

Nonmethane Hydrocarbon Chemistry in the Remote Marine Atmosphere

by

Neil McPherson Donahue

A. B. Physics, Brown University
(1985)

Submitted to the
Center for Meteorology and Physical Oceanography
in partial fulfillment of the requirements
for the degree of

Doctor of Philosophy
in Meteorology

at the

Massachusetts Institute of Technology
June, 1991

©Massachusetts Institute of Technology 1991
All rights reserved

Signature of Author _____

Center for Meteorology and Physical Oceanography
28 May, 1991

Certified by _____

Ronald G. Prinn
Professor of Meteorology
Thesis Supervisor

Accepted by _____

Thomas Jordan
Chairman, Department of Earth, Atmospheric and Planetary Sciences

WITHDRAWN
JUL 12 1991
FROM
LIBRARIES
MIT LIBRARIES
Lindgren

Nonmethane Hydrocarbon Chemistry in the Remote Marine Atmosphere

by
Neil McPherson Donahue

Submitted to the Center for Meteorology and Physical Oceanography
on May 28, 1991 in partial fulfillment of the requirements
for the degree of Doctor of Philosophy
in Meteorology

Abstract

We examine nonmethane hydrocarbon chemistry in the remote marine boundary layer theoretically and experimentally, with particular emphasis placed on the role it may play in hydroxyl radical (OH) chemistry. A photochemical model is used to consider the role the nonmethane hydrocarbons (NMHC) may have in the remote marine boundary layer, with (contradictory) constraints supplied by published observations of NMHC in the boundary layer and dissolved in ocean water. The atmospheric observations suggest a spectrum of roles for the NMHC in OH chemistry, ranging from secondary significance through primary importance as OH sinks and even approaching a governing role as dominant sources and sinks of OH. It is not possible to tell whether the range represents true variability or variable data quality. The oceanic observations suggest a much less important role, with NMHC fluxes to the atmosphere (and thus concentrations) roughly ten times lower than the low end of the range suggested by the atmospheric observations. Possibilities for this disagreement are discussed, though it is unclear whether the data are reliable enough to call into question current ideas about air-sea gas exchange. The experimental work begins with the development of absolute NMHC standards up to C₅ alkanes and alkenes. Finally, we describe our participation in the SAGA 3 expedition to the central Pacific in February - March, 1990, where we observed NMHC both in the atmosphere and the ocean. Our data continues to show the disagreement between air and water observations described above, and both our air and water data fall at the low ends of previous ranges. It is argued that the higher atmospheric observations probably reflect systematic problems with canister sampling, leading us to conclude that the role of NMHC in the remote atmospheric OH budget is indeed secondary though important, accounting (in conjunction with NMHC oxidation products) for 10 to 20 percent of all OH removal. The disparity between oceanic and atmospheric observations may be real, but enough uncertainty remains in the observations to prevent firm conclusions.

Thesis Supervisor: Dr. Ronald G. Prinn
Title: Professor of Meteorology

Acknowledgments

There is just no way I can thank all of the people who deserve it. I shall try. Ron Prinn, my advisor, gave me the latitude, the encouragement, the advice, and the money to allow me to pursue the wide range of topics contained in this work. I can not say too much. Thank you, Ron.

The atmospheric chemistry graduate students in our group have provided continuing and invaluable assistance and advice. Two deserve special recognition: Michele Sprengnether, who has been here the whole time, who developed the dilution system on which two of my gas standards were produced, and with whom I have shared so many trials and tribulations in the laboratory (excepting the move, which she dealt with herself...), and Bob Boldi, who has heard many of my looser thoughts (probably far too many) soon after their conception, and who has unhesitatingly provided more computer advice than I can relate. Yi Tang produced the standards already mentioned; without that work, this thesis would not yet have been completed. Dana Hartley and Kevin Gurney have also provided plenty of useful advice and good company.

The Undergraduate Research Opportunities Program provided support or waived overhead for many undergraduate researchers. Can I remember them all? Thieu Do started it all, followed by Nat Seymoure and Julie Callahan, then Jerco Fatovic and Cynthea Madras, and finally Michael Cabot, who has kept the lab going while I have written this thesis.

Ray Weiss lent the cylinders in which Yi Tang produced the standards upon the dilution system Michele Sprengnether built. Thanks Ray, even though one of the leaked. Ed Boyle and the captain of the RV Endeavor allowed me aboard for an instrumental test long ago, and Jim Johnson, Valentin Korapolov, and the captian of the RV Akademik Korolev provided the opportunity to participate in the SAGA III expedition. The soviet crew and scientists and the american participants on SAGA III made it a truly memorable experience.

For the first half of my tenure at MIT I was supported by the NASA Graduate Student Researchers Program, while for the second half, funds from NASA and NSF supported the work.

Finally, I would like to thank my housemates, Maren, and my parents.

Table of Contents

| | |
|---|-----|
| Chapter 1 -- Introduction | 8 |
| Chapter 2 -- NMHC Model | 10 |
| 2.1 Introduction | 10 |
| 2.2 Marine NMHC Abundances | 12 |
| 2.3 Marine Boundary Layer Chemical Model | 16 |
| 2.4 Model Chemistry | 23 |
| 2.5 Model Boundary Conditions | 37 |
| 2.6 Model Results | 38 |
| 2.6.1 Diurnal variability | 39 |
| 2.6.2 Sensitivity to NMHC emission fluxes | 42 |
| 2.6.3 Sensitivity to CO, O ₃ , H ₂ O and UV light | 49 |
| 2.6.4 Diurnal ozone variations | 53 |
| 2.6.5 Sensitivity to kinetics and isomeric composition | 54 |
| 2.7 Discussion | 56 |
| 2.8 Recommendations for future work | 58 |
| 2.9 Conclusions | 58 |
| Chapter 3 -- Calibration | 61 |
| 3.1 Introduction | 61 |
| 3.2 Permeation Tubes | 63 |
| 3.3 Tank Mixtures | 73 |
| 3.4 Capillary Flow Devices | 77 |
| 3.5 Instrument Response | 80 |
| 3.6 Tank Stability | 84 |
| 3.7 Standard Intercomparisons | 97 |
| 3.8 Suggestions for future work | 100 |
| 3.9 Conclusions | 102 |
| Chapter 4 -- Experimental Work | 103 |
| 4.1 Introduction | 103 |
| 4.2 Experimental | 107 |

| | |
|--|-----|
| 4.3 Data Analysis and Calibration | 117 |
| 4.4 Results and Discussion | 142 |
| 4.5 Recommended Improvements | 145 |
| 4.6 Conclusions | 164 |
| Chapter 5 -- Colclusions | 167 |
| References | 169 |
| Appendix 1 -- Model Reaction List | 174 |
| Appendix 2 -- Marine Air Samples from SAGA 3 | 195 |
| Appendix 3 -- Equilibrator Samples from SAGA 3 | 220 |
| Appendix 4 -- Curriculum Vita | 228 |

Chapter 1 -- Introduction

This thesis is an attempt at a fairly strict application of the classical scientific method: the use of observations, coupled with theoretical calculations, to inspire and guide further observations. The work described herein focuses on chemistry in the remote, tropical, marine boundary layer: that part of the atmosphere far from continental and human influences yet in close contact with a rich source of reactive compounds: the ocean. We shall argue that this region is central to global atmospheric chemistry because of the broad area underlain by the remote oceans, the high temperatures, intense sunlight and resulting high chemical reaction coefficients of the tropics, and finally the high pressure at the surface which again accelerates second and third order gas-phase reactions. As a result, a region in close contact with the surface, accounting for perhaps 15 percent of the mass of the troposphere, may be responsible for the oxidation of nearly half of the long lived trace compounds of current scientific and political interest, such as methane, methyl chloroform, and the hydrohalocarbons intended as chlorofluorocarbon replacements.

There is some history behind the thesis. We originally intended to study dimethylsulfide (DMS) chemistry, extending the work in sulfur chemistry begun by Mary Anne Carroll and described in her thesis (Carroll, 1983). Our intention was to combine DMS measurements with a photochemical model to facilitate both interpretation and the posing of further questions. The principal DMS sink in the remote atmosphere is believed to be the hydroxyl radical (OH) (Chatfield and Crutzen, 1990), so a photochemical sulfur model must include an adequate model of OH. Here our efforts ran into an obstacle. OH sinks include hydrocarbons; methane and carbon monoxide (CO) have long been recognized as globally important OH sinks, but a survey of existing nonmethane hydrocarbon (NMHC) measurements in the remote marine boundary layer showed that they too might be significant OH sinks, but the measurements were far too inclusive to establish their importance. We took that as a hint. The work became to explore NMHC chemistry in the remote marine boundary layer, using both a photochemical model and measurements. The measurement portion included development of standards for the analysis as well as actual field measurements.

The following thesis is thus divided into three main sections, one on modeling, one on standards, and one on the field measurements. The sections are not equal; the modeling chapter represents roughly half of the work, while each of the other two sections each amount

to roughly a quarter of the effort. Only modest changes have been made to transform Chapter 2 from a paper (Donahue and Prinn, 1990) into a thesis chapter. In particular, some new NMHC observations have not been added to the discussion of observations in Chapter 2 but have rather been taken up in Chapter 4 during the discussion of our own observations. The missing element is chemical kinetics. That is next.

Chapter 2 -- Chemical Modeling

2.1 Introduction

The lower tropical troposphere plays a disproportionately important role in removing long-lived trace gases from the atmosphere. The hydroxyl radical, OH, produced principally by the photodissociation of ozone followed by the reaction of resulting excited oxygen atoms ($O(^1D)$) with water, is widely recognized as the dominant tropospheric oxidizer. It removes most globally important trace gases, including carbon monoxide (Levy, 1971, Warneck, 1974), methane (Warneck, 1974; Logan *et al.*, 1981), and all halogenated alkanes with at least one hydrogen atom (Prinn, 1988). Because both trace gas densities and rate constants for reaction with OH maximize at the highest total pressures and temperatures, the lower tropical troposphere is a region of particularly intense chemical processing. Those factors which govern the OH concentration in the lower tropical troposphere are thus also disproportionately important to global tropospheric chemistry.

Figure 2.1.1 shows a simple example of this for two representative trace species: methyl chloroform (CH_3CCl_3) and carbon monoxide (CO). We compute the fraction of each compound removed below any given altitude using the appropriate rate constants (Atkinson *et al.*, 1989), profiles of temperature and pressure (15° latitude, US Standard Atmosphere Supplements, 1966), and mixing ratio profiles (taken to be constant for both methyl chloroform (Prinn, 1988), and CO in the remote tropics (Fishman *et al.*, 1987)). Results are shown for an OH summer profile from Kasting and Singh (1986) and for a second, *ad hoc*, profile which could represent the effect of significant surface emissions of strong OH sinks (it also corresponds roughly to the lower limit of surface OH in our chemical model). These two profiles are shown in Figure 2.1.1a. Figure 2.1.1a also shows the average OH concentration range deduced for the lower tropical southern hemisphere (1000–500 mb, 0–30°S) from 10 years of ALE/GAGE methyl chloroform data (Prinn *et al.*, 1987). From Figures 2.1.1b and 2.1.1c it is evident that about half of each compound is removed well below the half-height of the atmosphere (500 mb): depression of surface OH deflects the removal only slightly upwards (500 m at most). One-half of tropical methyl chloroform removal occurs in a layer between 1000 and 760 mb (which contains but one-quarter of the mass of the tropical atmosphere). Curves for other partially halogenated alkanes and methane are very similar to the methyl

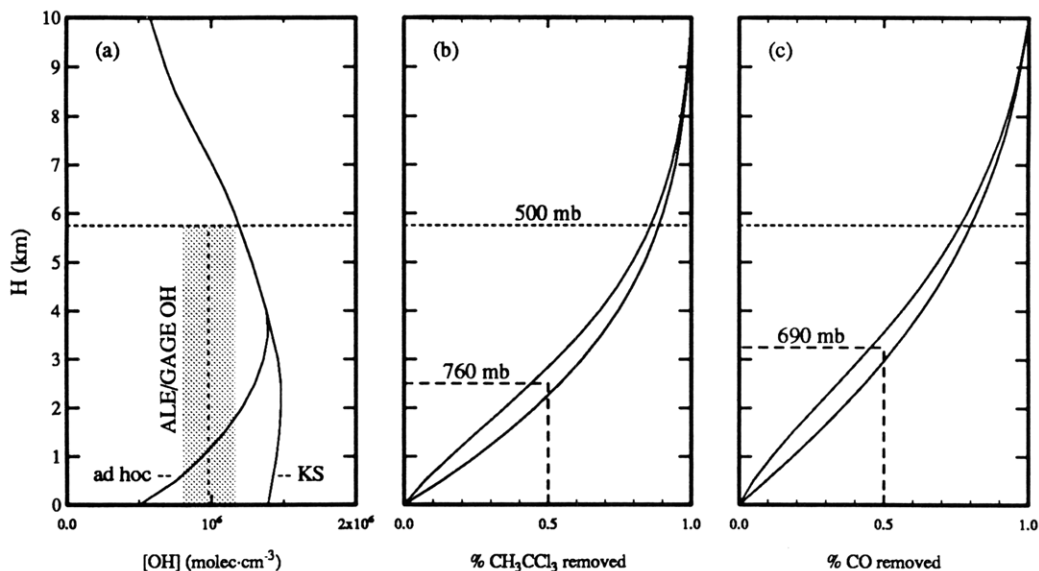


Figure 2.1.1. (a) OH vertical profiles in the tropical marine atmosphere. “KS” = Kasting and Singh (1984), “ALE/GAGE” = Prinn *et al.* (1987) (see text). (b) The fraction of CH_3CCl_3 removed below a given altitude, assuming that OH is the sole sink and that the two profiles in (a) apply. Long dashed line is height of 50% removal. (c) As (b), but for CO.

chloroform curve. Even CO, whose rate constant for reaction with OH is currently thought to be independent of temperature but strongly pressure dependent (Atkinson *et al.*, 1989), is processed far more efficiently in the lower troposphere than in the upper troposphere. The situation is much the same outside the tropics, but OH and temperature reach tropical levels for only half of the year, if that long. Therefore the lower tropical troposphere serves as a chemical crucible for the atmosphere, oxidizing up to twice the share of long-lived trace gases that its mass alone would indicate.

Because the chemistry of the lower marine atmosphere can be affected by very short-lived compounds emitted from the ocean surface, and because several measurements of short-lived non-methane hydrocarbon (NMHC) concentrations in the remote marine atmosphere suggest the existence of significant NMHC emission fluxes, we shall present here a theoretical examination of marine boundary layer (MBL) chemistry, focusing on the hydroxyl radical and the role NMHC’s may have in regulating its concentration. With existing measurements, we can constrain light (C_2 and C_3) hydrocarbon concentrations only to within roughly a factor of 4 (a factor of 2 on either side of the mean). There is much less of a consensus on the heavier NMHC’s (C_4 , C_5 and C_6), which we consider to be constrained only to within a factor of 25. To produce model NMHC concentrations consistent with this data we will

therefore consider a wide range of NMHC air-sea fluxes with various relative distributions of NMHC emissions: some weighted toward light NMHC's, and some allowing for substantial emissions of heavier NMHC's. We shall identify in particular the flux magnitude at which NMHC emissions become significant, and then dominant, players in MBL chemistry, and we shall show that this flux is well within the range of fluxes consistent with current observations.

2.2 Marine NMHC Abundances

Four of the published data sets on NMHC concentrations in the remote marine atmosphere (Singh and Salas, 1982; Greenberg and Zimmerman, 1984; Bonsang and Lambert, 1985; and Singh *et al.*, 1988) cover the Pacific marine boundary layer from roughly 40°N to 40°S. Two (Rudolph and Ehhalt, 1981; Tille and Bachmann, 1987) report observations over the equatorial Atlantic, and finally two publications from the STRAT0Z missions (Ehhalt *et al.*, 1985; Rudolph, 1988) contain data from the Pacific coast of South America in westerly winds as well as the equatorial Atlantic. Lamontagne *et al.* (1974), and Bonsang *et al.* (1988) report concentrations of light NMHC's in the ocean mixed layer. Bonsang *et al.* (1988) also report atmospheric NMHC data, along with tracer data (CO₂, ²¹⁰Pb, ²²²Rn) used to identify samples showing signs of continental influence. Their reported atmospheric NMHC concentrations are consistently at least an order of magnitude larger than the others discussed here, and some of our model runs therefore extend to fluxes large enough to produce the concentrations they report.

The existing atmospheric data are summarized in Table 2.2.1, which shows the range of (remote marine) observations for each publication. A blank indicates that there was no reference to the given compound in that paper. Where a significant interhemispheric gradient exists, we show the southern hemispheric values. This is important only for ethane and propane, which are secondary contributors to MBL chemistry. While these data show a great range of mixing ratios for each compound, the range within a given data set is generally comparable to the differences between the data sets. The data from the remote Pacific are generally a little higher than the mean, and the most recently published set (Singh *et al.*, 1988) falls generally below the mean for those hydrocarbons reported, although the data was collected at nearly the same time as most of the other Pacific data (Greenberg and Zimmerman, 1984; Bonsang and Lambert, 1985). Because of the very limited coverage of

Table 2.2.1 NMHC mixing ratios observed by various investigators in the remote marine atmosphere.

| | S88 | S82 | G84 | B85 | R81 | T87 | E85 | R88 | Range |
|--------------|-----|------------|-------------|------------|------------|------------|-----------|-------------|------------|
| (mdl, pptv:) | 50 | 50 | 25 - 50 | 20 | 5 - 20 | 1 - 100 | 20 - 50 | 5 - 10 | |
| ethane | 310 | 225 -- 300 | 450 -- 850 | 200 -- 600 | 675 -- 975 | 100 -- 200 | ~ 500 | 600 -- 1000 | 200 -- 800 |
| ethene | <50 | 25 -- 125 | 250 -- 750 | 100 -- 300 | 75 -- 425 | 100 -- 250 | 50 -- 100 | 100 -- 250 | 75 -- 300 |
| propane | 40 | 100 -- 300 | 250 -- 1000 | 40 -- 120 | 60 -- 180 | ~50 | 50 -- 100 | 75 -- 350 | 100 -- 400 |
| propene | -- | 50 -- 250 | 125 -- 375 | 100 -- 250 | 75 -- 275 | 100 -- 200 | 50 -- 200 | ~100 | 50 -- 200 |
| n-butane | 10 | 125 -- 175 | 50 -- 150 | 20 -- 80 | 25 -- 150 | ~50 | 10 -- 50 | 25 -- 250 | 25 -- 150 |
| i-butane | 20 | 150 -- 250 | 40 -- 80 | | 10 -- 30 | ~75 | 30 -- 50 | 10 -- 75 | 10 -- 100 |
| butene | | | | 25 -- 125 | | 25 -- 200 | | | 25 -- 150 |
| n-pentane | | 200 -- 400 | 10 -- 100 | 100 -- 250 | 10 -- 50 | 20 -- 150 | ~20 | 10 -- 100 | 10 -- 200 |
| i-pentane | | 50 -- 250 | 10 -- 50 | 50 -- 150 | 5 -- 20 | ~10 | <20 | 5 -- 150 | 5 -- 150 |
| pentene | | | | 100 -- 250 | | 5 -- 10 | | | 10 -- 250 |
| n-hexane | | | 10 -- 50 | 100 -- 300 | | ~20 | | | 5 -- 200 |
| hexene | | | | 100 -- 250 | | | | | 10 -- 250 |

Southern hemispheric values are shown for compounds showing large interhemispheric gradients (generally ethane and propane). S88 (Singh *et al.*, 1988), S82 (Singh and Salas, 1982), G84 (Greenberg and Zimmerman, 1984), B85 (Bonsang and Lambert, 1985) are from the remote Pacific; R81 (Rudolph and Ehhalt, 1981) and T87 (Tille and Bachmann, 1987) are from the equatorial and southern Atlantic; and E85 (Ehhalt *et al.*, 1985) and R88 (Rudolph, 1988) are culled from boundary layer observations made during STRATOZ flights over the equatorial Atlantic and on the western coast of South America in westerly winds. The detection limits given in each paper (mdl, in pptv) are shown in the header of each data set. 'Range' is the mixing ratio range used in this work. Listed mixing ratios are in pptv.

heavier (C₄ - C₆) alkenes, their concentrations are poorly constrained. In addition, there exists no isomeric data for the alkenes. The observations of heavy (C₄ - C₆) alkenes are in data sets in which concentrations of the lighter alkenes and alkanes do not differ significantly from those in the other data sets. We therefore include these heavy alkene observations in our investigation with the observed levels reported by Bonsang and Lambert (1985) as the upper limit to an indicated factor of 25 range. In our "base case" we consider heavy alkene concentrations less by a factor of 5 than the Bonsang and Lambert (1985) values.

Acetylene is not included because it is not abundant enough to strongly contribute to MBL chemistry. Other hydrocarbons, such as isoprene, the terpenes, and aromatics, are also excluded. While they may reach significant levels in the northern hemisphere (Greenberg and Zimmerman, 1984), they do not appear to be common enough in the southern hemisphere to play an important role (Nutmaguil and Cronn, 1985). We focus on the southern hemisphere because it should more closely represent "true" remote marine conditions, well removed

from continental and human influences.

Table 2.2.2 shows the NMHC values we adopt in this paper as representative of the remote marine atmosphere. Shown for each compound i considered here are the rate constants k_i for reaction with OH at 300K *, the lifetime (assuming a diurnally averaged OH concentration of 7×10^5 molec cm⁻³), the range and geometric mean value for the mixing ratio and concentration, and the product of the concentration C_i and rate constant (for low, mean, and high NMHC conditions). This last term ($k_i C_i$) is the frequency of removal of OH due to reaction with each species (v_{OH}). It is a far better indicator of a compound's importance in MBL chemistry than is concentration alone. To serve as a guide, we also include in Table 2.2.2 the values adopted in this work for three species (in addition to the NMHC's) known to be chemically important in the remote MBL: CO (Seiler and Fishmann, 1981), methane, and dimethyl sulfide (Andreae *et al.*, 1985). The range shown in $k_i C_i$ for these latter three species reflects the true variability of their MBL concentrations. The range shown for the NMHC's may represent either true variability or experimental uncertainty; until the various methods are suitably compared and more data is obtained, we will not know. If actual mean MBL NMHC concentrations *are* at or near the mean levels adopted here, NMHC's, particularly the alkenes, clearly cannot be ignored when one models MBL chemistry.

When considering ranges of concentrations, we divide the NMHC's into two groups: C₂ and C₃ hydrocarbons (the "light" group), and all heavier hydrocarbons (the "heavy" group). This reflects our judgement that the concentrations of the light hydrocarbons, as a group, are substantially better known than the heavier NMHC's. We also total the minimum and maximum values for all of the NMHC's. This is warranted because most observations do show high correlations between individual species. The assumed range in concentrations for the light group is a factor of 4, while for the heavy hydrocarbons it is a factor of 25. Because the range of heavy NMHC fluxes (as deduced from the relevant sums $\Sigma k_i C_i$) swamps that of the light NMHC's, the total NMHC flux is poorly constrained (or perhaps highly variable), with a factor of 25 range in magnitude.

* Throughout this thesis, rate constants are expressed in cm – molecule – sec units. The order of the reaction is indicated by the letter expressing the rate constant: j for first order (in units of sec⁻¹), k for second order (cm³molecules⁻¹sec⁻¹), and l for third order reactions (cm⁶molecules⁻²sec⁻¹.)

Table 2.2.2 OH removal frequencies, ν_{OH} , due to reaction with various carbon-containing compounds in the model.

| | k | τ (days) | χ (pptv) | | | C (molec \cdot cm $^{-3}$) | | | k \cdot C (10^{-3} sec $^{-1}$) | | |
|--------------|------|---------------|---------------|------|------|-------------------------------|----------|----------|---------------------------------------|-----|------|
| | | | low | med | high | low | med | high | low | med | high |
| CO | 0.24 | 69.0 | 50 | 62.5 | 75 | 1.25(12) | 1.56(12) | 1.88(12) | 294 | 367 | 442 |
| methane | .008 | 5.6(yr) | 1.64 | 1.65 | 1.66 | 4.10(13) | 4.12(13) | 4.15(13) | 329 | 331 | 333 |
| DMS | 6.17 | 2.68 | 75 | 150 | 250 | 1.99(9) | 3.75(10) | 6.25(10) | 12 | 23 | 39 |
| <hr/> | | | | | | | | | | | |
| ethane | 0.28 | 59.0 | 200 | 400 | 800 | 5.00(9) | 1.00(10) | 2.00(10) | 1 | 3 | 6 |
| ethene | 8.50 | 1.90 | 75 | 150 | 300 | 1.88(9) | 3.75(9) | 7.50(10) | 16 | 32 | 64 |
| propane | 1.20 | 13.8 | 100 | 200 | 400 | 2.50(9) | 5.00(9) | 1.00(10) | 3 | 6 | 12 |
| propene | 26.0 | 0.64 | 50 | 100 | 200 | 1.25(9) | 2.50(9) | 5.00(9) | 32 | 65 | 130 |
| <hr/> | | | | | | | | | | | |
| light NMHC's | | | | | | | | | 52 | 106 | 212 |
| <hr/> | | | | | | | | | | | |
| n-butane | 2.58 | 6.4 | 15 | 75 | 375 | 3.75(8) | 1.88(9) | 9.38(9) | 1 | 5 | 24 |
| i-butane | 2.39 | 6.9 | 10 | 50 | 250 | 2.50(8) | 1.25(9) | 6.25(9) | 1 | 3 | 15 |
| butene | 48.3 | 0.3 | 6 | 30 | 150 | 1.50(8) | 7.50(8) | 3.75(9) | 7 | 36 | 181 |
| n-pentane | 3.90 | 4.1 | 10 | 50 | 250 | 2.50(8) | 1.25(9) | 6.25(9) | 1 | 5 | 25 |
| i-pentane | 2.39 | 6.9 | 10 | 50 | 250 | 2.50(8) | 1.25(8) | 6.25(9) | 1 | 3 | 15 |
| pentene | 55.0 | 0.3 | 10 | 50 | 250 | 2.50(8) | 1.25(9) | 6.25(9) | 14 | 69 | 344 |
| n-hexane | 5.40 | 3.1 | 6 | 30 | 150 | 1.50(8) | 7.50(8) | 3.75(9) | 1 | 4 | 20 |
| hexene | 64.0 | 0.3 | 10 | 50 | 250 | 2.50(8) | 1.25(9) | 6.25(9) | 16 | 80 | 400 |
| <hr/> | | | | | | | | | | | |
| heavy NMHC's | | | | | | | | | 42 | 205 | 1024 |
| <hr/> | | | | | | | | | | | |
| total NMHC's | | | | | | | | | 94 | 311 | 1236 |

Shown are the ranges and geometric mean values for mixing ratio (χ), concentration (C) and removal frequency (k \cdot C), along with the rate constant (k) for reaction with OH and the compound lifetime, in days, assuming a diurnally averaged OH concentration of 7×10^5 molec cm $^{-3}$. All rate constants are in units of 10^{-12} cm 3 molec $^{-1}$ sec $^{-1}$. Note that CO mixing ratios are in ppbv, and methane mixing ratios are in ppmv.

In modeling remote MBL chemistry, we will consider ranges not only for the NMHC's but for several other variables whose values are fixed as model boundary conditions. These are: H $_2$ O, O $_3$, CO, and column ozone. Other species (NO $_x$, H $_2$, methane, and dimethyl sulfide) are fixed in the model and variations are not considered, either because they do not vary, or because they are not significant enough to warrant consideration in the OH chemistry. We do not explicitly consider variations in NO $_x$ levels in this paper, as we are modeling conditions where NO $_x$ is extremely scarce, and therefore the model chemistry is

Table 2.2.3 Initial concentrations in molec · cm⁻³ for compounds held fixed in the model.

| | | | |
|--------------------|--------------------------|----------------------|----------------------------|
| [N ₂] | = 2.0 × 10 ¹⁹ | [methane] | = 4.125 × 10 ¹³ |
| [O ₂] | = 5.3 × 10 ¹⁸ | [HCl] | = 2.5 × 10 ¹⁰ |
| [CO ₂] | = 1.0 × 10 ¹⁶ | [CH ₃ Cl] | = 1.0 × 10 ¹⁰ |
| [H ₂] | = 1.4 × 10 ¹³ | | |

relatively insensitive to NO_x levels. All assumed concentrations are shown in Table 2.2.3.

We assume water vapor in the MBL ranges between 60% relative humidity at 25°C and saturation at 35°C. The mean is taken to be 75% relative humidity at 29°C (US Standard Atm, 15°, 1966). For ozone, Piotrowitz *et al.* (1986), Fishman *et al.* (1987) and Johnson *et al.* (1989) all find similar ranges in the South Pacific. Johnson *et al.* (1989) have shown that ozone has strong seasonal variations and can reach very low mixing ratios in the southern tropics during the spring. We assume that ozone ranges between 2 and 30 ppbv, with a mean of 15 ppbv. Carbon monoxide appears to range between 50 and 75 ppbv in the southern hemisphere (Seiler and Fishman, 1981), with significant annual variation (Seiler *et al.*, 1984), and substantial diurnal variations of 10–20 ppbv peak-to-peak amplitude (Gammon and Kelly, 1988). We consider this latter range for CO with a “base case” of 62.5 ppbv. Odd nitrogen is extremely scarce in the remote, southern MBL (Liu *et al.*, 1983, Ridley *et al.*, 1987), with daytime maximum NO concentrations rarely exceeding 5 pptv. This places the remote, southern MBL firmly in a regime of photochemical ozone destruction, where odd nitrogen contributes to the chemical environment only tangentially.

2.3 Marine Boundary Layer Chemical Model

Remote MBL chemistry is dominated either by relatively long-lived compounds, such as CO, methane, and ozone, or by relatively short-lived non-methane hydrocarbons emitted from the ocean surface. The short-lived species are affected not only by MBL chemistry, but by MBL ventilation rates and NMHC air-sea fluxes. Ventilation rates are variable and difficult to predict, while the air-sea fluxes vary both with wind speed and NMHC concentrations in ocean water, for which little data exists. Because our focus here is on MBL chemistry rather than MBL meteorology or ocean processes, we consider the latter two effects only in a very simplified way. This is justified not only by our focus, but by the complete lack of data on any diurnality in NMHC sea-air fluxes. Also, to avoid the need for a

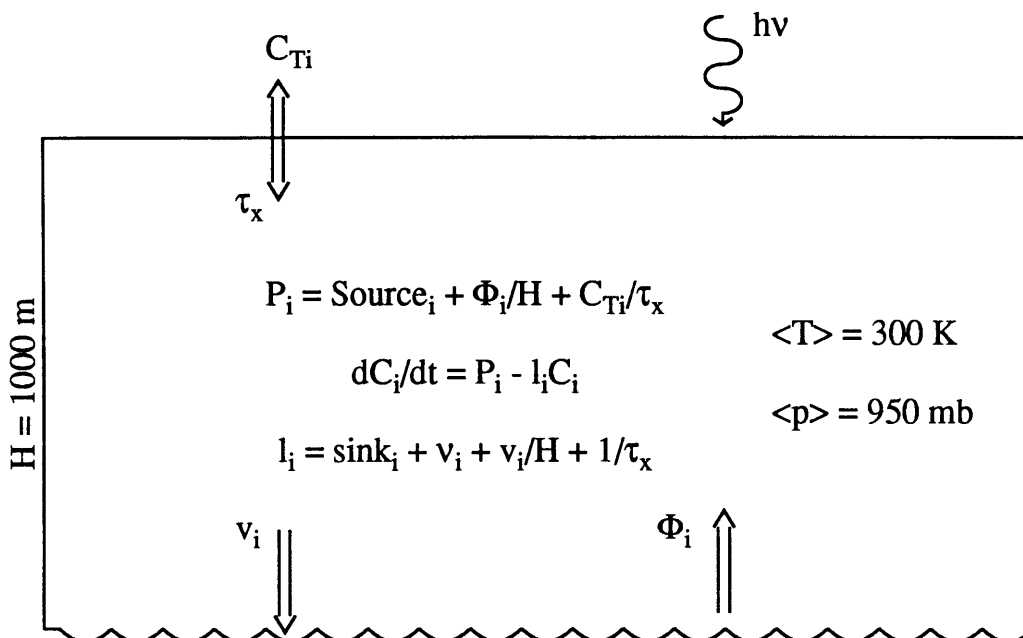


Figure 2.3.1. A schematic of the marine boundary layer chemical model. The concentration C_i of each species i is calculated, based on chemical production P_i and the inverse lifetime l_i . Contributors to these terms, in addition to homogeneous chemistry are fluxes from the ocean (Φ_i), heterogeneous removal (v_i), deposition to the ocean (v_i), and exchange with the free troposphere (τ_x).

large scale circulation model, the concentrations for the relatively long-lived compounds are assigned and not predicted. Specifically, to model remote MBL chemistry we consider a horizontally and vertically well-mixed layer (Figure 2.3.1) above the remote ocean surface, with exchange of predicted species between this layer and both the ocean and the free troposphere being parameterized using diurnally invariant exchange times. Heterogeneous chemistry and deposition to the ocean surface are also treated with similar parameterizations. To simulate the marine boundary layer, the model is run repeatedly through diurnal cycles of the various rate constants until the diurnally averaged concentrations for all compounds agree to within a small factor (generally 0.01) on two successive days.

We use a novel and very flexible prognostic code in which the timestep is continually adjusted to be appropriate to the time scale for chemical change intrinsic to the system. The equation solved for each compound, i , is

$$\begin{aligned} \frac{dC_i}{dt} &= \left(Source_i + \frac{\Phi_i}{H} \right) - \left(sink_i + v_i + \frac{v_i}{H} \right) C_i \\ &= P_i(t; \tau_{P_i}) - l_i(t; \tau_{l_i}) \cdot C_i(t; \tau_{C_i}) \end{aligned} \quad (2.3.1)$$

where

- C_i = concentration of i (molec cm⁻³),
 H = thickness of the layer (cm),
 $Source_i$ = homogeneous chemical source strength of i (molec cm⁻³sec⁻¹),
 Φ_i = flux of i into the layer (molec cm⁻²sec⁻¹),
 $sink_i$ = homogeneous chemical sink strength of i (sec⁻¹),
 v_i = removal frequency of i from the layer through ventilation or
heterogeneous reactions (sec⁻¹), and
 v_i = deposition velocity of i to the ocean surface (cm sec⁻¹).

There are four timescales pertinent to the evolution of C_i : τ_{C_i} is the timescale ($dt/d\ln C_i$) on which C_i changes, τ_i ($1/l_i$) is the chemical lifetime of i , and τ_{P_i} and τ_{l_i} are the characteristic times ($dt/d\ln P_i$ and $dt/d\ln l_i$) for changes in the production and loss terms of i . τ_{C_i} is a function of the other three timescales. Jointly, the production and loss terms constitute the chemical forcing of i , and we call τ_{P_i} and τ_{l_i} together the forcing timescales of i . The behavior of i depends strongly on whether the chemical lifetime, τ_i , is shorter or longer than the forcing timescales. To determine the time-evolution of the system we assume a constant coefficient solution, rather than a finite-difference solution, because the former allows longer timesteps and because errors will be more evenly distributed about the true solution. Given a known concentration at time t , the concentration at time $t + \delta t$ is thus:

$$C_i(t + \delta t) = C_{ssi}((t + \delta t); \tau_{fi}) + \{C_i(t) - C_{ssi}((t + \delta t); \tau_{fi})\} e^{(-t/\tau_i)} \quad (2.3.2)$$

where

$$C_{ssi} = P_i \tau_i,$$

$$\tau_i = 1/l_i,$$

and τ_{fi} (found *after* a model step of time δt) is the ‘‘reduced’’ forcing timescale, derived from the production and loss terms, *i.e.*

$$\begin{aligned}
\tau_{fi} &= \left(\frac{\tau_{P_i} \cdot \tau_{l_i}}{\tau_{P_i} + \tau_{l_i}} \right), \\
\tau_{P_i} &= \left(\frac{\min(P_i)}{\Delta P_i} \right) \delta t, \\
\tau_{l_i} &= \left(\frac{\min(l_i)}{\Delta l_i} \right) \delta t,
\end{aligned} \quad (2.3.3)$$

where $\min(x)$ is the minimum value obtained by x in the interval δt (a numerically safer choice than the average value).

The timescale over which the coefficients of our “constant” coefficient solution actually change is τ_{fi} . For a species i , the constant coefficient assumption is therefore valid for times small compared to τ_{fi} . Specifically, the constant coefficient solution for i will be within a desired accuracy, ϵ , of the actual solution for all times from t to $t + \epsilon\tau_{fi}$; we therefore find the timestep appropriate for each compound *following* each model step:

$$\delta t_i = \epsilon\tau_{fi}. \quad (2.3.4)$$

The “optimal” timestep for the (just passed) model step is then the shortest δt_i , excluding those compounds whose lifetimes, τ_i , are sufficiently shorter than τ_{fi} (these are *always* within ϵ of $C_{ssi}(t)$; they do not limit δt and are treated separately, as discussed below). If, after a model step, the optimal timestep for that step was significantly shorter (we use a factor of 2) than the one actually used, the step is repeated with the optimal timestep. Otherwise, this optimal timestep is used for the next step.

The timesteps used by the model are thus determined internally, and are continually adjusted based on the accuracy being demanded of the model and the rates of chemical change intrinsic to the system being modeled. Rate constants are interpolated from a sufficiently dense set of precalculated rate constants, allowing the model to determine them for arbitrary times without extensive computation, especially the computation involved in *a priori* determination of photodissociation frequencies. A substantial portion of the model time is spent at dawn and dusk (in excess of 80%), due to the rapid rate changes occurring at those times. To reduce run times, we have therefore introduced one relaxation from the strict definitions given above. Only compounds with sufficiently large reactive rates ($R_i = P_i + I_i C_i$) can be important to overall MBL chemistry. For example, no compound with a $1 \text{ molecule} \cdot \text{cm}^{-3} \text{sec}^{-1}$ reactive rate can influence OH, with a reactive rate around $10^6 \text{ molec cm}^{-3} \text{sec}^{-1}$. Only when an important compound demands a very short timestep is such a short step taken. To implement this when searching for the optimal timestep, the δt_i for compound i is multiplied by a weighting factor,

$$\begin{aligned} \delta t_i &= w \epsilon \tau_{fi} \\ w &= \frac{R_{max}}{F \cdot R_i}; \quad w \geq 1, \end{aligned} \tag{2.3.5}$$

where R_i and R_{max} are the reactive rates, respectively for compound i and the compound with the largest reactive rate in the previous timestep. All compounds with a reactive rate within F of R_{max} are given full consideration ($w = 1$) in the search for an appropriate timestep δt . All other compounds, with rates (R_i) less than R_{max}/F receive reduced consideration according to equation (2.3.5). For example, if i has a reactive rate 0.01 times the maximum rate, and $F = 10$, δt_i will be ten times longer than it would be without the weighting, and i will be less likely to determine the chosen timestep. Even if i *does* determine the timestep, the step will be ten times longer than it would be without the weighting. The factor F is included so that the odd hydrogen species will receive full weighting, although their reactive rates are roughly a factor of 10 less than the odd-oxygen species. This approximation causes compounds with relatively small reactive rates to be inaccurately modeled, but we assume that their small reactive rates render them unimportant. We have found that weighted model solutions with $F = 10$ agree to within one percent with the unweighted solutions for all important species while requiring approximately one tenth the computer time needed by an unweighted run.

Not all compounds are solved with the constant coefficient solution. Those with lifetimes (τ_i) much smaller than the timescale for changes in their chemical forcing ($\tau_i < \epsilon \tau_{fi}$) will always be within ϵ of the asymptotic, or steady state concentration (C_{ssi}), excepting transient behavior associated with initial conditions. These compounds are therefore identified by the model and excluded from the determination of an optimal timestep. Their concentrations are then iterated until the source and sink terms for each balance to within ϵ , subject to the constraint that the total concentrations of certain selected families ($\text{HO}_y = \text{OH} + \text{H} + \text{HO}_2 + 2\text{H}_2\text{O}_2$, for example) agree with values determined for those families by the explicit, constant coefficient solution. The iteration scheme used when $\tau_i < \epsilon \tau_{fi}$ is a simple, explicit iteration,

$$C_{i,n+1} = P_{i,n} \cdot \tau_{i,n}, \tag{2.3.6}$$

coupled with an intermittent (every 5th step) accelerator which finds the exponential asymptotic limit of the three most recent guesses. In the normal course of a diurnal model, the compounds for which $\tau_i < \epsilon \tau_{fi}$ are always very near their steady state values, and only two

or three iteration steps are generally required for convergence.

To further reduce computer time, the accuracy, ϵ , demanded of the solutions is started at a large number (0.5), and gradually reduced, day by day, as the evolving solution dictates. We consider a run to have converged when in two successive model days constrained to the final desired accuracy, ϵ_f , the diurnally averaged concentrations for all species agree to within $100\epsilon_f$ percent. In this way, a system of more than 800 reactions can be solved to the desired 1% accuracy ($\epsilon_f = 0.01$) in roughly one hour on an 80386-based micro computer.

This is a one layer model, and the free troposphere is not explicitly treated. We instead approximate its influence by including both an MBL (upward) ventilation rate and a (uni-directional) flux of material from the free troposphere to the MBL. Assuming a surface source, Φ_i , the continuity equations for i in the MBL and a layer (denoted by the subscript 'T') of equal mass just above the MBL are:

$$\begin{aligned}\frac{d\chi_i}{dt} &= \frac{\Phi_i}{H[M]} - \frac{\chi_i}{\tau_i} - \frac{\chi_i - \chi_{iT}}{\tau_x} \\ \frac{d\chi_{iT}}{dt} &= -\frac{\chi_{iT}}{\tau_{iT}} + \frac{\chi_i - \chi_{iT}}{\tau_x} \\ \tau_x &= 5 \times 10^4 \text{ sec } (\sim 14 \text{ hours})\end{aligned}\tag{2.3.7}$$

For relatively long-lived species, such as carbon monoxide and ozone, we simply specify a (diurnally invariant) free-tropospheric mixing ratio and calculate the uni-directional flux into the MBL. The exchange time τ_x (and thus the return flux) is incorporated into the removal frequency, ν_i . Shorter-lived species are handled differently. We assume that the chemical lifetimes in the MBL and the overlying free-tropospheric layer are identical ($\tau_{iT} = \tau_i$) and solve the two coupled continuity equations, assuming a diurnally invariant steady state. We eliminate χ_{iT} , yielding

$$\begin{aligned}\frac{d\chi_i}{dt} &= \frac{\Phi_i}{H[M]} - \frac{\chi_i}{\tau_i} - \frac{\chi_i}{\tau_x + \tau_i} \\ &= 0 \text{ (steady state)}.\end{aligned}\tag{2.3.8}$$

The third term on the right-hand side of (2.3.8) is the net upward flux of i . The larger τ_i is with respect to τ_x , the smaller will be the vertical mixing ratio gradient, and the smaller the net upward flux. Very short-lived species with a surface source will have relatively large net upward fluxes, but their loss will still be dominated by chemistry and not net upward mixing. Compounds with lifetimes between one hour and a few days will in contrast have

an important fraction of their loss associated with a net upward flux. For these compounds we include in the removal frequency, ν_i , an effective inverse exchange time consistent with the third term in equation (2.3.8) above:

$$\tau_{xi}(\text{eff})^{-1} = (\tau_x + \tau_{i(\text{dav})})^{-1}, \quad (2.3.9)$$

where $\tau_{i(\text{dav})}$ is the diurnally averaged lifetime of i . We include this term primarily to account for the incomplete oxidation of the NMHC's in the boundary layer, so that we can more accurately predict the NMHC air-sea fluxes required to sustain observed NMHC concentrations.

Ultraviolet fluxes needed in the above model are calculated as a function of time of day in a separate model. Specifically, we divide the atmosphere into 1 km thick layers, from the surface to 50 km, and, given an ozone concentration and a concentration of Rayleigh scatterers for each layer, solve analytically for the upwelling and downwelling scattered light intensities. We assume that the Rayleigh scattering phase function is a "double delta function," allowing scattering only directly forward or backward, and take the ocean surface albedo to be 0.06 (Houghton, 1985). Dawn and dusk are assumed to last for 1 hour each, with UV fluxes increasing exponentially from insignificant nocturnal values. To address average tropical conditions, fluxes are computed for 15°S at equinox. The results of the "double delta function" model agree to within a few percent with the Chandrasekhar two-stream model based on an isotropic phase function (Chandrasekhar, 1960). Column ozone typically varies in the tropics between 230 and 280 Dobson units (DU) (WMO 1985), with a mean of 255 DU. In addition to ozone absorption and Rayleigh scattering, cloud absorption also reduces the spherically integrated UV intensity. Logan *et al.* (1981) deduce a roughly 30% reduction in mid-latitude surface intensities when they include clouds in their model. They also indicate that the tropics have roughly half the mid-latitude cumulonimbus cover, and one third the mid-latitude stratus cover --- the major cloud types leading to integrated UV intensity reduction. We take as a base case a 15% reduction in UV intensity (and thus $O(^1D)$) due to clouds. We parameterize this reduction by shifting the average column ozone from 255 to 284 DU, producing a 12% drop in average $O(^1D)$ (and OH). To account for the expected range of MBL UV fluxes, we consider column ozone variations from 250 to 300 DU (Figure 2.6.10). This is obviously an oversimplified way to account for UV variations,

but we believe that it is sufficient to allow us to explore the sensitivity of MBL chemistry to variations in UV intensity.

2.4 Model Chemistry

Oxidation by OH, O₃, and various peroxy free radicals is included in the model. NO₃, while of demonstrated importance in the near-shore marine environment (Andreae *et al.*, 1985), is probably too rare in the remote MBL to be a major oxidant. Singh and Kasting (1988) argue that Cl can play a major role in marine alkane destruction. However, OH-alkene reactions are much too fast for Cl to compete with OH in alkene chemistry. Even hydrogen abstractions from oxidized hydrocarbons are dominated by OH and not Cl. Thus, while chlorine chemistry is included in the model, it has little chemical influence. IO may be important to DMS oxidation (Barnes *et al.*, 1987, Chatfield and Crutzen, 1990), but DMS is not an important regulator of OH. Since our emphasis is not on DMS, we do not include IO chemistry in this model.

The model contains some 750 chemical reactions, of which roughly 650 involve non-methane hydrocarbons. In Table 2.4.1 we show a subset of this reaction set, including the inorganic reactions, as well as those involving methane, ethane, and ethene. All of the essential chemistry and assumptions in our model are shown within this subset. The full reaction set is available, upon request, from the authors. We incorporate the known basic odd hydrogen chemistry for the remote atmosphere (see, e.g. Logan *et al.*, 1981; Thompson and Cicerone, 1982, Kasting and Singh, 1986). This is summarized in Figure 2.4.1, which shows the important odd-oxygen and odd-hydrogen species and the connections between them. The reactive rate shown in each arrow is the noon-time value from our “base-case” run (see Section 2.5). The dominant chemical source of odd oxygen is the formation of NO₂ by the reaction RO₂ + NO → RO + NO₂ (“RO₂” includes HO₂ this one time), followed by NO₂ photodissociation. The dominant odd-oxygen sink in the remote MBL is the pictured reaction, H₂O + O(¹D) → OH + OH, which produces a diurnally averaged odd-oxygen chemical lifetime of roughly 8 days. For the 15 ppbv of odd oxygen shown, an advective source is clearly required to augment the weak chemical source. Odd hydrogen is created by the reaction of O(¹D) with water vapor, and subsequent OH reactions lead to formation of hydroperoxy free radicals (HO₂). NMHC oxidation also involves many organic free radicals, including organo-

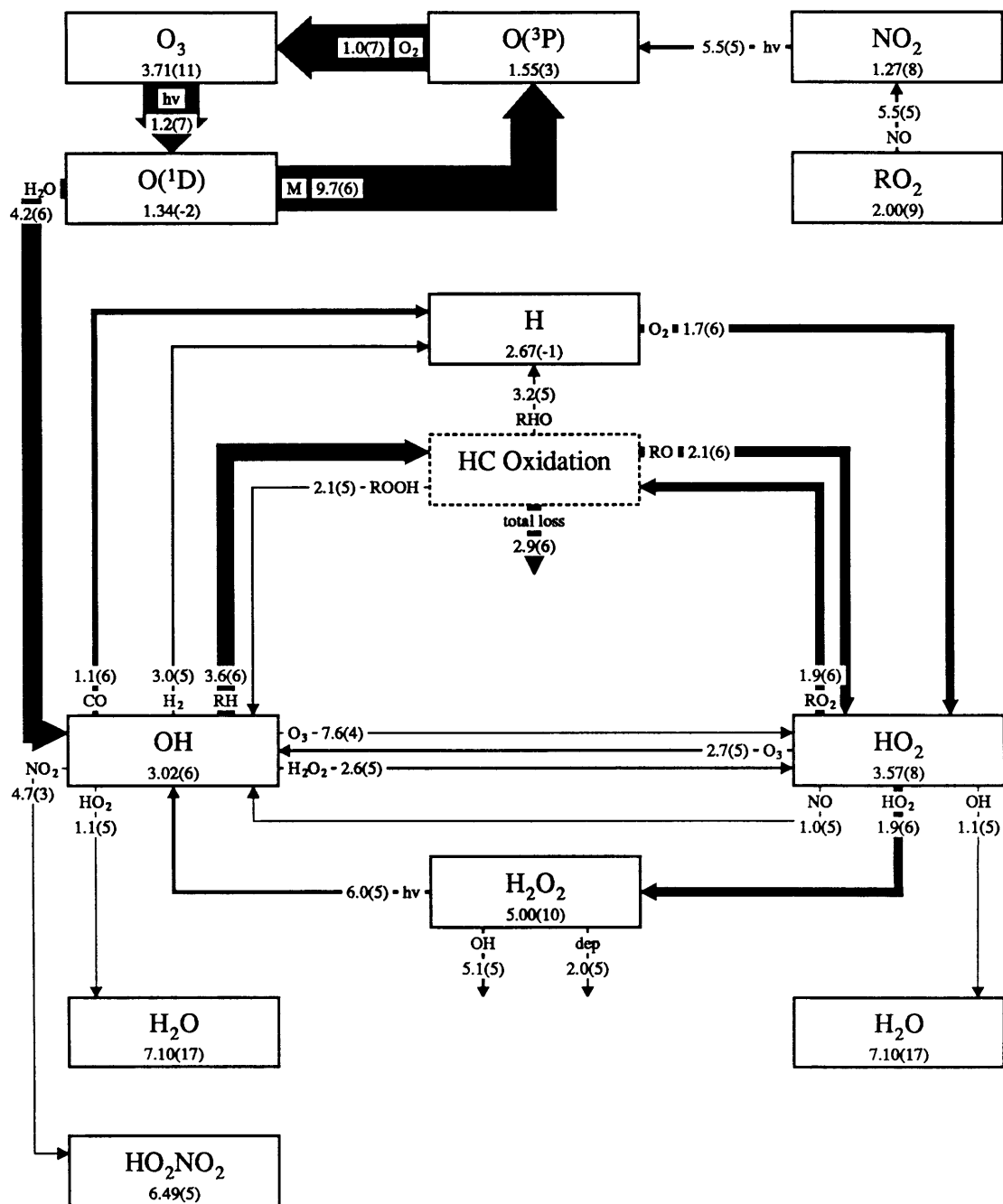


Figure 2.4.1. The odd-hydrogen cycle in the remote marine boundary layer. The case shown here is the “base case” adopted for this model at noon (see text). Numbers in the boxes are concentrations, in $\text{molec} \cdot \text{cm}^{-3}$, while the numbers in the arrows are reactive rates, in $\text{molec} \cdot \text{cm}^{-3} \text{sec}^{-1}$. “HC Oxidation” is the entire process for all hydrocarbons. Note that H_2O_2 is *not* in a steady state. The top half of the figure shows part of the odd oxygen chemistry, with only those reactions leading to odd oxygen formation or removal. For the roughly 15 ppbv of ozone shown here, photochemistry is a net odd oxygen sink (the reactive rate shown for $\text{O}(^1\text{D}) + \text{H}_2\text{O}$ is for odd hydrogen, which is twice the rate for odd oxygen).

peroxy free radicals (RO₂). The longer-lived reservoirs of odd hydrogen in the MBL are the peroxides: hydrogen peroxide (H₂O₂) and organic peroxides (ROOH). These can generally either photodissociate, closing the odd-hydrogen cycle by re-forming OH, or be permanently removed either through deposition or reaction with OH itself. Permanent peroxide removal is the major MBL odd-hydrogen sink. Hydrocarbon oxidation can potentially be either a net source or a net sink of odd-hydrogen; in the remote MBL, where there is very little NO_x, we find it to be a strong net odd-hydrogen sink. This is consistent with the findings in Crutzen (1979), and Logan *et al.* (1981) for methane in NO_x-poor environments.

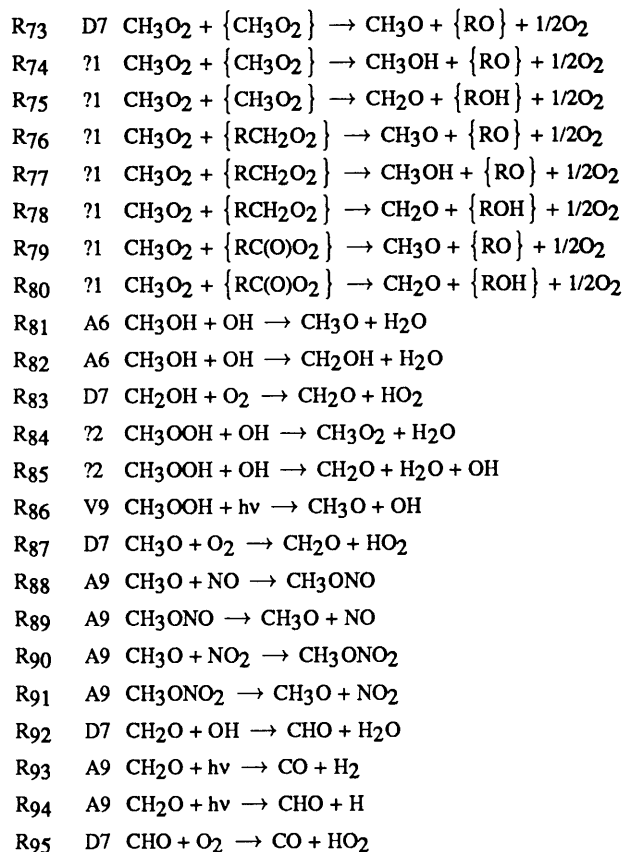
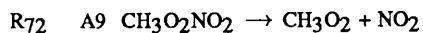
Table 2.4.1 Important reactions through ethene in the model.

| <u>Num</u> | <u>Ref</u> | <u>Reaction</u> | <u>Rate Constant</u> |
|-----------------|------------|---|--|
| R ₁ | D7 | O ₃ + hv → O ₂ + O(¹ D) | J ₁ = J(O ₃ - O(¹ D)) |
| R ₂ | D7 | O ₃ + hv → O ₂ + O(³ P) | J ₂ = J(O ₃ - O(³ P)) |
| R ₃ | A9 | O(¹ D) + N ₂ → O(³ P) + N ₂ | k ₃ = 1.8 × 10 ⁻¹¹ e ^{+107/T} |
| R ₄ | A9 | O(¹ D) + O ₂ → O(³ P) + O ₂ | k ₄ = 3.2 × 10 ⁻¹¹ e ^{+67/T} |
| R ₅ | A9 | O(¹ D) + H ₂ O → OH + OH | k ₅ = 2.2 × 10 ⁻¹⁰ |
| R ₆ | A9 | O(¹ D) + H ₂ O → O(³ P) + H ₂ O | k ₆ = 1.2 × 10 ⁻¹¹ |
| R ₇ | A9 | O(¹ D) + H ₂ O → H ₂ + O ₂ | k ₇ = 2.3 × 10 ⁻¹² |
| R ₈ | A9 | O(³ P) + O ₂ → O ₃ | I _{N28} = 5.7 × 10 ⁻³⁴ (T/300) ^{-2.8} I _{O28} = 6.2 × 10 ⁻³⁴ (T/300) ^{-2.0} k _{∞8} = 2.8 × 10 ⁻¹² F _{c8} = e ^{-T/696} |
| R ₉ | D7 | HO ₂ + O ₃ → OH + O ₂ + O ₂ | k ₉ = 1.1 × 10 ⁻¹⁴ e ^{-500/T} |
| R ₁₀ | N1 | H ₂ O ₂ + hv → OH + OH | J ₁₀ = J(H ₂ O ₂ - OH) |
| R ₁₁ | A9 | HO ₂ + NO → OH + NO ₂ | k ₁₁ = 3.7 × 10 ⁻¹² e ^{+240/T} |
| R ₁₂ | A9 | OH + H ₂ O ₂ → H ₂ O + HO ₂ | k ₁₂ = 2.9 × 10 ⁻¹² e ^{-160/T} |
| R ₁₃ | D7 | OH + HO ₂ → H ₂ O + O ₂ | k ₁₃ = 4.6 × 10 ⁻¹¹ e ^{+230/T} |
| R ₁₄ | A9 | OH + O ₃ → HO ₂ + O ₂ | k ₁₄ = 1.9 × 10 ⁻¹² e ^{-1000/T} |
| R ₁₅ | A9 | OH + CO → CO ₂ + H | k ₁₅ = 1.5 × 10 ⁻¹³ (1 + 0.59[M]/2.5 × 10 ¹⁹) |
| R ₁₆ | A9 | OH + NO ₂ → HONO ₂ | I _{N216} = 2.6 × 10 ⁻³⁰ (T/300) ^{-2.9} I _{O216} = 2.2 × 10 ⁻³⁰ (T/300) ^{-2.9} k _{∞16} = 5.2 × 10 ⁻¹¹ F _{c16} = e ^{-T/353} |
| R ₁₇ | A9 | HONO ₂ + hv → OH + NO ₂ | J ₁₇ = J(HONO ₂) |
| R ₁₈ | D7 | OH + HONO ₂ → H ₂ O + NO ₂ | k ₁₈ = k + {k ₃ [M]/{1 + k ₃ [M]/k ₂ }} k ₁ = 7.2 × 10 ⁻¹⁵ e ^{+785/T} k ₂ = 4.1 × 10 ⁻¹⁶ e ^{+1440/T} k ₃ = 1.9 × 10 ⁻³³ e ^{+725/T} |
| R ₁₉ | A9 | OH + NO → HONO | I _{N219} = 7.4 × 10 ⁻³¹ (T/300) ^{-2.4} I _{O219} = 7.4 × 10 ⁻³¹ (T/300) ^{-2.4} k _{∞19} = 1.0 × 10 ⁻¹¹ |

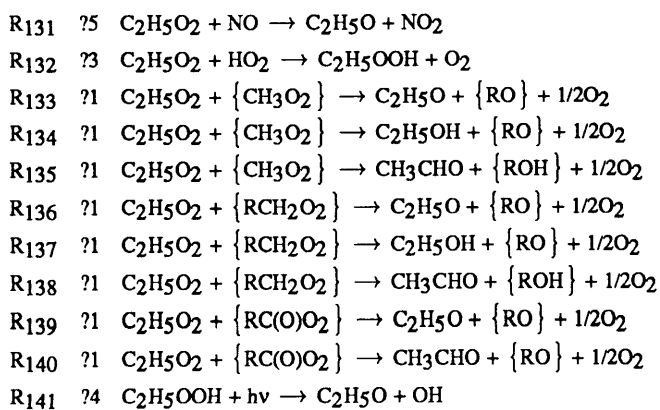
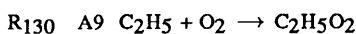
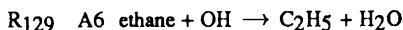
| | | | |
|-----|----|--|---|
| R20 | A9 | HONO + hv → OH + NO | $F_{c19} = e^{-T/1300}$ |
| R21 | D7 | OH + HONO → H ₂ O + NO ₂ | $J_{20} = J(\text{HONO})$ |
| R22 | D7 | OH + H ₂ → H ₂ O + H | $k_{21} = 1.8 \times 10^{-11} e^{-390/T}$ |
| R23 | D7 | H + O ₂ → HO ₂ | $k_{22} = 5.5 \times 10^{-12} e^{-2000/T}$ |
| | | | $l_{N_2 23} = 5.7 \times 10^{-32} (T/300)^{-1.6}$ |
| | | | $l_{O_2 23} = 5.7 \times 10^{-32} (T/300)^{-1.6}$ |
| | | | $k_{\infty 23} = 7.5 \times 10^{-11}$ |
| | | | $F_{c23} = e^{-T/502}$ |
| R24 | D7 | HO ₂ + HO ₂ → H ₂ O ₂ + O ₂ | $k_{24} = 2.3 \times 10^{-13} e^{+600/T}$ |
| | | | $k_{24} = k \cdot (1 + 7.4 \times 10^{-21} e^{+400/T} [M])$ |
| R25 | D7 | HO ₂ + HO ₂ + H ₂ O → H ₂ O ₂ + O ₂ + H ₂ O | $k_{25} = 3.2 \times 10^{-34} e^{+2800/T}$ |
| | | | $k_{25} = k \cdot (1 + 7.4 \times 10^{-21} e^{+400/T} [M])$ |
| R26 | D7 | HO ₂ + NO ₂ → HO ₂ NO ₂ | $l_{N_2 23} = 1.8 \times 10^{-31} (T/300)^{-3.2}$ |
| | | | $l_{O_2 26} = 1.8 \times 10^{-31} (T/300)^{-3.2}$ |
| | | | $k_{\infty 26} = 4.7 \times 10^{-12} (T/300)^{-1.4}$ |
| | | | $F_{c26} = e^{-T/517}$ |
| R27 | A9 | HO ₂ NO ₂ → HO ₂ + NO ₂ | $k_{oN_2 27} = 5.0 \times 10^{-6} e^{-10000/T}$ |
| | | | $k_{oO_2 27} = 3.6 \times 10^{-6} e^{-10000/T}$ |
| | | | $J_{\infty 27} = 3.4 \times 10^{+14} e^{-10420/T}$ |
| | | | $F_{c27} = e^{-T/517}$ |
| R28 | A9 | HO ₂ NO ₂ + hv → HO ₂ + NO ₂ | $J_{28} = J(\text{HO}_2\text{NO}_2)$ |
| R29 | A9 | O ₃ + NO → NO ₂ + O ₂ | $k_{29} = 1.8 \times 10^{-12} e^{-1370/T}$ |
| R30 | A9 | O ₃ + NO ₂ → O ₂ + NO ₃ | $k_{30} = 1.2 \times 10^{-13} e^{-2450/T}$ |
| R31 | D7 | NO + NO ₃ → NO ₂ + NO ₂ | $k_{31} = 1.7 \times 10^{-11} e^{+150/T}$ |
| R32 | D7 | NO ₂ + NO ₃ → N ₂ O ₅ | $l_{N_2 32} = 2.2 \times 10^{-30} (T/300)^{-4.3}$ |
| | | | $l_{O_2 32} = 2.2 \times 10^{-30} (T/300)^{-4.3}$ |
| | | | $k_{\infty 32} = 1.5 \times 10^{-12} (T/300)^{-0.5}$ |
| | | | $F_{c32} = e^{-T/280}$ |
| R33 | A9 | N ₂ O ₅ → NO ₂ + NO ₃ | $k_{oN_2 33} = 2.2 \times 10^{-3} (T/300)^{-4.4} e^{-11080/T}$ |
| | | | $k_{oO_2 33} = 2.2 \times 10^{-3} (T/300)^{-4.4} e^{-11080/T}$ |
| | | | $J_{\infty 33} = 9.7 \times 10^{+14} (T/300)^{+0.1} e^{-11080/T}$ |
| | | | $F_{c33} = e^{-T/280}$ |
| R34 | A9 | N ₂ O ₅ + hv → NO ₂ + NO ₃ | $J_{34} = J(\text{N}_2\text{O}_5)$ |
| R35 | A9 | NO ₂ + hv → NO + O(³ P) | $J_{35} = J(\text{NO}_2)$ |
| R36 | A9 | NO ₃ + hv → NO ₂ + O(³ P) | $J_{36} = J(\text{NO}_3 - \text{O})$ |
| R37 | A9 | NO ₃ + hv → NO + O ₂ | $J_{37} = J(\text{NO}_3 - \text{O}_2)$ |

Methane Chemistry

| | | | |
|-----|----|---|--|
| R67 | A9 | OH + methane → CH ₃ + H ₂ O | $k_{67} = 2.4 \times 10^{-12} e^{-1710/T}$ |
| R68 | D7 | CH ₃ + O ₂ → CH ₃ O ₂ | $l_{N_2 68} = 4.5 \times 10^{-31} (T/300)^{-2.0}$ |
| | | | $l_{O_2 68} = 4.5 \times 10^{-31} (T/300)^{-2.0}$ |
| | | | $k_{\infty 68} = 1.8 \times 10^{-12} (T/300)^{-2.0}$ |
| | | | $F_{c68} = e^{-T/446}$ |
| R69 | ?3 | CH ₃ O ₂ + HO ₂ → CH ₃ OOH + O ₂ | $k_{69} = 3.2 \times 10^{-12}$ |
| R70 | D7 | CH ₃ O ₂ + NO → CH ₃ O + NO ₂ | $k_{70} = 4.2 \times 10^{-12} e^{+180/T}$ |
| R71 | A9 | CH ₃ O ₂ + NO ₂ → CH ₃ O ₂ NO ₂ | $l_{N_2 71} = 2.3 \times 10^{-30} (T/300)^{-4.0}$ |
| | | | $l_{O_2 71} = 2.3 \times 10^{-30} (T/300)^{-4.0}$ |



Ethane Chemistry



$$k_{\infty 71} = 8.0 \times 10^{-12}$$

$$F_{c71} = e^{-T/327}$$

$$k_{\text{O}_2 72} = 9.0 \times 10^{-5} e^{-9690/T}$$

$$k_{\text{O}_2 72} = 9.0 \times 10^{-5} e^{-9690/T}$$

$$J_{\infty 72} = 1.6 \times 10^{+16} e^{-10560/T}$$

$$F_{c72} = 0.4$$

$$k_{73} = 4.8 \times 10^{-13}$$

$$k_{74} = 1.6 \times 10^{-13}$$

$$k_{75} = 1.6 \times 10^{-13}$$

$$k_{76} = 3.40 \times 10^{-13}$$

$$k_{77} = 1.13 \times 10^{-13}$$

$$k_{78} = 1.13 \times 10^{-13}$$

$$k_{79} = 1.39 \times 10^{-12}$$

$$k_{80} = 4.64 \times 10^{-13}$$

$$k_{81} = 1.7 \times 10^{-12} e^{-806/T}$$

$$k_{82} = 9.8 \times 10^{-12} e^{-806/T}$$

$$k_{83} = 9.6 \times 10^{-12}$$

$$k_{84} = 5.9 \times 10^{-12}$$

$$k_{85} = 2.9 \times 10^{-12} e^{(-900+712)/T}$$

$$J_{86} = J(\text{CH}_3\text{OOH})$$

$$k_{87} = 3.9 \times 10^{-14} e^{(-900/T)}$$

$$k_{88} = 2 \times 10^{-11}$$

$$k_{89} = 7.0 \times 10^{+16} e^{-20500/T}$$

$$k_{90} = 1.2 \times 10^{-11}$$

$$k_{91} = 1.7 \times 10^{+17} e^{-20125/T}$$

$$k_{92} = 1.0 \times 10^{-11}$$

$$J_{93} = J(\text{CH}_2\text{O} - \text{H}_2)$$

$$J_{94} = J(\text{CH}_2\text{O} - \text{H})$$

$$k_{95} = 3.5 \times 10^{-12} e^{+140/T}$$

$$k_{129} = 1.37 \times 10^{-17} T^2 e^{-444/T}$$

$$I_{\text{N}_2 130} = 2 \times 10^{-28} (T/300)^{-3.8}$$

$$I_{\text{O}_2 130} = 2 \times 10^{-28} (T/300)^{-3.8}$$

$$k_{\infty 130} = 5 \times 10^{-12}$$

$$F_{c130} = e^{-T/840}$$

$$k_{131} = 4.2 \times 10^{-12} e^{+180/T}$$

$$k_{132} = 3.2 \times 10^{-12}$$

$$k_{133} = 3.40 \times 10^{-13}$$

$$k_{134} = 1.13 \times 10^{-13}$$

$$k_{135} = 1.13 \times 10^{-13}$$

$$k_{136} = 2.40 \times 10^{-13}$$

$$k_{137} = 8.00 \times 10^{-14}$$

$$k_{138} = 8.00 \times 10^{-14}$$

$$k_{139} = 9.84 \times 10^{-13}$$

$$k_{140} = 3.28 \times 10^{-13}$$

$$J_{141} = J(\text{CH}_3\text{OOH})$$

| | | | |
|------------------|----|---|--|
| R ₁₄₂ | ?? | $C_2H_5OOH + OH \rightarrow C_2H_5O_2 + H_2O$ | $k_{142} = 5.9 \times 10^{-12}$ |
| R ₁₄₃ | ?? | $C_2H_5OOH + OH \rightarrow CH_3CHO + H_2O + OH$ | $k_{143} = 2.9 \times 10^{-12} e^{(-367+712)/T}$ |
| R ₁₄₄ | ?? | $C_2H_5O + O_2 \rightarrow CH_3CHO + HO_2$ | $k_{144} = 3.9 \times 10^{-14} e^{-900/T}$ |
| R ₁₄₅ | A9 | $CH_3CHO + hv \rightarrow \text{methane} + CO$ | $J_{145} = J(CH_3CHO - 2)$ |
| R ₁₄₆ | A9 | $CH_3CHO + hv \rightarrow CH_3 + CHO$ | $J_{146} = J(CH_3CHO - 1)$ |
| R ₁₄₇ | A9 | $CH_3CHO + hv \rightarrow CH_3CO + H$ | $J_{147} = J(CH_3CHO - 3)$ |
| R ₁₄₈ | A6 | $CH_3CHO + OH \rightarrow CH_3CO + H_2O$ | $k_{148} = 6.9 \times 10^{-12} e^{260/T}$ |
| R ₁₄₉ | ?? | $CH_3CO + O_2 \rightarrow CH_3C(O)O_2$ | $I_{N_2 149} = 4.5 \times 10^{-31} (T/300)^{-2.0}$ $I_{O_2 149} = 4.5 \times 10^{-31} (T/300)^{-2.0}$ $k_{\infty 149} = 1.8 \times 10^{-12} (T/300)^{-2.0}$ $F_{c149} = e^{-T/446}$ |
| R ₁₅₀ | ?? | $CH_3C(O)O_2 + HO_2 \rightarrow CH_3C(O)OOH + O_2$ | $k_{150} = 3.2 \times 10^{-12}$ |
| R ₁₅₁ | A9 | $CH_3C(O)O_2 + NO \rightarrow CH_3COO + NO_2$ | $k_{151} = 1.4 \times 10^{-11}$ |
| R ₁₅₂ | A9 | $CH_3C(O)O_2 + NO_2 \rightarrow CH_3C(O)O_2NO_2$ | $k_{152} = 6 \times 10^{-12}$ |
| R ₁₅₃ | ?1 | $CH_3C(O)O_2 + \{CH_3O_2\} \rightarrow CH_3COO + \{RO\} + 1/2O_2$ | $k_{153} = 1.39 \times 10^{-12}$ |
| R ₁₅₄ | ?1 | $CH_3C(O)O_2 + \{CH_3O_2\} \rightarrow CH_3C(O)OH + \{RO\} + 1/2O_2$ | $k_{154} = 4.64 \times 10^{-13}$ |
| R ₁₅₅ | ?1 | $CH_3C(O)O_2 + \{RCH_2O_2\} \rightarrow CH_3COO + \{RO\} + 1/2O_2$ | $k_{155} = 9.84 \times 10^{-13}$ |
| R ₁₅₆ | ?1 | $CH_3C(O)O_2 + \{RCH_2O_2\} \rightarrow CH_3C(O)OH + \{RO\} + 1/2O_2$ | $k_{156} = 3.28 \times 10^{-13}$ |
| R ₁₅₇ | ?1 | $CH_3C(O)O_2 + \{RC(O)O_2\} \rightarrow CH_3COO + \{RO\} + 1/2O_2$ | $k_{157} = 4.02 \times 10^{-12}$ |
| R ₁₅₈ | ?? | $CH_3COO \rightarrow CH_3 + CO_2$ | $k_{158} = 1 \times 10^{+7}$ |
| R ₁₅₉ | A9 | $CH_3C(O)O_2NO_2 \rightarrow CH_3C(O)O_2 + NO_2$ | $k_{159} = 1.12 \times 10^{+16} e^{-13330/T}$ |
| R ₁₆₀ | A9 | $CH_3C(O)O_2NO_2 + hv \rightarrow CH_3C(O)O_2 + NO_2$ | $J_{160} = J(PAN)$ |
| R ₁₆₁ | KS | $CH_3C(O)O_2NO_2 + OH \rightarrow CH_2O + CO_2 + NO_2 + H_2O$ | $k_{161} = 1.23 \times 10^{-12} e^{-651/T}$ |
| R ₁₆₂ | ?4 | $CH_3C(O)OOH + hv \rightarrow CH_3 + CO_2 + OH$ | $J_{162} = J(CH_3OOH)$ |
| R ₁₆₃ | ?2 | $CH_3C(O)OOH + OH \rightarrow CH_3C(O)O_2 + H_2O$ | $k_{163} = 5.9 \times 10^{-12}$ |
| R ₁₆₄ | A6 | $C_2H_5OH + OH \rightarrow CH_3CHOH + H_2O$ | $k_{164} = 2.9 \times 10^{-12} e^{-84/T}$ |
| R ₁₆₅ | A6 | $C_2H_5OH + OH \rightarrow HOC_2H_4 + H_2O$ | $k_{165} = 2.9 \times 10^{-12} e^{-430/T}$ |
| R ₁₆₆ | ?? | $CH_3CHOH + O_2 \rightarrow CH_3CHO + HO_2$ | $k_{166} = 9.6 \times 10^{-12}$ |

Ethene Chemistry

| | | | |
|------------------|----|---|--|
| R ₁₆₇ | A6 | $\text{ethene} + OH \rightarrow HOC_2H_4$ | $k_{167} = 2.15 \times 10^{-12} e^{+411/T}$ |
| R ₁₆₈ | ?? | $HOC_2H_4 + O_2 \rightarrow HOC_2H_4O_2$ | $k_{168} = 1 \times 10^{-12}$ |
| R ₁₆₉ | ?5 | $HOC_2H_4O_2 + NO \rightarrow HOC_2H_4O + NO_2$ | $k_{169} = 4.2 \times 10^{-12} e^{+180/T}$ |
| R ₁₇₀ | ?3 | $HOC_2H_4O_2 + HO_2 \rightarrow HOC_2H_4OOH + O_2$ | $k_{170} = 3.2 \times 10^{-12}$ |
| R ₁₇₁ | ?1 | $HOC_2H_4O_2 + \{CH_3O_2\} \rightarrow HOC_2H_4O + \{RO\} + 1/2O_2$ | $k_{171} = 3.40 \times 10^{-13}$ |
| R ₁₇₂ | ?1 | $HOC_2H_4O_2 + \{CH_3O_2\} \rightarrow HOC_2H_4OH + \{RO\} + 1/2O_2$ | $k_{172} = 1.13 \times 10^{-13}$ |
| R ₁₇₃ | ?1 | $HOC_2H_4O_2 + \{CH_3O_2\} \rightarrow HOCH_2CHO + \{ROH\} + 1/2O_2$ | $k_{173} = 1.13 \times 10^{-13}$ |
| R ₁₇₄ | ?1 | $HOC_2H_4O_2 + \{RCH_2O_2\} \rightarrow HOC_2H_4O + \{RO\} + 1/2O_2$ | $k_{174} = 2.40 \times 10^{-13}$ |
| R ₁₇₅ | ?1 | $HOC_2H_4O_2 + \{RCH_2O_2\} \rightarrow HOC_2H_4OH + \{RO\} + 1/2O_2$ | $k_{175} = 8.00 \times 10^{-14}$ |
| R ₁₇₆ | ?1 | $HOC_2H_4O_2 + \{RCH_2O_2\} \rightarrow HOCH_2CHO + \{ROH\} + 1/2O_2$ | $k_{176} = 8.00 \times 10^{-14}$ |
| R ₁₇₇ | ?1 | $HOC_2H_4O_2 + \{RC(O)O_2\} \rightarrow HOC_2H_4O + \{RO\} + 1/2O_2$ | $k_{177} = 9.84 \times 10^{-13}$ |
| R ₁₇₈ | ?1 | $HOC_2H_4O_2 + \{RC(O)O_2\} \rightarrow HOCH_2CHO + \{ROH\} + 1/2O_2$ | $k_{178} = 3.28 \times 10^{-13}$ |
| R ₁₇₉ | A6 | $HOC_2H_4OH + OH \rightarrow HOCH_2CHOH + H_2O$ | $k_{179} = 7.7 \times 10^{-12}$ |
| R ₁₈₀ | A6 | $HOCH_2CHOH + O_2 \rightarrow HOCH_2CHO + HO_2$ | $k_{180} = 9.6 \times 10^{-12}$ |
| R ₁₈₁ | ?4 | $HOC_2H_4OOH + hv \rightarrow HOC_2H_4O + OH$ | $J_{181} = J(CH_3OOH)$ |
| R ₁₈₂ | ?2 | $HOC_2H_4OOH + OH \rightarrow HOC_2H_4O_2 + H_2O$ | $k_{182} = 5.9 \times 10^{-12}$ |
| R ₁₈₃ | ?2 | $HOC_2H_4OOH + OH \rightarrow HOCH_2CHO + OH + H_2O$ | $k_{183} = 2.9 \times 10^{-12} e^{(-291+712)/T}$ |

| | | | |
|------|----|---|--|
| R184 | ?? | $\text{HOC}_2\text{H}_4\text{OOH} + \text{OH} \rightarrow \text{HOCHCH}_2\text{OOH} + \text{H}_2\text{O}$ | $k_{184} = 2.9 \times 10^{-12} e^{+74/T}$ |
| R185 | KS | $\text{HOC}_2\text{H}_4\text{O} \rightarrow \text{CH}_2\text{OH} + \text{CH}_2\text{O}$ | $k_{185} = 1.4 \times 10^{+5}$ |
| R186 | CA | $\text{HOC}_2\text{H}_4\text{O} + \text{O}_2 \rightarrow \text{HOCH}_2\text{CHO} + \text{HO}_2$ | $k_{186} = 7.4 \times 10^{-15}$ |
| R187 | ?? | $\text{HOCH}_2\text{CHO} + h\nu \rightarrow \text{CH}_3\text{OH} + \text{CO}$ | $J_{187} = J(\text{CH}_3\text{CHO} - 2)$ |
| R188 | ?? | $\text{HOCH}_2\text{CHO} + h\nu \rightarrow \text{CH}_2\text{OH} + \text{CHO}$ | $J_{188} = J(\text{CH}_3\text{CHO} - 1)$ |
| R189 | A7 | $\text{HOCH}_2\text{CHO} + \text{OH} \rightarrow \text{HOCH}_2\text{CO} + \text{H}_2\text{O}$ | $k_{189} = 2.1 \times 10^{-11}$ |
| R190 | ?? | $\text{HOCH}_2\text{CO} + \text{O}_2 \rightarrow \text{HOCH}_2\text{C(O)O}_2$ | $k_{190} = 2 \times 10^{-12}$ |
| R191 | ?3 | $\text{HOCH}_2\text{C(O)O}_2 + \text{HO}_2 \rightarrow \text{HOCH}_2\text{C(O)OOH}$ | $k_{191} = 3.2 \times 10^{-12}$ |
| R192 | N1 | $\text{HOCH}_2\text{CO} + \text{O}_2 \rightarrow \text{HOCH}_2\text{C(O)O}_2$ | $k_{192} = 2 \times 10^{-12}$ |
| R193 | KS | $\text{HOCH}_2\text{C(O)O}_2 + \text{NO}_2 \rightarrow \text{HOCH}_2\text{C(O)O}_2\text{NO}_2$ | $k_{193} = 4.7 \times 10^{-12}$ |
| R194 | ?5 | $\text{HOCH}_2\text{C(O)O}_2 + \text{NO} \rightarrow \text{HOCH}_2\text{COO} + \text{NO}_2$ | $k_{194} = 4.2 \times 10^{-12} e^{+180/T}$ |
| R195 | ?1 | $\text{HOCH}_2\text{C(O)O}_2 + \{\text{CH}_3\text{O}_2\} \rightarrow \text{HOCH}_2\text{COO} + \{\text{RO}\} + 1/2\text{O}_2$ | $k_{195} = 1.39 \times 10^{-12}$ |
| R196 | ?1 | $\text{HOCH}_2\text{C(O)O}_2 + \{\text{CH}_3\text{O}_2\} \rightarrow \text{HOCH}_2\text{C(O)OH} + \{\text{ROH}\} + 1/2\text{O}_2$ | $k_{196} = 4.64 \times 10^{-13}$ |
| R197 | ?1 | $\text{HOCH}_2\text{C(O)O}_2 + \{\text{RCH}_2\text{O}_2\} \rightarrow \text{HOCH}_2\text{COO} + \{\text{RO}\} + 1/2\text{O}_2$ | $k_{197} = 9.84 \times 10^{-13}$ |
| R198 | ?1 | $\text{HOCH}_2\text{C(O)O}_2 + \{\text{RCH}_2\text{O}_2\} \rightarrow \text{HOCH}_2\text{COO} + \{\text{ROH}\} + 1/2\text{O}_2$ | $k_{198} = 3.28 \times 10^{-13}$ |
| R199 | ?1 | $\text{HOCH}_2\text{C(O)O}_2 + \{\text{RC(O)O}_2\} \rightarrow \text{HOCH}_2\text{COO} + \{\text{RO}\} + 1/2\text{O}_2$ | $k_{199} = 4.02 \times 10^{-12}$ |
| R200 | EA | $\text{HOCH}_2\text{C(O)OH} + \text{OH} \rightarrow \text{CH}_2\text{OH} + \text{CO}_2 + \text{HO}_2$ | $k_{200} = 1.3 \times 10^{-12} e^{-170/T}$ |
| R201 | ?? | $\text{HOCH}_2\text{COO} \rightarrow \text{CH}_2\text{OH} + \text{CO}_2$ | $k_{201} = 1 \times 10^{+7}$ |
| R202 | ?? | $\text{HOCH}_2\text{C(O)OOH} + h\nu \rightarrow \text{CH}_2\text{OH} + \text{CO}_2 + \text{OH}$ | $J_{202} = J(\text{CH}_3\text{OOH})$ |
| R203 | ?2 | $\text{HOCH}_2\text{C(O)OOH} + \text{OH} \rightarrow \text{HOCH}_2\text{C(O)O}_2 + \text{H}_2\text{O}$ | $k_{203} = 5.9 \times 10^{-12}$ |
| R204 | ?A | $\text{HOCH}_2\text{C(O)OOH} + \text{OH} \rightarrow \text{HOCHC(O)OOH} + \text{H}_2\text{O}$ | $k_{204} = 2.9 \times 10^{-12}$ |
| R205 | ?N | $\text{HOCHC(O)OOH} + \text{O}_2 \rightarrow \text{CHO} + \text{CO}_2 + \text{OH} + \text{HO}_2$ | $k_{205} = 1.9 \times 10^{-15} e^{-900/T}$ |
| R206 | KS | $\text{HOCH}_2\text{C(O)O}_2\text{NO}_2 \rightarrow \text{HOCH}_2\text{C(O)O}_2 + \text{NO}_2$ | $k_{206} = 1.1 \times 10^{+16} e^{-13330/T}$ |
| R207 | ?5 | $\text{HOCH}_2\text{C(O)O}_2\text{NO}_2 + \text{OH} \rightarrow \text{CH}_2\text{O} + \text{CO}_2 + \text{NO}_3 + \text{H}_2\text{O}$ | $k_{207} = 2.9 \times 10^{-12}$ |
| R208 | ?? | $\text{HOCHCH}_2\text{OOH} + \text{O}_2 \rightarrow \text{OCHCH}_2\text{OOH} + \text{HO}_2$ | $k_{208} = 1 \times 10^{-12}$ |
| R209 | ?? | $\text{OCHCH}_2\text{OOH} + h\nu \rightarrow \text{CHO} + \text{CH}_2\text{O} + \text{OH}$ | $J_{209} = J(\text{CH}_3\text{CHO} - 1)$ |
| R210 | ?? | $\text{OCHCH}_2\text{OOH} + h\nu \rightarrow \text{CHO} + \text{CH}_2\text{O} + \text{OH}$ | $J_{210} = J(\text{CH}_3\text{OOH})$ |
| R211 | ?2 | $\text{OCHCH}_2\text{OOH} + \text{OH} \rightarrow \text{OCHCH}_2\text{O}_2 + \text{H}_2\text{O}$ | $k_{211} = 5.9 \times 10^{-12}$ |
| R212 | ?2 | $\text{OCHCH}_2\text{OOH} + \text{OH} \rightarrow \text{OCHCHO} + \text{H}_2\text{O} + \text{OH}$ | $k_{212} = 2.9 \times 10^{-12} e^{(-449+712)/T}$ |
| R213 | ?2 | $\text{OCHCH}_2\text{OOH} + \text{OH} \rightarrow \text{OCCH}_2\text{OOH} + \text{H}_2\text{O}$ | $k_{213} = 1.3 \times 10^{-12} e^{+835/T}$ |
| R214 | ?3 | $\text{OCHCH}_2\text{O}_2 + \text{HO}_2 \rightarrow \text{OCHCH}_2\text{OOH} + \text{O}_2$ | $k_{214} = 3.2 \times 10^{-12}$ |
| R215 | ?5 | $\text{OCHCH}_2\text{O}_2 + \text{NO} \rightarrow \text{OCHCH}_2\text{O} + \text{NO}_2$ | $k_{215} = 4.2 \times 10^{-12} e^{+180/T}$ |
| R216 | ?1 | $\text{OCHCH}_2\text{O}_2 + \{\text{CH}_3\text{O}_2\} \rightarrow \text{OCHCH}_2\text{O} + \{\text{RO}\} + 1/2\text{O}_2$ | $k_{216} = 3.40 \times 10^{-13}$ |
| R217 | ?1 | $\text{OCHCH}_2\text{O}_2 + \{\text{CH}_3\text{O}_2\} \rightarrow \text{HOCH}_2\text{CHO} + \{\text{RO}\} + 1/2\text{O}_2$ | $k_{217} = 1.13 \times 10^{-13}$ |
| R218 | ?1 | $\text{OCHCH}_2\text{O}_2 + \{\text{CH}_3\text{O}_2\} \rightarrow \text{OCHCHO} + \{\text{ROH}\} + 1/2\text{O}_2$ | $k_{218} = 1.13 \times 10^{-13}$ |
| R219 | ?1 | $\text{OCHCH}_2\text{O}_2 + \{\text{RCH}_2\text{O}_2\} \rightarrow \text{OCHCH}_2\text{O} + \{\text{RO}\} + 1/2\text{O}_2$ | $k_{219} = 2.40 \times 10^{-13}$ |
| R220 | ?1 | $\text{OCHCH}_2\text{O}_2 + \{\text{RCH}_2\text{O}_2\} \rightarrow \text{HOCH}_2\text{CHO} + \{\text{RO}\} + 1/2\text{O}_2$ | $k_{220} = 8.00 \times 10^{-14}$ |
| R221 | ?1 | $\text{OCHCH}_2\text{O}_2 + \{\text{RCH}_2\text{O}_2\} \rightarrow \text{OCHCHO} + \{\text{ROH}\} + 1/2\text{O}_2$ | $k_{221} = 8.00 \times 10^{-14}$ |
| R222 | ?1 | $\text{OCHCH}_2\text{O}_2 + \{\text{RC(O)O}_2\} \rightarrow \text{OCHCH}_2\text{O} + \{\text{RO}\} + 1/2\text{O}_2$ | $k_{222} = 9.84 \times 10^{-13}$ |
| R223 | ?1 | $\text{OCHCH}_2\text{O}_2 + \{\text{RC(O)O}_2\} \rightarrow \text{OCHCHO} + \{\text{ROH}\} + 1/2\text{O}_2$ | $k_{223} = 3.28 \times 10^{-13}$ |
| R224 | ?? | $\text{OCHCH}_2\text{O} \rightarrow \text{CHO} + \text{CH}_2\text{O}$ | $k_{224} = 1 \times 10^{+7}$ |
| R225 | P3 | $\text{OCHCHO} + h\nu \rightarrow \text{CHO} + \text{CHO}$ | $J_{225} = 8 \times 10^{-3} J(\text{NO}_2)$ |
| R226 | P3 | $\text{OCHCHO} + \text{OH} \rightarrow \text{CO} + \text{CHO} + \text{H}_2\text{O}$ | $k_{226} = 2.2 \times 10^{-12} e^{+500/T}$ |
| R227 | ?? | $\text{OCCH}_2\text{OOH} \rightarrow \text{CO} + \text{CH}_2\text{O} + \text{OH}$ | $k_{227} = 1 \times 10^{+5}$ |
| R228 | A4 | $\text{ethene} + \text{O}_3 \rightarrow \text{CH}_2\text{OO} + \text{CH}_2\text{O}$ | $k_{228} = 2.63 \times 10^{-14} e^{-2830/T}$ |
| R229 | A4 | $\text{CH}_2\text{OO} \rightarrow \text{CH}_2\text{O}_2$ | $k_{229} = 4.0 \times 10^{+3}$ |

| | | | |
|------|----|--|---|
| R230 | A4 | $\text{CH}_2\text{OO} \rightarrow \text{CO} + \text{H}_2\text{O}$ | $k_{230} = 4.2 \times 10^{+3}$ |
| R231 | A4 | $\text{CH}_2\text{OO} \rightarrow \text{CO}_2 + \text{H}_2$ | $k_{231} = 1.2 \times 10^{+3}$ |
| R232 | A4 | $\text{CH}_2\text{OO} \rightarrow \text{CHO}_2 + \text{H}$ | $k_{232} = 6 \times 10^{+2}$ |
| R233 | A4 | $\text{CHO}_2 + \text{O}_2 \rightarrow \text{CO}_2 + \text{HO}_2$ | $k_{233} = 2 \times 10^{-11}$ |
| R234 | A4 | $\text{CH}_2\text{O}_2 + \text{H}_2\text{O} \rightarrow \text{HC(O)OH}$ | $k_{234} = 1 \times 10^{-17}$ |
| R235 | D8 | $\text{HC(O)OH} + \text{OH} \rightarrow \text{H}_2\text{O} + \text{CO}_2 + \text{H}$ | $k_{235} = 3.6 \times 10^{-13} e^{-77/T}$ |

The references are as follows: A9 : Atkinson *et al.* 1989; D7 : DeMore *et al.* , 1987; A6 : Atkinson, 1986; KS : Kasting and Singh, 1986; P3 : Plum *et al.* , 1983; V9 : Vaghjiani and Ravishankara, 1989a; ?1 : RO₂ self reactions (see text); ?2 : ROOH + OH (see text); ?3 : RO₂ + HO₂ (see text); ?4 : ROOH + hv (see text); ?5 : RO₂ + NO (see text). Note that rate constants with a sum for an activation energy have been estimated based on Atkinson (1987). 3-body reactions are treated according to A9. Units are sec⁻¹ for j's, cm³sec⁻¹ for k's and cm⁶sec⁻¹ for l's. Species enclosed in brackets ({---}) denote reactive families (see text) and are not included in the stoichiometry of the relevant reactions.

We have attempted to construct hydrocarbon oxidation sequences which are as complete as possible, allowing for multiple oxidation channels where such may exist. Because of this, some of the pathways considered involve poorly-known reactions and rate constants. We will show that OH is far more sensitive to the total NMHC flux than to uncertainties in any specific mechanisms and rates in our model. However, this uncertain chemistry does limit our ability to model and understand in detail the MBL chemistry, especially our ability to predict the abundances and identities of the eventual hydrocarbon oxidation products.

Our oxidation pathways for C₂–C₆ alkanes and alkenes in the absence of significant odd-nitrogen levels draw on the work of Aikin *et al.* (1982), Kasting and Singh (1986), and Calvert and Madronich (1988), as well as available reviews directed toward polluted air containing high odd-nitrogen levels (Atkinson and Lloyd, 1984; Carter and Atkinson, 1985; Leone and Seinfeld, 1985). The task is complicated because the OH-substituted oxidation products of unsaturated hydrocarbons have received very little experimental attention. Following Carter and Atkinson (1985) we generally treat these latter compounds as if they were their non-OH substituted equivalents. For other reactions which lack experimental data we have used rate constants from analogous reactions, adjusting them for differences between the studied and actual reactions if a clear technique is available (specifically, for OH abstraction reactions we follow Atkinson, 1987, and for RO₂ self reactions we follow Calvert and Madronich, 1987, and Madronich and Calvert, 1988).

Organo-peroxy RO₂ radicals are almost certainly the immediate products of either OH- or Cl- initiated hydrocarbon oxidation (Calvert and Madronich, 1987; Calvert, 1987). One of the major differences between NO_x-rich and NO_x-poor environments is the fate in each case

of these RO₂ radicals (Logan *et al.*, 1981, Kasting and Singh, 1986). In addition to reacting with NO to form RO radicals and with NO₂ to form organic nitrates (the dominant pathways in more polluted conditions), RO₂ can react with HO₂ to form organic hydroperoxides (DeMore *et al.*, 1987), and with RO₂ to form RO radicals, alcohols, and carbonyl compounds, including organic acids (Calvert and Madronich, 1987). At low NMHC levels, the reaction with HO₂ is expected to dominate, while at higher NMHC levels the RO₂ self reactions may gain prominence. Finally, RO₂ radicals are generally long enough lived (~ 1000 sec) that they can collide with several aerosol particles before reacting in the gas phase. For example, assuming an MBL aerosol of 1 micron radius and a particle concentration of 10 molec cm⁻³ (Houghton, 1985), an RO₂ radical should generally encounter an aerosol every 100 seconds. If the aerosol chemistry resembles that of a cloud drop, this will be of no consequence, as RO₂ radicals have a low solubility in water and will not remain in a drop long enough for aqueous reactions to compete with homogeneous gas-phase reactions, even in the extreme case of a marine cloud (Jacob, 1987). If RO₂ radicals are far more soluble in the MBL aerosol than in water, heterogeneous RO₂ removal could be important. In addition, the observed importance of water in the HO₂+HO₂ self-reaction (DeMore *et al.*, 1987) should serve as a warning that even the homogeneous chemistry of the RO₂ radicals may have some surprises in store. In this model we will focus on known homogeneous gas-phase RO₂ removal, though we feel that heterogeneous RO₂ removal on marine aerosols may well deserve more attention.

To summarize, RO₂ can undergo the following reactions in our model:



We divide the RO₂ radicals into 5 separate families, according to the scheme of Madronich and Calvert (1988): CH₃O₂, primary peroxy radicals such as CH₃CH₂O₂, secondary and tertiary peroxy radicals, and finally peroxy acyl radicals such as the peroxy acetyl radical, CH₃C(O)O₂. A scheme very similar to this is described in Madronich and Calvert (1990).

These families are used to simplify the model. In particular, in reaction (2.4.4) instead of reacting with individual RO₂ radicals, an RO₂ radical will react with the five families, the concentration of each family being the sum of the concentrations of its member compounds. Reactions R₇₃ through R₈₀ in Table 2.4.1 are an example of this. Reaction (2.4.1) is assumed to be identical for all RO₂ radicals, and two rates are considered:

$$k_{2.4.1a} = 3.2 \times 10^{-12}.$$

$$k_{2.4.1b} = 7.7 \times 10^{-14} e^{(+1300/T)}$$

$$= 5.9 \times 10^{-12} \text{ at 300K}$$

These cover the range of current measurements (Cox and Tyndall, 1980; Kurylo *et al.*, 1987; Daugut *et al.*, 1987; and McAdam *et al.*, 1987) and reflect the large uncertainty in this rate. Reaction 2.4.2 is also assumed to have the same rate for all RO₂, equal to the rate for CH₃O₂ (Atkinson *et al.*, 1989) unless direct measurements suggest otherwise (e.g. for CH₃C(O)O₂):

$$k_{2.4.2} = 4.2 \times 10^{-12} e^{(+180/T)}$$

$$= 7.6 \times 10^{-12} \text{ at 300K}$$

Because NO is so scarce in the remote MBL, we do not consider an additive pathway for reaction (2.4.3). Reaction (2.4.4) potentially has 3 channels if the oxygenated carbon on each reacting RO₂ radical also has a hydrogen (which must be given up for channels b and/or c). Following Madronich and Calvert (1988) we estimate the rate constant $k_{2.4.4(m,n)}$ for a member of the RO₂ family m reacting with the RO₂ family n , using the formula $k_{2.4.4(m,n)} = (k_{2.4.4(m,m)} \cdot k_{2.4.4(n,n)})^{1/2}$, where,

$$k_{2.4.4(0,0)} = 8.0 \times 10^{-13},$$

$$k_{2.4.4(1,1)} = 4.0 \times 10^{-13},$$

$$k_{2.4.4(2,2)} = 1.6 \times 10^{-15},$$

$$k_{2.4.4(3,3)} = 7.5 \times 10^{-17}, \text{ and}$$

$$k_{2.4.4(4,4)} = 6.7 \times 10^{-12}.$$

For branching ratios we take $R_a = 0.6$ (always), $R_b = 0.2$ (if allowed), and $R_c = 0.2$ (if allowed). For these purposes, we do *not* require that the sum of the branching ratios be unity; if pathways are not allowed, the reaction will simply run slower than an analogous reaction with all pathways allowed. This produces rate constants consistent with those recommended

by Madronich and Calvert (1988). Note that $k_{2.4.4(0,0)}$ is *not* the actual rate constant for the reaction

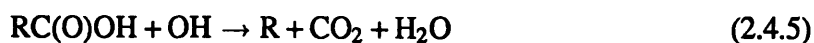


for which $k = 4.0 \times 10^{-13}$ (Atkinson *et al.*, 1989), but twice that rate. This is because our scheme treats the reacting radical as separate from the family with which it reacts, whether or not the specific radical is in that family. Our branching ratios and products are consistent with Calvert and Madronich (1987). In particular, we do not consider a channel forming ROOR', as suggested by DeMore *et al.*, 1987; such a channel could be included in the scheme, but there is not currently enough evidence to warrant its inclusion. In the "base-case" reaction set we omit all RO₂ + RO₂ reactions involving secondary and tertiary RO₂ families, which are too slow to compete with the others listed (except when a secondary or tertiary RO₂ is being treated explicitly). RO₂ reactions do play a major role in the model, and to help assess the largest possible error due to poorly known rate constants we have considered the pathological case in which all of the RO₂ radicals react rapidly (all the $k_{2.4.4(n,n)}$ were taken to be either 8.0×10^{-13} , $n = 0, 1, 2$ or 6.7×10^{-12} , $n = 3, 4$). The effect on diurnally averaged OH is only about 10%.

In NO_x-poor environments, a large portion of the RO₂ radicals may proceed to react with HO₂ to form organic peroxides, ROOH. These organic peroxides can be photodissociated, splitting into an RO and an OH radical, they can react with OH in at least two ways (removal by OH of the terminal OOH hydrogen or abstraction by OH of a hydrogen on the adjacent carbon group), and they can be removed by deposition to the ocean surface. For the ROOH UV cross-sections we use the recent results of Vaghjiani and Ravishankara (1989a), which are qualitatively similar to but ~ 25% lower than those of Molina and Arguello (1979). This cross-section for methyl hydroperoxide is applied to all ROOH. Two studies of the CH₃OOH + OH reaction have been published (Niki *et al.* 1978, Vaghjiani and Ravishankara, 1989b), in addition to one of t-butyl hydroperoxide (Anastasi *et al.*, 1978) (which should have only one fast pathway, the terminal OOH hydrogen abstraction). All three studies agree to within a factor of 2 on abstraction from the OOH group (5.7×10^{-12} , 3.7×10^{-12} , and 3.0×10^{-12} , respectively), with considerably better agreement between the second two studies (which are both absolute measurements). Niki *et al.* (1975) and Vaghjiani and Ravishankara (1989b) differ by more than a factor of 2 on the methyl group abstraction

rate ($4.3 \times 10^{-12} \text{ cm}^3 \text{ sec}^{-1}$ compared to 1.8×10^{-12}). The former rate (based on relative determination in a complicated chemical system) is extraordinarily fast for hydrogen abstraction from a methyl group (Atkinson, 1987), and in addition the latter results are based on an absolute technique. We therefore use the results of Vaghjiani and Ravishankara (1989) and the method of Atkinson (1987) to define rate constants for all abstraction reactions involving an OOH group.

With these considerations, we have constructed oxidation sequences for the $C_2 - C_6$ hydrocarbons. All of the sequences follow a similar pattern, shown in Figure 2.4.2. The sizes of the flux arrows in this figure are illustrative. One can easily see the central importance of the RO_2 radicals, as well as the emergence of ROOH when NO_x levels drop. The oxidation sequences differ in their relative strengths for certain reactions and in the occasional opening up of parallel pathways. Several processes lead to carbonyl compound formation, including organic acids, which are indicated as "O = R'" in Figure 2.4.2. O = R' can generally be fed back into the chemistry as base compounds, RH, with abstractable hydrogens (and, of course, with other sinks, such as deposition and photolysis). When organic acids are formed, we assume two dominant sinks: deposition and reaction with OH



We know of measured rate constants for formic, acetic, propionic and i-butyric acids (Dagaut *et al.*, 1988). We apply the rate for propionic acid to all C_3 organic acids and the i-butyric rate to all heavier acids.

Ozone is also an NMHC sink, and we adopt the mechanism ($R_{228} - R_{235}$ in Table 2.4.1) suggested in Atkinson and Carter (1984). Particularly noteworthy is the production of odd-hydrogen in this mechanism. Both OH and H are produced with 20 - 25% yield. This produces odd hydrogen at night in our model.

We have assembled a relatively complete set of reactions for hydrocarbons through C_4 . We also include simplified reaction sequences for 2 - pentene and 2 - hexene, which we choose to represent all of the C_5 and C_6 alkenes, while all alkanes heavier than the butanes are treated as if they were a butane. By treating all of the butene isomers we can examine the influence of the different isomers on MBL chemistry (remembering that measurements of specific alkene isomers are not yet available) without having to include all of the heavier

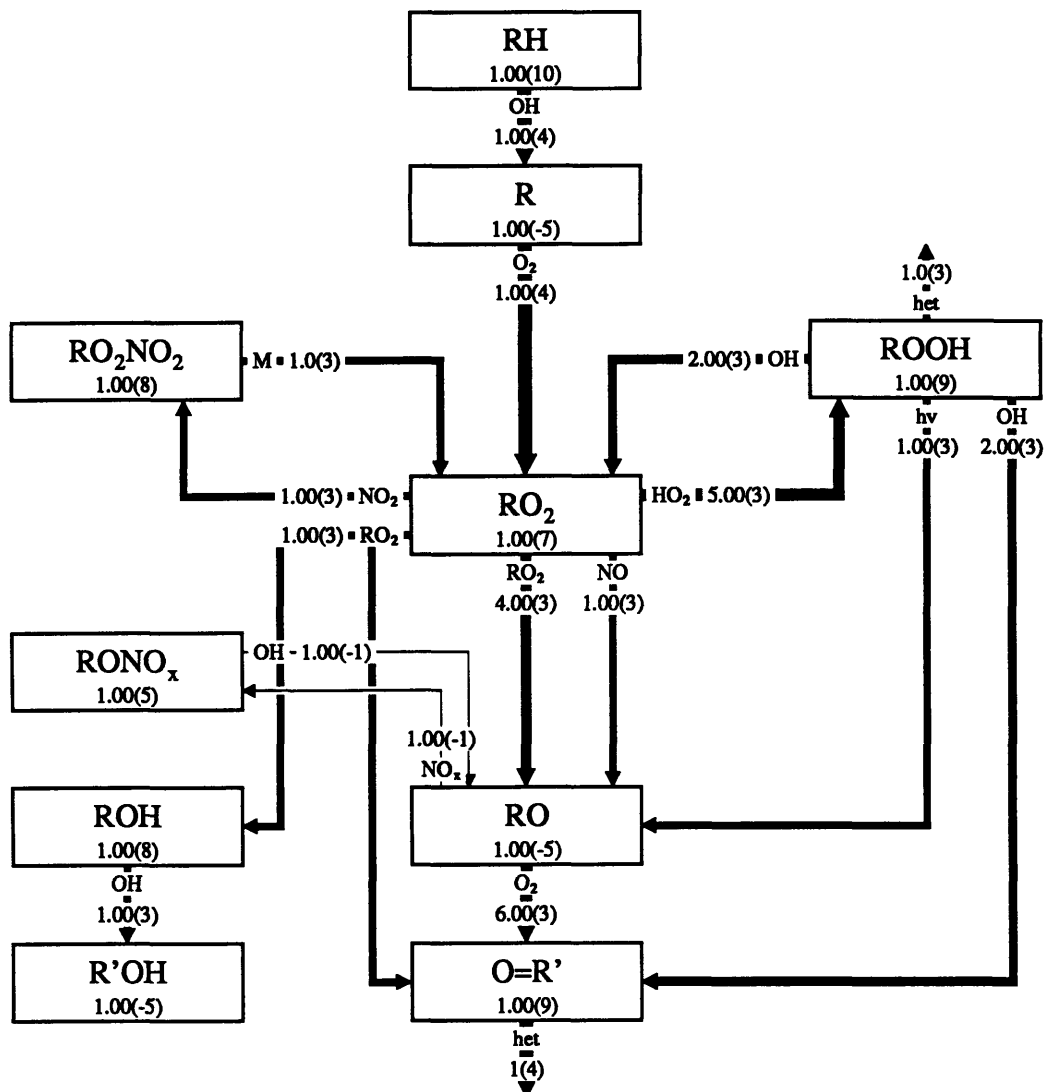


Figure 2.4.2. The basic hydrocarbon oxidation pattern used in this model. Reactive rates here are illustrative. We emphasize the central role of RO₂.

alkene isomers. The full reaction set contains 752 reactions, (see Appendix 1) and in Table 2.4.1 we show the reaction set through ethene. Figure 2.4.3 graphically shows the chemistry initiated by OH addition to the central carbon of propene, with noon-time reactive rates from our “base-case” simulation described later (Section 2.5).

Despite the greater complexity, the modeling uncertainty is not vastly greater for a heavy hydrocarbon like hexene than it is for the lighter ethene. In neither case are very many rate constants past the initial OH reaction known directly, and the basic assumptions leading to our estimations of the needed rate constants are the same for each. The complete hexene oxidation sequence, including the reactions of all of the eventual products, is certainly much

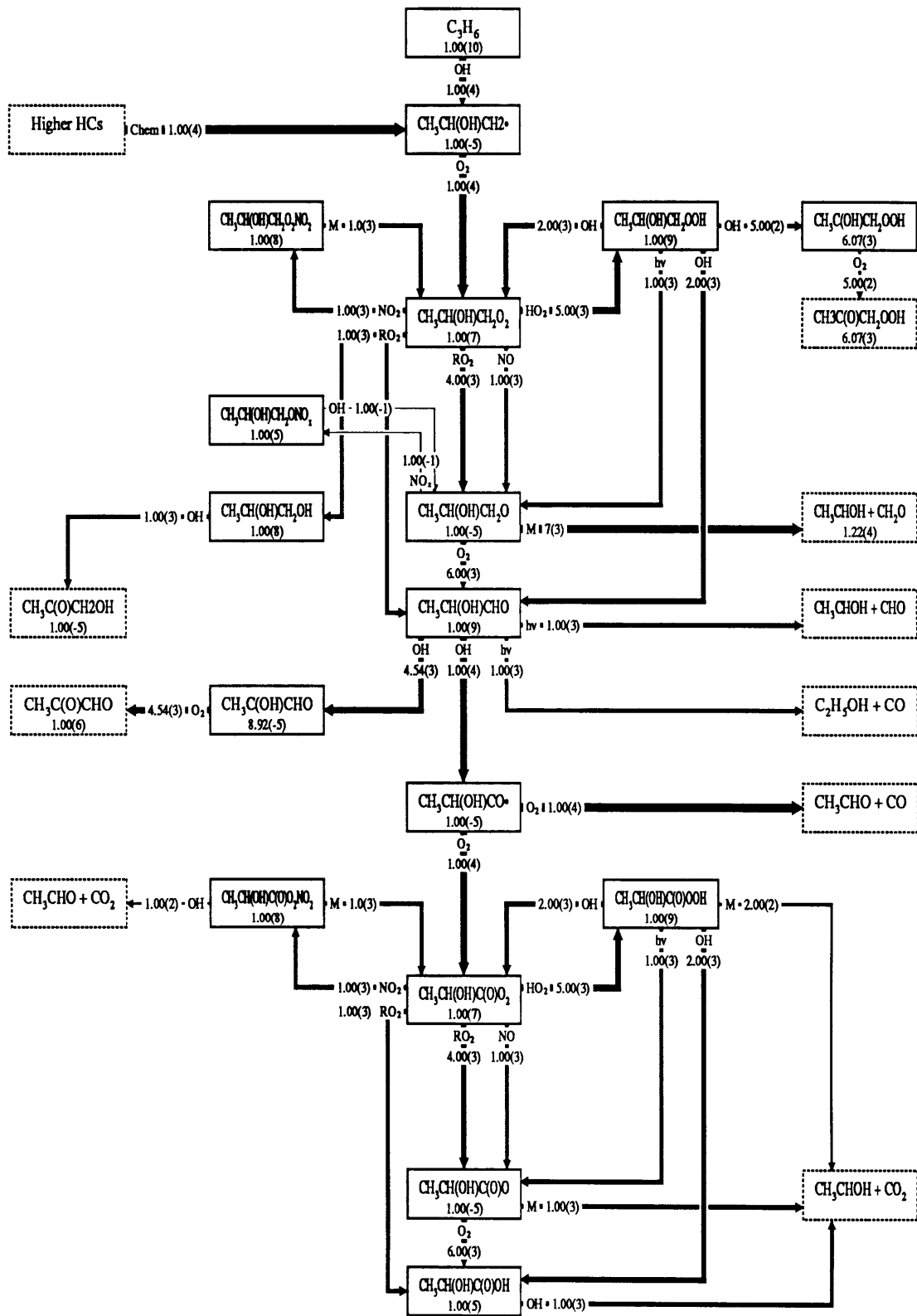


Figure 2.4.3. The sequence initiated by OH addition to the central carbon in propene. Compounds in dashed boxes are treated in other sequences. Reactive rates are qualitative.

longer and more complicated than ethene's, but if there is abundant hexene in the remote marine atmosphere, that complexity is there as well.

2.5 Model Boundary Conditions

One of the purposes of this investigation is to determine at what level the air-sea flux of short-lived NMHC's begins to play a potent role in governing marine boundary layer chemistry. Rather than separately examining the full possible emission range of all species, we split them into the two groups already described, the "light" NMHC's (C₂ and C₃) and the "heavy" NMHC's (all the rest). We define a "base case" flux for each compound as that flux which produces a diurnally averaged concentration equal to the mean observed value shown in Table 2.2.2. The relative NMHC fluxes in this base case are the initial case for our "normal" emissions scenario; a scenario being a series of runs with different absolute NMHC fluxes but identical relative NMHC fluxes. The absolute fluxes for each run within a scenario are determined by multiplying the initial case fluxes for each hydrocarbon in that scenario by a gain factor, ranging from 0.01 or less to at least 100. We use four scenarios in all:

- a. the "normal" scenario,
- b. the "very light" scenario, which involves only the light hydrocarbons, with the heavy NMHC fluxes held fixed at one percent of their value in the base-case run,
- c. the "light" scenario, in which the heavy hydrocarbon fluxes are reduced by a factor of five relative to the "normal" scenario, and finally
- d. the "heavy" scenario in which the heavy NMHC fluxes are doubled relative to the "normal" scenario.

The purpose of these four scenarios is to investigate whether the heavy hydrocarbons, with their vastly longer and more complicated oxidation sequences, affect MBL chemistry in a quantitatively or qualitatively different way from the light hydrocarbons.

Our primary intent is not so much to support or refute any particular set of observations - with such short-lived and sparsely measured compounds they could all be correct - but rather to determine at what average flux NMHC's begin to play a leading role in remote equatorial MBL chemistry. Beyond that, we shall comment on the consistency of emissions above this threshold and the consequent chemistry with existing observations of such species

as CO and ozone, as well as with NMHC observations themselves. We shall also suggest future observation strategies and point out reactions which should receive further attention in the laboratory.

To examine the importance of NMHC fluxes we shall use two measures. In all four emission scenarios we vary the gain factor from a value low enough that the NMHC's have no important role in MBL chemistry, through the gain factor of 1 (the initial case), and on above 1 to at least a gain factor of 100. The most direct measure of importance is obtained by tracking the diurnally averaged OH concentration as NMHC fluxes are increased from negligible levels. We deem NMHC fluxes "important" when the OH concentration deviates by more than 10% from the asymptotic (low flux) value, and "very important" when the deviation exceeds 30% (30% is a suggested benchmark precision for OH observation according to Crosley and Hoell, 1985). A second way to gauge NMHC importance is to examine the sources and sinks of OH. When the total OH sink due to all NMHC's and their oxidation products exceeds any other OH sink (particularly CO or methane and its oxidation products), we say that the NMHC's "dominate" MBL chemistry. Complete dominance would occur if NMHC's controlled both OH sources *and* sinks. This is possible only when NMHC fluxes are high and ozone is scarce.

We also vary the boundary conditions associated with the other governing parameters (H_2O concentrations, ozone and CO fluxes, and ultraviolet intensity). Each of these parameters is varied using a gain factor in three scenarios, with NMHC fluxes equal to the base-case value, one fifth, and twice the base-case value. This roughly brackets the range of NMHC fluxes we deem to be most likely. We generally reduce the gain factor in each case until the parameter being varied loses significance, thus finding its importance to MBL chemistry in the same way we explore the importance of the NMHC's.

Soluble compounds produced in the model are assigned deposition velocities depending on the expected solubility of the individual compound and consistent with other studies of the marine atmosphere the boundary layer (Kasting and Singh, 1986, Thompson and Cicerone, 1982). Generally, deposition velocities range from 1 cm sec^{-1} for very soluble acids, such as HONO_2 , to 0.1 cm sec^{-1} for less soluble compounds. Deposition velocities for hydrocarbon oxidation intermediates range between 0.1 and 0.5 cm sec^{-1} .

2.6 Model results

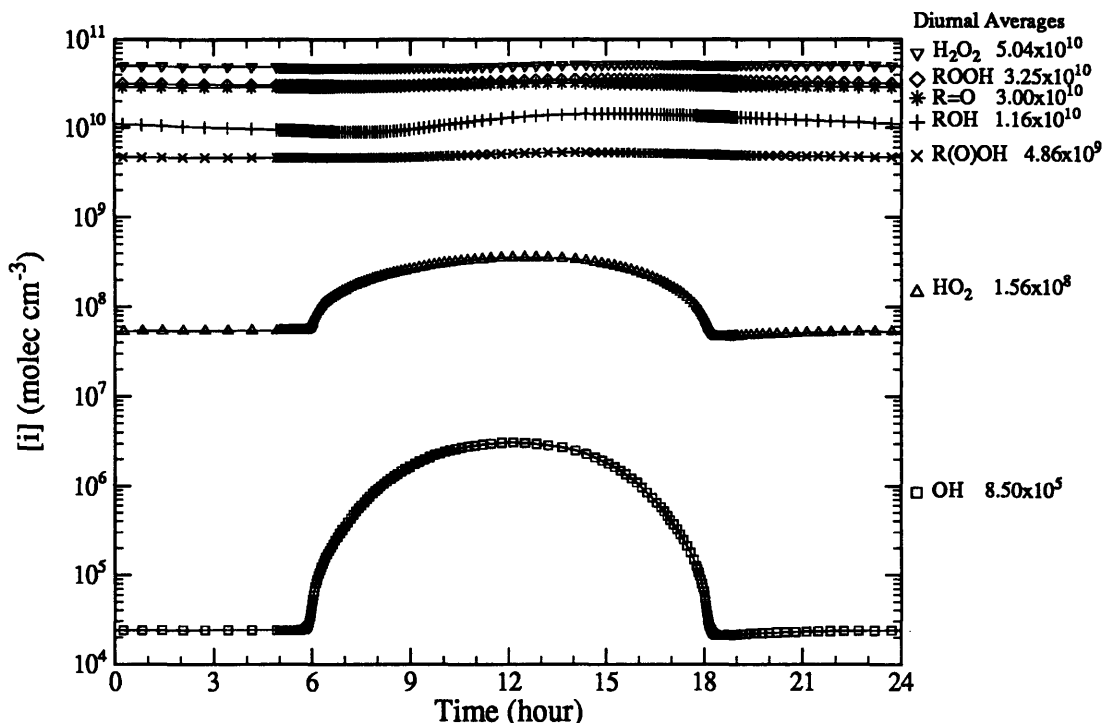


Figure 2.6.1. Diurnal behavior of HO_y and the important oxidized hydrocarbon families in the base-case run. Every tenth model time-step is indicated with a symbol. Diurnally averaged concentrations are displayed on the right-hand edge of the figure, along with the symbol used for each compound. Note the asymmetry in OH and HO₂ caused by the diurnal variations of the NMHC's (Figure 2.6.4).

2.6.1 Diurnal variability

The diurnal variation of several major compounds in the base-case run are shown in Figures 2.6.1 - 5. This run does not use the computational time-saving feature described in Section 2.3 and used in all other runs; another run which uses this feature but is otherwise identical to the base-case run differs from it by less than 1% for most important compounds. The convergence value ϵ is 0.01, and concentrations at every tenth timestep are shown on the graphs by a symbol. The very short timesteps required to resolve rapid variations near dawn and dusk are apparent. The timesteps shorten at 5:00 a.m. due to our assumption that dawn begins an hour before sunrise, with light intensities increasing exponentially from their low nighttime values between 5:00 and 6:00 a.m.. The same assumption applies to the interval between 6:00 and 7:00 p.m. at dusk.

In Figure 2.6.1 we show the odd-hydrogen species (OH, HO₂, H₂O₂) as well as the long-lived oxidized carbon species, shown here as families (total organic peroxides, ROOH; total aldehydes and ketones, R = O; total alcohols, ROH; and total organic acids, RC(O)OH).

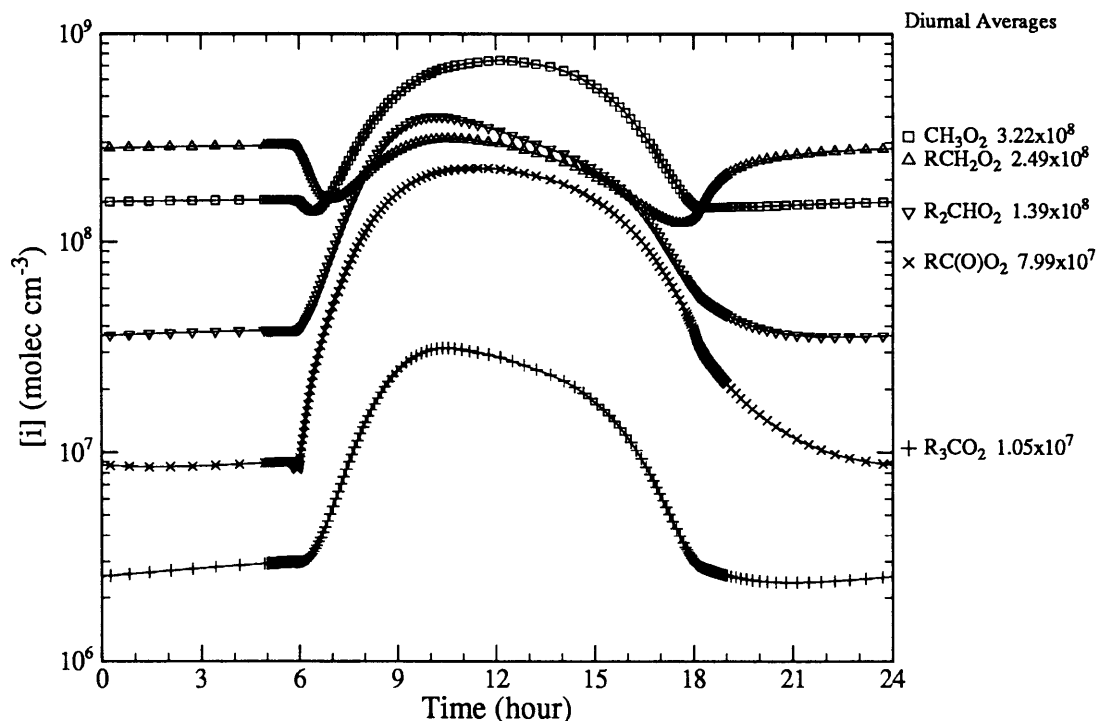


Figure 2.6.2. Diurnal behavior of the RO_2 radicals, shown as families (see text). As with odd-hydrogen, the asymmetry is caused by NMHC diurnal variations. Dips at dawn and dusk are caused by the high concentrations of HO_2 at those times, relative to OH.

Figure 2.6.2 shows the various RO_2 radical families: CH_3O_2 , primary, secondary and tertiary peroxy alkyl radicals, (RCH_2O_2 , R_2CHO_2 , R_3CO_2), and peroxy acyl radicals (RC(O)O_2). The diurnal behavior of these species is qualitatively similar to that predicted in previously published models (Logan *et al.*, 1981; Thompson and Cicerone, 1982). There is, however, one exception: the high alkene fluxes combined with the alkene-ozone reactions serve as a strong nighttime source of odd hydrogen. HO_2 therefore persists through the night at approximately one-quarter of its daytime value, while OH falls to roughly 1% of its daytime maximum. $\text{R} = \text{O}$ and ROOH are, not surprisingly, considerably more abundant in our model than in the above-mentioned models, which assume lower NMHC fluxes.

Figure 2.6.3 shows diurnal variations of the modeled alkenes for the base-case run. The constant NMHC emissions used in this run are shown in Table 2.6.1. All of the NMHC's show the expected behavior for compounds with constant emissions and a diurnally variable sink with a daytime maximum. The amplitude of this cycle depends both on the species' lifetime and the relative importance of OH and ozone as oxidizers. Ozone will tend to dampen a diurnal signal by providing a strong nocturnal sink for reactive hydrocarbons. There is no

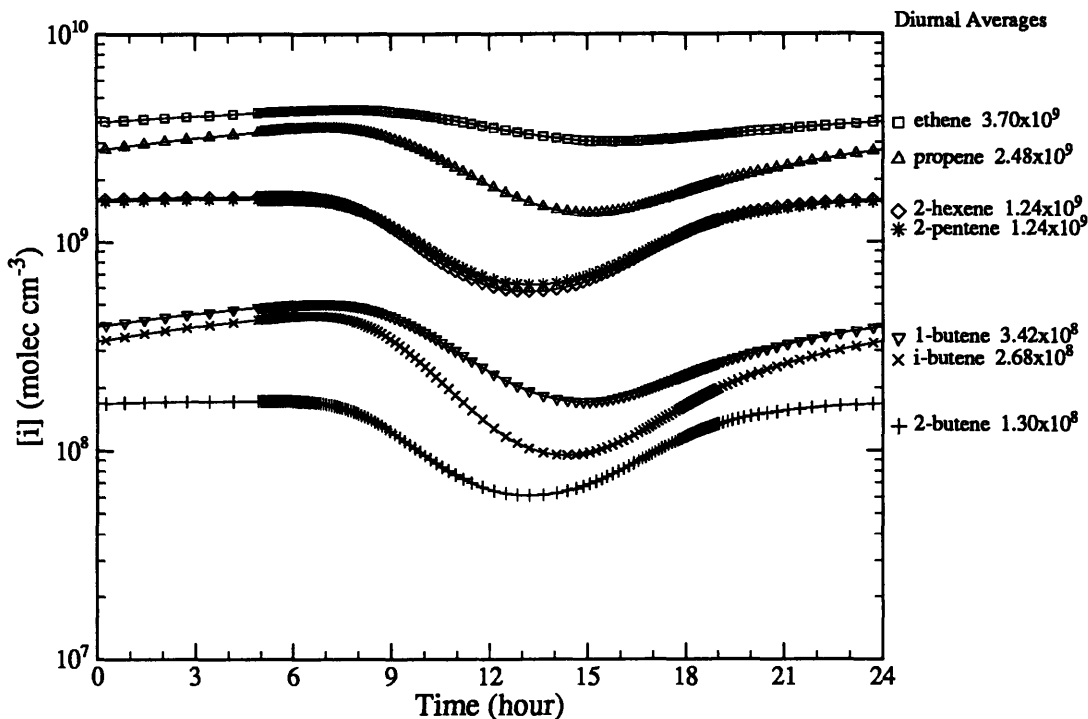


Figure 2.6.3. Diurnal variations of modeled alkenes in the base-case run. Amplitudes increase with increasing OH rate-constants, while nocturnal recoveries are suppressed with high O₃ rate constants (e. g. the 2-alkenes).

data against which to compare these heavy alkene results. Rudolph and Ehhalt (1981) report six samples of heavy alkanes taken during one week over the Equatorial Atlantic which show little correlation between time of day and mixing ratios, and Singh *et al.* (1988) show diurnal data for alkanes on the California coast, but neither measured the short-lived heavier alkenes.

Odd-nitrogen diurnal variations are shown in Figure 2.6.4. They are consistent with Thompson and Cicerone's (1982) simulations without a major surface NO source. The organic nitrates in this model are quite short-lived, and their concentrations increase considerably during the day, when NO₂ and peroxy acyl radicals are available. Figure 2.6.5 shows predictions for O₃ from the base-case run. Ozone shows behavior consistent with an ozone-destroying photochemical environment, (Thompson and Lenschow, 1986) with a diurnal amplitude of roughly 1 ppbv, quite consistent with observations (Johnson *et al.*, 1989). We discuss the ozone diurnal behavior in greater detail later. It is important to note that, while odd-nitrogen concentrations are extremely low in the remote marine atmosphere, in our model the NO - peroxy radical reaction is still the dominant chemical source of odd oxygen. In model runs where we introduce a flux of odd oxygen to the MBL, thereby forc-

Table 2.6.1 Fluxes in the base-case model run producing atmospheric NMHC concentrations consistent with observations.

| | Φ_{mod} | C_{B} | Φ_{B} | C_{L} | Φ_{L} |
|--------------|---------------------|----------------|-------------------|----------------|-------------------|
| ethane | 2.7 | 11 ± 10 | 6.6 ± 6.0 | 0.5 | 0.3 ± 0.2 |
| ethene | 54 | 38 ± 30 | 23 ± 21 | 10 ± 5 | 6 ± 4 |
| propane | 5.6 | 6.2 ± 5.2 | 3.7 ± 3.6 | 0.75 | 0.45 ± 0.3 |
| propene | 88 | 18 ± 13 | 11 ± 9.5 | 5 ± 3 | 3 ± 2.5 |
| n-butane | 25 | 2.9 ± 2.5 | 1.7 ± 1.5 | 0.25 | 0.15 ± 0.1 |
| i-butane | 14 | 1.8 ± 1.6 | 1.1 ± 1.1 | 0.25 | 0.15 ± 0.1 |
| butene | 43* | 5.1 ± 4.1 | 3.1 ± 2.9 | | |
| n-pentane | * | 1.6 ± 1.6 | 1.0 ± 1.1 | | |
| i-pentane | * | 2.3 ± 4.1 | 1.4 ± 2.5 | | |
| pentene | 153 | 4.4 ± 4.2 | 2.6 ± 2.8 | | |
| n-hexane | * | 3.6 ± 3.6 | 2.2 ± 2.5 | | |
| hexene | 158 | 2.2 ± 2.3 | 1.3 ± 1.5 | | |
| TOTAL | 543 | | 59 ± 57 | | 10.5 ± 7 |

Model fluxes (Φ_{mod}) are compared with those calculated from Bonsang *et al.*, 1988 (Φ_{B}) and Lamontagne *et al.*, 1974 (Φ_{L}). Fluxes are in $10^8 \text{ molec} \cdot \text{cm}^{-2} \text{sec}^{-1}$ and sea-water concentrations are in $10^{10} \text{ molec} \cdot \text{cm}^{-3}$. Fluxes are calculated from sea-water concentrations using a piston velocity of $v_p = (6 \pm 3) \times 10^{-3} \text{ cm} \cdot \text{sec}^{-1}$ (Rother, 1986). Only for ethane, ethene and propane do Φ_{mod} and Φ_{B} agree, while Φ_{L} is consistently far lower than Φ_{mod} . All atmospheric NMHC concentrations in the base-case model run are, however, at least an order of magnitude lower than the atmospheric concentrations reported in Bonsang *et al.*, (1988). (* Note that, in the model, butene fluxes are distributed among three isomers, while pentane and hexane fluxes have been assigned to the respective butane isomers.)

ing ozone levels to roughly 15 ppbv, the chemical source of odd oxygen from this reaction is insignificant and model photochemistry leads to a net chemical removal of odd oxygen. This is consistent with the general understanding of tropospheric ozone chemistry (Crutzen, 1988). Johnson *et al.* (1989) have recently noted that ozone mixing ratios over the southern Pacific ocean in the southern autumn often fall to a few ppbv. If we shut off the ozone flux into our model, crudely simulating long term isolation from continental or stratospheric odd oxygen sources, the ozone mixing ratio reaches a diurnal average of a few pptv, the exact value depending on the fluxes of NMHC's and odd-nitrogen into the model. The balance dominating this ozone steady state is between NO-derived production and removal through the interaction of $\text{O}(^1\text{D})$ and water. Remote oceanic regions with very low ozone and NO mixing ratios are therefore *not* ozone destruction regions but are rather ozone neutral, having already reduced ozone mixing ratios to a low steady state value.

2.6.2 Sensitivity to NMHC emission fluxes

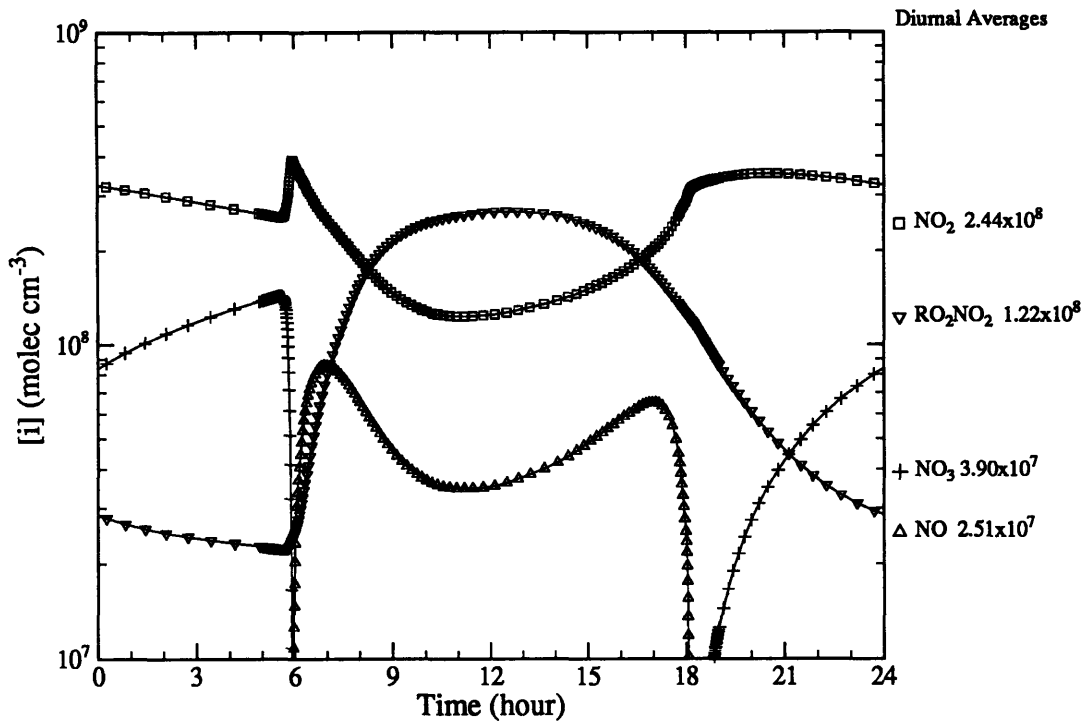


Figure 2.6.4. Diurnal variations of important NO_y species. NO_3 and NO control the model timesteps near dawn and dusk. Note the high resolution of rapid changes.

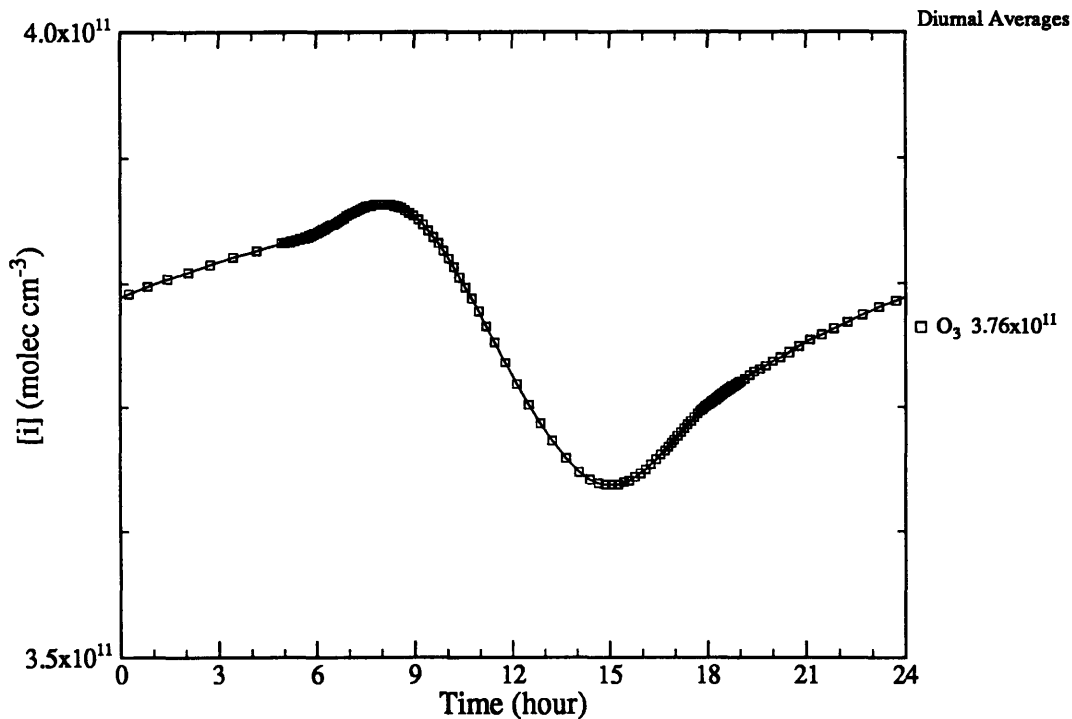


Figure 2.6.5. Diurnal behavior of ozone in the base case run. Note the small range of the y-axis, which is linear. The entire y-axis range is roughly 2 ppbv.

Diurnally averaged OH as a function of the *total* NMHC flux is shown in Figure 2.6.6 for

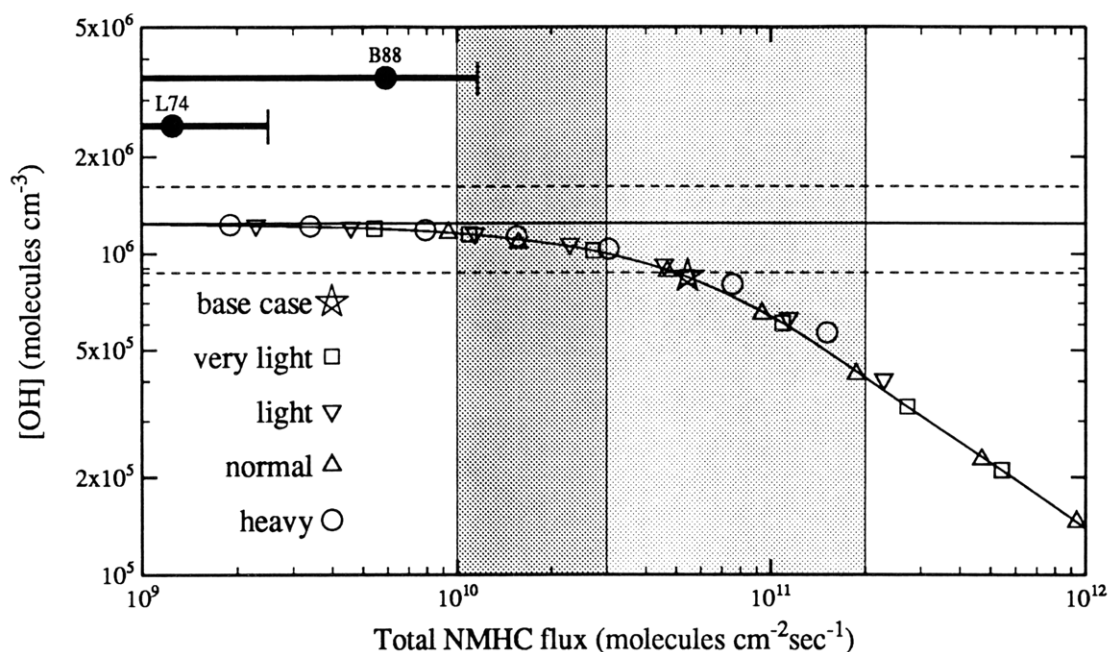


Figure 2.6.6. Dependence of diurnally averaged OH concentrations on the total NMHC flux. See text for a description of the emission scenarios. The entire shaded region corresponds to flux-range consistent with the range of atmospheric NMHC observations (Table 2.2.1), while the the darker region is the flux range required to support only light (C_2 and C_3) NMHC observations. The heavy horizontal bars show the flux ranges based on oceanic water observations (Table 5). The upper bar (B88) is based on Bonsang *et al.* (1988), while the lower bar (L74) is based on Lamontagne *et al.*, (1974). The vertical positions of the bars have no significance. The light horizontal dashed lines are 30% deviations from the solid low-flux asymptote.

the four scenarios described in Section 2.5: “normal,” “very light,” “light,” and “heavy.” The base-case run is shown in the figure by a star. The range of total fluxes producing modeled NMHC concentrations consistent with current atmospheric NMHC observations (Table 2.2.2) is shown by the shaded region, with two gradations: the darker shaded region between 1×10^{10} and 3×10^{10} molecules \cdot cm $^{-2}$ sec $^{-1}$ shows the consistent flux range resulting from consideration only of the light (C_2 and C_3) hydrocarbons, while the lighter shaded region extending to 2×10^{11} molecules \cdot cm $^{-2}$ sec $^{-1}$ includes the heavier NMHC’s. Note that the base-case run lies inside the lighter shaded region. The asymptotic diurnally averaged OH concentration reached when total NMHC fluxes drop to insignificance is shown as a solid horizontal line at 1.24×10^6 cm $^{-3}$. The horizontal dashed lines indicate a 30% deviation from this asymptotic value, the threshold we adopted in Section 2.5 as a sign that a compound is “very important” to OH chemistry.

The NMHC’s clearly could play a very important role in MBL chemistry. For example, the diurnally averaged OH in our base-case run is reduced by just over 30% from its value

in the absence of significant NMHC fluxes. This agrees well with the recent result of Liu *et al.* (1989), who predict a 25% reduction of MBL OH for unspecified NMHC fluxes (modeled as isoprene) in a 1-dimensional model. Note that this conclusion is relatively insensitive to the chosen NMHC distribution; the difference between the very light and heavy scenarios is only roughly 10% of the total effect on OH at any given flux. This is *not* the flux of carbon atoms but rather the flux of hydrocarbon molecules. The NMHC flux is best represented this way, at least in terms of its effect on OH. The additional chemistry introduced by increasingly complex hydrocarbons is OH-neutral in the absence of significant odd-nitrogen concentrations. The significance of heavy NMHC's is therefore not that they are heavy but that they are highly reactive, and even very low concentrations of them still indicate a large flux into the MBL.

In Figure 2.6.6 and Table 2.6.1 we also show total fluxes consistent with the existing *oceanic* NMHC measurements. In the figure these appear as bold horizontal error bars; only the horizontal extents and not the vertical positions are meaningful. These are calculated based on a diffusive microlayer model, for greatly supersaturated oceanic water (which is the case for the NMHC's):

$$\Phi_i = v_p \cdot C_{wi} \text{ (molec} \cdot \text{cm}^{-3}\text{)}$$

(Liss and Slater, 1974). We assume that v_p is $(6 \pm 3) \times 10^{-3} \text{ cm} \cdot \text{sec}^{-1}$ (Roether, 1986). We compute a flux based on the Lamontagne *et al.* (1976) oceanic concentrations C_{wi} of $(1.3 \pm 1.2) \times 10^9 \text{ molec} \cdot \text{cm}^{-2}\text{sec}^{-1}$, while for Bonsang *et al.*'s (1988) reported oceanic NMHC observations we compute a flux of $(5.9 \pm 5.7) \times 10^9 \text{ molec} \cdot \text{cm}^{-2}\text{sec}^{-1}$. In each case, we assume strong covariance among the NMHC's, so this is a conservative estimate of the possible flux uncertainty. These fluxes are below those which our model requires to maintain even the lowest observed MBL NMHC concentrations. The high end of the computed air-sea total NMHC fluxes just overlaps with the low end of the total fluxes capable of producing concentrations in our model which are consistent with atmospheric observations. This is a stretch for both; we must ignore all heavy NMHC measurements and assume that even the lighter alkenes are generally at the low end of the reported concentrations to get model fluxes as low as $1 \times 10^{10} \text{ molec} \cdot \text{cm}^{-2}\text{sec}^{-1}$, while we must combine high piston velocities with high oceanic NMHC concentrations and strong NMHC covariance to push the predicted NMHC fluxes that high. Only Bonsang *et al.* (1988) actually observed NMHC's in both

the atmosphere and ocean, but we excluded their atmospheric observations because they are much larger than other reports. Their high oceanic NMHC observations allow the tenuous overlap between fluxes predicted from oceanic and atmospheric observations in Figure 2.6.6. However, they generally saw 1 – 5ppbv in the atmosphere of all reported (C₂ – C₆) alkenes, which can only be supported in our model if the NMHC flux is nearly 1×10^{12} molecules · cm⁻²sec⁻¹. To predict a flux that large based on their reported oceanic measurements, we would need to assume an average piston velocity of roughly 900 cm sec⁻¹! If both our MBL model and the simple bulk-flux model are correct, there is therefore a serious discrepancy between current atmospheric and oceanic NMHC observations. Because there are very few oceanic observations, and because it is very easy to lose NMHC's from ocean water samples (Henry's law constants of roughly 50 mean that even small air pockets can severely perturb water concentrations), we are inclined to favor the atmospheric measurements. We must, however, regard the subject as an open one; one to be closed only when simultaneous oceanic and atmospheric samples give consistent predictions of air-sea fluxes.

In Figures 2.6.7 a and b we show the dependence of actual NMHC concentrations on total NMHC flux and the summed OH removal frequency due to the NMHC's (this is the same frequency shown in Table 2.2.2). Figure 2.6.7a is for the "normal" scenario. Particularly noteworthy are the very low predicted concentrations of the various butene isomers, which lie below the current instrumental detection levels over much of the flux range for all but the most sensitive systems currently described in the literature. (As shown in Table 2.2.2 and Figure 2.6.7a, those systems based on packed column gas chromatography generally have detection limits of 20 pptv or more, and only capillary gas chromatograph systems are sensitive to 1 pptv.) While we know nothing about the isomeric composition of the heavier alkenes in the MBL, we do know that the heavy alkane isomers are fairly evenly distributed (Table 2.2.1). Like the alkenes, heavy alkanes are also short-lived and must have a local (surface) source, so there is no reason to expect anything different for the alkenes. Distribution among two or three isomers for pentene and hexene would push their individual isomeric concentrations down very close to the current detection limits of many systems over much of the flux range covered in this paper; for the base-case run, most of the isomers would have mixing ratios below 20 pptv. Therefore, while most of the observational studies summarized in Table 2.2.1 did not indicate significant levels of the heavier alkenes, the

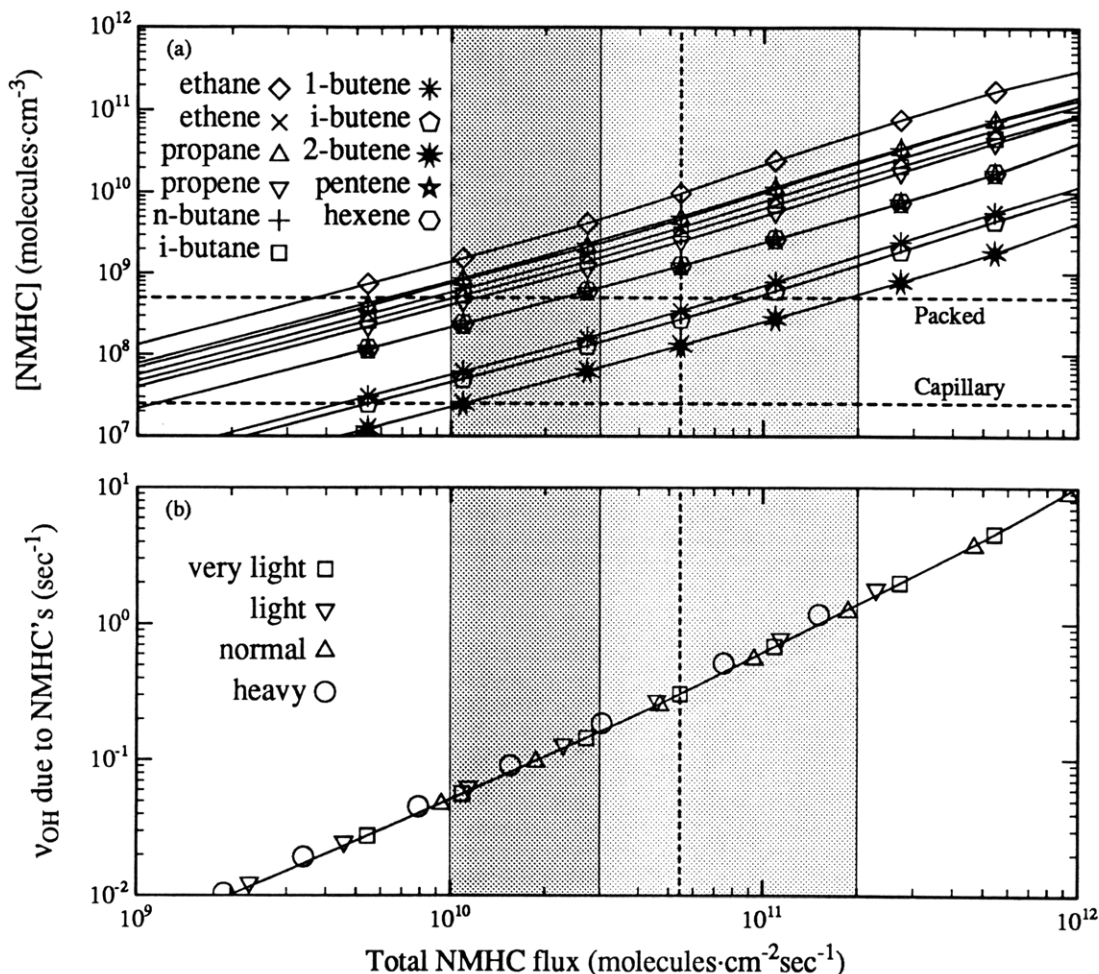


Figure 2.6.7. (a) Diurnally averaged NMHC concentrations as a function of total NMHC flux for the base-case run. Horizontal dashed lines show instrumental detection limits for the best packed (20 pptv) and capillary (1 pptv) GC systems. The dashed vertical line shows the base-case run. (b) Diurnally averaged OH removal frequency due to NMHC's only as a function of *total* NMHC flux for the four described scenarios. This allows a rough estimation of the total NMHC flux given a complete set of NMHC measurements (see text).

techniques used were generally not sensitive enough to see highly significant levels of these very reactive compounds.

While the distribution shown in Figure 2.6.7a depends strongly on the actual emissions scenario used, Figure 2.6.7b shows that the OH removal frequency (defined as $\nu_{\text{OH}} = \sum k_i C_i$, where the sum is over all of the NMHC's) depends only weakly on the emission scenario. Note that the *total* NMHC flux required to sustain a given set of measured NMHC concentrations can be determined by computing ν_{OH} from these measurements and then reading the appropriate flux from Figure 2.6.7b. Because this approach gives the total flux, the set must include all of the important NMHC's. This indirect method for flux determinations can be

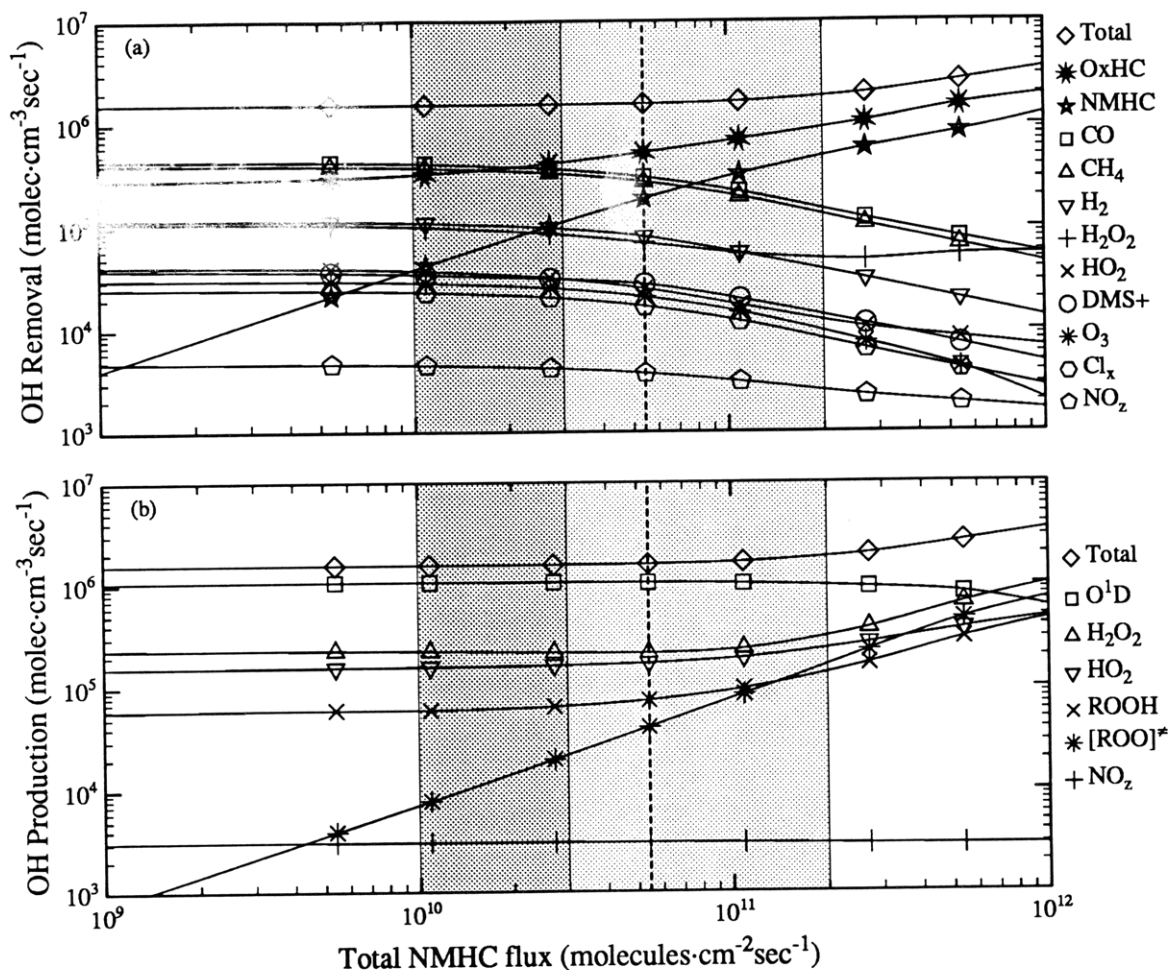


Figure 2.6.8. Diurnally averaged OH removal (a) and production (b) rates from specific sinks or sources in the MBL as a function of total NMHC flux for the “normal” scenario. NO_z is all nitrogen species, including HONO_2 , and $[\text{ROO}]^*$ is the source from ozone oxidation of alkenes.

regarded as complementary to measurements of ocean water NMHC supersaturations, combined with assumptions about the surface microlayer piston velocity (Liss and Slater, 1974). Ideally, the two predictions should agree (but as already noted, with currently available measurements they do not).

Figures 2.6.8 a and b show, respectively, the diurnally averaged OH removal and production rates. The NMHC's and their oxidation products take over as the dominant OH sink (Figure 2.6.8a) at a flux of roughly 2.5×10^{10} molecules \cdot $\text{cm}^{-2}\text{sec}^{-1}$. This is well within the likely flux range even excluding the heavy NMHC's from consideration. The total OH removal rate is influenced not only by reactions involving pure hydrocarbons but also by their oxidation products (mostly organic hydroperoxides and carbonyl compounds, including aldehydes, ketones and organic acids). Indeed, the contribution by these oxidation products,

excluding methyl hydroperoxide and formaldehyde derived from methane, exceeds that for the pure hydrocarbons over the whole range of NMHC fluxes considered in Table 2.2.2.

In the NO_x -poor environments modeled here, there are three major sources of OH (Figure 2.6.8b): reaction of $\text{O}(^1\text{D})$ with water, photolysis of peroxides, and recycling of HO_2 to OH via the reaction of HO_2 and ozone. At the higher NMHC fluxes, production of OH as a by-product of the ozone-alkene reaction (Atkinson and Lloyd, 1984) also contributes (see reactions R₂₂₈–R₂₃₅ in Table 2.4.1). In Figure 2.6.8b, we divide up the peroxides into hydrogen peroxide and the organic peroxides. At NMHC fluxes below about 10^{11} molecules·cm⁻²sec⁻¹, the $\text{O}(^1\text{D})$ source dominates OH production. Above that threshold, however, the hydroperoxides (H_2O_2 and ROOH combined) begin to compete with $\text{O}(^1\text{D})$, becoming dominant at an NMHC flux of roughly 3×10^{11} molecules · cm⁻²sec⁻¹. The relevant hydroperoxides are produced almost exclusively by the combination of peroxy radicals (HO_2 and RO_2) with HO_2 . The NMHC's are a strong source not only of RO_2 but of HO_2 as well, through the scavenging of weakly bound hydrogens on hydrocarbon fragments by molecular oxygen (see e. g. R83 in Table 2.4.1).

2.6.3 Sensitivity to CO, O₃, H₂O and UV light

Figures 2.6.9 - 12 show the variation of diurnally averaged OH with variations of assumed CO and O₃ input fluxes, O₃ column amounts, and H₂O concentrations. For this purpose we consider three of the NMHC flux strengths from our “normal” scenario (the base case, roughly one-fifth the base-case, and twice the base case). In each case the expected range of the assumed fluxes, column amounts, or concentrations is shown as a shaded region. As before, the base case run shown uses our full numerical scheme and thus differs, albeit slightly, from the given “normal” scenario curve, which uses our accelerated (weighted) numerical scheme.

The sensitivity of OH to carbon monoxide shows the expected behavior (Figure 2.6.9). OH concentrations vary only slightly over the range of assumed CO input fluxes, and even at the highest CO input fluxes, the OH concentration is not very significantly lower than it would be in the total absence of CO (specifically, the reductions from asymptotically low CO fluxes are 23%, 19% and 14% for the three total NMHC fluxes considered). CO therefore fails to meet the criterion we have advanced to establish a compound as “very important.” To add

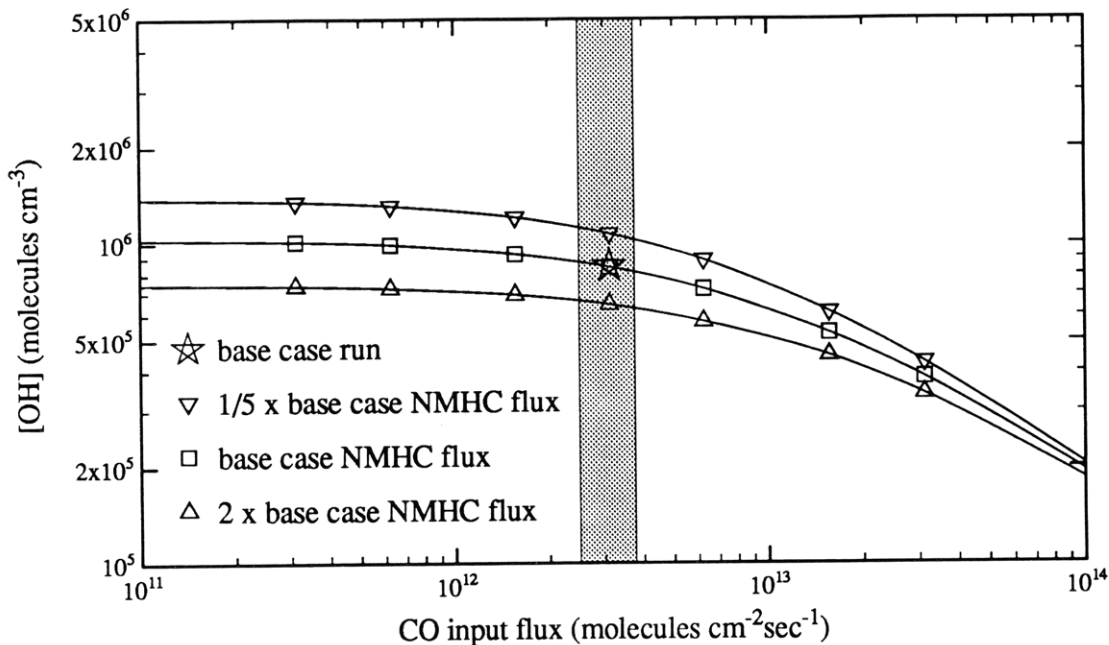


Figure 2.6.9. Dependence of OH concentrations on the flux of CO into the MBL. (This flux, as well as the flux of ozone in Figure 18, is *not* the net downward flux but rather the uni-directional flux described in Section 3.) The shaded region shows the flux range consistent with available CO observations. Three different NMHC fluxes were used in these model runs, as shown.

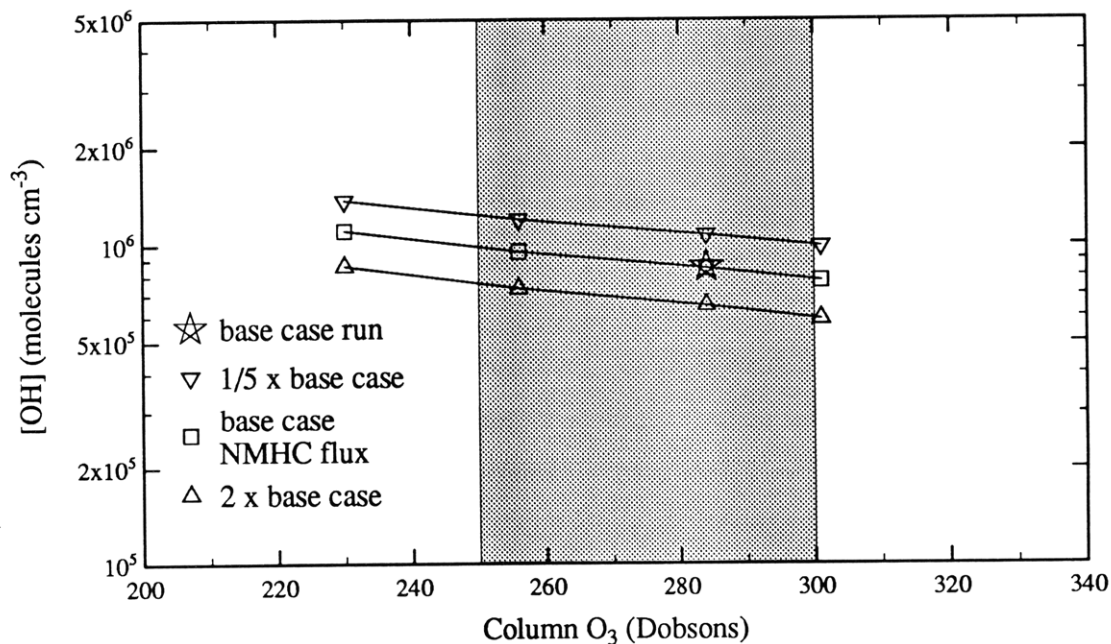


Figure 2.6.10. Dependence of OH concentrations on total column ozone, adjusted to simulate cloud-cover (see text).

perspective, the CO + OH rate constant is known only to within roughly 10% (Atkinson *et al.*, 1989). Note that methane, while an important OH sink, is not variable enough for the sensitivity of OH to its concentration to be relevant here.

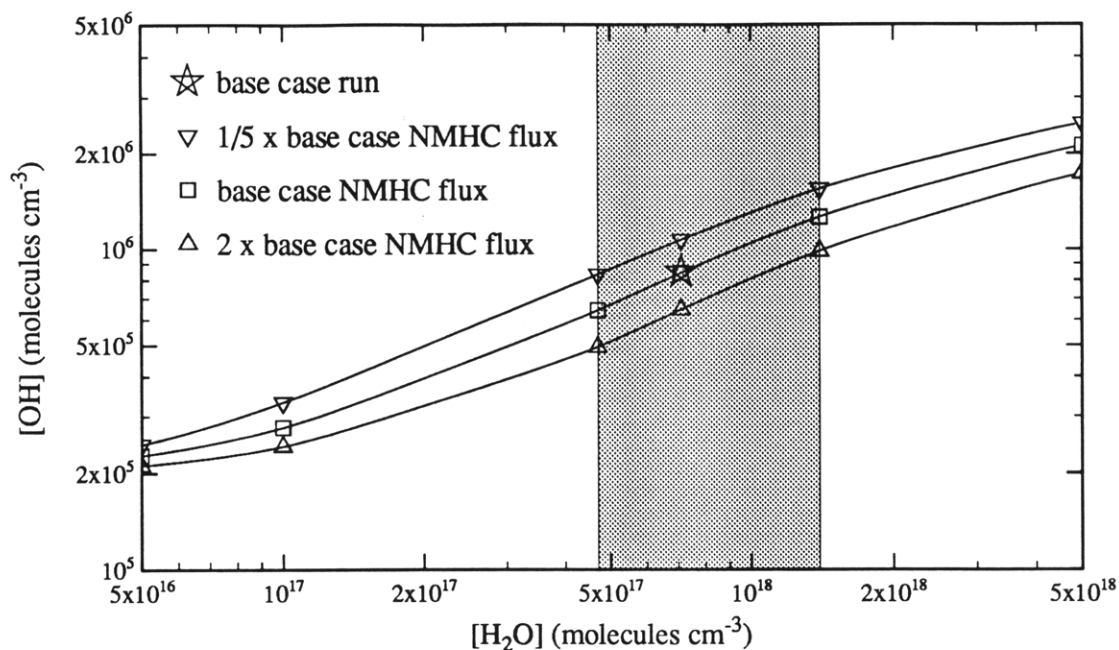


Figure 2.6.11. Dependence of OH concentrations on water vapor concentrations.

OH variations with changing column ozone are smooth and unremarkable (Figure 2.6.10). Over the range we consider, OH concentrations vary by about 20%, which is not so large as the variations caused by changing NMHC or ozone fluxes. Actual atmospheric UV intensity is certainly highly variable, more so than the other variables relevant to OH, such as ozone, CO and methane concentrations. Our approach addresses only the probable variation in *average* MBL UV intensity, but certainly does not include extreme situations such as the MBL immediately below a deep, precipitating cumulonimbus. Modeling would be greatly simplified were concurrent, accurate, spherically integrated UV spectra available. We should add that the uncertainty in the product of the relevant ozone cross-sections and O(¹D) quantum yields is estimated to be $\pm 40\%$ (DeMore *et al.*, 1987), introducing additional uncertainty in the predicted average and instantaneous OH concentrations.

Water, which reacts with O(¹D) to produce OH, is highly variable, even in the MBL. We assume that water vapor ranges between 65% relative humidity at 25C to 100% relative humidity at 35C, as discussed earlier. Figure 2.6.11 shows that, given this (factor of 3) range, variations in water vapor contribute significantly to MBL OH variability. For extremely dry conditions never realized in the tropical marine atmosphere the sensitivity of OH to H₂O becomes small and OH production from NMHC chemistry dominates.

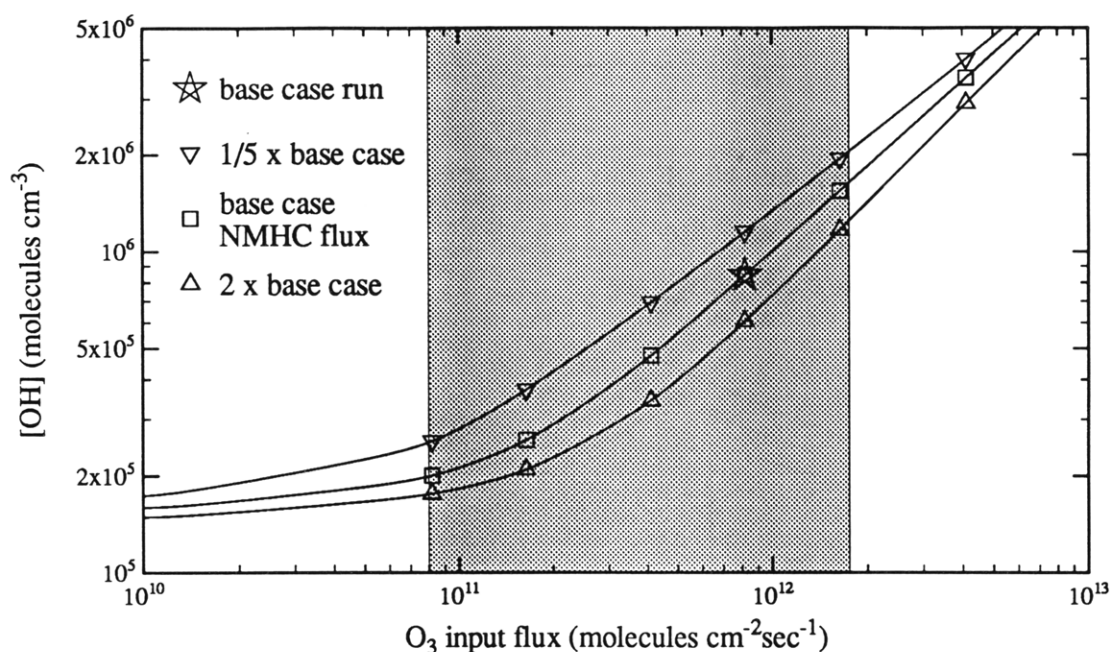


Figure 2.6.12. Dependence of OH concentrations on ozone fluxes in the MBL. The shaded region corresponds to the range of ozone observations in the remote MBL. Note the flattening near the lower limit of the flux, especially for higher NMHC fluxes.

Figure 2.6.12 shows the sensitivity of OH to ozone input flux. Recent observations by Johnson *et al.* (1989) show that ozone reaches very low levels (a few pptv) during the spring in the remote tropical Pacific MBL. In the model runs shown in Figure 2.6.12, the OH source is ozone-controlled, and the diurnally averaged OH therefore drops to a very low value when ozone fluxes are small, reaching $2 \times 10^5 \text{ cm}^{-3}$ at an ozone flux of $8 \times 10^{10} \text{ molecule cm}^{-2}\text{sec}^{-1}$ (equivalently a level of 3 ppbv). As NMHC fluxes are increased much beyond those shown in Figure 2.6.12, the peroxide OH sources take over from ozone as its level falls, and the sensitivity of OH to ozone is much smaller. Since ozone and OH are the dominant NMHC sinks, and their concentrations should be strongly correlated, one would expect a strong anti-correlation between ozone (and OH) and NMHC concentrations if NMHC sources were annually invariant. Unfortunately, the three data sets with reasonable coverage in the southern Pacific (Singh and Salas, 1982; Bonsang and Lambert, 1985; and Singh *et al.*, 1988) are all from the fall, when ozone in the tropical South Pacific tends to be higher than normal (Johnson *et al.*, 1989). If NMHC emissions are reasonably constant throughout the year we would expect NMHC concentrations to peak in the spring, when ozone levels are reduced. If actual NMHC fluxes are nearer the high end of those we consider, OH in the autumnal tropical South Pacific may well be governed largely by hydrocarbons. Note that the detection

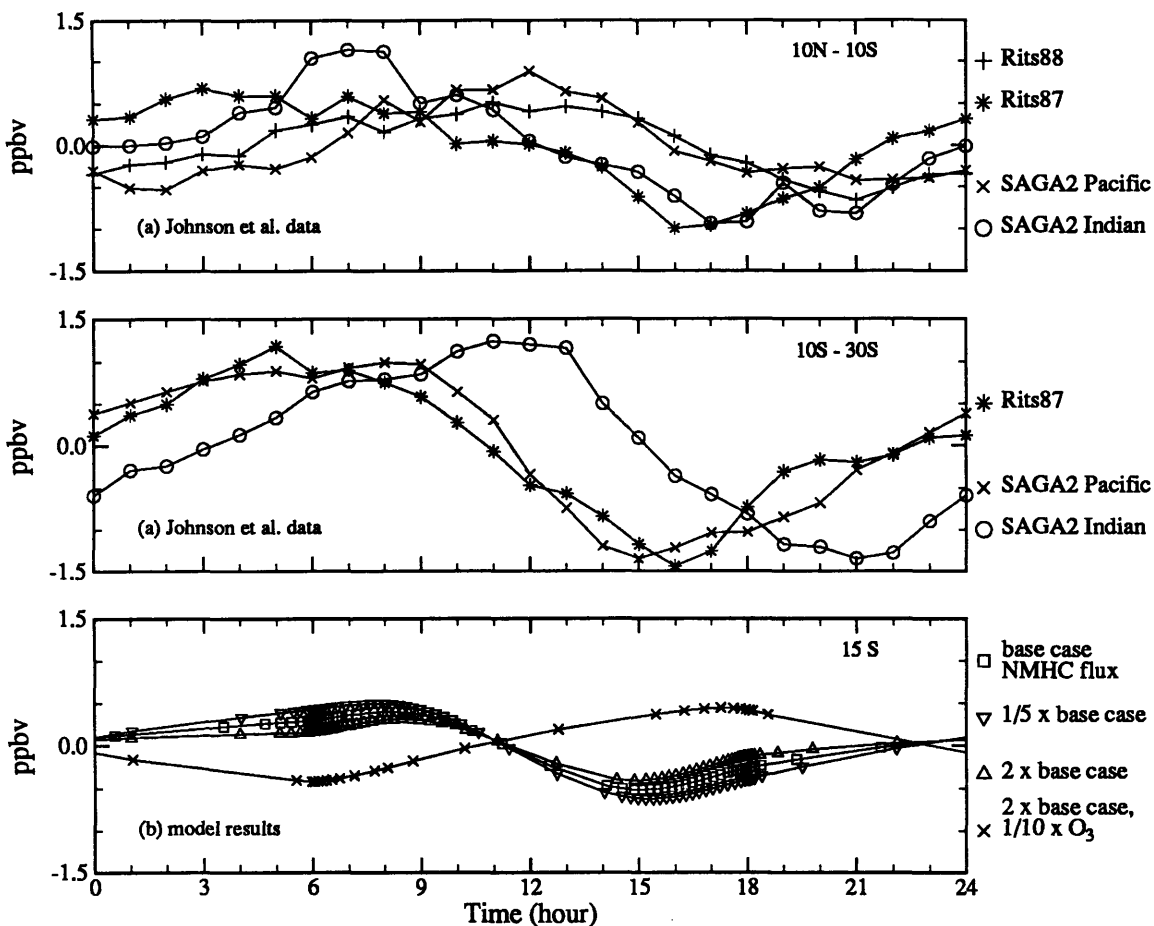


Figure 2.6.13. Ozone diurnal variations (a) from Johnson *et al.* (1989) and (b) for various model runs (see text). Note the flattening of the nocturnal variations with increasing NMHC fluxes.

limit of the Dasibi instrument used by Johnson *et al.* (1989) is 1 ppbv, so for ozone mixing ratios below 10 ppbv, observational imprecision for ozone will significantly contribute to uncertainties in modeled OH concentrations.

2.6.4 Diurnal ozone variations

Johnson *et al.* (1989) have reported observations of the diurnal cycles of ozone in the remote MBL as a function of latitude. Their southern hemispheric results are reproduced in Figure 2.6.13a. The majority of the cycles show ozone to be constant or slowly rising at night, with a maximum shortly after dawn (never after noon) and a minimum near dusk. The peak to peak amplitude of this diurnal cycle is generally between 1 and 1.5 ppbv. Our model predictions of diurnal cycles are shown in Figure 2.6.13b for 4 assumptions: 1/5, 1, and 2

times the base-case NMHC emissions, and 2 times the base-case NMHC emissions with a low (8×10^{10} molecules \cdot cm⁻²sec⁻¹) ozone input flux. A fifth run, with the base-case NMHC emissions and the exchange time between the MBL and the free troposphere doubled, did not produce diurnal ozone variations significantly different from the base case. The diurnal ozone amplitude increases with decreasing NMHC fluxes and is relatively insensitive to the diurnally invariant exchange time constant. Higher NMHC concentrations reduce the amplitude of the ozone diurnal variations because the alkenes are an ozone sink, and they peak at night. Our predicted diurnal amplitudes range between 0.7 and 1 ppbv, which is somewhat lower than those seen by Johnson *et al.* (1989). Many of the observed cycles are, however, quantitatively and qualitatively similar to our predicted cycles for relatively high NMHC flux conditions. Particularly evident is the lack of significant nocturnal ozone recovery. However, this could also be explained by a sudden MBL deepening at dawn (not considered in our model), which would entrain free tropospheric air with high ozone concentrations. Two of the Johnson *et al.* (1989) diurnal cycles, both labeled “RITS 88” in Figure 2.6.13a, correspond to very low ozone conditions. Our model results (Figure 2.6.13b) for very low ozone conditions generally show ozone declining at night, when alkene concentrations are high, and increasing during the day, which is distinctly different from the Johnson *et al.* (1989) data for equatorial regions in 1988.

2.6.5 Sensitivity to kinetics and isomeric composition

We have also explored the effects of uncertainties in the RO₂ loss mechanisms and kinetics, as well as in the isomeric distribution of the heavier alkenes. The important uncertainty associated with RO₂ is the ratio of the HO₂ and RO₂ sinks. For comparison to the base-case run, we considered a case where the RO₂ + HO₂ rate constant is almost twice its base-case value (5.9×10^{-12} instead of 3.2×10^{-12}). The resulting diurnally averaged OH concentration was 7.95×10^5 cm⁻³, compared to a base case value of 8.44×10^5 cm⁻³ (a 6% shift). It is hard to assess from the literature the actual uncertainty in this rate constant, but it may lie between a factor of two and five, causing an uncertainty in modeled OH of between 3% and 15%. Recently, several studies have provided new insight into RO₂ chemistry, producing findings which could alter conclusions based on the reaction scheme we used for the model runs discussed so far: the reactions of organoperoxy radicals with themselves (Moortgat *et*

al. , 1989a, and Lightfoot *et al.* , 1990a) and with hydroperoxy (Moortgat *et al.* , 1989b, and Lightfoot *et al.* , 1990b) radicals are faster than we have assumed; the branching ratios of the organoperoxy interactions also appear to favor the molecular channel more strongly than we have assumed; and finally, there appear to be additional active channels in the RO₂ – HO₂ reactions. Jenken *et al.* , 1988 have found an analog to the molecular channel in organoperoxy interactions for the HO₂ – CD₃O₂ reaction, with a roughly 40% CD₂O yield, and Moortgat *et al.* , 1989b find a 33% yield of ozone in the self-reaction of acetylperoxy radicals. To assess how these new findings might affect the results described here, we carried out model runs with all of the new rates and channels included. We assumed that all acylperoxy radicals react like acetylperoxy radicals (consistent with the described reactive family concept), and also assumed that the rate of the carbonyl generating branch of the RO₂ – HO₂ reaction is proportional to the number of hydrogens on the carbon atom in question. With these adjustments, the diurnally averaged OH concentrations rose by roughly 10% over the entire flux range considered in this paper. In addition, in spite of the additional odd oxygen sources, the dominant chemical source of odd oxygen in the model remained the removal of peroxy radicals by NO.

To explore uncertainty associated with isomeric composition, we added three runs to the base case run. In the first, all pentene and hexene fluxes were assigned instead to 2-butene (we make no distinction between the cis- and trans- isomers). Following that, the (now large) 2-butene flux was assigned to 1-butene, and finally to i-butene. Compared to the base-case OH concentration of 8.44×10^5 molec cm⁻³, these runs yielded concentrations 9.04×10^5 , 8.39×10^5 and 8.77×10^5 molec cm⁻³. These changes result mainly from the changing secondary chemistry associated with the relevant butene isomers. Note that the error in predicted OH levels caused by treating all pentene and hexene as butene is no greater than that caused by misassignments in the isomeric composition of butene. The total range of the above four OH concentration predictions is only 9% of the mean, and the 1σ uncertainty is 3.5%. This is consistent with our earlier observation that it is the total NMHC flux, and not the precise NMHC composition, that primarily influences MBL OH. It also suggests that models with far simpler chemistry, using even ethene as a proxy for all the unsaturated NMHC's, would not do very badly in predicting MBL OH. Such a drastic assumption would of course prevent prediction of specific NMHC and NMHC oxidation product concentrations,

preventing crucial comparisons between models and observations.

2.7 Discussion

We can compare these results with several existing chemical models of the marine atmosphere. Specifically, we shall consider the models of Thompson and Lenschow (1984) (and Thompson and Cicerone, 1982) and Kasting and Singh (1986). These two models are one-dimensional photochemical models. The first has variable height resolution (fine resolution in the boundary layer) and considers diurnal variability with prescribed (uneven) timesteps at 30° N and equinox. The second has a constant 1km resolution and solves for diurnally averaged mixing ratios, instead focusing on annual variability at 45° N. Of the two, only Kasting and Singh (1986) consider NMHC chemistry in detail. Our model is zero-dimensional, assuming rapid internal mixing in the boundary layer and including only a crude parameterization of exchange with the free troposphere. We focus on diurnal variability at 15° S and equinox and include far more complicated chemistry than either of the other two models.

Diurnal behaviors in our model and Thompson and Cicerone (1982) for both odd-hydrogen and odd-nitrogen species are qualitatively consistent. Our base case model has roughly half as much ozone as their model (15 ppbv opposed to 30 ppbv) but four times the water vapor. In both models the HO₂ to OH ratio is roughly 200, but we have roughly five times as much H₂O₂. (Kasting and Singh's (1986) marine summer model produces a similar HO₂ to OH ratio and they do not report results for H₂O₂.) The major qualitative difference in odd hydrogen is the high nighttime concentrations displayed in our model. These result directly from high alkene concentrations and the alkene - ozone reaction, which is a source of odd hydrogen. Our model sustains more H₂O₂ because we use a deposition velocity consistent with a rapidly mixed boundary layer (0.1 cm sec⁻¹), while the figures in Thompson and Cicerone (1982) are for a very thin layer near the surface with a 1 cm sec⁻¹ deposition velocity. The reason for the 200:1 HO₂ to OH ratio is alluded to in Kasting and Singh (1986): in a low-NO_x, low-ozone environment, the direct recirculation of HO₂ to OH is cut off, and HO₂ is instead forced to react with itself and other RO₂ to form peroxides. This is a very inefficient means of recirculating odd hydrogen. HO₂ has a long lifetime against reacting with RO₂ (hence the large HO₂ to OH ratio) and the recirculation

channels are very leaky; they are collectively the dominant odd-hydrogen sink in a low NO_x environment. This is graphically illustrated in Figure 2.4.1, which shows the various channels in the odd-hydrogen cycle with arrows proportional in size to their strength. Note that HO_2 is removed equally by self reaction and reaction with RO_2 , and both H_2O_2 and ROOH are far stronger odd-hydrogen sinks than recirculation agents. Note as well that hydrocarbon oxidation is a major odd-hydrogen sink; were NO_x levels one to two orders of magnitude higher, hydrocarbon oxidation would become instead a strong odd-hydrogen source.

We fix our NMHC fluxes just as Kasting and Singh (1986) do: we adjust the fluxes until concentrations agree with our prescribed values. The total molecular flux used in their marine simulation is 2×10^{10} molec cm^{-3} , which falls in the middle of our low flux (light NMHC only) range (the darker region in Figure 2.6.6). The compounds considered by Kasting and Singh (1986) are just those we classify as light (with the exception of n-butane), so we are in good agreement about the flux required to support observed light NMHC concentrations in regions lacking heavier NMHC's. At this flux, we find a roughly 10% depression of OH from its asymptotic (zero NMHC flux) limit, with a diurnally averaged concentration of 1.2×10^6 molec cm^{-3} . Both values are consistent with Kasting and Singh (1986), though their OH concentrations are some 20% higher than ours. This agreement is comforting if expected. It indicates that our crude free-tropospheric mixing parameterization is sufficient to quantitatively reproduce other model results, and it indicates that ignoring diurnal variability does not greatly harm Kasting and Singh (1986). This is also no surprise. In low NO_x environments, both of our models lack any significant compounds with nocturnal maxima. They are dominated by diurnally peaked species and longer lived species with only small diurnal fluxuations. There is thus no substantial error introduced by considering only diurnally averaged interactions because few important compounds have strong covariances. HO_2 (RO_2 in general) is the major exception to this, and the Kasting and Singh (1986) HO_2 to OH ratio is 20% larger than ours (HO_2 is removed more efficiently in our model because of its strong covariance with RO_2).

Our model explores two regimes untouched by these other models: high NMHC fluxes in low NO_x , and very low ozone concentrations. These models share with other models the common problem of producing too much OH with respect to independent estimations of globally averaged OH concentrations. Both lower ozone and higher NMHC environments

sustain less OH than the more traditionally modeled regimes, and there is observational evidence (reviewed earlier in this paper) to indicate that significant portions of the marine atmosphere may have higher hydrocarbon and/or lower ozone levels than those traditionally considered. These situations thus deserve more attention in dynamically more complicated models capable of producing meaningful global concentration averages.

2.8 Recommendations for future work

Models of this sort have two major uses: they can include a great deal of chemistry because they focus on a single location and almost entirely ignore advection, and they can be run rapidly, even in real time, in conjunction with experimental programs, to provide a check of local fast (steady-state) photochemistry. The atmospheric chemistry community needs to grapple with the problem of how best to probe the chemistry of moderately short-lived compounds such as the NMHC which are subject to advection but are far too heterogeneously distributed for global or even regional averages to have any real meaning. One solution is to carry out measurements in reasonably homogeneous, well understood environments, such as the remote marine boundary layer. Models such as this one should be put to the task of assessing the consistency of ensembles of measurements taken in these well-chosen environments; one such set was gathered, in part by us, on the SAGA 3 experiment in February - March, 1990 (which will be described in Chapter 4 of this thesis). That data set is ideal for this model, and should be examined with it. A second area of great potential use for this model is in examining kinetic uncertainties; Monte-Carlo or other techniques can be applied to a large reaction set to find, for instance, the reactions to which the OH radical is most sensitive, and those which contribute the greatest uncertainty to its calculated levels. Such information for the troposphere will be an invaluable tool for kineticists. The ability of this model to easily digest arbitrary reaction sets makes it ideally suited for adaptation to this task.

2.9 Conclusions

We have constructed a model of the remote tropical marine boundary layer containing the most extensive treatment to date of NMHC chemistry in NO_x -poor air. Model runs covering a wide range of NMHC air-sea fluxes show that, in the range consistent with current

observations, the NMHC's may either dominate MBL chemistry, or simply be contributors at the 10% level. These model runs also show that existing observations of NMHC's in ocean water find them too scarce for fluxes from bulk-flux air-sea gas exchange models to be consistent with the fluxes needed in our model to maintain even the lowest observed MBL NMHC concentrations. The model OH values for our assumed NMHC fluxes are consistent with the tropical lower tropospheric OH values deduced by inverse methods from ALE/GAGE CH_3CCl_3 data (Prinn *et al.*, 1987). The *ad hoc* OH profile shown in Figure 2.1.1 is a crude combination of our results with a one dimensional model OH profile (Kasting and Singh, 1986). It was designed to represent the effect of a strong surface source of OH destroying compounds. This *ad hoc* profile is clearly more consistent with the ALE/GAGE results than the unaltered profile, which has a surface OH concentration similar to our low NMHC flux limit, as discussed in the previous section. However, important uncertainties in the chemistry, including the $\text{O}(^1\text{D})$ quantum yield and in the observations of NMHC species in the MBL, prevent definitive conclusions about the precise role of the NMHC's in tropical atmospheric chemistry.

In addition to NMHC observations, ozone measurements provide important information on NMHC chemistry. Alkenes are known ozone sinks, and will, if present, tend to deplete ozone at night relative to the daytime. The diurnal observations of Johnson *et al.* (1989) show ozone mixing ratios characteristically rising slowly at night and through dawn, and declining during the day. This is consistent with (but does not necessarily validate) our model results for normal ozone levels and no diurnal variation in NMHC fluxes. The nearly 1 ppbv amplitude cycle with a nocturnal minimum predicted by our model for low ozone conditions with high NMHC fluxes is not evident in available observations. This suggests that, in low ozone conditions (typically tropical spring), NMHC sea-air fluxes are either no larger than in our base-case model run or possess a daytime maximum. Unfortunately, what little NMHC data there is was not collected at times when ozone was expected or observed to be at extremely low levels. Our model results for the 10 – 15 ppbv of ozone likely in the fall (when most of the existing NMHC data from the Pacific was collected) and for our assumed range of NMHC fluxes are generally consistent with observations with agreement being best for the higher NMHC fluxes.

To improve our understanding, it is apparent that we need NMHC observations with

systems capable of detecting unsaturated hydrocarbons out to at least hexene and down to 1 pptv. Definition of the diurnal and seasonal cycles in NMHC atmospheric and oceanic concentrations is needed, along with concurrent water vapor, ozone, UV flux and CO observations. Modeling tropospheric OH is currently limited by the large uncertainty in the O(¹D) quantum yield near the 310 nm cutoff. Finally, further kinetic data will be needed, if the NMHC's do prove to be significant. Their already acknowledged role in the continental boundary layer, and their potential role in low-NO_x regions addressed in this paper, should provide impetus for further investigation of the relevant hydrocarbon chemistry. Further examination of RO₂ self reactions, possibly RO₂ heterogeneous chemistry, and the fate of various organic hydroperoxides (including OH substituted hydroperoxides) should be given high priority.

While there is tantalizing evidence, including some of the results given in this chapter, that the lower tropical troposphere may be chemically governed by very short-lived NMHC's emitted from the ocean surface, this has not been established with certainty. If this is so, there exists an important connection between small and large scales within tropospheric chemistry revolving around the role of marine OH radicals as an oxidizer of both short- and long-lived chemically and/or radiatively important species. The observations reported here leave these questions unresolved; the rest of this thesis details the progress we have made toward a resolution.

Chapter 3 -- Calibration

3.1 Introduction

Our calibration philosophy is to develop at least two independent methods of absolute calibration and apply them separately to the system, demanding agreement between the two methods before considering the calibration complete. In addition to these primary standards, we seek to generate secondary standards which mimic the real atmosphere in both concentration and composition; these secondary standards are analyzed in the field under conditions essentially identical to ambient air analyses. In this work, primary standards were generated both by precise dynamic dilution of flows from permeation tubes and by volumetric static dilution of pure hydrocarbon samples into an electropolished, medium pressure, stainless steel cylinder. A secondary (field) standard was generated by precisely diluting a regulated flow from a second tank to produce standards with near ambient hydrocarbon concentrations. For hydrocarbons we also favor dynamically diluted standards over standards actually maintained at remote tropospheric levels (of as low as a few pptv) for two reasons; the problem of long-term stability is much more tractable at 100 ppbv than at 10 pptv, and the highly variable mixing ratios observed in the atmosphere call for a calibration technique with the flexibility to adjust to the observed conditions. Consistent with our philosophy, the leading sources of uncertainty in these techniques are independent from one another. Uncertainty in the permeation tube standards is caused by inaccuracy in weighing the tubes and the difficulty of establishing with certainty that changes in the tube's mass are caused entirely by flow of the calibration gas into the dilution stream. On the other hand, uncertainty in tank standards, as we prepare them, is caused by inaccurate pressure measurements and incomplete diffusive mixing during standard preparation.

It is conventional to discuss the quality of a standard in terms of its absolute accuracy (hereafter referred to as "accuracy" for brevity), meaning the confidence with which the mixing ratio of a given compound in the standard is known, including both random and systematic errors. A benchmark for accuracy is 1 percent. Accuracy is distinct from precision, which is generally taken to mean the repeatability of a given technique. We modestly expand the common definition of precision to include our ability to assess the relative mixing ratios of different compounds in the standard. This increases the utility of the definition, as much

of our analysis will focus on the relative importance of the various hydrocarbons in the tropospheric OH budget. It is also convenient and justifiable because our confidence in the relative abundance of the various hydrocarbons in a standard is directly proportional to the more conventional definition of precision. While our confidence in trace hydrocarbon standards preparation is growing, it will take significantly more work to develop and verify standards that are accurate to 1 percent. We currently assess the accuracy of our standards to be roughly 30 percent, while the precision is roughly 10 percent.

We have so far produced three standards: one uses a set of permeation tubes, and the other two are stored in tanks. We have assessed the stability of these standards, intercompared them, and tested their consistency with the notion of relative molar (carbon) response on a Flame Ionization Detector (FID). Some of the permeation tubes were not stable over time, and as a group they were not consistent with the relative molar response (RMR) model. The tank standards appear to have been stable, though the second (more accurate) one developed a small leak. The first tank was also not completely consistent with the RMR model, but the second tank was. Two of the standards, the permeation tubes and the second tank mixture, were prepared with sufficient care to be called absolute standards. We intentionally produced the first standard tank quickly, with an eye toward assessing stability and making a working standard well in advance of taking a system into the field. This tank became our working field standard, and we have three separate determinations of the NMHC mixing ratios in it. The first is the set of mixing ratios determined during the preparation of the mixture, while the other two are based on comparisons of chromatographic analyses of this tank with analyses of the other two standards. Our assessments of the precision and accuracy of the standards are in large part based on the consistency of these three determinations. The hydrocarbons in this first tank have been stable over the last year; the ratios of chromatographic peak areas for most compounds have not varied by more than 5 percent, which is roughly the precision of analysis. Though our confidence in the accuracy of the mixing ratio assignments for this tank is not enormous, eight of the twelve compounds none-the-less compare well with the corresponding permeation tube standards. For these eight compounds the two standards agree to within 50 percent. The same eight compounds in the tank mixture also produce chromatographic peaks whose areas are consistent with the relative molar response model. After we found that the NMHCs were stable in the electropolished stainless steel cylinders, we carefully prepared the

second standard tank as an absolute standard. However, we discovered after manufacturing it that it had a pinhole leak, allowing a flow of roughly 2 scc/min to escape from the tank. Fortunately, this did not interfere with the mixing ratios of the hydrocarbons it contained; analyses of this tank are consistent to within 10 percent with the relative molar response model for all compounds, a result we consider improbable had the leak affected compound mixing ratios. Furthermore, there is generally good agreement between this tank and the other two standards for the eight compounds for which the other two standards agreed, as discussed above.

Though we see considerable potential for further improvement our standards, they proved more than good enough to provide calibrations for the type of field work we conducted. In particular, our modest goal was to assess the importance of NMHC's to the OH budget in the marine atmosphere; our current standards are certainly up to that task. A more ambitious undertaking was the comparison of air and water samples to examine the consistency of fluxes predicted by air- sea gas exchange models with fluxes required in our MBL photochemical model as boundary conditions in order to maintain the observed atmospheric NMHC concentrations. To first order this consistency test depends only on the ratios of water and air concentrations and is completely independent of the absolute standards. Second order corrections arise because NMHCs in the remote MBL influence the OH concentration, and the consistency check involves modeling OH. Our measurements suggest that the NMHCs account for perhaps 10 percent of the total OH removal, so a 30 percent inaccuracy in NMHC mixing ratios produces roughly a 3 percent error in the consistency check. That is one of the smaller error terms in the calculation. Finally, because of the excellent stability of our working standard, as we continue to improve our absolute calibration technique we will be able to adjust all the absolute assignments based on that working standard.

3.2 Permeation Tubes

Permeation tubes consist of a pure reservoir of some compound separated from a dilution flow by a permeable membrane, generally teflon. If the tube is maintained at a constant temperature (stable to within 0.1 K), the vapor pressure of the compound, its solubility in the teflon, and its diffusion constant through the teflon will all remain constant; therefore the flow of the compound out of the tube into zero air will be constant. If this loss is the

only process acting to change the tube's mass, the permeation flow rate can be determined by measuring the change in mass of the tube over time.

In practice, the smallest measurable mass loss rate from a permeation tube is $\sim 2 \times 10^{-8} \text{ g min}^{-1}$ ($2 \times 10^{-4} \text{ g week}^{-1}$). For a compound with a molecular weight of 50, this is equal to $1 \times 10^{-5} \text{ cc min}^{-1}$. Because we use the permeation tubes only as primary standards, we need only dilute the permeation flow (f_p) to roughly 100 ppbv in order to calibrate the working standard. This requires a dilution flow (f_1) of 100 scc/min, a simple task with a single stage dilution (all flows are molar, or standard flows) and the resulting standard has a mixing ratio (χ_i) given by:

$$\chi_i = \frac{f_p + \chi_1 f_1}{f_p + f_1} \quad (3.2.1)$$

$$\simeq \frac{f_p}{f_1 + \chi_1} \quad (3.2.2)$$

assuming that the permeation flow is very much smaller than the dilution flow. χ_1 is an error term - for standards diluted to 100 ppbv, it is necessary to establish that the dilution gas has less than 1ppbv of the compound of interest. While expected to be true, this must always be demonstrated. The accuracy of this standard is:

$$(\delta \ln(\chi))^2 = (\delta \ln(f_p))^2 + (\delta \ln(f_1))^2 + \frac{(\delta \chi_1)^2}{\chi^2}. \quad (3.2.3)$$

where

$\delta \ln(f_p)$ = percentage uncertainty in permeation flow, largely from uncertainty in the rate of mass loss from the tube,

$\delta \ln(f_1)$ = percentage uncertainty in the regulated dilution flow, including inaccuracy due to calibration volume errors,

$\delta \chi_1$ = uncertainty of the contamination level in the dilution gas (often the instrumental detection limit, making this an upper limit).

We will specifically address each of these terms later. Generally speaking, we know f_1 to better than 1 percent and χ_1 is much less than 1 percent of χ , leaving the permeation flow (f_p) itself as the leading cause of uncertainty.

Our permeation tubes are inward flowing devices, with the calibration liquid confined in a sealed stainless steel union. A 1/16 inch teflon tube passes through the union, generally

a bored-through 1/8 inch Valco union, and calibration gas permeates into the tubing. The tubing in turn is flushed by a controlled flow, producing the standard. To prepare a tube standard, the compound must be in the liquid phase inside the tube. Using a freezer reaching -50 °C, we were able to make tubes for propane and propene, but ethane and ethene were beyond reach. We manufactured a set of these tubes in October 1989 (C₃ and C₄ NMHC) and November 1989 (C₅ NMHC). These tubes were kept in a 40 °C oven and continuously swept with a dilution flow of several scc/min. From time to time the tubes were removed from the oven and weighed on a Mettler balance (2×10^{-5} g sensitivity and accuracy). All masses were corrected for buoyancy. While the theoretical precision of these measurements should be as good as 2×10^{-5} g, early tests showed variability in repeated tube weighings of up to five times this theoretical value (in contrast, tests on standard stainless steel weights showed roughly the theoretically expected precision). Some portion of this additional imprecision was caused by small magnetic moments in the steel fittings we used for the tubes. The fittings were degaussed, and this generally removed any magnetic effect. Other potential causes of imprecision include variable adsorption of water by the steel fittings and the teflon tubes as well as incomplete thermal equilibration of the tubes with the environment of the balance. To minimize this latter effect, the tubes were weighed at least two hours after being removed from the oven, and occasionally up to twelve hours after removal. Longer equilibration periods would however run counter to the requirement for a constant mean temperature for the permeation tubes.

The most vexing problem associated with this design is leakage. The flows associated with permeation devices are very small, of order 1×10^{-4} scc/min or less, so very small leaks pose a severe threat. The inward flowing devices eliminate potential leakage problems associated with often hard-to-seal dilution chambers and allow a long series of tubes to be strung together in a chain, saving a great deal of space over a system requiring a dilution chamber large enough to hold 20 or 30 devices. The tradeoff is the assumption that none of the calibration material leaks out of the confining fitting instead of permeating through the central teflon tube. In recent studies on pentane devices, we have isolated a permeation device inside of a dilution chamber, keeping separate the flows around and through it. When the through-tube and around-tube flows are fixed at identical levels, chromatograms of samples taken from each flow can be directly compared to determine the fraction of material leaking

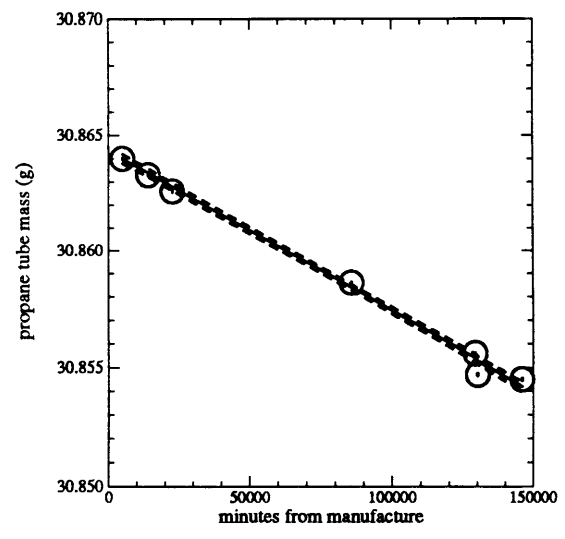
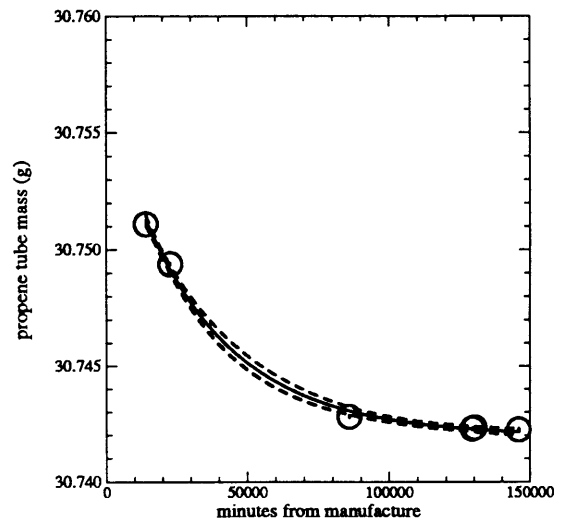
out of the device rather than permeating into the central teflon tube. For one particular tube, roughly 30 percent of the pentane was leaking out of the device. Note that leakage would cause us to overestimate the permeation flow by invalidating the assumption that all of the mass loss could be ascribed to permeation. This is consistent with the permeation tube based assignments for our working standard being generally higher than the assignments based on our primary tank standard. A leakage on the order of a few tens of percent for a device of this design, while severe for the particular device, does not endanger the design itself; it does indicate that the sealing mechanisms need to be studied more carefully. The testing applied to the one pentane device described here should become a regular part of permeation device manufacturing and monitoring.

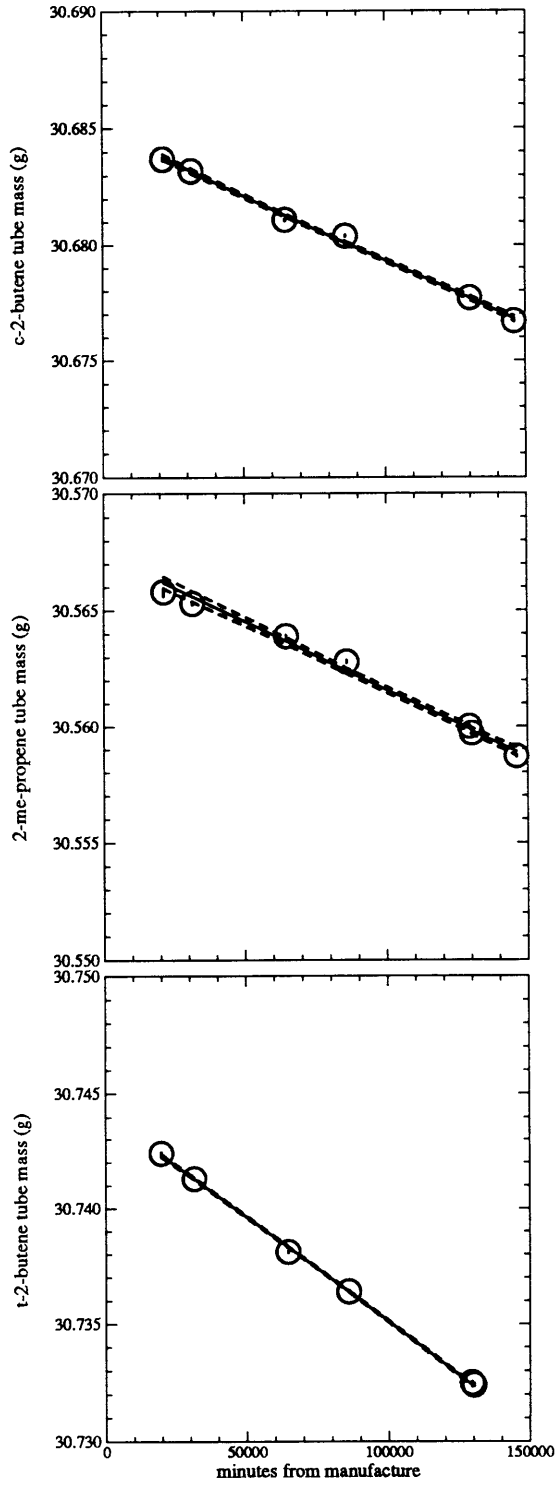
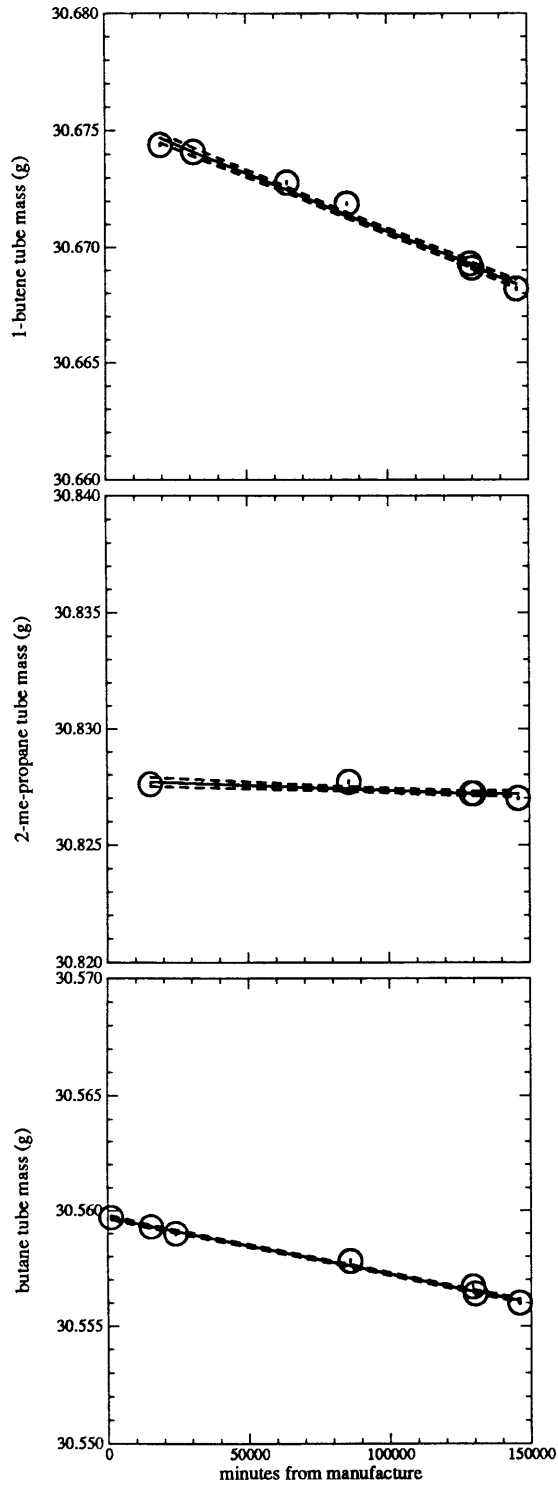
The mass record for each device is shown graphically in Figure 3.2.1, together with a least-squares fit and 65 percent confidence lines for linear or exponential models of mass loss. So long as liquid remains in a tube, its mass loss should obey a linear model; once the liquid runs out, the tube mass will exponentially approach a constant value as the residual gas evolves from the tube. Mass loss rates determined from linear fits are listed in Table 3.2.1. For all compounds but propene we used a linear model. For the propene tube, which expired, we used an exponential model. The results of this modelling show that the technique has great promise. The least-squares errors (1σ) in the linear coefficients are generally 5 percent or better.

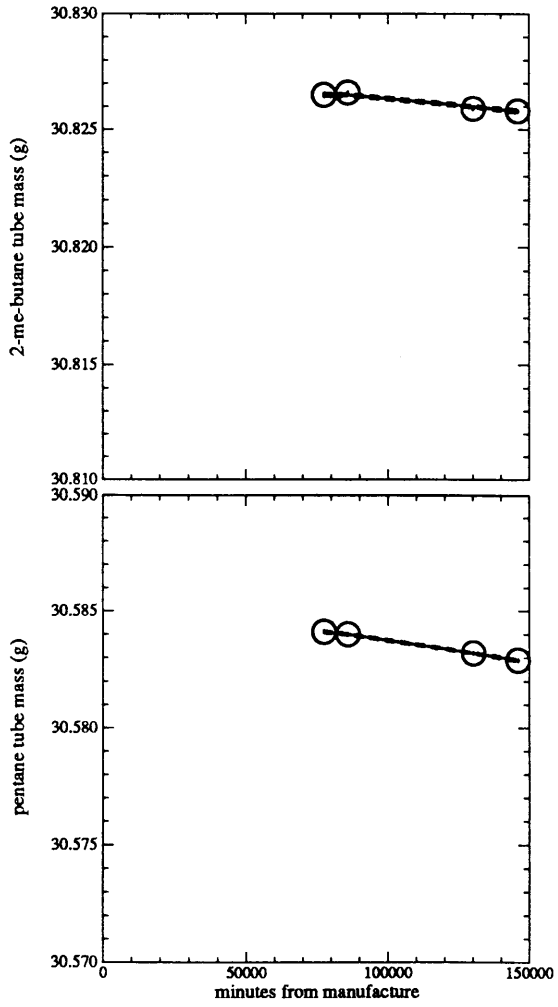
The chromatograms of samples taken from this set of tubes show a problem; the ratios of the various areas are not stable. Results from two chromatograms are shown in Table 3.2.2, with integrated peak areas and the ratio of peak areas for each compound. One chromatogram is from 22 November, 1989, and the other from 21 January, 1990; the relative peak sizes have changed. We have no reason to believe that the instrumental sensitivity to the various NMHC's (in particular the relative sensitivity) varies significantly with time; all other indicators suggest that the instrument is very stable. In addition, the FID is also very linear, as we will show later. The first chromatogram was a direct (1 cc) injection of an NMHC-N₂ dynamic mixture with an 11.4 scc/min N₂ flow. The mixture for the second chromatogram was prepared with an 81.86 scc/min N₂ flow. The peak area ratio for each compound should thus be 7.18 (Nov / Jan), barring any sensitivity changes or changes in permeation rates. One cause of a higher ratio would be a decreased permeation flow; propene,

Figure 3.2.1

This figure shows the mass records for the 15 permeation tubes manufactured in the fall of 1990. The placement of graphs in this figure will be repeated throughout the work; many compounds are missing from this figure, leaving the gaps. All C₂ and C₃ NMHC will be on the first page of each figure, all C₄ NMHC will be on the second page, all pentanes on the third, and all pentenes on the fifth. The mass records for all permeation tubes excepting propene are fitted to a straight line; the slope of this fit is the experimentally determined permeation flow. The propene tube expired quickly, and so the propene data is fitted to an exponential. Confidence limits are 67 percent for the model values. One mass point in the 3-methyl-1-butene record was rejected. It is indicated with an asterisk. The range on all of these graphs, 0.02 g, is roughly the mass of hydrocarbon in each tube, though occasionally it was somewhat less. There are error bars on each point; they are too small to see. Note that the relative position of each graph in this figure is determined by the compound corresponding to that graph; this pattern will remain the same in all subsequent figures dealing with multiple hydrocarbons. All C₂ and C₃ compounds are on the first page, all C₄ compounds on the second page, the pentanes on the third, and finally the pentenes on the fourth.







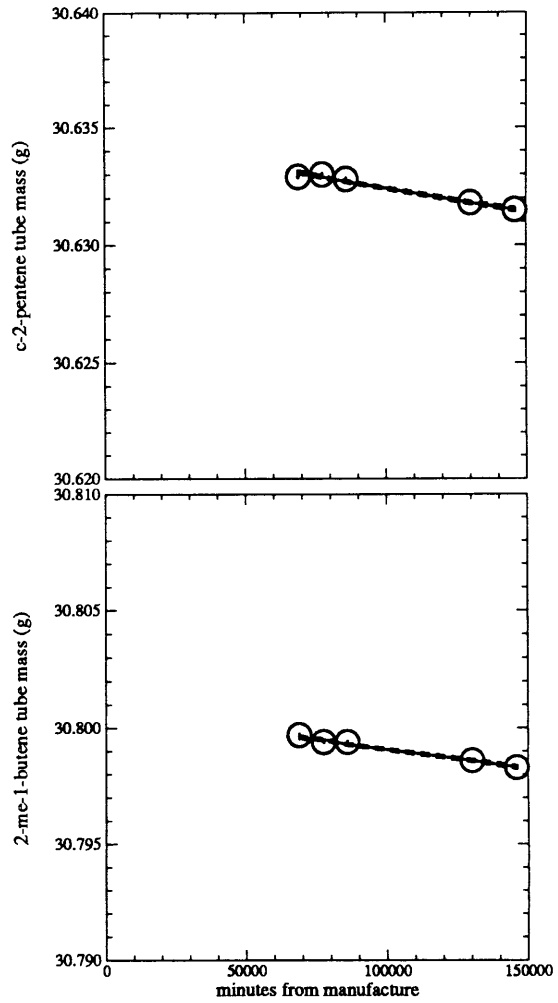
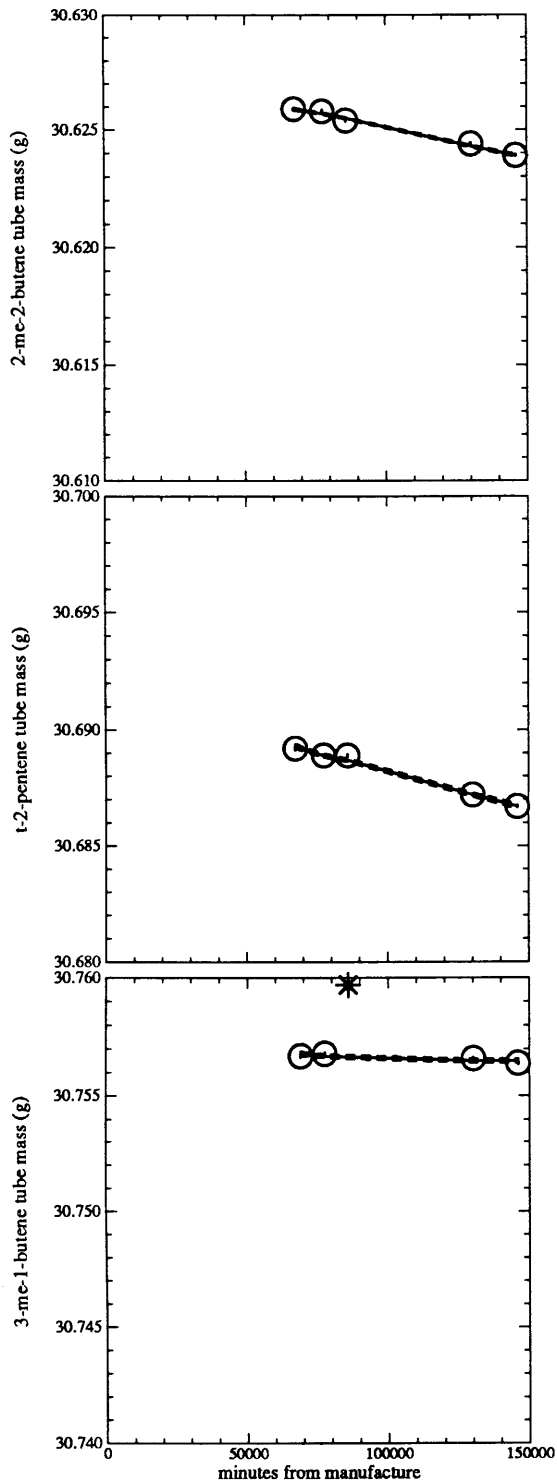


Table 3.2.1. Mass loss rates in ng min^{-1} for permeation tubes shown in Figure 3.2.1, along with 67 percent confidence limits from the linear fits.

| Compound | dm/dt ng min^{-1} | \pm |
|---------------|-------------------------------|-------|
| propane | 69.2 | 2.2 |
| 2-me-propane | 43.0 | 2.0 |
| butane | 24.34 | 0.97 |
| t-2-butene | 90.00 | 0.93 |
| 1-butene | 49.6 | 2.6 |
| 2-me-propene | 58.8 | 2.9 |
| c-2-butene | 56.0 | 1.6 |
| 2-me-butane | 10.8 | 1.7 |
| pentane | 17.2 | 1.1 |
| 3-me-1-butene | 35.6 | 1.7 |
| t-2-pentene | 32.4 | 2.0 |
| 2-me-2-butene | 25.7 | 1.0 |
| 2-me-1-butene | 17.1 | 1.4 |
| c-2-pentene | 20.5 | 1.6 |

for instance, has a ratio of 519, and trans-2-butene, whose mass-record also shows liquid expiration by late January, has a ratio of 34. For no other permeation tube does the mass data show an obvious sign of expiration; however, all compounds show area ratios higher than 7.18. The expected ratio appears to be a lower limit for the observed ratios, suggesting that some or all of the tubes suffered a decrease in permeation flow over the interval being considered. As the lower limit of the observations is more nearly 7.7, rather than 7.18, part of the ratio change could be explained as a 7 percent change in FID sensitivity. However, only 6 compounds have area ratios within 10 percent of 7.7: 2-methyl-propene, 2-methyl-1-butane, 3-methyl-1-butene, trans-2-butene, 2-methyl-1-butene, and cis-2-pentene. Seven others, excluding the two already mentioned, have significantly higher area ratios. The tubes contained roughly 1.5×10^{-2} g of material when manufactured, and several tubes other than propene and trans-2-butene had lost about that much mass by late January. The list of those tubes which had lost close to their estimated capacity by January is similar, but not identical, to the list with anomalously high area ratios. It is probable that several tubes were beginning to run out of liquid by late January, but that the change was not great enough to appear in the mass records. Unfortunately the tubes were then removed from their temperature controlled environment for transport to the field, so no further data is available. Because several permeation tubes appear to have expired during January, and because the FID has show stability to within a few percent over a year, when comparing the permeation tubes to

Table 3.2.2 Areas from two chromatograms of diluted permeation tube flows.

| Compound | A _{Nov} | A _{Jan} | A _{Nov} /A _{Jan} |
|---------------|------------------|------------------|------------------------------------|
| propane | 142.40 | 6.32 | 22.53 |
| propene | 409.87 | 0.79 | 519 |
| 2-me-propane | 14.68 | 1.81 | 8.11 |
| butane | 63.01 | 6.55 | 9.61 |
| t-2-butene | 217.20 | 6.41 | 33.88 |
| 1-butene | 87.46 | 9.08 | 9.63 |
| 2-me-propene | 86.44 | 9.51 | 9.09 |
| c-2-butene | 128.81 | 14.12 | 9.12 |
| 2-me-butane | 6.06 | 0.77 | 7.87 |
| pentane | 31.32 | 2.96 | 10.06 |
| 3-me-1-butene | 8.08 | 1.05 | 7.69 |
| t-2-pentene | 29.51 | 3.52 | 8.38 |
| 2-me-2-butene | 34.53 | 2.98 | 11.59 |
| 2-me-1-butene | 18.37 | 2.37 | 7.75 |
| c-2-pentene | 24.27 | 3.10 | 7.82 |

The first standard, from 22 Nov 1989, had a dilution flow of 11.4 scc/m, while the second, from 21 Jan 1990, had a dilution flow of 81.86 scc/m. Ratios of all areas are listed, which should be compared to the expected ratio of 7.18.

the tank standards we will use tube analyses from November and tank analyses from January (the earliest date when good tank analyses exist). This is not ideal, but we feel that in this case it is justified.

3.3 Tank Mixtures

We used the static dilution system originally developed for halocarbons by Michele Sprengnether (MIT) to prepare in tanks absolute mixtures of hydrocarbons. The system will be described in detail in her doctoral thesis and will thus be only briefly discussed here. The tanks were prepared by Yi Tang (MIT). The standards were manufactured using an evacuated dilution manifold; each compound was diluted with nitrogen in a glass bulb down to a volume mixing ratio of between 5 and 15 percent, determined with precise pressure measurements. A small portion of this mixture was then expanded into a nearly evacuated, specially prepared, steel tank; this step required accurate pressure measurements and accurate knowledge of the mixing manifold volume. It is the step which contributed most to the uncertainty in the standard. Finally, once all of the constituents were added to the tank, it was filled to 400 psi with UHP (analyzed) nitrogen and weighed. The contribution of the weighing to the total

standard uncertainty was minor. When we refer to the precision of the standard, we mean the uncertainty in relative mixing ratios. This uncertainty was caused largely by imprecision in pressure measurements during the first dilution stage, assuming that no significant differential wall problems existed. The accuracy of the standard is, of course, the absolute uncertainty in the final mixing ratios, including the uncertainty in all dilution steps, as well as weighing the tank.

The tanks used in this work were both refurbished, 34 liter, type 304 stainless steel, military oxygen tanks which we had commercially cleaned and electropolished (Electromatic, LA). Before any hydrocarbons were added to a tank, it was evacuated and flushed several times with UHP nitrogen, evacuated again, weighed, monitored for leaks, and filled with roughly 15 torr of water vapor to neutralize the walls. Buoyancy corrections were not applied, as the entire correction to the tank mass is of order 3×10^{-4} , and the change in the correction before and after gas is added is of order 5×10^{-5} , while the added N_2 is roughly 10 percent of the total tank mass, leaving the error caused by neglecting buoyancy less than one tenth of one percent. One of the important questions we addressed in this work was the stability of hydrocarbons in these tanks. The methods and results of the stability testing are presented in the following section. Each tank mixture was prepared in the following fashion:

1. the manifold and a mixing volume were evacuated,
2. the constituent was added, with the exact procedure depending on the individual compound (liquids were injected through a septum with a microliter syringe, while gases were introduced directly through a needle valve),
3. the manifold and volume pressure was monitored for 15 minutes to detect any pressure change due to wall adsorption,
4. the manifold and volume were filled to roughly 350 torr with UHP nitrogen,
5. the volume was isolated from the manifold and allowed to homogenize for at least one hour, while the manifold was evacuated,
6. the mixture in the volume was reintroduced to the manifold, and the manifold was again isolated from the volume,
7. using as an airlock a very small volume between the valve terminating the line connecting the manifold and the tank (this volume was considered to be part of the manifold volume), a small quantity of gas was injected into the tank and the pressure change in

the entire manifold was measured, and

8. after all constituents were added, the tank was filled to roughly 400 psig with UHP nitrogen and re-weighed.

In the completed tank, each constituent volume mixing ratio (χ_i) can be expressed in terms of the known or measured quantities in the calibration procedure:

$$\begin{aligned}
 \chi_i &= \frac{n_i}{n_{\text{tot}}} \\
 &= \frac{M(N_2)}{\delta m} \times \chi_1 \times \frac{V_m}{RT} \times \delta p_{\text{inj}} \\
 &= \frac{M(N_2)}{\delta m} \times \frac{p_1}{p_{\text{all}}} \times \frac{V_m}{RT} \times \delta p_{\text{inj}} \\
 &= \underbrace{\frac{M(N_2)}{\delta m}}_{1/n_{\text{tot}}} \times \underbrace{\frac{E_1 - E_0}{E_{\text{all}} - E_{\text{vac}}}}_{\chi_1} \times \underbrace{\frac{E_{\text{both}} - E_{\text{low}}}{E_{\text{man}} - E_{\text{both}} \times \frac{V_s}{RT}}}_{V_m/RT} \times \underbrace{M_p \times (E_b - E_a)}_{\delta p_{\text{inj}}}
 \end{aligned} \tag{3.3.1}$$

where

n_i = the number of moles of i in the tank,

n_{tot} = the total number of moles of gas in the tank,

$M(N_2)$ = molecular weight of $N_2 = 28.013 \text{ g mole}^{-1}$,

δm = change in mass of tank after filling with gas,

δp_{inj} = pressure change in manifold when i is injected into the tank,

p_1 = pressure of i during stage 1 dilution,

p_{all} = total pressure after stage 1 dilution,

R = gas constant = $8.3193 \times 10^4 \text{ mb cm}^3 \text{ moles}^{-1} \text{ K}^{-1}$,

T = temperature at time of injection into tank,

V_m = manifold volume,

V_s = a calibrated standard volume used to calibrate the manifold,

with:

E = pressure voltage, $p = M_p(E - E_{\text{vac}})$

M_p = slope of pressure transducer response function

Constituent dilution pressures:

E_{vac} = voltage for a vacuum,

E_0 = voltage before introduction of constituent to manifold,

E_1 = voltage after introduction of constituent,

E_{all} = voltage after dilution with UHP nitrogen,

Manifold calibration pressures:

E_{low} = voltage of evacuated manifold + standard volume,

E_{man} = voltage of filled manifold (std evacuated),

E_{both} = voltage of manifold + standard volume after Eman,

Constituent injection pressures:

E_{b} = voltage before injection,

E_{a} = voltage after injection.

We estimate that the uncertainty in each mixing ratio is

$$\begin{aligned}(\delta \ln(\chi_i))^2 &= (\delta \ln(\delta m))^2 + (\delta \ln(\chi_1))^2 + (\delta \ln(V))^2 + (\delta \ln(\delta p))^2 + (\delta \ln(T))^2 \\ &\sim (2 \times 10^{-3})^2 + (7 \times 10^{-3})^2 + (1.6 \times 10^{-3})^2 + (4.4 \times 10^{-3})^2 + (3 \times 10^{-3})^2 \quad (3.3.2) \\ \delta \ln \chi_i &\sim 0.009\end{aligned}$$

for a roughly 1ppm standard. The leading cause of uncertainty is associated with pressure voltage measurements, which contribute to both the $\delta \ln \chi_1$ and $\delta \ln(\delta p)$ terms. It is not yet clear whether this pressure voltage uncertainty is caused by reading inaccuracies or by true variability of the pressure in the manifold, perhaps due to wall effects. Because the leading causes of uncertainty are contributors to both inaccuracy and imprecision of the standard, we shall assume that the precision and accuracy of the tank mixtures are the same. Only after preparing several tank mixtures will we be able to assess them independently.

Mixing ratios for the second (absolute) tank are shown in Table 3.3.1., along with the manifold pressure before (E_{b}) and after (E_{a}) each injection, the first-stage mixing ratio (χ_1), and the temperature at each injection (T). For this standard, the manifold volume (V_{m}) was 27.268 ± 0.037 cc, and the change in tank mass due to added N_2 (δm) was 1127 g. For all compounds but ethane and propane, the pressure transducer calibration was

$$p(\text{mb}) = 275.1((1 \pm 7.2 \times 10^{-4}) \times E - (0.79 \pm 1.8 \times 10^{-3})).$$

After an overpressure, the transducer was recalibrated at

$$p(\text{mb}) = 279.0((1 \pm 1.3 \times 10^{-3}) \times E - (2.76 \pm 3.6 \times 10^{-3})).$$

Note that the theoretical uncertainties based on the above analysis and shown in Table 3.3.1 for each compound are all roughly 1 percent. Later analysis will show strong evidence that

Table 3.3.1 Tank Calibrations

| Compound | E_b | E_a | χ_1 (v/v) | T | χ_i (ppbv) | % error |
|---------------|-------|-------|----------------|--------|-----------------|---------|
| ethane | 5.684 | 4.456 | 1.0000 | 294.15 | 9,492 | 0.9 |
| ethene | 2.819 | 1.970 | 0.2949 | 295.65 | 1,898 | 0.7 |
| propane | 4.455 | 3.864 | 1.0000 | 295.45 | 4548 | 1.4 |
| cyclopropane | 2.997 | 2.376 | 0.2026 | 296.75 | 951 | 1.0 |
| propene | 3.083 | 2.440 | 0.1963 | 295.35 | 958 | 0.9 |
| 2-me-propane | 3.048 | 2.100 | 0.2655 | 294.75 | 1,914 | 0.7 |
| butane | 3.198 | 2.344 | 0.2933 | 294.45 | 1,907 | 0.7 |
| t-2-butene | 2.057 | 1.656 | 0.1657 | 293.95 | 507 | 1.2 |
| 1-butene | 2.299 | 1.882 | 0.1504 | 293.05 | 480 | 1.3 |
| 2-me-propene | 2.393 | 1.948 | 0.1411 | 294.15 | 479 | 1.2 |
| c-2-butene | 2.308 | 1.889 | 0.1498 | 294.55 | 478 | 1.3 |
| pentane | 2.847 | 1.994 | 0.2904 | 296.45 | 1873 | 0.7 |
| 2-me-butane | 2.778 | 1.953 | 0.3004 | 296.15 | 1876 | 0.7 |
| 3-me-1-butene | 2.092 | 1.734 | 0.1820 | 292.95 | 499 | 1.2 |
| t-2-pentene | 2.323 | 1.898 | 0.1478 | 292.95 | 481 | 1.3 |
| 2-me-2-butene | 2.287 | 1.875 | 0.1524 | 294.85 | 477 | 1.3 |
| 1-pentene | 2.380 | 1.939 | 0.1420 | 291.85 | 481 | 1.3 |
| 2-me-1-butene | 2.563 | 1.941 | 0.2003 | 297.45 | 939 | 1.0 |
| c-2-pentene | 2.331 | 1.905 | 0.1467 | 293.15 | 478 | 1.4 |

Mixing ratios (χ_i) and percent uncertainties in the second tank standard, along with pressure voltages before and after compound addition (E_b and E_a), first stage mixing ratios (χ_1), and the temperature at the time of injection (T). The manifold volume (V_m) was 27.268 ± 0.037 cc, and the added mass of N_2 (δm) was 1127 ± 2 g. Refer to equation 3.3.1 to calculate χ_i .

the actual standard precision may be as poor as 10 percent, while the actual standard accuracy may be as poor as 30 percent. We do not yet know why this is the case; identifying the causes of this unexplained inaccuracy will be a major goal of future standards work.

3.4 Capillary Flow Devices

We have recently been testing a third absolute calibration method. Instead of using a permeable membrane such as teflon to force a small, steady, flow for use in a dynamic dilution system, one can use a very small bore capillary tube. These devices can achieve flows ranging from the high end of standard permeation devices (1×10^{-4} scc/min) and up. Though the concept is mathematically identical to the permeation tube calibration method, error in the permeation tube standards is dominated by errors in mass-loss measurement,

with systematic errors arising when the devices leak, while capillary flow devices with large enough flows will have high but easy to measure mass losses, forcing multiple stage dilution and leaving the dilution, and not the mass loss measurements, as the dominant error term. Because of the difference in dominant error, it rates as an independent calibration technique.

The expression for laminar flow of an ideal gas through a narrow tube is:

$$f = \frac{3.75\pi r^4 T_s}{M\mu T l} \times \frac{p_h^2 - p_o^2}{p_s} \quad (3.4.1)$$

$$\frac{d \ln f}{dT} = 2 \frac{d \ln p_h}{dT} \left(1 - \frac{p_o^2}{p_h^2}\right)^{-1} - \frac{d \ln \mu}{dT} - \frac{1}{T} \quad (3.4.2)$$

where

f = flow in standard cc per minute,

l = length of the capillary in cm,

M = Molecular weight,

μ = viscosity in poise,

T_s = 273.15 K,

T = temperature of capillary in Kelvin,

r = capillary radius in cm,

p_s = 1.01323×10^6 dynes cm^{-2} ,

p_h = head pressure of capillary,

p_o = outlet pressure of capillary.

For absolute standards made with liquids, p_h will be the saturation vapor pressure of the compound in question, while p_o will generally but not necessarily be atmospheric pressure. Capillary tubing is available with radii ranging from 2.65×10^{-2} cm to 1.23×10^{-3} cm, yielding a very wide range in r^4 of 4.9×10^{-7} cm^4 to 2.4×10^{-12} cm^4 . Assuming an internal pressure of roughly 2 atm and using the smallest tubing available, with a viscosity of 5×10^{-5} poise and a molecular weight of 50 gm mole^{-1} , one would obtain a flow from such a device of $10^{-2}/1$ scc/min, or 10^{-3} scc/min for a 10 cm capillary. We expect that flow variability will be caused mostly by unstable temperatures. From 3.4.2 it is evident that the error so caused grows without bound as the head and outlet pressures approach the same value; this is not a surprising result, but it runs counter to the need to maintain small mixing ratios and thus small flows.

For a more concrete example, we will consider pentane, writing its saturation vapor pressure and viscosity respectively as

$$p_s = 2.36 \times 10^5 e^{\left\{\frac{10.63(T-273.15)}{T-45.22}\right\}} \text{ dyne cm}^2 \quad (3.4.3)$$

$$\mu = 8.05 \times 10^{-6} T^{-1/2} - 71.3 \times 10^{-6} \text{ poise} \quad (3.4.4)$$

based on values from CRC (1986) and assumed functional forms. At 60 °C, calculating both the values and temperature derivatives of these quantities, we find:

$$p_s = 2.16 \times 10^6 \text{ dynes cm}^{-2}$$

$$\frac{d \ln p_s}{dT} = 2.92 \times 10^{-2}$$

$$\left(1 - \frac{p_0^2}{p_s^2}\right)^{-1} = 1.28$$

$$\mu = 7.56 \times 10^{-5} \text{ poise}$$

$$\frac{d \ln \mu}{dT} = 2.9 \times 10^{-3}$$

Again assuming a 10 cm tube,

$$f_s = 1.4 \times 10^{-3} \text{ scc/min,}$$

$$\frac{d \ln f_s}{dT} = (3.7 \times 10^{-2} + 2.9 \times 10^{-3} + 3.0 \times 10^{-3})$$

$$= 3.3 \times 10^{-2},$$

which one could easily dilute to 100 ppbv, and which would have to be held in an oven stable to 0.3 K for the flow to be stable to within 1 percent. Note that easily the leading cause of flow variability with temperature is the dependence of the saturation vapor pressure on temperature. The above device would lose $4.5 \times 10^{-6} \text{ g min}^{-1}$, in principle allowing real time mass loss measurement, and in practice meaning that a device could be manufactured, weighed, placed in an oven, used to produce standards, and removed in a day after losing $6.5 \times 10^{-3} \text{ g}$, leaving the uncertainties in dilution as the largest contributors to the absolute uncertainty associated with the standard. These devices are not long-term standards, but they will provide independent point-checks of both permeation tubes and tank standards. Testing of the design is still in the early stages. So far we have used a prototype tube to identify ethyne on our column, using the device not as a standard but as a simple restrictor to produce stable small flows for our dilution system.

3.5 Instrument Response

At this point it is necessary to discuss the response characteristics of the Flame Ionization Detector (FID). The concentration of compound i in the detector as a function of time will be:

$$e_i(t - t_i; w_i), \int_0^{\infty} e_i(t') dt' = l_i \quad (3.5.1)$$

where

e_i = the elution function of compound i (often assumed to be gaussian),

t_i = the retention time of compound i ,

w_i = a measure of peak width for compound i ,

l_i = the total loading of i on the column.

Still focusing on compound i , the response ($r_i(t)$) of the instrument at time t will be a function of both i and any co-eluting compounds, j :

$$r_i = e_i(t; \sum_{j \neq i} e_j(t)) + r_0, \quad (3.5.2)$$

where r_0 is the baseline response. This includes linear addition, as well as any non-linear effects (quenching, square-response, etc..). The flame ionization detector (FID) is very linear; however, even if a detector responds linearly to a compound when no interfering compounds are present, there remains the possibility that it will lose its linearity when one compound co-elutes with another. Furthermore, even if the response remains linear through all possible interferences, the software used to integrate peak areas and apportion the total response among all co-eluting peaks may display systematic behavior. Thus the second set of dependencies, $e_j(t)$, in r_i represent not only incomplete separation and the resulting difficulties of peak integration, but also possible complex response by the detector to multiply eluting peaks. For the FID, this includes negative responses caused by strongly electron-capturing species such as oxygen and many halocarbons.

For a nearly linear detector, and i far removed from other peaks, the response function will be:

$$r_i = r_0(t) + m_i(t)e_i(t) + n l_i(e_i(t)) \quad (3.5.3)$$

where

r_o = baseline response,

m_i = linear response of the detector to species i

nl_i = non-linear portion of the detector response to i .

Each of these terms may be time-dependent as well. The long-term stability of m_i is a secondary issue we would also like to address during standards analyses. For this nearly linear detector, overlapping peaks can be expressed as a linear sum of response terms:

$$r(t) = r_o(t) + m_i e_i(t) + m_j e_j(t) + nl_i(e_i) + nl_j(e_j) + nl_{ij}(e_i, e_j) \quad (3.5.4)$$

The cross term represents the interactions mentioned earlier.

If i is well separated from all of its neighbors, the integrated response (peak area A_i) above the baseline (r_o) due to a total loading of compound i (E_i) will be:

$$\begin{aligned} A_i &= m_i \int_0^\infty e_i(t') dt' + \int_0^\infty nl_i(e_i(t')) dt' \\ &= m_i E_i + NL_i(E_i) \end{aligned} \quad (3.5.5)$$

$$E_i = \frac{A_i}{m_i} - \frac{NL_i(E_i)}{m_i} \quad (3.5.6)$$

We will assume that this holds for all of the compounds being discussed here: even where separation is not complete, it is good enough that accurate estimations of peak areas can be made for both peaks. If one has a stable standard, m_i can be determined from that standard:

$$m_i = \frac{R_{is} - NL(E_{is})}{E_{is}} \quad (3.5.7)$$

$$\begin{aligned} E_i &= \frac{R_i E_{is}}{R_{is} - NL(E_{is})} - \frac{NL(E_i) E_{is}}{R_{is} - NL(E_{is})} \\ &\simeq E_{is} \frac{R_i}{R_{is}} + E_{is} NL(E_{is}) \frac{R_i}{R_{is}^2} - NL(E_i) \frac{E_{is}}{R_{is}} \\ &= E_{is} \frac{R_i}{R_{is}} + NL(E_{is}) \frac{E_i}{R_{is}} - NL(E_i) \frac{E_{is}}{R_{is}} \\ &\approx E_{is} \frac{R_i}{R_{is}} \end{aligned} \quad (3.5.8)$$

where the non-linear terms cancel each other out, provided that the total amount of injected standard is sufficiently close to the total amount of injected sample. The flame ionization detector is linear enough that "sufficiently close" is usually determined by causes other than

concerns about linearity. The need to treat standards and samples similarly is generally a more pressing reason to keep standard and sample concentrations similar. Figure 3.5.1 shows the response for propene over a concentration range of 100; this is typical of all of the NMHC. The small deviations from perfect linearity appear to be randomly distributed about the best fit line and are ascribable to uncertainties in the integrated peak areas.

A powerful concept in hydrocarbon analysis on the FID is that of relative molar response (RMR). Ackman (1968) showed that the responses of a broad range of hydrocarbons can be described by the expression

$$\text{RMR}_i = 100C\#_i \frac{C\%_i}{C\%_{\text{hept}}} \quad (3.5.9)$$

where

$C\#_i$ = the carbon number of i ,

$C\%_i$ = the mass fraction of carbon in i ,

$C\%_{\text{hept}}$ = the mass fraction of carbon in heptane (0.839).

The RMR are thought to be generally good to within 10 percent or better. We will use them as a check of our standards and also as a tool for testing tank stability, assuming that the time variation of the RMR, even if they do not perfectly obey equation 3.5.9, are far more stable than the overall response characteristics of the instrument itself.

Assuming that the detector is linear, we can write down a general equation describing the response of the system to an individual hydrocarbon:

$$A_i(t) = I_i(t)c(t)\text{RMR}_i(t)e_i(t)\chi_i(t)v(t) \quad (3.5.10)$$

where

$A_i(t)$ = the peak area determined for i ,

$I_i(t)$ = the integration efficiency for i , normally near 1,

$c(t)$ = the common instrumental response term,

$\text{RMR}_i(t)$ = the relative molar response for i

$e_i(t)$ = the system efficiency for i , including any cryogenic trapping efficiencies, chemical losses or additions during trapping, and column losses.

$\chi_i(t)$ = the mixing ratio of i in the sample

$v(t)$ = the standard volume sampled, either pV/RT for direct injections or $f\delta t$ for cryogenic samples with a controlled flow.

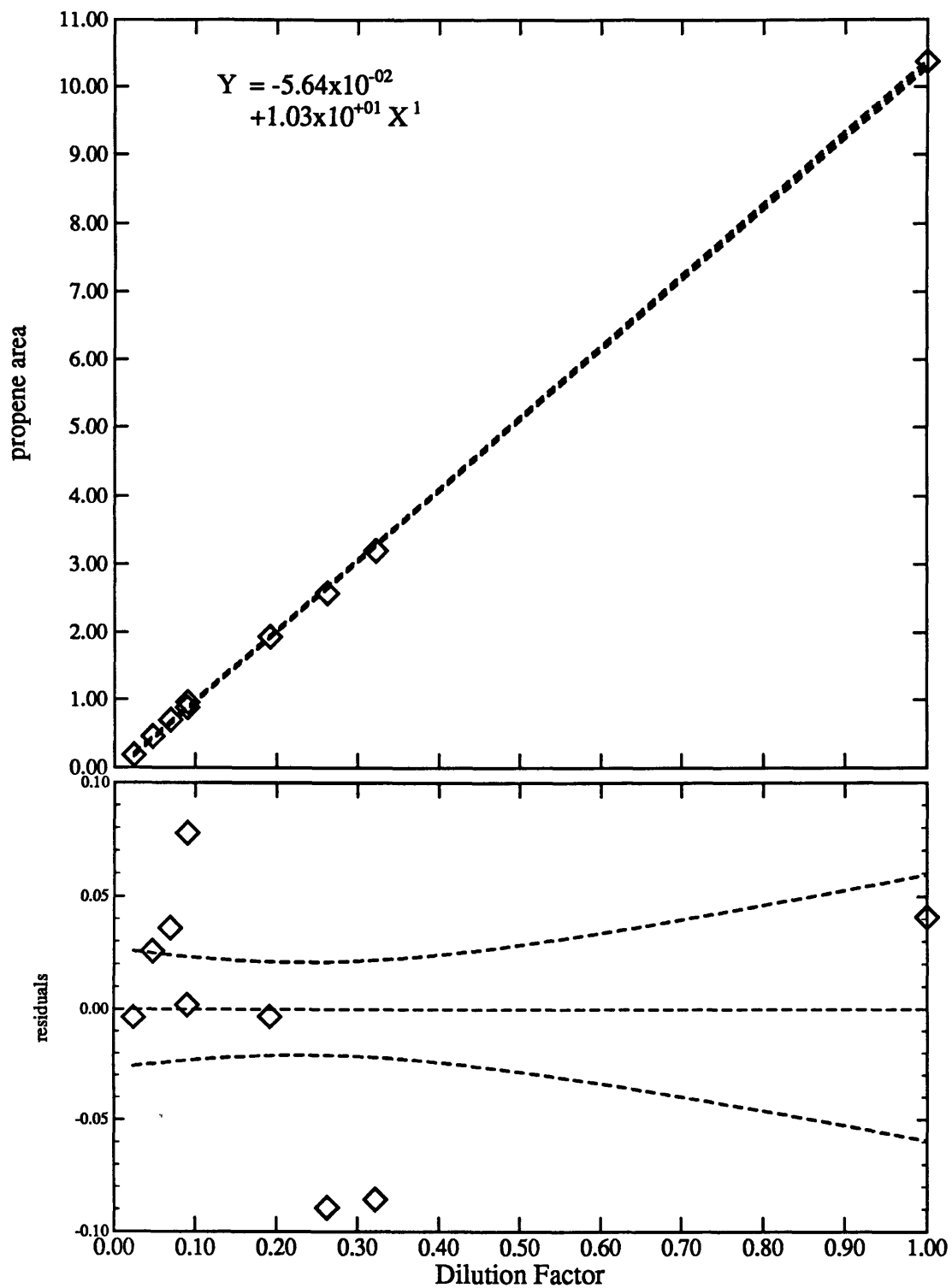


Figure 3.5.1. Linearity check for propene. Propene is shown here as a typical NMHC.

The response term, m_i , in equation 3.5.7 has now been separated into 4 components; $m_i = I_i c RMR_i e_i$. We emphasize that all of the terms in 3.5.10 will be time dependent, meaning that they all must be either controlled or measured. The utility of the RMR appears when we divide the response to one compound by the response to another:

$$\frac{A_i}{A_j} = \frac{I_i RMR_i e_i \chi_i v_i}{I_j RMR_j e_j \chi_j v_j} \quad (3.5.11)$$

The common response term has gone away. We will generally report instrumental response not as an area but as an area per unit volume as heptane (ie, divided by the RMR),

$$R_i = \frac{A_i}{I_i RMR_i v_i} \quad (3.5.12)$$

The integration efficiency is retained because it conveniently carries the uncertainty associated with integration, and because it serves as a reminder that there may be systematic errors associated with the integration. Substitution of 3.5.12 into 3.5.11 yields

$$\frac{R_i}{R_j} = \frac{e_i \chi_i}{e_j \chi_j} \quad (3.5.13)$$

If the system efficiencies are the same, 3.5.13 allows one to calibrate a system with a single hydrocarbon standard; medium-weight alkanes are frequently used (ie, Greenberg and Zimmerman, 1984, used neohexane). However, by far the safest way of eliminating e_i is to calibrate with the same compound at a mixing ratio close to the sample mixing ratio. Because of this, we favor producing standards containing all the hydrocarbons to be analyzed.

3.6 Tank Stability

In studying the stability of various compounds in the standard tanks, we encounter many of the issues important to field measurements. We shall therefore consider this issue before turning to that broader issue. Good tank stability is critical to both primary standards maintained in the laboratory and secondary standards taken into the field; while permeation tubes can be constantly weighed to verify that the permeation rate is constant, the only direct calculation of mixing ratios in a tank standard is carried out when the tank is manufactured. After that, the most reliable way to again measure the mixing ratios in the tank is to compare it to a fresh tank which has not had time to degrade.

One method commonly used to assess the stability of primary standards is to regularly intercompare different tanks from a common batch. While this will effectively detect "rogue" tanks, it will not detect systematic drifts common to a set of similar tanks. If several tanks have similar construction and preparation, contain nearly identical gas mixtures, and are kept at nearly identical pressures, homogeneous gas-phase reactions and some wall losses will proceed at similar rates in the various tanks and thus evade detection by simple tank inter-comparisons. If we consider two species (or one species in two tanks) whose concentrations are changing exponentially with time:

$$\begin{aligned}
 I_i &= \chi_{i0} e^{a_i t} \\
 Ra_{ij} &= \frac{R_i \chi_{i0}}{R_j \chi_{j0}} e^{(a_i - a_j)t} \\
 &= Ra_{ij0} e^{T_{ij} t} \\
 T_{ij} &= a_i - a_j.
 \end{aligned}
 \tag{3.6.1}$$

This expression is quite general, and it shows clearly the basic problem confronting anyone attempting to assess compound stability (in one tank or in an ensemble of tanks) without repeatedly manufacturing new standards with techniques that do not drift. The only solid information obtainable from these intercomparisons is the *difference* in trends between two compounds. The individual trends can be adjusted by any arbitrary constant without affecting the resulting difference. This problem renders particularly questionable those techniques which rely only on repeated intercomparisons of an ensemble of very similar tanks. A drift common to all of the tanks would go completely undetected. Standards can be prepared in different types of tanks, at different pressures and with different mixes of gases. This will help to expose many potential drift problems.

Another method, which we prefer and use, relies on intercomparisons among various compounds in the same mixture. Our NMHC standards are mixtures of some 20 compounds, ranging in reactivity from ethane to the pentenes. It is therefore improbable that each compound would interact similarly with the storage tank, so we assess compound stability by monitoring the ratio R_i/R_j for all compounds. Our assumption is that we have a diverse enough mixture, ranging from alkanes with very long lifetimes to alkenes with very short lifetimes, that any common trend among the constituent compounds will be very much smaller

than the relative trends among them. Returning to 3.5.11:

$$\frac{A_i}{A_j} = \frac{I_i \text{RMR}_i e_i \chi_i v_i}{I_j \text{RMR}_j e_j \chi_j v_j} \quad (3.5.11)$$

$$= \frac{I_i \text{RMR}_i e_i \chi_i}{I_j \text{RMR}_j e_j \chi_j} \quad (3.6.2)$$

we see that ratioing compounds in the same tank not only eliminates any common instrumental response drift, it eliminates the injected volume term as well (for a linear detector). Our experience has shown that for our compounds even the common instrumental response is very stable for our FID. The RMR are much more stable. As usual, this measurement cannot distinguish between changes in χ and changes in either the two efficiency terms, or the RMR. For this reason, chromatographic conditions should be kept constant over the entire period for which tank stability is tested.

We currently have a record of repeated chromatographic measurements of the first tank that we prepared (tank 1) spanning more than one year. These are shown graphically in Figure 3.6.1, in the form of peak area ratios of the various hydrocarbons in the tank to ethane. Ordinate tick-marks correspond to 1 percent changes in ratio. The gap in the data from roughly days 60 to 180 is the time when our instrument was either on Akademik Korolev during the SAGA 3 experiment or in transit; the tank was also on the cruise, serving as our working standard. In Figure 3.6.1 two least squares fits are shown for each set of ratios; the fit shown spanning the entire figure with a solid line encompasses all of the data, while the fit shown with a dashed line encompasses only that data which it spans (the data taken since SAGA 3). The confidence bands in each case are 67 percent limits of the modeled function. The results of these fits are tabulated in Table 3.6.1, which lists the trends in percent per year along with uncertainties and the r-values for each linear fit. The fits are quite evidently poor and in many cases the direction of the trend reverses itself when the pre-SAGA data is excluded. The trends are also relatively small, however, seldom exceeding 5 percent over the year represented, and there is little evidence that the variations represent a trend rather than simply random deviations from a mean value. During SAGA 3, the chromatographic conditions we used for NMHC analysis were changed. This change is obvious in the figures, which serves to emphasize the importance of keeping the chromatographic conditions constant during tank trend studies. Even with the more stable conditions since the cruise, seemingly random variations in the various ratios considerably exceed the variability on any given day,

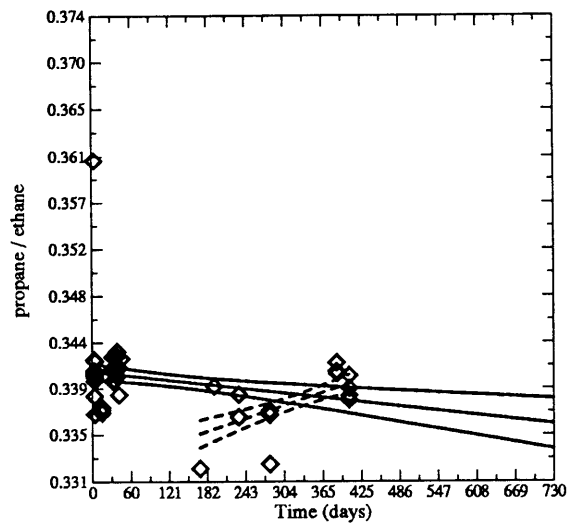
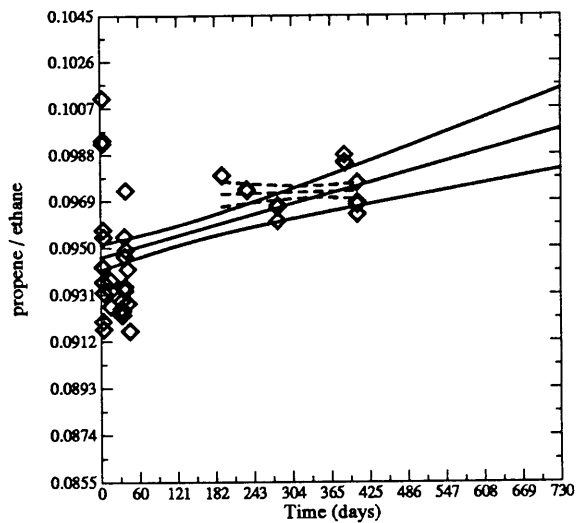
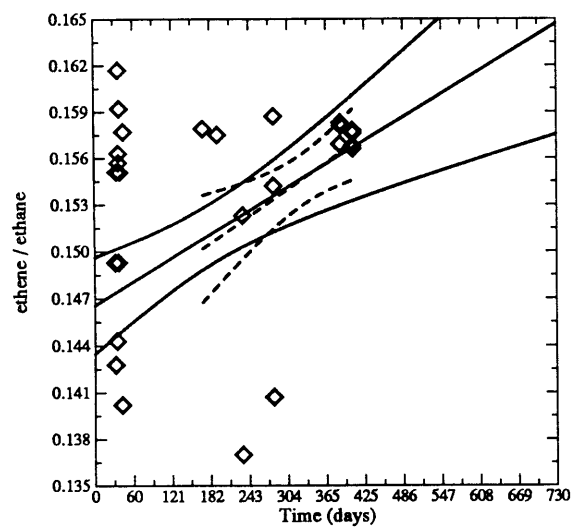
suggesting that the RMR, while more stable than the overall instrument response, may be subject to causes of variation that we have not yet identified. Variability in the efficiencies retained in equation 3.6.1 could also have caused the observed variations in these ratios. In order to minimize the chance that either the RMR, the integration efficiencies, or the system efficiencies will cause variability in these measurements, future work on standard stability should be done with a GC dedicated to the task, with an unchanging method.

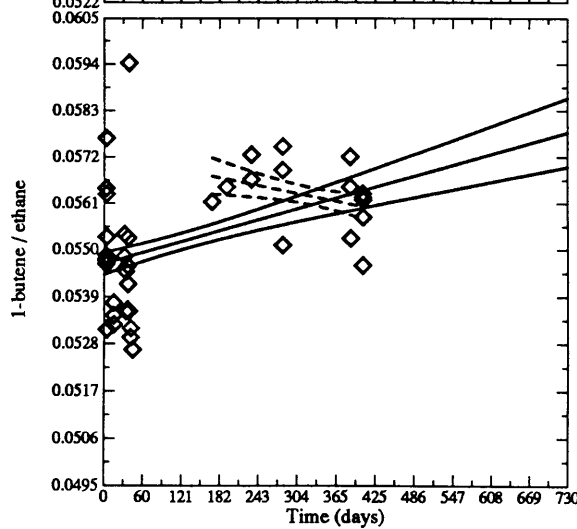
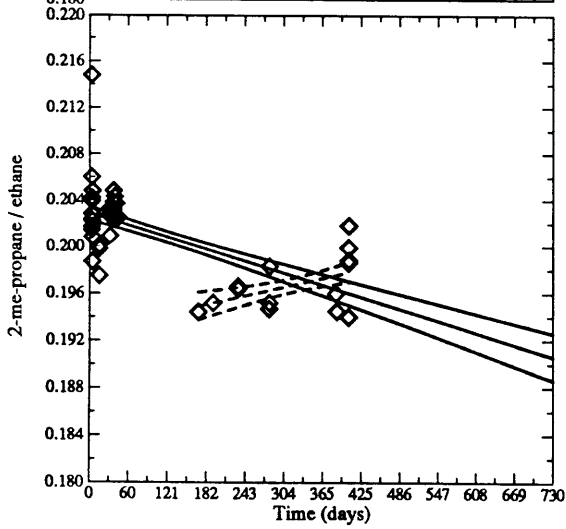
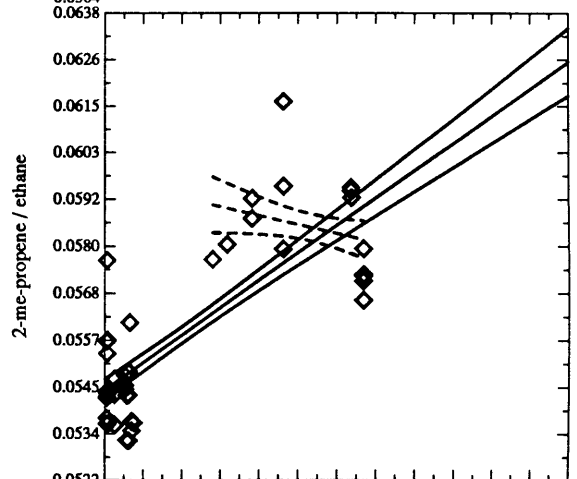
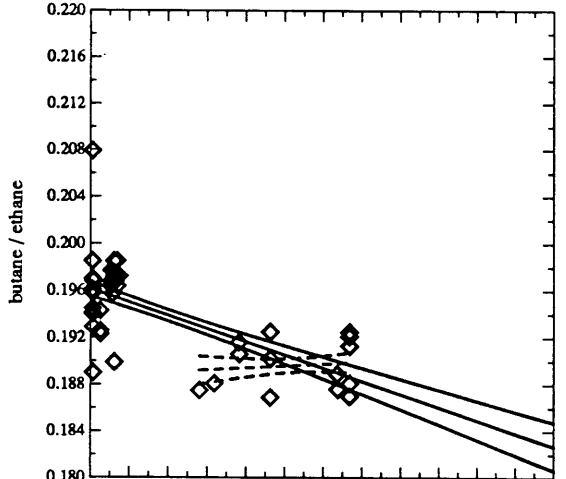
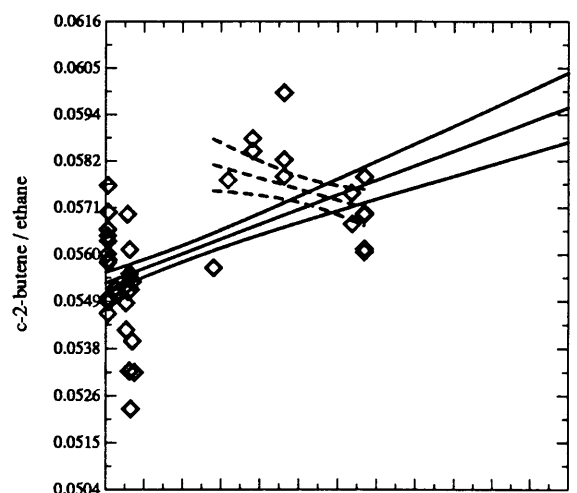
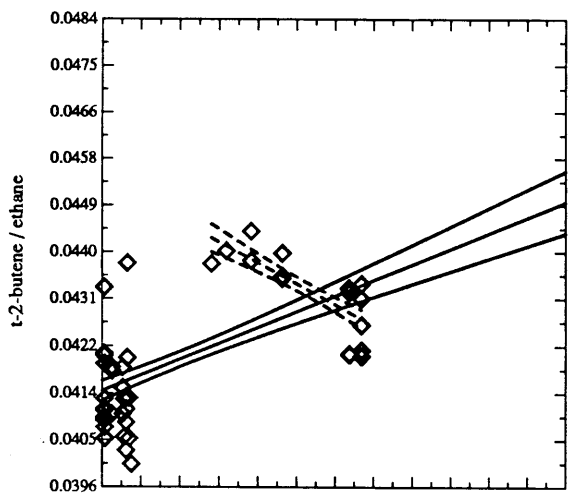
Based on the plots and least squares fits, we can conclude that there is little evidence that many mixing ratios in this tank have changed by more than 5 percent during the past year, relative to ethane. There is, however, no proof that changes smaller than that have not occurred, with the possible exception of propane and ethane, which appear to be quite stable with respect to each other. One thing not shown in the figure is the record of ethene over the first 30 days; the ethene areas increased from values we considered to be unreasonably low to levels we consider to be reasonable during this period. Ethene was one of the last (though not the last) compound added to the tank as it was made, so we have tentatively concluded that it was not well mixed until day 30. The two other possible explanations are that the ethene was produced during this time, or that it initially deposited on the walls of the tank, then came back off of the walls during those first 30 days. It must also be noted that the discontinuity before and after SAGA3 need not be due to changed chromatography; either rapidly progressing reactions begun when the tank was made or chemistry induced by the month and more the tank spent in the tropics could have caused real changes in the constituent mixing ratios. Regardless of these concerns, over the past year the tank has been stable compared to the precision to which we know the relative mixing ratios in it, which is roughly 10 percent. In the future, as the precision and accuracy of our standards production improves, these concerns will become more important.

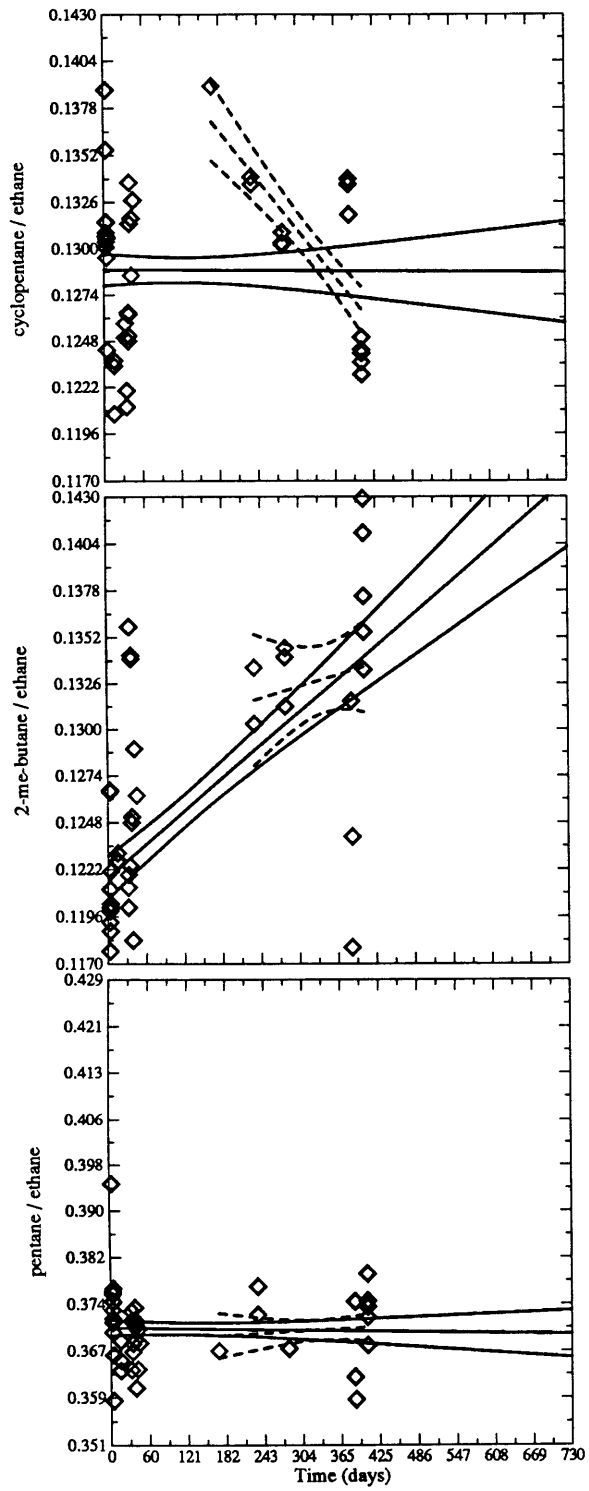
Independent linear least squares fits to the time series of each of these ratios is not the optimal technique for determining the relative trends of each constituent in the tank. One set of ratios, using a stable compound as the base (denominator), contains all of the information about the tank, but there is considerable covariance among the various ratios. There should be. We shall outline the use of the Kalman filter, as described in Gelb (1974), to optimally estimate the trends of the constituents. Optimal estimation techniques described in Gelb (1974) are also designed specifically to continually revise estimated parameters as

Figure 3.6.1

The one-year record of the first static dilution tank manufactured (with a two-year range). Shown are the ratios of the various peak areas to ethane, in addition to two linear fits with 67 percent model confidence limits. Ordinate tick marks correspond to roughly one percent changes in ratio. The first fit (shown as a solid line spanning the entire frame) includes all the data, while the second fit (shown as a limited dashed line) includes only data gathered after the SAGA 3 cruise. Note that the deduced trends are quite different for the two fits, often even changing sign. There are two possible causes for this: either the concentrations in the tank actually jumped, or system changes made during SAGA 3 led to slight (a few percent) changes in the relative response to the various hydrocarbons. Similar stepwise behavior for both alkanes and alkenes tends to favor the second possibility.







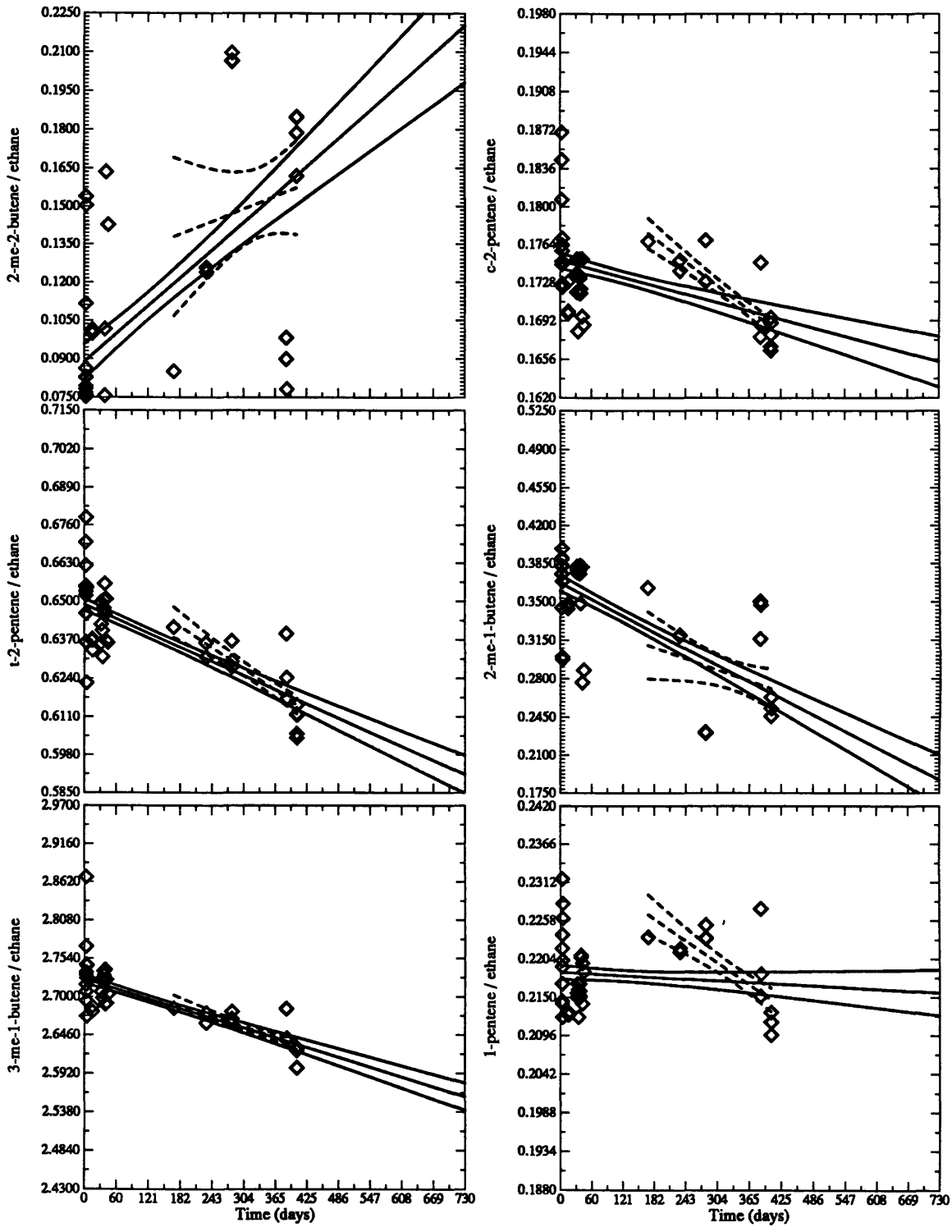


Table 3.6.1 Least-squares trends for the first standard tank.

| Compound | All Data | | | After Saga | | |
|---------------|--------------------|-----|------|--------------------|------|------|
| | % yr ⁻¹ | ± | r | % yr ⁻¹ | ± | r |
| ethene | 6.2 | 3.2 | 0.35 | 7.1 | 4.8 | 0.38 |
| propane | -0.7 | 0.4 | 0.26 | 1.8 | 0.8 | 0.61 |
| propene | 2.8 | 1.8 | 0.4 | 0.2 | 0.1 | 0.68 |
| 2-me-propane | -3.0 | 0.6 | 0.63 | 2.3 | 1.3 | 0.45 |
| butane | -3.4 | 0.6 | 0.65 | 0.5 | 1.3 | 0.12 |
| t-2-butene | 4.3 | 0.8 | 0.62 | -5.2 | 1.2 | 0.77 |
| 1-butene | 2.8 | 0.9 | 0.44 | -2.0 | 1.5 | 0.33 |
| 2-me-propene | 7.5 | 0.9 | 0.78 | -2.2 | 2.4 | 0.25 |
| c-2-butene | 3.8 | 0.9 | 0.56 | -2.7 | 2.1 | 0.33 |
| pentane | -0.1 | 0.6 | 0.04 | 0.6 | 2.0 | 0.08 |
| 2-me-butane | 9.1 | 1.8 | 0.62 | 13 | 8 | 0.43 |
| cyclopentane | 0.0 | 1.3 | 0.01 | -11 | 3 | 0.74 |
| 3-me-1-butene | -3.0 | 0.4 | 0.75 | -2.4 | 0.08 | 0.78 |
| t-2-pentene | -4.4 | 0.6 | 0.76 | -6.6 | 1.5 | 0.78 |
| 2-me-2-butene | 74 | 15 | 0.62 | 24 | 50 | 0.14 |
| 1-pentene | -0.7 | 0.9 | 0.12 | -7.9 | 2.3 | 0.69 |
| 2-me-1-butene | -24 | 4 | 0.71 | -18 | 18 | 0.28 |
| c-2-pentene | -2.7 | 0.8 | 0.47 | -7.4 | 1.5 | 0.82 |

These are the trends, in percent per year, shown in Figure 3.6.1, along with the trend error and the correlation coefficients for each fit. The first set of values is for fits including the entire set, while the second set is for fits including only data gathered after our participation in the SAGA 3 expedition. Note that many trends reverse sign.

new sources of information are obtained. The techniques are ideally suited to the problem of maintaining a set of standards whose values are to be estimated from several different sources of data (in our case, the calibration values from the three absolute techniques we have described). We have not been able to apply the filter directly to the existing standard, because it is sensitive to the model being sufficient to describe the data. The fluctuations in response from month to month often greatly exceed the noise observed on a given day, which causes the Kalman filter to diverge exponentially. While the estimated error in individual groups of measurements can be arbitrarily increased until the filter becomes stable, this also eliminates the ability of the filter to correctly assess the error in estimated parameters, which is the reason for using it. The existing data simply cannot be well enough described by a line to warrant using a Kalman filter with a linear model. Our assumption is that future tank data will be of higher quality.

The Kalman filter applies to systems developing in time for which one has a set of

measured parameters (in our case the ratios) which are not the ones one wants to actually know. Assuming that the measured and unknown quantities can be related through a linear model, the situation at time t can be written as:

$$\mathbf{A}_t = \mathbf{P}_t \mathbf{a} + \mathbf{s}_t \quad (3.6.3)$$

$$\boldsymbol{\alpha}_t = \mathbf{a}_t + \boldsymbol{\sigma}_t \quad (3.6.4)$$

where

\mathbf{A}_t = the array of observed ratios,

\mathbf{a} = the array of parameters describing the system (ie, slopes and intercepts in our case),

\mathbf{P} = the partial derivative matrix modeling the relationship between \mathbf{A} and \mathbf{a} ,

\mathbf{s}_t = the array of errors in the observations

$\boldsymbol{\alpha}_t$ = the optimally estimated array of parameters \mathbf{a}

$\boldsymbol{\sigma}_t$ = the array of errors in the optimal estimation.

To apply the Kalman filter, we assume that the unknown parameters \mathbf{a} are invariant, and start with an initial guess at time t_0 of both the unknowns themselves and the variance-covariance matrix containing the optimally estimated uncertainties of the unknowns. The working equations of the Kalman filter are:

$$\boldsymbol{\alpha}_t = \boldsymbol{\alpha}_{t-1} + \mathbf{G}_t [\mathbf{A}_t - \mathbf{P} \boldsymbol{\alpha}_{t-1}] \quad (3.6.6)$$

$$\mathbf{C}_t = \mathbf{C}_{t-1} - \mathbf{G}_t \mathbf{P}_t \mathbf{C}_{t-1} \quad (3.6.6)$$

$$\mathbf{G}_t = \mathbf{C}_{t-1} \mathbf{P}_t^T [\mathbf{S}_{pt} + \mathbf{N}_t]^{-1} \quad (3.6.7)$$

$$\mathbf{S}_{pt} = \mathbf{P}_t \mathbf{C}_{t-1} \mathbf{P}_t^T \quad (3.6.8)$$

$$\mathbf{S}_{at} = \mathbf{P}_t \mathbf{C}_t \mathbf{P}_t^T \quad (3.6.9)$$

where

\mathbf{G}_t = the Kalman gain matrix for timestep t ,

\mathbf{C}_t = the variance-covariance matrix of the optimally estimated parameters,

\mathbf{N}_t = the noise matrix; the variance-covariance matrix of the observations,

\mathbf{S}_{pt} = the predictive uncertainty matrix, used in conjunction with the noise matrix to find the gain matrix, and

\mathbf{S}_{at} = the analyzed model uncertainty matrix; the confidence interval in the case of one dependent variable.

The array α and the matrix C , along with the matrix S_{at} , are the outputs of the filter, given inputs A and N . From equation 3.6.5 we can see that α is updated by applying the gain matrix G to the difference between the observations at time t , A_t , and the model prediction of those observations, $P\alpha_{t-1}$, based on the optimal estimation of the parameters at time $t-1$. The greater the disagreement between model and observations, and the greater the gain, the larger will be the adjustment made to α . Equation 3.6.6 shows a similar situation for the variance-covariance matrix C ; it will tend to decrease in time, provided that the gain is high and the model is sensitive to the parameters (ie, P is large). This is akin to the standard error of the mean decreasing with increasing N . Finally, equation 3.6.7 generates the gain itself, which will be large if the model is potent, the covariance matrix is large (indicating that the filter is not confident in the parameter estimations and will thus allow large changes), and uncertainties (the sum of the model uncertainty S_{pt} and the observational noise N) are small. We include the two model uncertainty matrices S because they help clarify the filter and because S_{at} is a multi-dimensional version of the confidence interval used in standard least-squares analysis, including covariance among the predicted quantities. Thus considered, the Kalman filter is a very intuitive beast.

The filter can be applied to any linear model which can adequately describe a set of measurements. In our case, we assume that each ratio can be described by a linear trend:

$$A_{ij} = a_{ij0} + a_{ij1}t \quad (3.6.10)$$

where from 3.6.1,

$$a_{ij1} = a_{i1} - a_{j1} \quad (3.6.11)$$

which generates the coupling of the various A_{ij} . Given a set of n peaks, there are $n-1$ independent A_{ij} , using a well chosen base compound for j (well chosen meaning a compound which appears to fit 3.6.10 well), all coupled through j . Note that j in these equations is not really an index, but rather an indicator of the base compound; A_{ij} is an array in i of $n-1$ elements, while N_{ikj} is an $n-1 \times n-1$ square matrix. If the area of each peak is

$$a_i + s_i, \text{ or } a_i(1 + d_i), \quad d_i = \frac{s_i}{a_i} \quad (3.6.12)$$

where s_i is the error in the observation,

$$A_{ij} = \frac{a_i}{a_j} \frac{1 + d_i}{1 + d_j}$$

$$\simeq \frac{a_i}{a_j} (1 + d_i - d_j), \quad (3.6.13)$$

$$d_{ij} = d_i - d_j \quad (3.6.14)$$

$$s_{ij} = (d_i - d_j) \frac{a_i}{a_j}$$

assuming that the errors are small ($d \ll 1$). The noise matrix N is the variance-covariance matrix of the expectation values of the various products $s_{ij}s_{kj}$:

$$\begin{aligned} N_{ikj} &= E[s_{ij}s_{kj}] \\ &= E[(d_i - d_j)(d_k - d_j)] \frac{a_i}{a_j} \frac{a_k}{a_j} \\ &= E[d_i d_k + d_j d_j - d_i d_j - d_k d_j] \frac{a_i a_k}{a_j^2} \end{aligned} \quad (3.6.15)$$

If there is no covariance (aside from common instrumental drift) among the various peak areas themselves, the two negative terms will drop out, leaving

$$N_{ijj} = (d_i^2 + d_j^2) A_{ij}^2 \quad (3.6.16)$$

for the diagonal terms, and

$$N_{ikj} = d_j^2 A_{ij} A_{ik} \quad (3.6.17)$$

for the off-diagonal terms. Clearly, one criterion for choosing a base compound is that it be well separated from other compounds, thus reducing the possibility that it will co-vary with the others.

To construct the Kalman filter for this problem, we shall re-write 3.5.10, given m independent observed ratios ($m = n-1$) and p model parameters ($p = 2m$),

$$A_{ij} = a_i + a_{i+m}; i = 0, \dots, m-1 \quad (3.6.18),$$

we can write down the partial derivative matrix,

$$\begin{aligned} P_{ikj} &= \frac{dA_{ij}}{da_k} \\ &= 1; k = 1, \\ &= t; k = i + m, \\ &= 0; \text{ all others.} \end{aligned} \quad (3.6.19)$$

The final step is to concoct a good first guess of both the model parameters and their uncertainties. We suggest initializing the parameters with the intercepts equal to the initial ratios and the slopes equal to zero. The variance-covariance matrix C should be initially diagonal, with elements corresponding to intercept errors equal to the appropriate diagonal terms from the initial noise matrix N , and slope errors equal to a value suggested by the data, perhaps 5 percent per year. Note that for two compounds and thus one independent ratio, the Kalman filter with a good first guess and a weighted least squares fit produce identical results on randomly generated data. In a test with identically small errors in random data, the slope errors in 20 ratios were roughly 12 percent smaller with the coupled Kalman filter than with individual least squares fit. Aside from this modest decrease in uncertainty, the additional advantages in the optimal estimation methods are their ability to quantitatively accrete information as it is generated from several sources, assuming that the information has realistically estimated error.

In the future, data about tank stability will come not only from this RMR method, but also from repeatedly generated dilution standards, both permeation tubes and capillary flow devices, as well as tank standards manufactured at intervals rather than in a group. Comparison to the independent standards introduces their absolute uncertainty into the stability analysis, which is a drawback, but eliminates any variation in the RMR. The overall success of the stability studies thus depends on both reducing absolute errors and reducing or at least quantifying the variability of the RMR. The great power of the optimal estimation methods is their ability to absorb these various inputs, once their errors are properly defined.

3.7 Standard Intercomparisons

The results of intercomparisons of the three standards are shown in Table 3.7.1. The primary calibration goal was to calibrate our working standard (tank 1), so, as was described in section 3.1, the intercomparison is framed in terms of assignments of the mixing ratios in tank 1. Our current accepted calibration is based on tank 2, and the steps in calibrating tank 1 from tank 2 are detailed in the first four columns of Table 3.7.1. These show in turn: the tank 2 mixing ratios, the ratio of these mixing ratios to analyzed peak areas, the relative molar response expected on the FID for each compound, and the product of the latter two values. Mixing ratios enclosed in parentheses are highly uncertain. We draw two major conclusions

Table 3.7.1 Standard Intercomparisons

| Compound | Tank 2 RMR | | | | Tank 1 Cal | | | |
|---------------|------------|----------|-----|--------------|------------|----------|----------|-----------------|
| | χ | χ/A | RMR | $\chi RMR/A$ | χ_o | χ_p | χ_a | χ_a/χ_p |
| ethane | 9940 | 370 | 191 | 7071 | 1752 | | 4666 | |
| ethene | 1898 | 380 | 204 | 7746 | 350 | | 630 | |
| propane | 4548 | 253 | 293 | 7425 | 812 | 868 | 1025 | 1.18 |
| cyclopropane | 951 | 216 | 306 | 6613 | | | | |
| propene | 958 | 253 | 306 | 7733 | 171 | | 283 | |
| 2-me-propane | 1914 | 191 | 394 | 7510 | 344 | (231) | 442 | (1.91) |
| butane | 1907 | 194 | 394 | 7675 | 344 | 284 | 427 | 1.50 |
| t-2-butene | 507 | 135 | 408 | 5524 | 88 | 66 | 94 | 1.42 |
| 1-butene | 480 | 191 | 408 | 7780 | 87 | 121 | 122 | 1.01 |
| 2-me-propene | 479 | 205 | 408 | 8189 | 88 | 143 | 126 | 0.88 |
| c-2-butene | 478 | 201 | 408 | 8197 | 88 | 90 | 129 | 1.43 |
| pentane | 1876 | 156 | 496 | 7752 | 347 | 600 | 655 | 1.09 |
| 2-me-butane | 1873 | 155 | 496 | 7757 | 96 | (670) | 234 | (0.35) |
| cyclopentane | | | | | 170 | | 229 | |
| 3-me-1-butene | 499 | 157 | 510 | 7817 | 4685 | 3685 | 4611 | 1.25 |
| t-2-pentene | 481 | 160 | 510 | 8140 | 203 | 2153 | 1089 | 0.50 |
| 2-me-2-butene | 477 | 127 | 510 | 6487 | 86 | 171 | 294 | 1.72 |
| 1-pentene | 481 | 165 | 510 | 8430 | (178) | | 386 | |
| 2-me-1-butene | 939 | 206 | 510 | 10491 | 172 | 1087 | 459 | 0.47 |
| c-2-pentene | 478 | 167 | 510 | 8532 | 160 | 446 | 298 | 1.32 |

Intercomparison of two static dilution tanks and permeation tubes and the resulting mixing ratio assignments for the working standard (tank 1). The first four columns are a check of the relative molar response model against tank 2, where χ is the mixing ratio in the tank in ppbv, (see table 3.3.1), χ/A is the mixing ratio divided by the integrated peak area, RMR is the relative molar response factor (eqn. 3.5.9), and $\chi RMR/A$ is the ratio of observed to expected response for each compound, neglecting a proportionality constant. The next three columns are three different assignments of the mixing ratios in tank 1. χ_o are the original assignments made when tank 1 was prepared, χ_p are based on a comparison of tank 1 with the permeation tube standards, and χ_a are the assignments based on a comparison of tank 1 with tank 2, adjusted for a mean RMR ratio of 7730. χ_a is the assignment actually used. The last column shows the ratios of the second and third assignments.

from this table: the tank 2 standard is consistent with the relative molar response model; and both the tank 1 initial assignments and the permeation tubes show mixed consistency with tank 2.

Column 4 of Table 3.7.1 shows the ratio of the expected relative molar response and the

actual response (A/χ) for each compound in tank 2. Were both the model and our assessment of relative concentrations in tank 2 correct, all the numbers in column 4 would be the same. The actual numbers do show fair agreement. Specifically, the mean ratio is 7700, plus or minus 1000 (13 percent) for all compounds, and plus or minus 560 (7.5 percent), excluding the two outliers. There are no obvious groupings; variability is as large within a chemically related group, such as the butene isomers, as it is between groups. There appears to be a consistent relationship between the ratios (RMR/R and carbon number for the alkanes, with the ratio proportional to carbon number, but there is no such relationship discernible for the alkenes. This apparent relationship for the alkanes is the only seemingly non- random feature in column 4 of the table. We cannot now say whether the observed variance is due to imprecision in the standards or limitations of the relative molar response model; after we have manufactured many more standards we will be able to examine far more accurately the relative molar response model.

Based on alternating analyses of tanks 1 and 2, we have calibrated tank 1 with tank 2. This is our primary assessment of the mixing ratios in tank 1. We can compare the results of this calibration of tank 1 with the other two calibrations (the original tank assessment and the permeation tubes). Nine of the permeation tubes lead to tank 1 calibrations higher than those based on tank 2, while three lead to lower assignments, excluding the tubes with high uncertainty. Considering only those nine tubes, the ratio between the two sets of assessments is 1.32 ± 0.23 . There is no relationship between these nine tubes and the tubes discussed earlier as showing no signs of expiration. The spotty consistency with permeation tubes is both comforting and disturbing; it is comforting because there is enough agreement between the permeation tubes and the absolute standard to suggest strongly that our absolute standards are good, and it is disturbing because there is no clue in the permeation tube measurements suggesting which tubes should be trusted. The problems with permeation tube leakage we have discussed would tend to lead to overestimations based on the perm tubes, and could also produce the spotty performance. Because the tank standard obeys the relative molar response model, we regard it as our best standard, and all calibrations in the analysis of our field data will be based on this tank. We estimate the precision of the standard to be roughly 10 percent for the relative mixing ratios of all compounds, and the absolute accuracy to be 30 percent for all compounds in the tank. The absolute accuracy may be much better than

that, but we will not be able to confidently assess accuracy until at least two, and ideally all three, of our calibration methods are consistently agreeing.

3.8 Suggestions for future work

In order of priority, we offer the following suggestions for the continuation of this work:

1. A separate chromatographic system must be dedicated solely to the standards work. A very stable method should be employed which might differ from the field instrument method because certain coeluting unknowns will not be in the standards; development of this method should be the first priority. We generally recommend using a method similar to the current one, but adding sub-ambient initial oven temperatures in order to increase light hydrocarbon retention and eliminate the peak-splitting currently present for those compounds.
2. The capillary standards technique now in development should be completed and employed. This will offer a third, independent calibration technique, permitting voting among the three techniques to expose problems in any one of them. The short lifetimes of these devices will be an advantage when standards are developed for highly reactive hydrocarbons which might be unstable in both stainless steel tanks and permeation tubes.
3. The leakage problems in the current permeation tube design should be eliminated. There is every indication that this will be possible, as the rough equality between leakage and permeation flows (favoring permeation in pentane by a factor of two) in the current design suggests that improvements could reduce total leakage to less than 1 percent. Barring that, outward flowing devices should be used, with which dilution is accomplished by diluent surrounding the tube, thus eliminating any possibility of leakage into anything but the diluent. All inward flowing tubes and all capillary devices should be periodically checked for leakage by placing them in dilution chambers and sampling gas flowing around but not through them.
4. Pressure measurements in the static dilution system should be improved. The leading source of error in the static dilutions is pressure measurement (eqn. 3.3.2), caused by a combination of line noise and limitations of the transducer used (Omega). Shielding around the dilution system should be improved, and it should be positioned as far as possible from obvious sources of noise. A higher precision absolute pressure transducer

(MKS) should be purchased which has internal temperature regulation and an integral power supply/readout module in order to minimize noise problems.

5. A suitably stable optimal estimation method should be developed in which all information about standard mixing ratios and their development through time is employed to optimally estimate those mixing ratios at all times.
6. A protocol for making and monitoring standards should be developed and strictly adhered to. This is placed below the other items in priority only because one important aspect of the protocol should be constant techniques. The above suggestions are refinements which should be completed before a firm protocol is established. They are mostly relatively simple refinements and can thus be accomplished in short order. The key elements of the protocol, in addition to invariance, will be:
 - a. Regular, routine, and dense data collection. Tanks should be monitored at a minimum monthly, with at least ten analyses in order to confidently establish the variance and covariance of the data. Permeation tubes and capillary flow devices should be monitored at least as frequently as they are weighed, in order to look for correlations between peak areas and mass-loss rates.
 - b. Careful consideration to sources of systematic error. Permeation and capillary devices must be removed from temperature controlled environments in order to be weighed. The maximum duration of disturbances to their operating temperatures must be calculated for all such devices, and the limits strictly adhered to. Issues such as wall effects for tank standards need to be continually examined, both in the dilution manifold during their manufacture and afterwards in the tanks themselves. Mass-flow controllers and pressure transducers should be regularly calibrated, and in all dilution gases should be regularly examined for blanks.
 - c. Periodic standards production. Standards cannot be made once, then monitored as a group. To ensure stability, new standards must be regularly added to the ensemble. The most pressing problem will be reducing imprecision caused by the introduction of newly generated standards.
7. Some of the more exotic and unstable hydrocarbons should at a minimum be synthesized or purchased at least once, in order to put them in a capillary flow device and determine their retention index on our system. A reasonable order would be their elution order,

which on the PLOT column is alkane - alkene - diene - alkyne, with cycloalkanes eluting relatively earlier for heavier compounds (cyclopropane elutes near propene, while cyclopentane elutes near 2- methyl-butane), and alkynes and dienes generally eluting two to three carbon numbers later than the alkanes.

3.9 Conclusions

Our calibration work so far shows both the advantages of relying on several independent calibration techniques (tanks and permeation tubes in our case) and the pitfalls of relying on only one. Both the tank standard and the permeation tubes were carefully prepared. Error analyses based on theoretical considerations (as well as least-squares fits for the tubes) suggest very good accuracy, on the order of a few percent in each case. Further analysis, independently applied to each set but using theoretical models of FID response, indicate poorer precision in each set; 10 percent excluding outliers for the tank, and 20 percent (excluding one quarter of the data points) for the tubes. Finally, an intercomparison of the two standards shows that the absolute accuracy of these standards for some or all of the compounds may be as poor as 30 percent. Clearly these differences must be pursued and eliminated; because our working standards have proven to be stable, we will be able to revise the absolute assignments used in this work if that should prove necessary. However, the absolute accuracy of these standards is generally sufficient to answer the questions we shall consider in the rest of this work, since current disagreement between various investigators as to the actual NMHC levels in the remote atmosphere is as great as an order of magnitude. Future work should, however, be able to produce standards with absolute accuracies at the 1 percent level.

Chapter 4 - Experimental Work

4.1 Introduction

Between 12 February and 16 March, 1990, we participated in the joint Soviet and American Gases and Aerosols experiment (SAGA 3), aboard the RV Akademik Korolev (Vladivostok), sailing on a zig-zag course from Hilo, Hawaii, to Pago Pago, American Samoa which crossed the equator 5 times with meridional southward legs and diagonal northward legs (Figure 4.1.1). One major objective of the cruise was to measure a comprehensive suite of variables either important to chemistry in the remote marine boundary layer or useful as tracers of non-local influences. Included in this suite were: local ozone (Jim Johnson, NOAA PMEL, and Vladimir Egorov, Laboratory for Atmospheric Monitoring, Moscow), column ozone (Alexander Shaskov, Main Geophysical Laboratory, Leningrad), NO (Arnold Torres, NASA WFF), organic nitrates (Anne Thompson, NASA Goddard, and Eliot Atlas, Texas A&M), carbon monoxide and methane (Kim Kelley, PMEL), dimethyl sulfide (Johnson), C₂–C₅ nonmethane hydrocarbons (in-situ measurements by ourselves and flask samples by Thompson and Atlas), hydrogen peroxide and organic peroxides (Brian Hiekes, URI), organic acids (Bayard Mosher, UNH), ultraviolet insolation (Anne Thompson, NASA Goddard, and FarEast Hydrometeorological Research Institute, Vladivostok), and ²²²Rn (Institute for Applied Geophysics, Moscow).

Two types of NMHC measurements were conducted on the cruise. We carried an in-situ system built around a commercial GC, while Thompson and Atlas filled electropolished stainless steel cannisters for subsequent laboratory analysis. In this work we will focus on the NMHC measurements. The goals of the work, in order of importance, are:

1. To verify the in-situ measurement technique.
2. To assess the role of NMHCs in the OH budget of the remote atmosphere.
3. To observe latitudinal gradients of the longer-lived NMHCs near the ITCZ.
4. To assess the consistency of air and water NMHC measurements with simple local balance models of the NMHCs.

Our original intention was to measure NMHCs in the atmospheric mixed layer only, using an in-situ gas chromatographic system located as far forward as possible to minimize contamination problems potentially associated with a long bow sampling line. Other investigators,

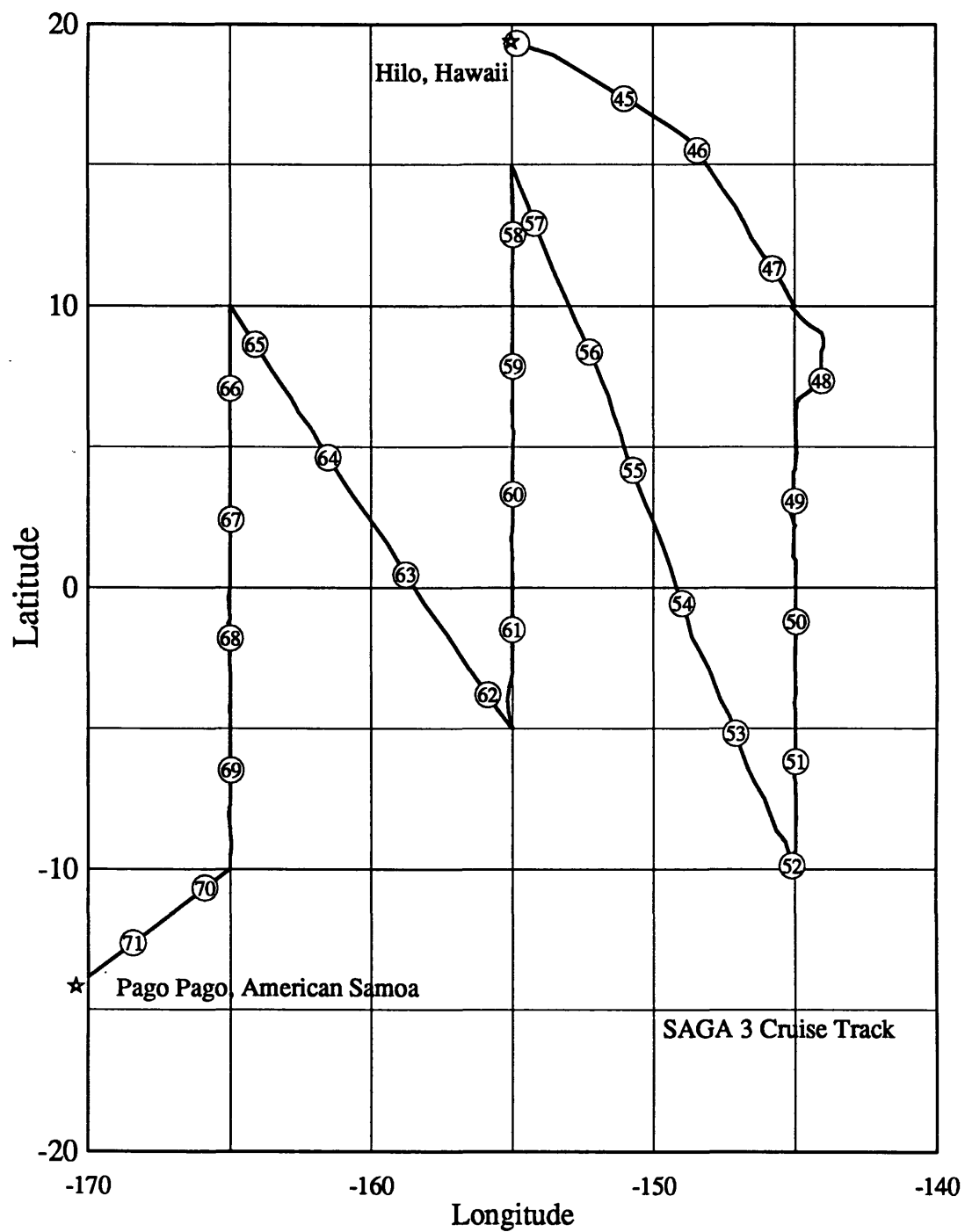


Figure 4.1.1. SAGA 3 cruise track. Julian days (1990) are indicated on the track.

however, brought two high flow sea water equilibrators to measure conservative compounds in ocean surface waters. While equilibration sampling is not ideal for NMHCs, which are sparingly soluble in water and presumably have a biogenic source (Plass *et al.* 1991), we decided to draw samples from the equilibrator, thus providing us with untested water measurements for the final 10 days of the cruise.

It is our belief that technique verification should be ongoing and inherent to the system design. Particularly, we must continually show that air containing oxidants such as ozone can be sampled without destroying the unsaturated hydrocarbons, as suggested by Singh and Zimmerman (1991), and that no significant positive or negative interferences are associated with any part of the sampling procedure, including the sample line, conditioning traps, cryogenic preconcentration, or the chromatography itself. In the in-situ system, these effects were constantly monitored through a cycle of calibration and standard additions in which the standards are treated as much as possible like real air samples. We shall demonstrate that standard additions showed the expected response when a small flow from our working hydrocarbon standard was added to an incoming air sample, indicating that no significant losses occurred in the system for any of the measured compounds under real sampling conditions.

To conclusively establish the importance of each NMHC in the OH budget, the detection limit for each hydrocarbon must be low enough to rule it out as an important OH sink (NMHCs become significant OH sinks at a lower concentration than they become OH sources (Donahue and Prinn, 1990)). The constraint is actually stricter than that; we would like to have a sufficiently low detection limit for each hydrocarbon to assess the collective role of the assembled hydrocarbons in the OH budget. Ideally, we would therefore like to be capable of assessing each hydrocarbon as a contributor to the total OH destruction rate at well below the 1 percent level. Assuming a net OH lifetime of 1 second, we therefore require a detection limit for each hydrocarbon such that its partial contribution to the OH sink is less than 0.01 per second. If we further assume that roughly ten different compounds will have concentrations very near this limit, we would actually like ten times this sensitivity. Table 4.1.1 shows the required detection limit for each hydrocarbon; assuming that the detection limits are similar for all compounds. The overall detection limit should thus be 0.5 ppbv. The table also contains the rate constants for reaction with OH and ozone for each compound, the removal rates due to OH and ozone, assuming 5×10^5 OH per cc and 2.5×10^{11} ozone

Table 4.1.1 Values used in analyzing NMHC data.

| Compound | dl (pptv) | OH | | | O ₃ | | τ (days) | H |
|---------------|--------------|------------------------|------|----------------------------------|------------------------|---|-------------|-------|
| | | k ×10 ¹² | dlnk | k × [OH] (day ⁻¹) | k ×10 ¹⁷ | k × [O ₃] (day ⁻¹) | | |
| ethane | 150 | 0.27 | 0.20 | 0.012 | | | 86 | 20.4 |
| ethene | 5 | 8.52 | 0.15 | 0.37 | 0.18 | 0.04 | 2.5 | 8.8 |
| ethyne | 45 | 0.88 | | 0.038 | | | 26 | 0.98 |
| propane | 35 | 1.15 | 0.30 | 0.050 | | | 20 | 28.9 |
| cyclopropane | 500 | 0.08 | ? | 0.003 | | | 289 | ? |
| propene | 1.5 | 26.8 | 0.15 | 1.12 | 1.13 | 0.24 | 0.73 | 8.6 |
| 2-me-propane | 17 | 2.34 | 0.25 | 0.10 | | | 9.9 | 48.4 |
| butane | 16 | 2.54 | 0.20 | 0.11 | | | 9.1 | 38.7 |
| t-2-butene | 0.6 | 64.0 | 0.20 | 2.8 | 20 | 4.3 | 0.14 | (7.8) |
| 1-butene | 1.3 | 31.4 | 0.20 | 1.36 | 1.1 | 0.24 | 0.63 | 10.3 |
| 2-me-propene | 0.8 | 51.4 | 0.20 | 2.22 | 1.21 | 0.26 | 0.40 | 8.7 |
| c-2-butene | 0.7 | 56.4 | 0.20 | 2.44 | 13.0 | 2.81 | 0.19 | (5.8) |
| pentane | 10 | 3.94 | 0.25 | 0.17 | | | 5.9 | 50.4 |
| 2-me-butane | 10 | 3.90 | 0.40 | 0.17 | | | 5.9 | 48.4 |
| cyclopentane | 8 | 5.16 | 0.20 | 0.22 | | | 4.5 | 7.5 |
| 3-me-1-butene | 1.3 | 31.8 | 0.20 | 1.36 | (1.2) | 0.2 | 0.62 | 22.1 |
| t-2-pentene | 0.6 | 66.9 | 0.30 | 2.89 | (20) | 4.3 | 0.14 | (10) |
| 2-me-2-butene | 0.5 | 86.9 | 0.20 | 3.75 | 42 | 9.07 | 0.08 | (6.3) |
| 1-pentene | 1.3 | 31.4 | 0.20 | 1.36 | (1.2) | 0.3 | 0.62 | 16.3 |
| 2-me-1-butene | 0.7 | 60.0 | 0.30 | 2.59 | (1.2) | 0.3 | 0.35 | (9.7) |
| c-2-pentene | 0.6 | 65.6 | 0.30 | 2.83 | (13) | 2.8 | 0.18 | 9.2 |

Shown are: the threshold mixing ratios (dl) at which each NMHC removes less than 10^{-3} OH per second; the rate constant for reaction with OH at 300 K ($\times 10^{12}$) (Atkinson, 1989), the uncertainty in that rate constant, and the NMHC removal frequency due to ($5 \times 10^5 \text{ cm}^{-3}$) OH, (per day); the rate constant for reaction with O₃ at 300 K ($\times 10^{17}$) (Atkinson and Carter, 1984), and the NMHC removal frequency due to ($2.5 \times 10^{11} \text{ cm}^{-3}$) O₃ (per day); the overall NMHC lifetime in days (τ), and the dimensionless Henry's law constant (H) (Mackay and Shiu, 1981). Values enclosed in parentheses are estimations.

per cc (10 ppbv), the overall compound lifetimes, and Henry's law data used in analyzing equilibrator data. OH rate constants are from Atkinson (1989) while ozone rate constants are from Atkinson and Carter (1984). Note that the required detection limits for essentially all alkenes are below many of the detection limits reported by many investigators who have studied hydrocarbons in the remote atmosphere.

Proper assessment of the remote marine NMHC budgets is very important. Data pub-

in the marine boundary layer (Donahue and Prinn, 1990). Recently, Singh and Zimmerman (1990) have suggested that advection from continental sources could account for the evidently high atmospheric observations, while Koppmann *et al.* (1991) have shown that simultaneous measurements of NMHCs in and above the remote Atlantic ocean may not be mutually inconsistent. In this paper we shall show that the atmospheric distribution of all the observed alkenes and many of the heavier alkanes is consistent with a marine source and not a continental one. However we shall also present sea-water observations which corroborate the existing apparent inconsistency of atmospheric and oceanic observations. We shall discuss five possible (and not necessarily mutually exclusive) explanations of this inconsistency:

1. the marine air measurements are falsely high,
2. the ocean water measurements are falsely low,
3. air-sea flux models under-predict NMHC fluxes,
4. atmospheric models over-predict NMHC column removal rates,
5. continental advection significantly affects NMHC mixing ratios in the remote marine atmosphere.

Assessment of this issue using the measurements that we report here is hampered somewhat because half of the measurements necessary for the comparison, those in the ocean water, are based on a system which we have not been able to test adequately. Our inferences from these combined atmospheric and oceanic measurements will therefore be more suggestive than conclusive. The complete data set from SAGA 3 does, however, allow us to carefully examine atmospheric explanations of this problem, including column removal and the above suggestion that advection from continental sources may be able to explain the observed ethene levels in the remote marine atmosphere, enabling us to eliminate possibilities (4) and (5) from the list.

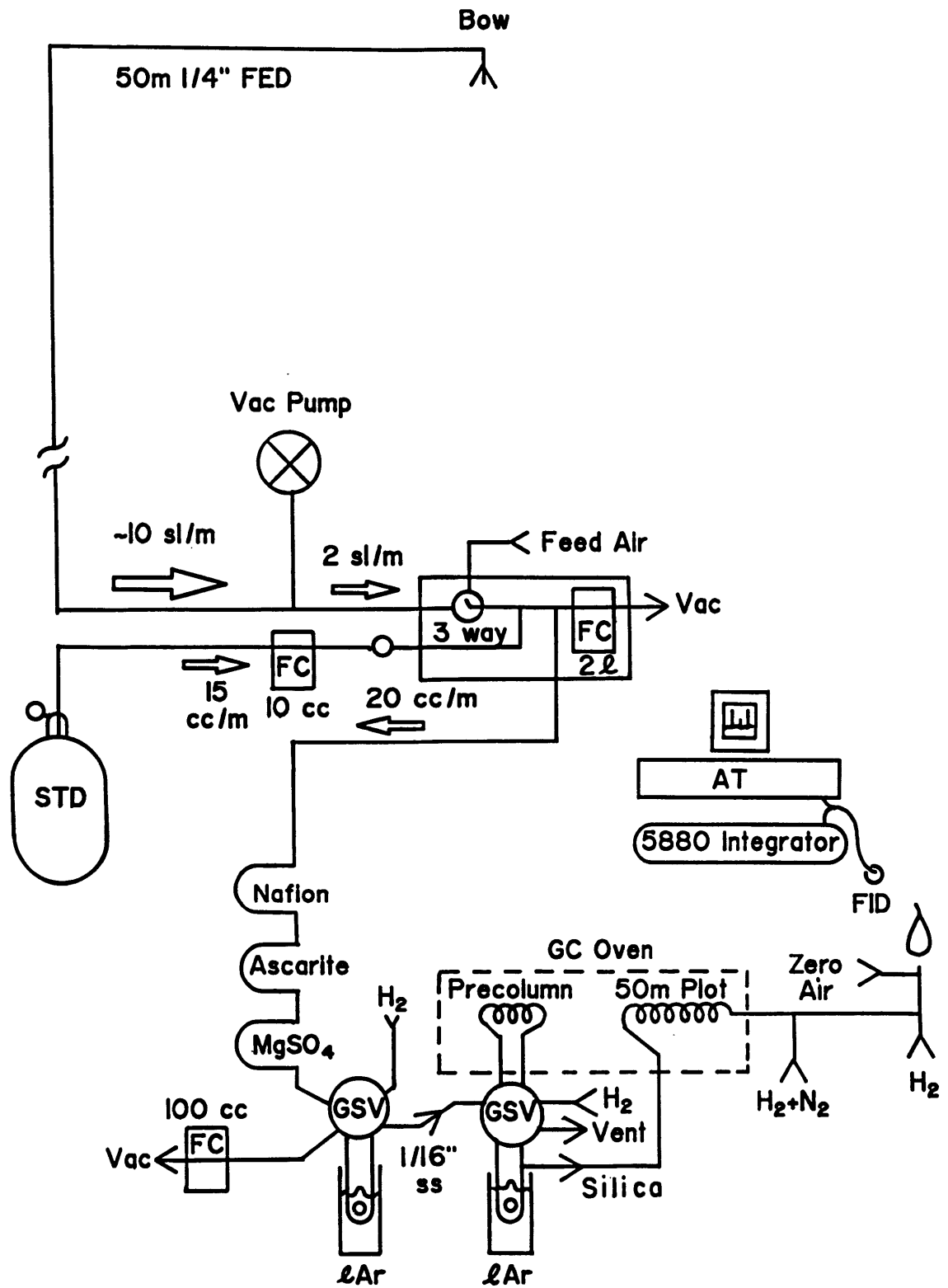
4.2 Experimental

Our system is built around an HP 5880a temperature programmable gas chromatograph equipped with a flame ionization detector. The entire system is shown schematically in Figure 4.2.1. It is based loosely on a system described by Schmidbauer and Oehme (1985). To optimize both separation and detection, we chose to use a medium bore (0.32 mm id) 50 m capillary column internally coated with a porous layer of aluminum oxide (Chrompack

PLOT, the Netherlands). This column can separate C₂ – C₅ NMHCs from each other and from interfering compounds during a temperature programmed 15 minute run, starting at 50 °C and finishing at 200 °C (with three stages; initially isothermal (3 min), followed by a period ramping at 10 °C min⁻¹ (2 min) and culminating in a period ramping at 15 °C min⁻¹. We use H₂ as a carrier gas, as it allows optimal separation at higher flows and over a broader range of flows than either N₂ or He. The exact chromatographic conditions used on SAGA 3 were changed during the cruise in order to better separate various hydrocarbons from unanticipated interfering compounds, but in general the carrier gas was maintained at a 30 psig head pressure, resulting in a roughly 2 scc/m carrier flow. This was supplemented by a make-up flow comprising 10 scc/m of H₂ and 20 scc/m of N₂. Finally, in the detector (held at 300 °C), 25 scc/m of H₂ and 250 scc/m of zero air were added to make a hydrogen-oxygen flame with optimal hydrocarbon sensitivity. A sample chromatogram is shown in Figure 4.2.2. The peaks are consistently very sharp, with peak widths of from 1 to 5 seconds, and can be fit as gaussians with slight to moderate tails.

Gas sampling with a medium bore capillary column requires cryofocusing. Between the sample loop and the column we placed a loop of 0.32 mm id silica tubing. The internal volume of this loop was very small (0.01 cc per coil), so it was swept in less than one second. Before a gas sample was injected, this cryofocus loop was immersed in liquid argon, allowing us to transfer the contents of the sampling loop to the smaller cryofocus loop. Once the transfer was complete, the cryofocus loop was quickly transferred to boiling water to desorb its contents and inject them onto the column. (Since the SAGA 3 cruise we have found that simply pulling the cryofocus loop from the cryogen and leaving it in the air helps to reduce peak splitting for ethane and ethene.) While having two loops added to the complexity of the system, it also allowed us to protect the column from undesirable contaminants by placing a pre-column between the gas sampling loop and the cryofocus loop. Ideally, this pre-column would separate all the constituents of an air sample into two parts: first a part containing all the compounds being analyzed, and second a part containing everything else. With the PLOT column, undesirable compounds are all highly polar species, including water and oxidized organics (the latter bond almost permanently to active sites on the column). Additionally, heavier organics would only force longer intervals between runs and would best be left on the precolumn. A pre-column could be used to separate one sample

Figure 4.2.1. A schematic of the system aboard RV Akademik Korolev. Air was drawn down the 50 meter 1/4 inch FEP teflon line at more than 10 liters per minute by an oil-less vacuum pump. Either 2 sl/min of that flow or 2 sl/min of generated zero air was then drawn into the sampling system. To that flow roughly 1 scc/min of standard from the calibration tank shown could be added. 20 scc/min were drawn from the 2 sl/min sample flow, through three traps, and thence through a 1cc 1/16 inch stainless steel loop immersed in liquid argon. The three traps served to dry the air and remove O₃ and CO₂; Nafion removed most of the water, Ascarite the CO₂, and magnesium sulfate the O₃ and any residual water. Note that both standards and samples (at similar mixing ratios) passed through these traps. No effect on the NMHCs was observed. After collection of from 1 to 3 standard liters of air in the steel loop, the first sampling valve was switched and the collected sample passed onto the pre-column (1 m Al₂O₃-coated PLOT) in order to retard water, polar organics, and heavier NMHCs. After the light NMHCs were collected in a capillary cryofocus loop, also immersed in liquid argon, the second 6-port valve was switched so that the material remaining on the pre-column was backflushed off during the subsequent GC run. Finally, the cryofocus loop was warmed rapidly and a temperature programmed GC run begun, with data collected both on an HP integrator and a personal computer.



stream for analysis on several columns (in our case, we might collect the oxidized organics on a second cryofocus loop at the head of a column designed for polar species). On SAGA 3 our system was simpler than that; we used a short (1 m) piece of Al₂O₃ PLOT column as the pre-column and back-flushed off all of the undesirable compounds after the C₂ – C₅ hydrocarbons eluted at 100 °C.

For direct, 1cc injections, the detection limit of the system was roughly 500 pptv for all hydrocarbons, the increased response for heavier NMHCs being roughly cancelled by increased peak widths. This detection limit was clearly insufficient in light of our requirements. To solve this problem, concentrations in a 1cc gas sample loop had to be boosted by at least a factor of 1000. By immersing the sample loop in liquid argon and drawing through it a controlled flow slow enough that all hydrocarbons are quantitatively trapped on the loop walls, one can cryogenically collect ambient air samples of almost arbitrary size. One must, however, prevent plugging by water vapor, carbon dioxide, or any of the less abundant trace gases. Practically, we could gather 1 - 3 liter air samples without a problem. Once a sufficiently large sample was collected, the sample loop was removed from the cryogen and quickly immersed in boiling water. From that time on the analysis was identical to a direct injection. It is during this cryogenic stage that moderately long lived oxidants can destroy samples. Just as the compounds of interest are trapped in the sample loop, so are oxidants such as ozone. Not only is the ozone concentration enhanced by the same factor of 1000, directly reducing the homogeneous gas phase lifetimes of the more reactive alkenes after evaporation from the loop from several hours to several seconds, but the whole process occurs near a potentially catalytic metal surface. However, laboratory tests prior to SAGA 3 on synthetically generated air streams containing several tens of pptv of C₂ – C₅ alkenes and roughly 100 ppbv of ozone showed no signs of alkene removal during cryotrapping. As an additional safeguard, the magnesium sulfate we used as a desiccant was able to effectively remove at least 100 ppbv of ozone from the sample air stream.

Our goal was to treat samples and standards identically. On SAGA 3 we fell slightly short of that goal, since standards and samples were accorded very similar but not identical treatment. Central to our approaching this goal is a combined sampling/calibration system using electronic mass flow controllers (Tylan Corp). The controllers were all calibrated with gravimetrically calibrated bubble flow meters shortly before and six months after SAGA 3,

Figure 4.2.2.

Example of a processed chromatogram from SAGA 3. This was a 3 standard liter air sample, collected from the bow of the RV Akademik Korolov on 10 March 1990 (JD 69) at 20:30 Z and roughly 10 S, 165 W. This sample contained roughly 450 pptv ethane, 40 pptv ethene, and 5 pptv t-2-butene, to give a sense of scale. This data has been processed with our integration software, which involved the following steps:

1. Peaks were identified by having large second derivatives.
2. All points not identified as peaks or near peaks were considered baseline points. Gaps caused by peaks were filled in, and the baseline data was smoothed with a wide (50 point) filter.
3. The smoothed baseline was subtracted from the data, leaving the chromatogram shown in the figure. Both signal noise and the discrete nature of the data are evident in the baseline residuals; areas where the baseline was curved, such as between propane and propene, show up as "folds" in the discretized processed data.
4. Peaks tentatively identified in (1) were confirmed and valley points adjusted to true minima.
5. Using a simulated annealing procedure, the peaks from (4) were compared against a list of known peak locations, with translation and some stretching allowed. The "minimum energy" configuration resulted in the identifications shown.
6. To determine peak areas, the peaks were each fitted to a tailing gaussian function:

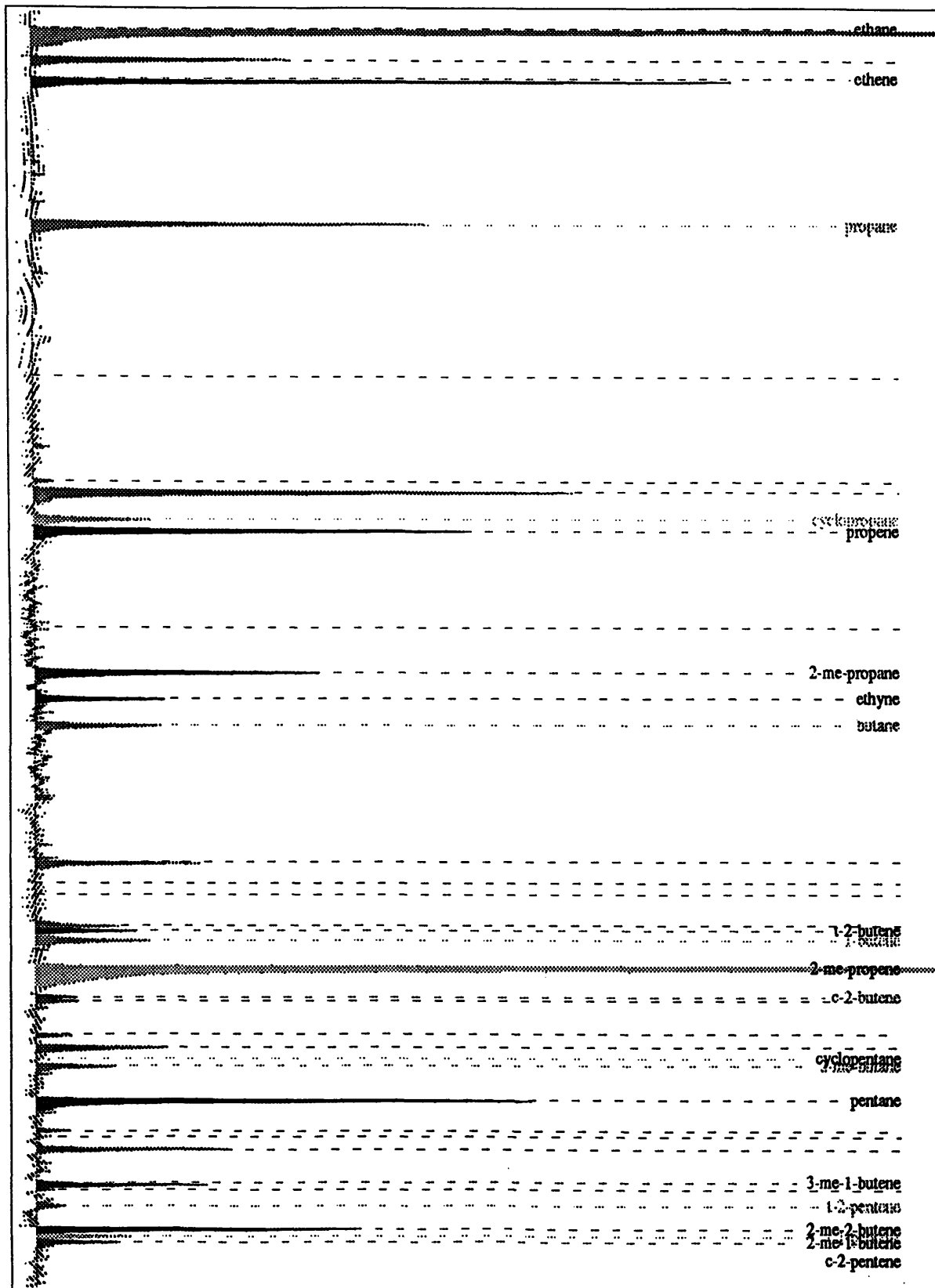
$$f(t) = a_1 e^{-X^2/T},$$

where

X = the normalized distance from the peak center, $X = (t - a_2)/a_3$,

T = a tailing parameter: $T = 1 - a_4 X^{a_5} - a_6 X^{a_7}$ for $X > 0$.

The tailing parameter is 1 for a symmetric gaussian. In addition to fitting all of the identified peaks, the fitting procedure searched for any known but not identified peaks, thus finding a lower concentration limit for each known but undetected compound.



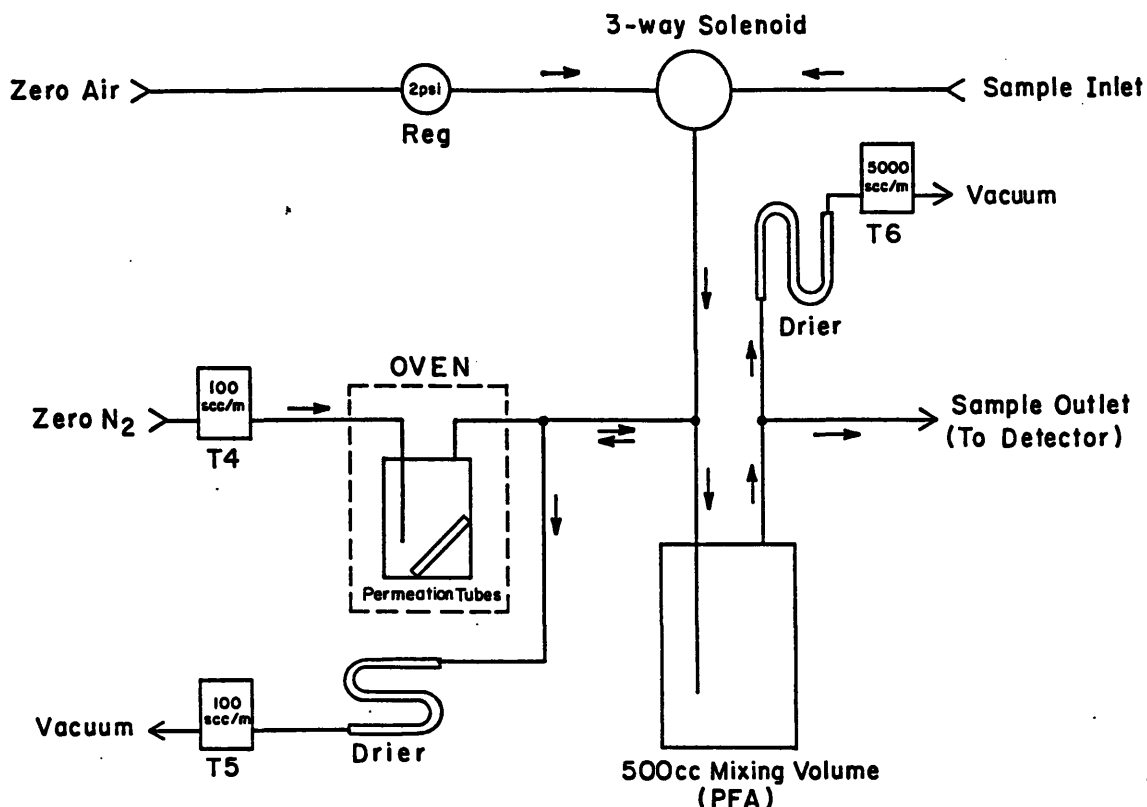


Figure 4.2.3. Detail of our dilution/sampling system. All whetted parts are FEP teflon. Switching between bow samples and generated zero air regulated at slightly above 1 atm is accomplished with the 3-way solenoid valve. Standards from either permeation tubes or a tank may be introduced just up-stream of a mixing volume, and samples are extracted to the GC at a "T" just down-stream of the volume. We currently use a 2 meter 1/8 inch teflon tube as a mixing volume, rather than the indicated 500 cc vessel.

showing no signs of significant change over that period. and the entire system is temperature controlled, preventing any temperature induced drifts. Originally designed for sulfur analysis, the system is built with teflon whetted parts. A detail of the system is shown in Figure 4.2.3. On SAGA 3 we sampled air at the bow, through a 50 m 1/4" FEP teflon line beginning in a funnel facing back toward the ship in order to shield the inlet from sea spray and rain. Tests without the funnel in calm conditions showed the funnel and its configuration to cause no interferences. Sampling was conducted only when the Korolev was underway with a strong effective wind off of the bow. Air samples entered through a 1/4" port into the main flow line, proceeding to a teflon 3-way valve on the main flow line which allowed selection between this sample flow and a pressure-regulated source of hydrocarbon-free zero air. The line terminated at a 5 sl/min flow controller in front of an oil-less vacuum pump. After the

fourth day of the cruise, we configured the system so that in excess of 10 sl/min were drawn through all but the final 3 meters of the main sampling line, where a smaller flow, regulated at 2 sl/min, was shunted from the main flow to the instrument. Before then 2.5 sl/min were drawn down the entire line. Standards were introduced into the main flow line through a "T" below the 3-way valve in the sampling system, which in turn allowed us to switch the main flow between bow and zero air. The standard flow was controlled by a 10 scc/min mass flow controller, generally set to 1 scc/min. In this way the standards were diluted by a factor of 4.80×10^{-4} , from a range of 100 - 1000 ppbv down to a range of 50 - 500 pptv, depending on the compound. All told, there were four possible sample configurations on SAGA 3: pure zero-air could be sampled as a blank, the standard could be mixed with zero air to make a calibration standard, the standard could be mixed with ambient air to make a standard addition as a test for interferences in real air, and pure ambient air could be sampled. The major drawback with this design was that both the zero air and the standard were introduced into the system near the instrument, while the bow sample traveled through a 50 m FEP tube before reaching the sampling system. Thus any contamination or losses occurring in the sample line were not easily observable. A better design would have both the standard and the zero air added very close to the air inlet. Ideally, the sampling line would also be very short. To address these shortcomings on SAGA 3 we conducted several tests, which we will describe in detail later. The first was to connect the bow line to a tank of zero air; the second was to carry the standard to the bow, set its flow with a needle valve, and introduce the standard into the bow sampling line with a short tube; and the third was to vary the flow through the sample line and look for accompanying changes in observed NMHC levels. The test showed that losses were not a problem, though contamination for some compounds could not be ruled out early in the cruise.

Water and carbon dioxide pose special problems when one relies on cryotrapping. Water will quickly clog a sample loop, and even barring clogging, it would severely interfere with the chromatography. CO₂, while uncommon enough not to clog the cryogenic sample loop, could partially clog the 0.32 mm id cryofocus loop, causing a pressure surge at the beginning of each chromatogram and occasionally preventing complete transfer from the sample loop. On SAGA 3, each of these problems was solved with a trap. Water was removed with a semipermeable Nafion membrane (Perma-Pure), or in a magnesium sulfate trap, and generally

with both, the Nafion acting as a preliminary desiccator. Pre-cruise lab tests showed no losses at the ppt level in either trap, and mild contamination of only one compound, 2-methylpropene. Both traps also removed ozone; the magnesium sulfate completely, and the Nafion partially. The CO₂ problem described above was only noticed after the cruise began. It was solved by adding an Ascarite trap to the system, lent by Jim Butler of NOAA/GMCC. While the trap was not tested in the lab beforehand, neither the standards nor the standard additions showed signs of significant contamination or loss after the Ascarite was added.

Because this was the first cruise for this system, the analytical procedures changed during the cruise. As much as possible, we tried to run for long periods in one configuration and not tinker with the system. Most of the significant changes were made over a period of a few days roughly two-thirds of the way into the cruise. The exact nature and timing of each change will be noted in the discussion of the cruise data.

We did not participate in SAGA 3 with the intention of sampling ocean water. Other participants, however, did. Two air-sea water equilibrators of a type designed by Ray Weiss of the Scripps Institution of Oceanography (described in Butler *et al.*, 1989) were brought on board to measure N₂O, chlorofluorocarbons, methyl chloroform, CO, CO₂ and methane. We tapped into one of these systems roughly two thirds of the way into the cruise, providing us with 20 samples of sea water. We had no opportunity to test this system for NMHCs. The system was designed by Ray Weiss to measure highly soluble, conservative gases, though NOAA PMEL has used the system extensively for methane analysis over the past several years, apparently with success (Kim Kelly, personal communication). The nonmethane hydrocarbons are neither conservative nor highly soluble, with Henry's law constants H (see Table 4.1.1) ranging from 8 to 50 (the Henry's law constant we use is the dimensionless ratio of air to water concentration at equilibrium), and they have unknown lifetimes in water. The equilibrators had a roughly 20 liter internal air volume and a 20 liter per minute water flow, so the equilibration time scale was roughly equal to H minutes. Specifically the equilibration time scales for the NMHC ranged from 8 to 50 minutes. Fortunately, the more reactive alkenes are also more soluble, with Henry's law constants near the lower end of the range. The system was sealed, except for occasional (small) sample extractions, so if hydrocarbon concentrations in the incoming water varied only slowly the system should always have been near equilibrium. In the future, measurements from a system like this must be compared

with measurements from a quantitative stripping system that extracts all of the hydrocarbons from a water sample.

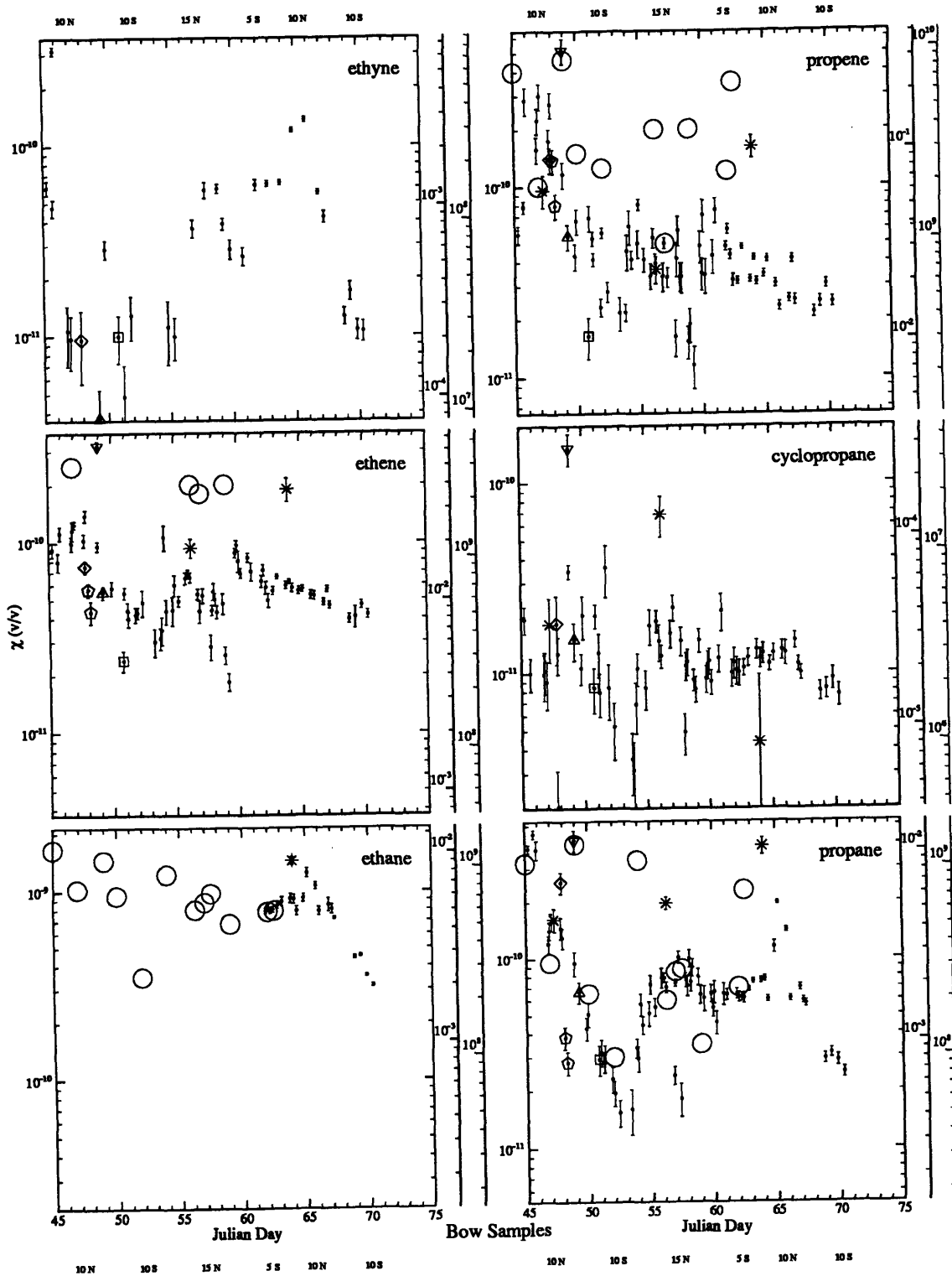
4.3 Data Analysis and Calibration

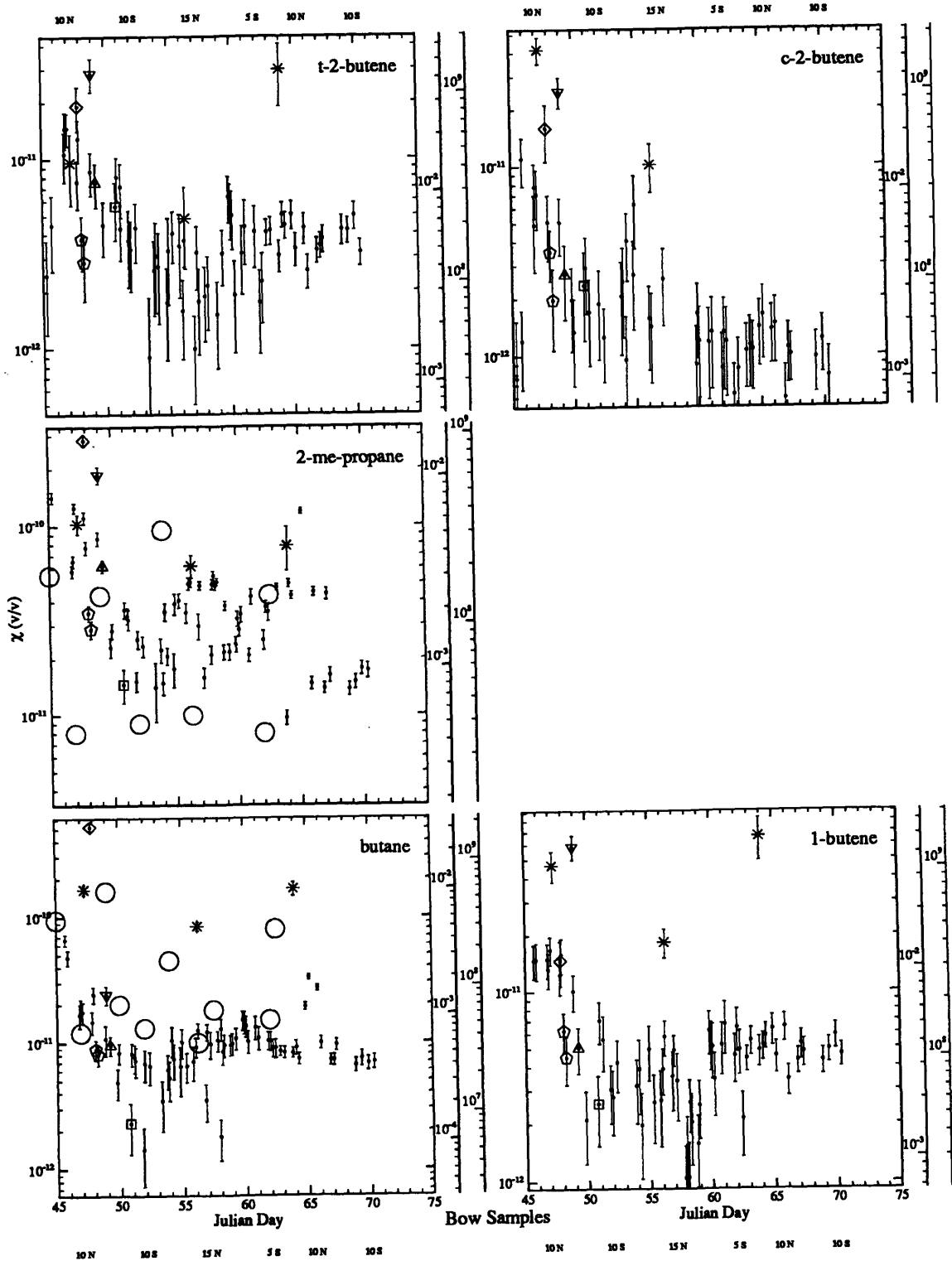
The chromatographic data was stored on disk and analyzed with an integration program written in our laboratory. Peaks were automatically identified and fitted to a tailing gaussian function, generally leaving very small residuals. This enabled us to accurately apportion areas among partially merged peaks and peaks resting on tails of other peaks. The results are summarized in Figures 4.3.1 through 4.3.3, which show, respectively, ambient air analyses, equilibrator air analyses, and standard analyses. Data is shown for all identified C₂–C₅ alkanes excepting 2-methyl-propene, which suffered from contamination throughout the cruise. Ethane data begins on day 61, before which it also suffered from contamination (Figure 4.3.3). Water sampling commenced on day 62.

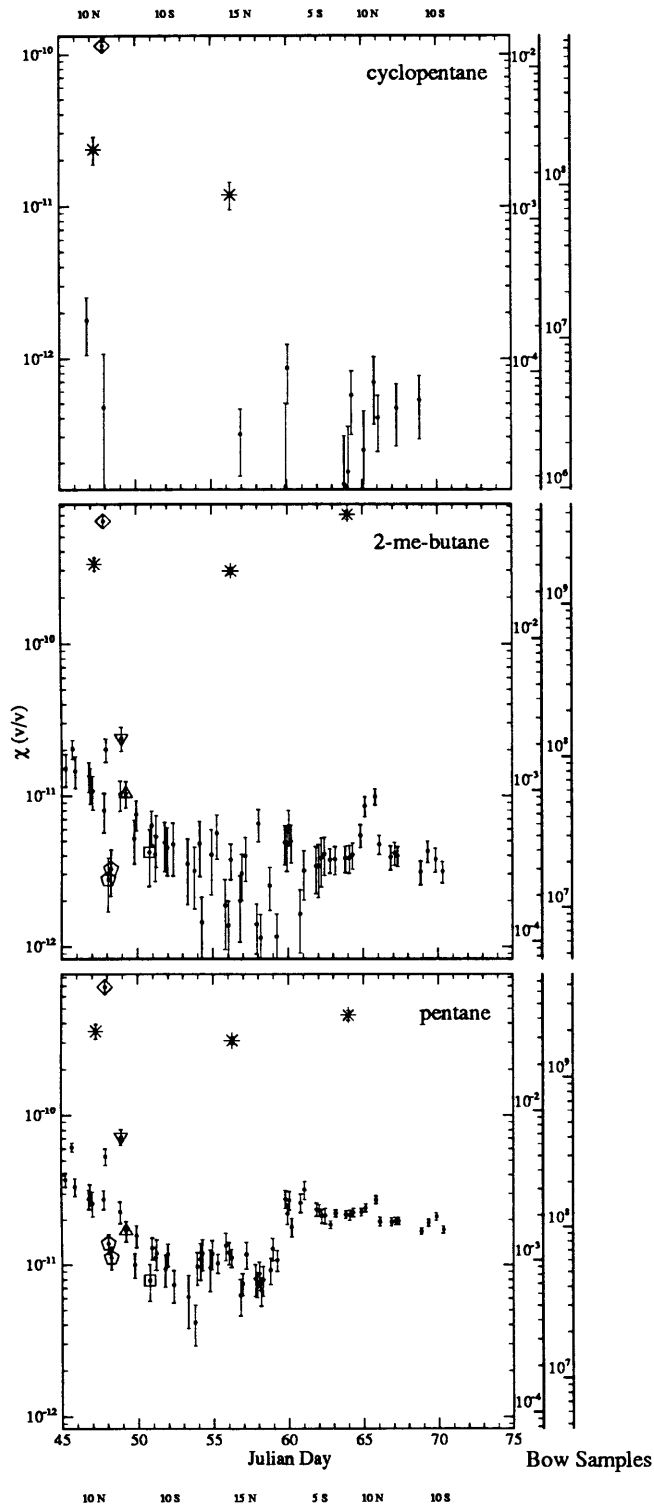
Both atmospheric and oceanic measurements are presented with three axes. The raw atmospheric measurements are of mixing ratio, but the more useful quantity when one is concerned with local photochemistry is the product of concentration and a compound's rate coefficient for reaction with OH. Thus the primary axis on each graph of atmospheric measurements is the mixing ratio (volume of NMHC / volume of dry air), while the secondary axes are the product of those mixing ratios, the bulk number density of dry air (2.36×10^{19} molec cm⁻³) based on a mean temperature of 27 °C and a mean relative humidity of 80 percent), and the appropriate rate constant. The rate constants are taken from Table 4.1.1. This axis is thus a direct scale of each compound's importance in removing OH from the MBL. The values should be compared with the total OH removal rate of about 1 per second. Finally, the tertiary axis is a rough estimation of the column removal rate for each NMHC, assuming reaction only with OH, a mean OH level of 6×10^5 molec cm⁻³, and one of three scale heights: 2 km for ethane, ethyne, propane, and cyclopropane, 1 km for the shorter-lived ethene, butane, 2-methyl-propane, pentane, cyclopentane, and 2-methyl-butane, and 500 meters for the rest. These values are based loosely on simple models of tropical vertical structure (Sarachik, 1985) with a mixed layer (500 - 600 m) mixing on a scale of hours, and a cloud layer (1000 m thick) mixing on a scale of one to two days. Inclusion of an ozone sink would increase the column removal rate for some compounds, particularly the 2-alkenes

Figure 4.3.1

NMHC Mixing ratios in the marine boundary layer. Error bars indicate the precision of each calibrated measurement. The primary axes are mixing ratios, with an absolute accuracy of $\pm 20\%$. The secondary axes are the OH removal frequency due to each NMHC, in sec^{-1} , with an absolute accuracy of $\sim \pm 30\%$. Finally, the tertiary axes are the NMHC column removal rates, in $\text{molec cm}^{-2} \text{ sec}$, with an accuracy of $\sim \pm 100\%$ (see text). The cruise turning points are indicated along the time axis by latitude. Samples from before JD 64 were 1 sl, those from after JD 64 were 3 sl. Symbols indicate special samples (see text): * -- lab air, \diamond -- air from port beam, ∇ -- lowered (1 sl/min) bow line flow, Δ -- increased (10 sl/min) bow line flow (maintained for remainder of cruise), [] alternate bow line, and the pentagons -- zero air in bow line. \bigcirc are Atlas *et al.*, 1990. All NMHCs were calibrated directly against the same compound in our standard except ethyne and cyclopropane, for which an instrument calibration factor of 8×10^4 was used (see text).







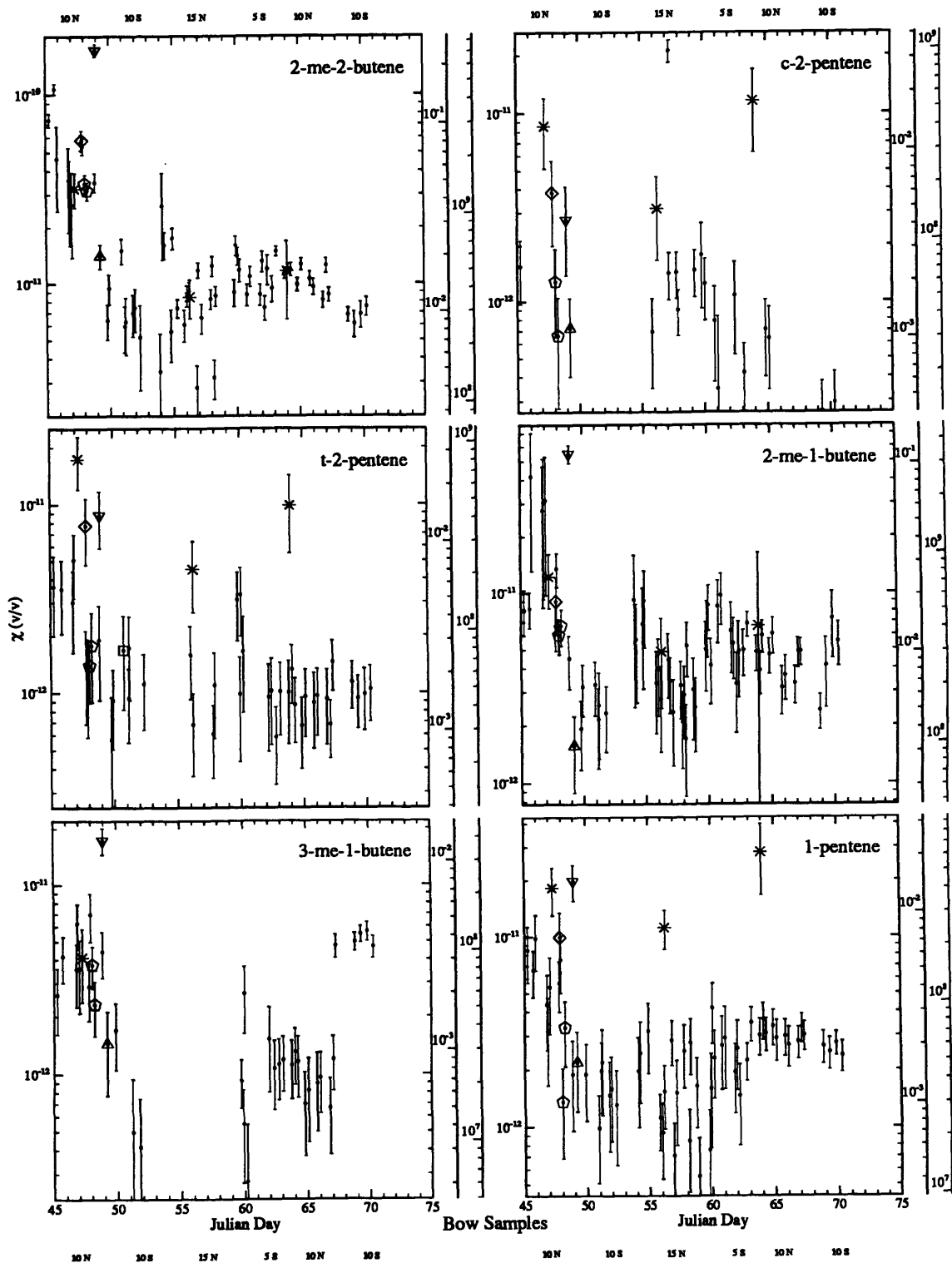
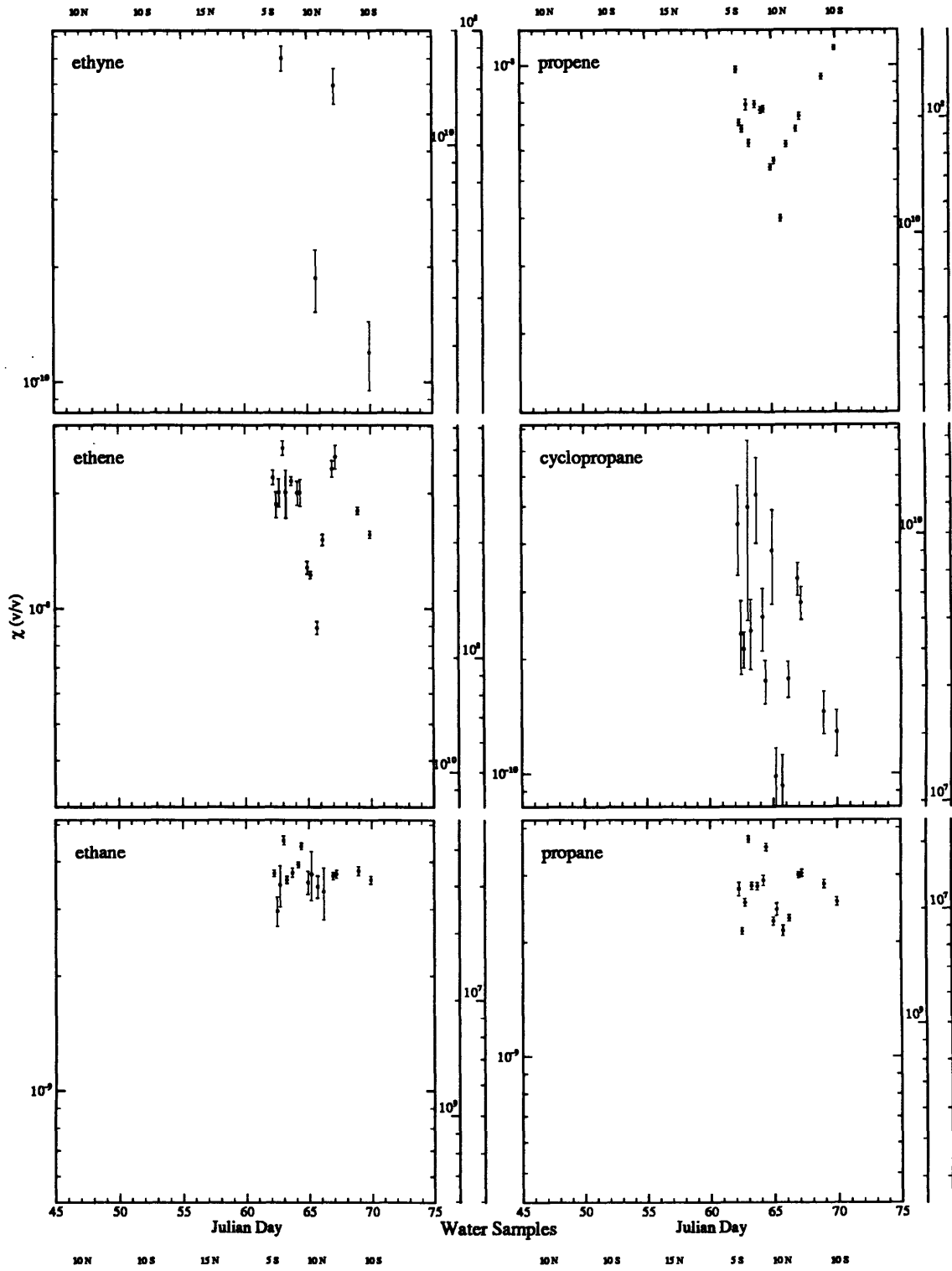
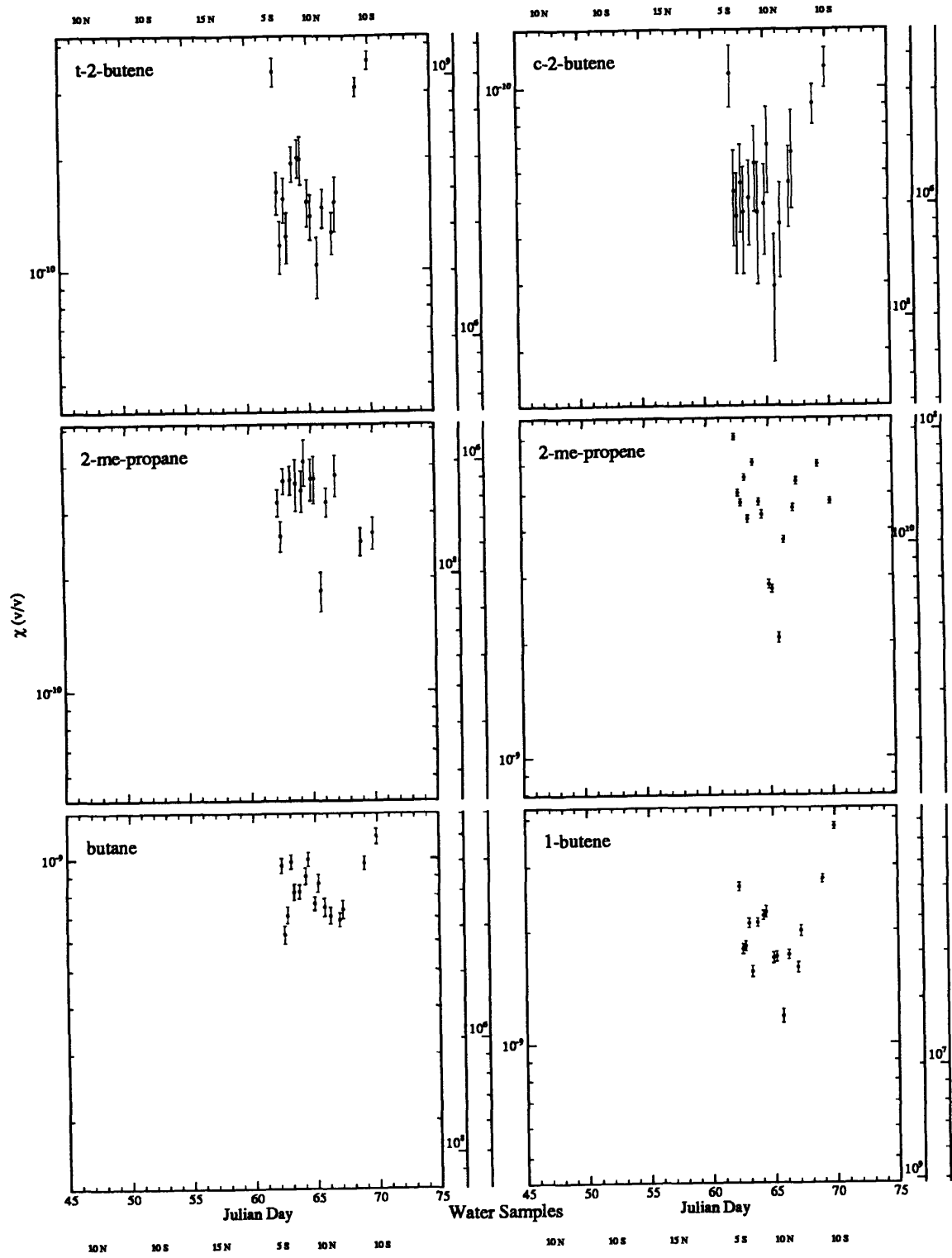
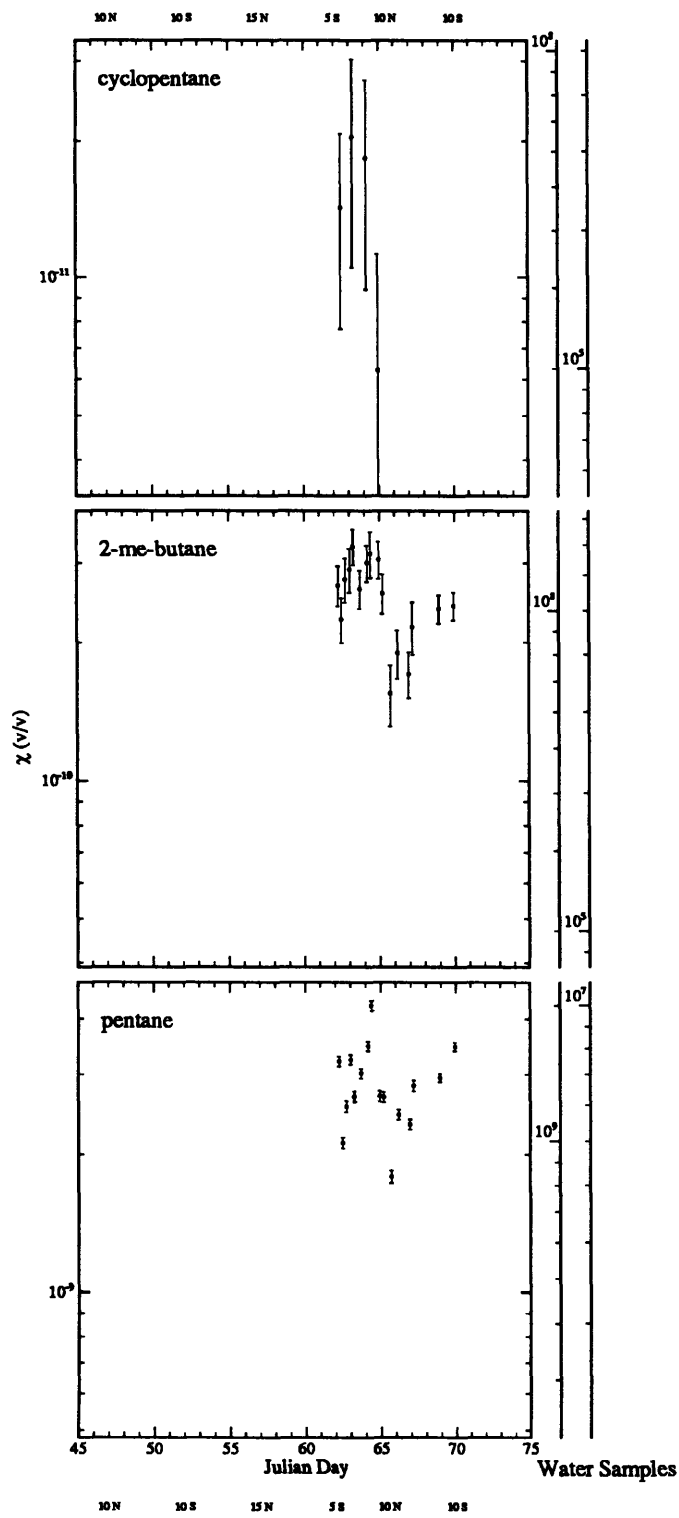


Figure 4.3.2.

NMHC Mixing ratios for air in equilibrium with ocean water (see text). The primary axes are mixing ratios, with an absolute accuracy of $\pm 20\%$. The secondary axes are the NMHC concentrations in ocean water ($C_w = C_{eq}/H$) in molec cm^{-3} , with absolute accuracies of $\sim \pm 30 - 50\%$. Finally, the tertiary axes are the NMHC sea-air fluxes in molec $\text{cm}^{-2} \text{ sec}$, with an accuracy of $\sim \pm 100\%$ (see text). The cruise turning points are indicated along the time axis by latitude. Samples were 100 scc. All NMHCs were calibrated directly against the same compound in our standard except ethyne, cyclopropane, and 2-methyl-propene, for which an instrument calibration factor of 8×10^4 was used (see text).







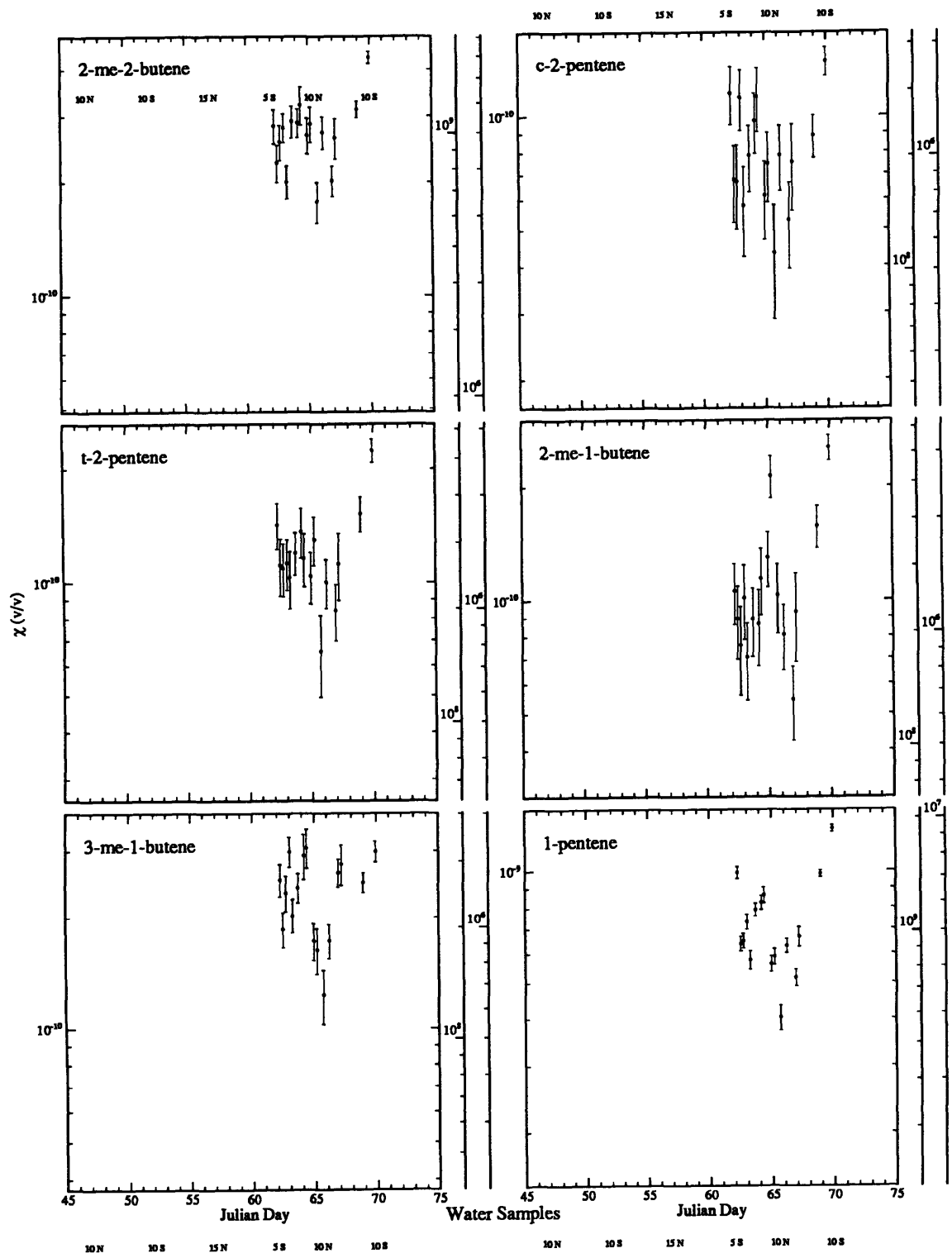
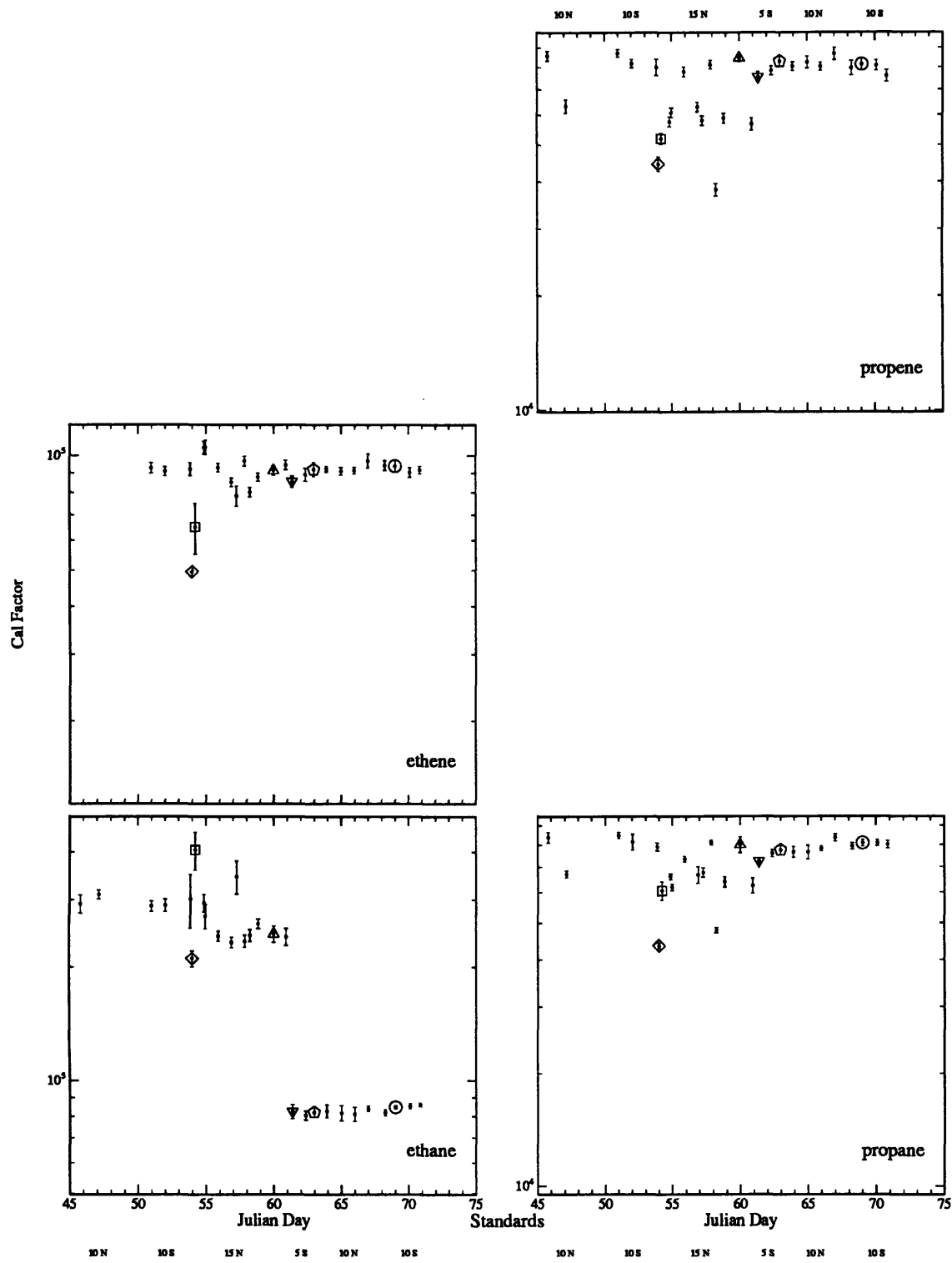
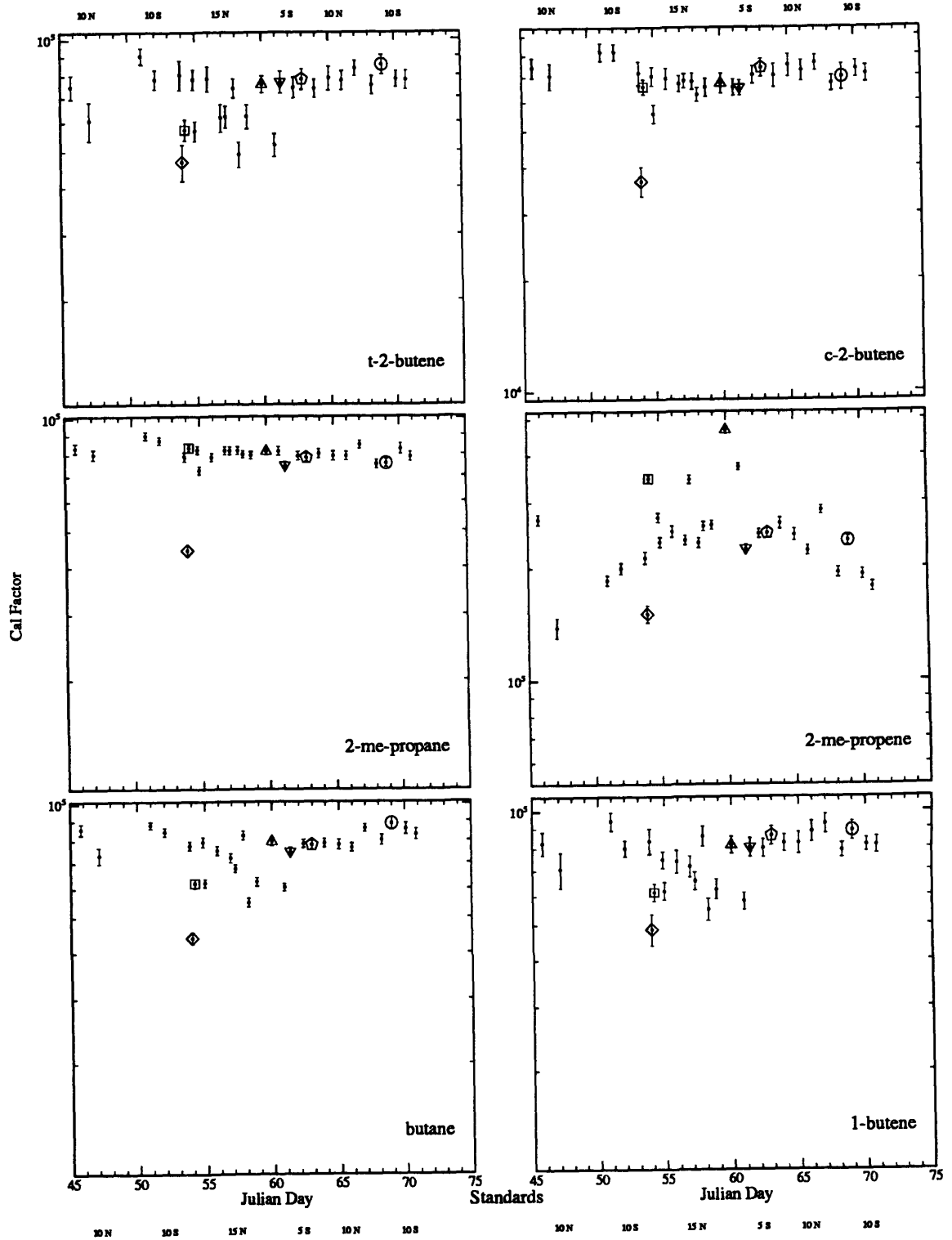
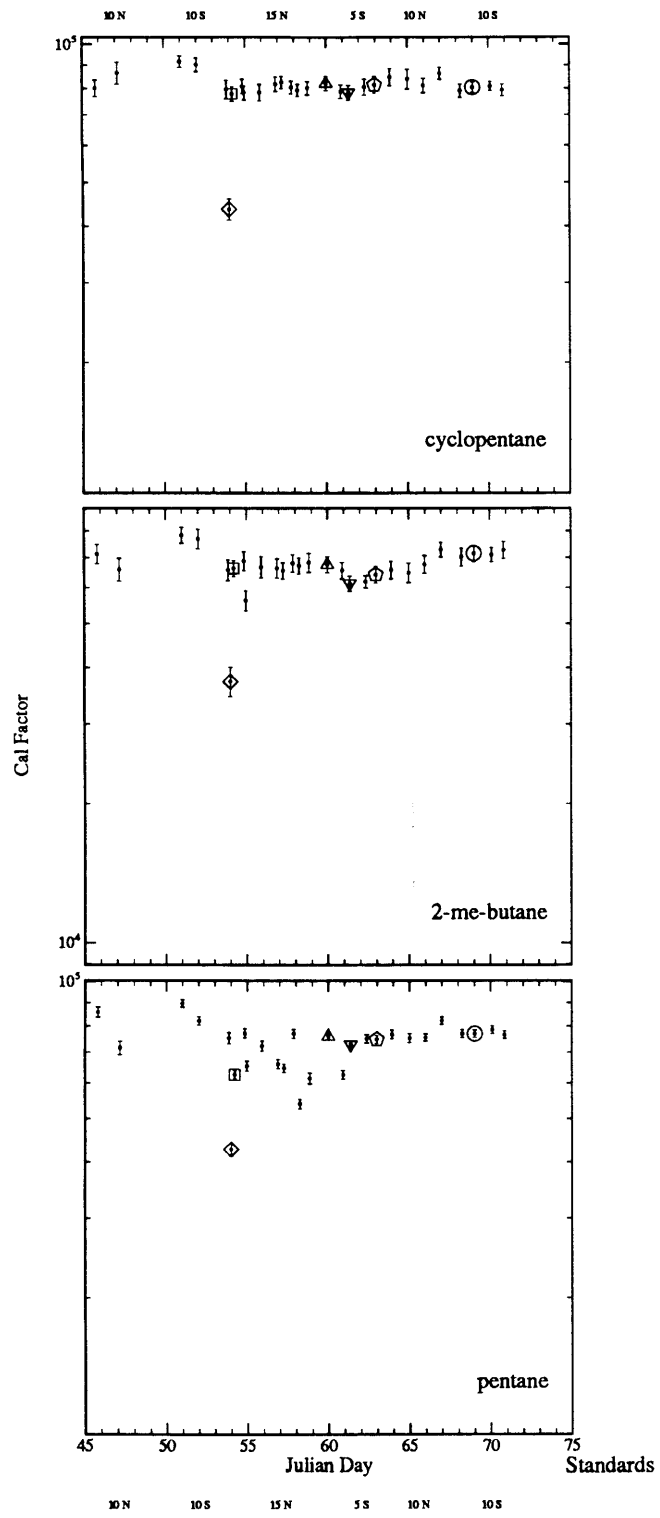


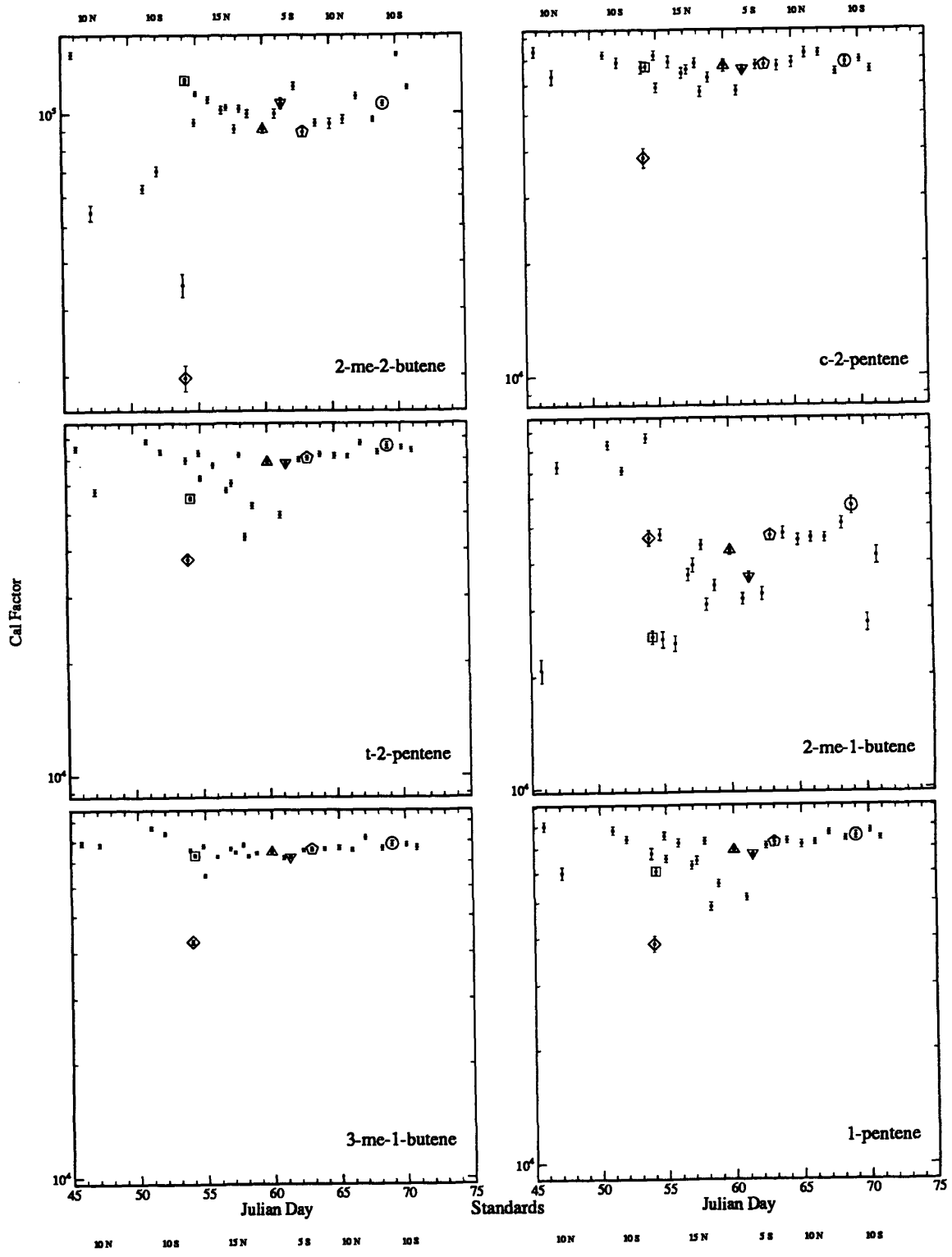
Figure 4.3.3

NMHC standard analyses. Standards were diluted from our calibration tank by a factor of 4.80×10^{-4} . The analyses are plotted as a calibration factor: $c = (v \text{ RMR}) / (A \chi_{\text{std}})$. The cruise turning points are indicated along the time axis by latitude. Symbols indicate procedural changes (see text): \diamond -- drier saturated, \square new drier, \triangle -- Ascarite added to remove CO_2 , ∇ -- chemical traps removed from carrier gas, pentagon -- 3 sl samples, \bigcirc -- new temperature program and carrier flow. Note contamination in ethane before JD 61 and 2-methyl-propene for the entire cruise, indicated by a response different from the otherwise common value of 8×10^4









(see Table 4.1.1). There are uncertainties in the placement of each axis; for the primary axis the absolute calibration uncertainty is estimated at 20 percent for each compound, for the secondary axis the rate constants are generally known to between 20 and 40 percent (Table 4.1.1), making a total uncertainty of 28 to 45 percent in the secondary axis placement, because of our crude assessment of both [OH] and H the tertiary axis uncertainty is very large, approaching a factor of two.

The oceanic measurements are of mixing ratio in equilibrium with air. This measure can be compared directly with the atmospheric mixing ratios to determine whether each compound is super- or under-saturated in the air with respect to the surface waters of the ocean. In all cases excepting ethyne the NMHCs were enormously supersaturated, indicating that there was a sea-to-air flux of all NMHCs. The actual flux for greatly supersaturated compounds is, however, proportional to the compound's water concentration, not the equilibrium concentration (Liss and Slater 1974). The equilibrium concentrations are therefore divided by the appropriate Henry's Law constants to produce the secondary presentation of ocean water measurements. The Henry's law constants themselves are listed in Table 4.1.1. They are taken, where possible, from Mackay and Shiu (1981) who drew heavily on the work of McAuliffe (1966). (The Henry's law constants listed in Mackay and Shiu for 1-butene and 2-methyl propene were miscalculated. We use correctly calculated values.) Where data were absent, we calculated solubilities based on the inverse relationship demonstrated in McAuliffe (1966) between the logarithm of the solubility with the molar volume for hydrocarbons in a homologous series. Henry's law constants so calculated are enclosed in parentheses in Table 5.1.1. The ethyne Henry's law constant is taken from Wilhelm *et al.* (1977). Note that Wilhelm's data are generally lower than the others (especially for propene, which is 35 percent lower); they specifically reject McAuliffe's (1966) data, but later studies quoted in Mackay and Shiu (1981) have generally supported McAuliffe (1966), and we adopt his values. We have made no corrections for salinity. The secondary axis on the water measurements is the sea water concentration (molecules per cc water) thus calculated, with an estimated standard error of roughly 28 percent; half due to calibration uncertainty and half to uncertainty in the solubilities of the NMHCs in sea water. Finally, the tertiary axis for each NMHC sea-water graph is the calculated flux to the atmosphere, using a mean transfer velocity of $5 \times 10^{-3} \text{ cm sec}^{-1}$, which is generally consistent with both the values used by Plass *et al.*

(1991) and those suggested by Roether (1986). Uncertainties in these bulk flux calculations are very large. Accounting for the propagating errors from the Henry's law constants, they probably range between 50 and 100 percent. Just as the equilibrium measurements can be compared directly with the atmospheric mixing ratios to find the supersaturation for each NMHC, the flux values should balance the column removal rates show on the tertiary axes of the atmospheric data. In general, they are too low.

Where possible, the NMHCs were calibrated individually, using bracketing standard analyses around each measurement to determine a calibration factor. During the final third of the cruise (after JD 61) the standard analyses were stable to within 5 to 10 percent, depending on the compound. Before then, 8 of the 16 compounds for which the standard analyses were stable (for 3 they were not) occasionally showed dips in response approaching 20 percent. There are no evident correlations among the groups which did and did not experience these sensitivity drops. Both alkanes and alkenes are in each group; for instance, *trans*-2-butene showed them, while *cis*-2-butene did not. The worst drop, which alone appeared in all compounds, occurred just as a Nafion drier was saturating, suggesting that water may have played a role. However, the problem finally vanished on JD 61 when some traps on the carrier and flame gas lines were removed after we discovered that they caused the ethane contamination we saw during the first two-thirds of the cruise.

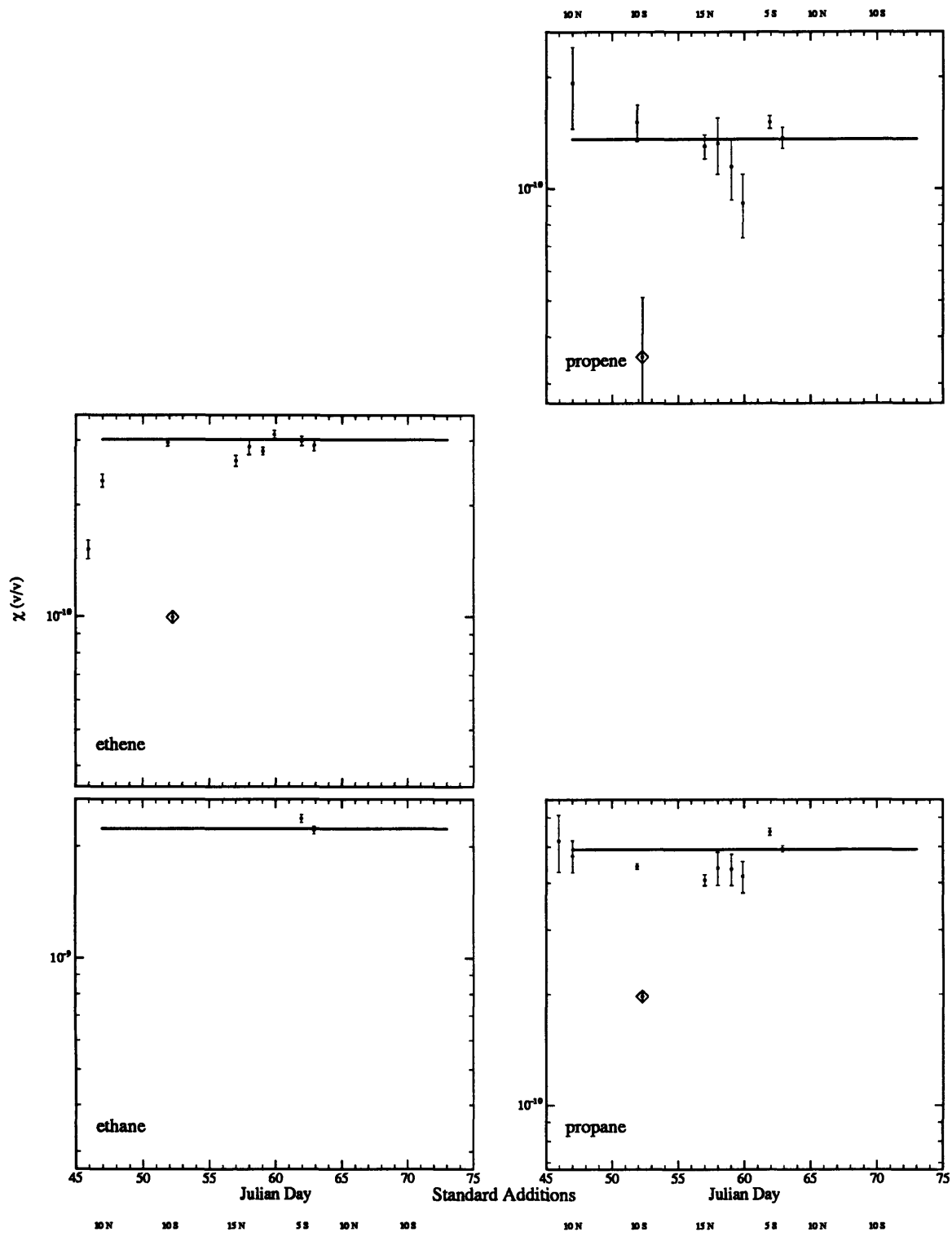
An alternate, and less desirable, calibration method is to rely on the relative molar response (RMR) of each NMHC (Ackman, 1968). In the process of analysis, we divided the area per unit volume (A/V) of each NMHC peak by the appropriate RMR, thus providing us with an additional check of system performance. For 16 of the 18 compounds for which we had a specific standard (excluding 2-methyl-propene), the calibration factor (by which the instrument response, $A/(V \times \text{RMR})$, is divided to yield the mixing ratio) was $(8.0 \pm 0.6) \times 10^4$. The precision is actually better than the relative precision we have assigned to the standard itself (which is 13 percent for relative concentrations), showing that there were no significant problems associated with standard analyses at levels ranging from 50 pptv (for the butenes) to 2 ppbv (for ethane and 3-methyl-1-butene). As the standards passed through all stages of the instrument except the bow sampling line, this provides strong evidence that the system was conservative for these 18 compounds. The calibration factor derived above was used to calibrate ethyne and cyclopropane, for which we did not have independent standards.

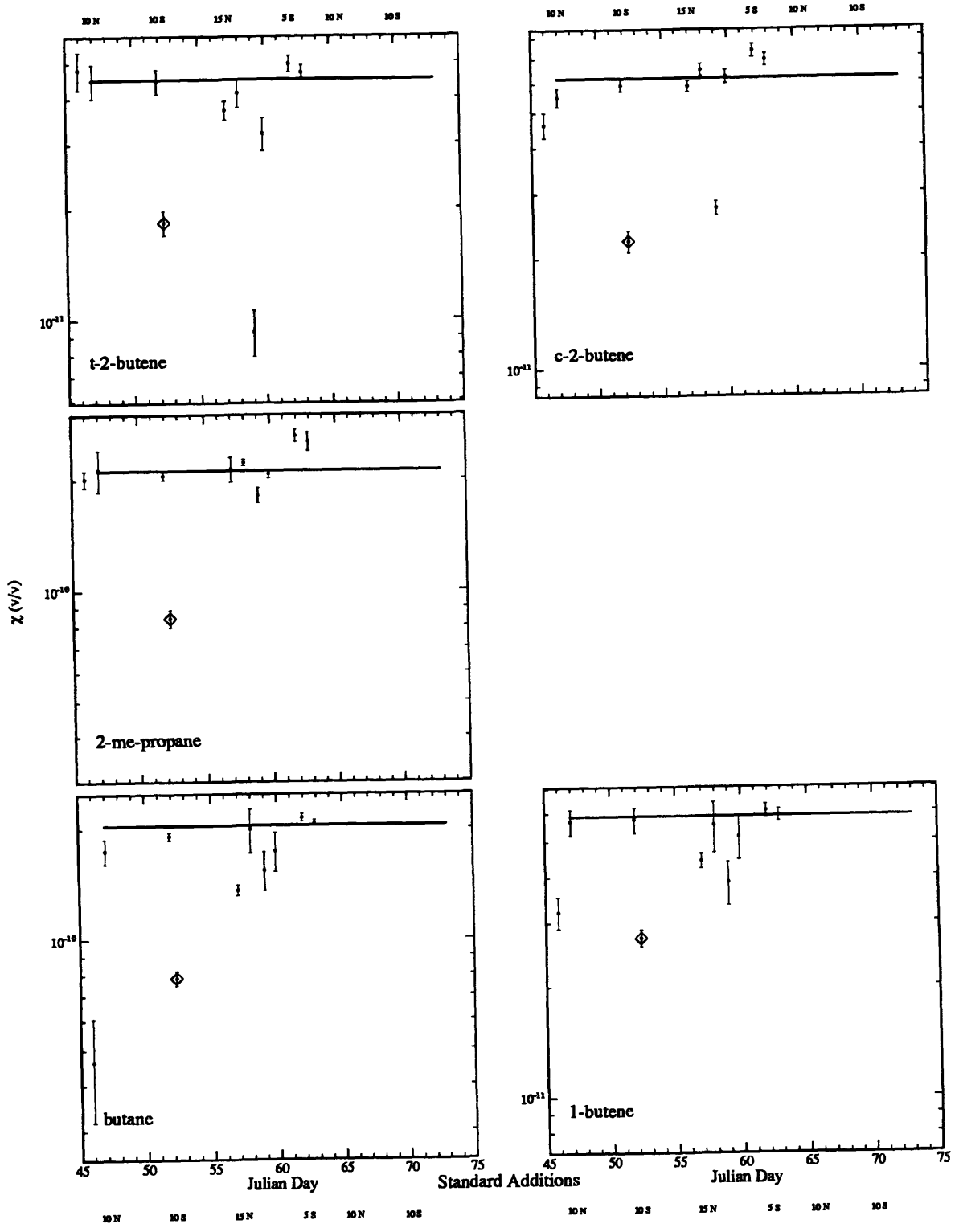
Another test of the analyses involved frequent performance of standard additions. For these tests, a standard was diluted in air from the bow line, rather than zero air. Any destruction problems associated with the sampling lines, passage through the traps, or cryotrapping of the samples would equally affect these standard additions. To perform these tests, we subtracted off the average response for the two air samples bracketing the standard addition and then calculated the mixing ratio of the residual peak. For ideal standard additions, the resulting mixing ratios should be the mixing ratios of the standard, the dilution factors being identical. An offset factor common to all peaks would indicate not loss or addition but sensitivity to air composition (particularly humidity) of the flow controllers regulating either the main bow line flow or the sample flow. The results are shown in Figure 4.3.4, with the solid horizontal bar in each graph indicating the standard mixing ratio. Excepting the first run for some compounds, the mixing ratios are nearly identical to our standard analyses. Note that the problem of occasional sensitivity drops in the standards before JD 61 is also apparent in the standard additions. On JD 52 we lashed the standard tank to the bow, regulating the standard flow with a needle valve. This run is indicated with a diamond in the figure. The exact dilution factor is unknown, since neither the standard flow nor the (unregulated) bow line flow were well known. However, real production or loss problems absent, all mixing ratios from this test should be different from the standard mixing ratios by only a common factor. This is the case. We interpret these tests to indicate that no major losses commonly occurred in any part of our system for any of the compounds for which we had a working standard. It remains to show that no contamination occurred at levels too small to detect with these tests.

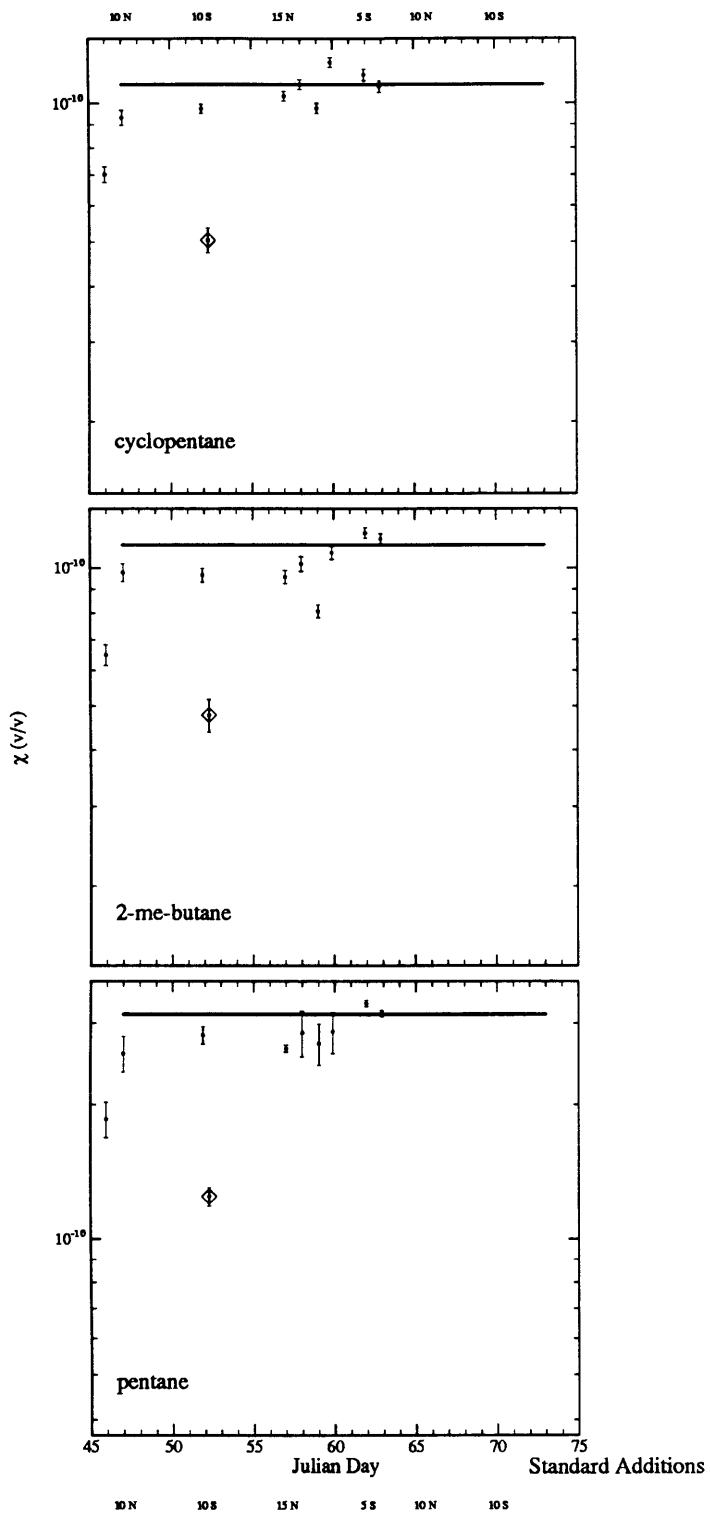
Two compounds did not show a stable standard response. Specifically, 2-methyl-1-butene and 2-methyl-2-butene, which were the initial and terminal peaks in a resolved triplet, along with 1-pentene. For reasons we do not yet understand, the areas of these two peaks (but not 1-pentene) exhibited strong covariance, both before and after the peaks have been fitted to tailing gaussian peak functions with minimal residuals. The sum of the two peak areas was relatively stable. The covariance may therefore be real, and not an integration artifact, but we do not yet understand it. As a consequence of this covariance, the calibrated levels for these two compounds differ by roughly a factor of two when they are calibrated with the specific standard and the RMR calibration factor.

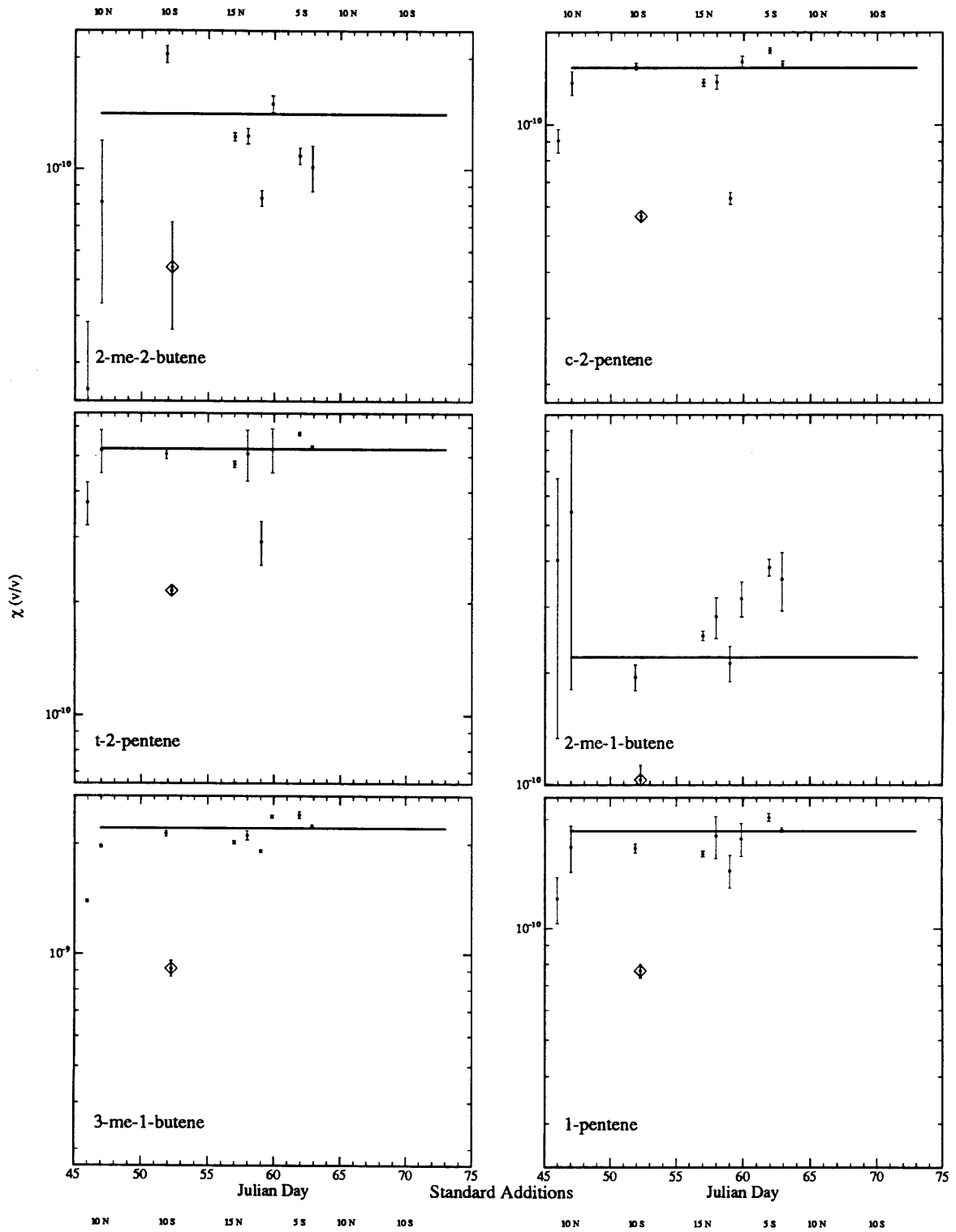
Figure 4.3.4

NMHC standard addition tests, (see text). The ambient contribution has been removed from the signal. Nominal standard mixing ratios are indicated by a horizontal bar. The diamond is a standard addition at the bow with unknown flows (see text), which should be (and is) equidistant from the bar on all NMHC (log) plots.









In addition, before JD 60, and in some cases before the final 5 analyses of the cruise, the chromatographic conditions for some compounds were less than ideal. Of particular concern was the coelution of 2-methyl-propane and ethyne, which produced peaks which may have merged from time to time. Occasionally the peaks were sufficiently merged to obscure the valley point between them, though both peaks were integrated with our peak fitter. The early results for these compounds should therefore be considered with caution. For the final 5 analyses, the separation was complete. Both trans- and cis-2-butene eluted near unknown compounds which produced peaks of similar size. While positive identification was generally not a problem, it is less certain for data taken before JD 60 (which were 1 as opposed to 3 sl samples). Again, for the final 5 air analyses the separation was complete in each case. Cyclopropane and propene were the final two peaks in a resolved quadruplet in all but the final 5 analyses. The first peak was very small, but the second, unknown, compound produced a peak similar in size to propene. The separation and identification of these peaks was generally not a problem. Ethane and ethene suffered peak splitting during cryofocusing. This was distinguished from coelution because the splitting was observed during pure standard analysis as well as during sampling.

The error bars on each measurement include three contributions: the uncertainty of the peak integration, as estimated by our integration software, any imprecision in sample volume (generally less than 1 percent), and the calibration uncertainty (which is a weighted mean of the integration uncertainties for the two bracketing standards, including any differences in the peak areas for the two standards). Note that accurate determination of sample volume was not necessary because both samples and standards were gathered identically; none-the-less, the absolute accuracy of sample volumes was of order 1 percent. One can easily see the increase in precision caused by several changes made around day 60, including the removal of the ethane contamination and the subsequent improvement in standard precision. Not included in the individual error bars is the overall calibration accuracy of (± 20 percent). Unquantifiable errors are not included either. Two could be important: misidentification or coelution, and contamination from the bow line. As just discussed, misidentification is only suspected as a potential problem for ethyne and 2-methyl-propane. Because the FID is a non-specific detector, strictly speaking the identifications are always tentative, and coelution is never ruled out. The combination of the capillary GC with the peak-fitting integrator

does, however, reduce the risk of coelution problems. Peaks were typically 1 second wide (gaussian width) and, with the exceptions already noted, did not show signs of humps or irregularities which one would associate with coelution. There were, however, many near co-elutions, which could easily have caused problems on a column producing broader peaks.

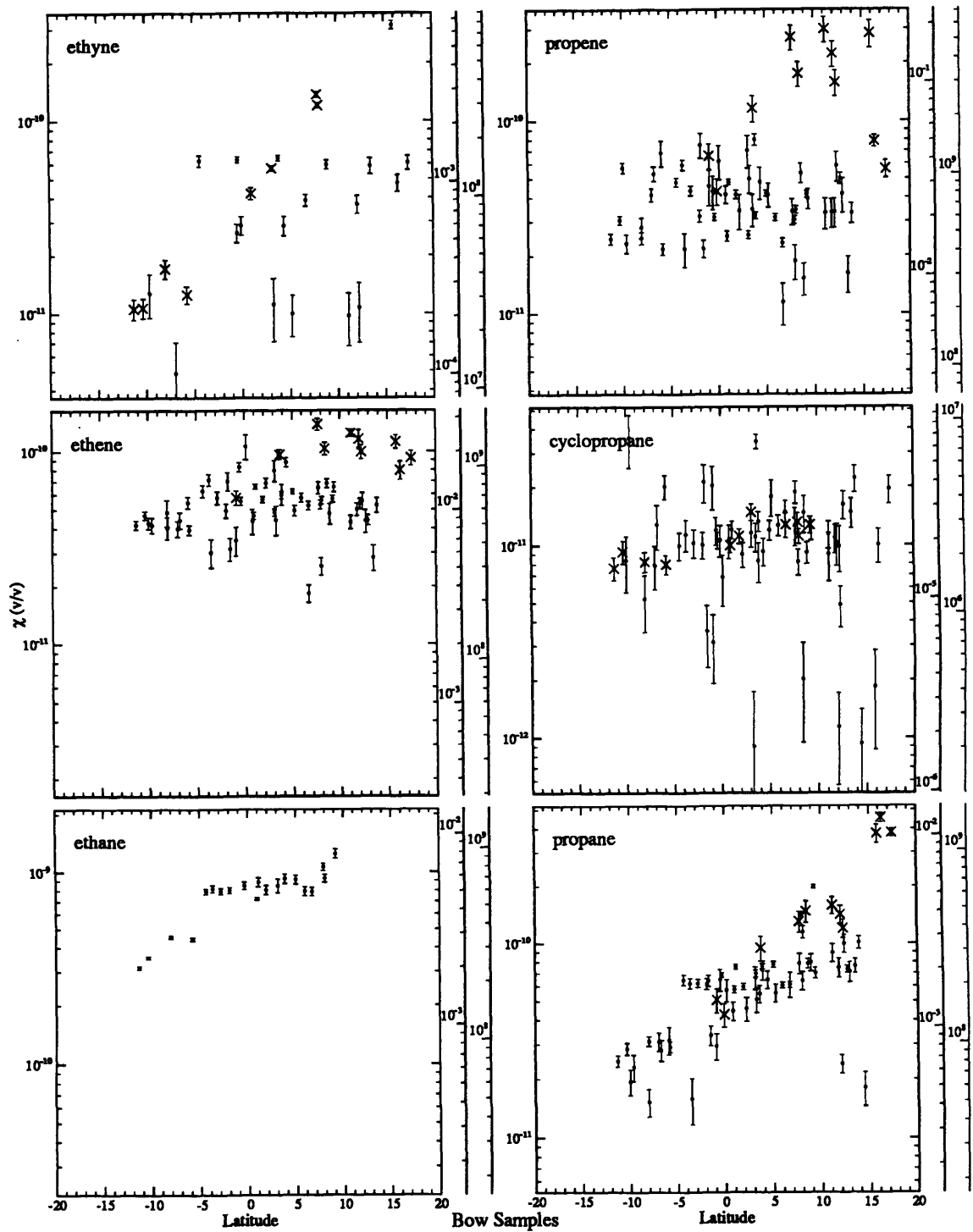
4.4 Results and Discussion

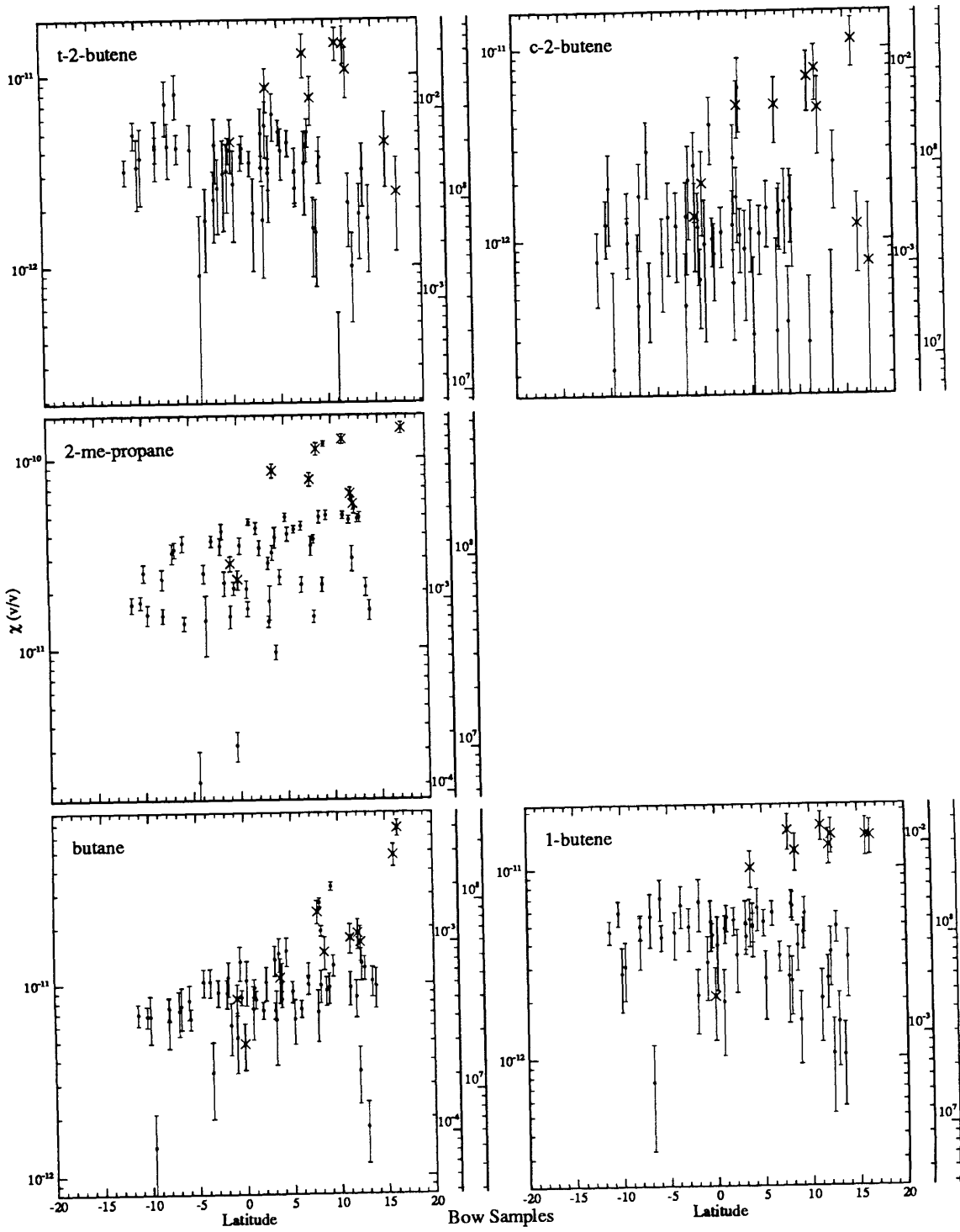
Latitudinal plots of the atmospheric measurements are shown in Figure (4.4.1). Generally speaking, the atmospheric data can be divided into two groups: those compounds showing a consistent, reproducible latitudinal gradient (ethane, ethyne, and propane), and those that do not. Each group has a representative compound; propane for the former, and pentane for the latter. A few compounds, notably the butanes, appear to be a combination. Cyclopropane also appears to belong in the first group, but the data is too noisy to be conclusive. The final 5 data points for ethyne (for which the chromatographic identification is beyond doubt) clearly show a strong gradient. The remaining data appears to follow this trend, indicating that the earlier identifications were generally correct. The division is almost perfectly between those compounds with atmospheric lifetimes longer than 5 days and those with shorter lifetimes, the patterns being particularly evident in the time-series (Figure 4.3.1). The short lived compounds do show a common structure, which is most obvious for pentane. The mixing ratios generally dropped for the first 10 days of the cruise, through the first southward leg and into the beginning of the return northward. They then remained roughly stable until the northward leg was complete, increased during the second southward leg, and declined (slightly to moderately) for the remainder of the cruise, through a northward and a final southward leg. For many of the compounds the initial decline was considerable, up to an order of magnitude, while in general the variations after that were confined to less than a factor of two. Several compounds in both groups show occasional sudden dips between days 55 and 60. It is not known whether these are real or were caused by the same phenomenon mentioned in connection with the standards. The drops are generally substantial, between a factor of 2 and 5, which greatly exceeds the 20 percent observed for the standards.

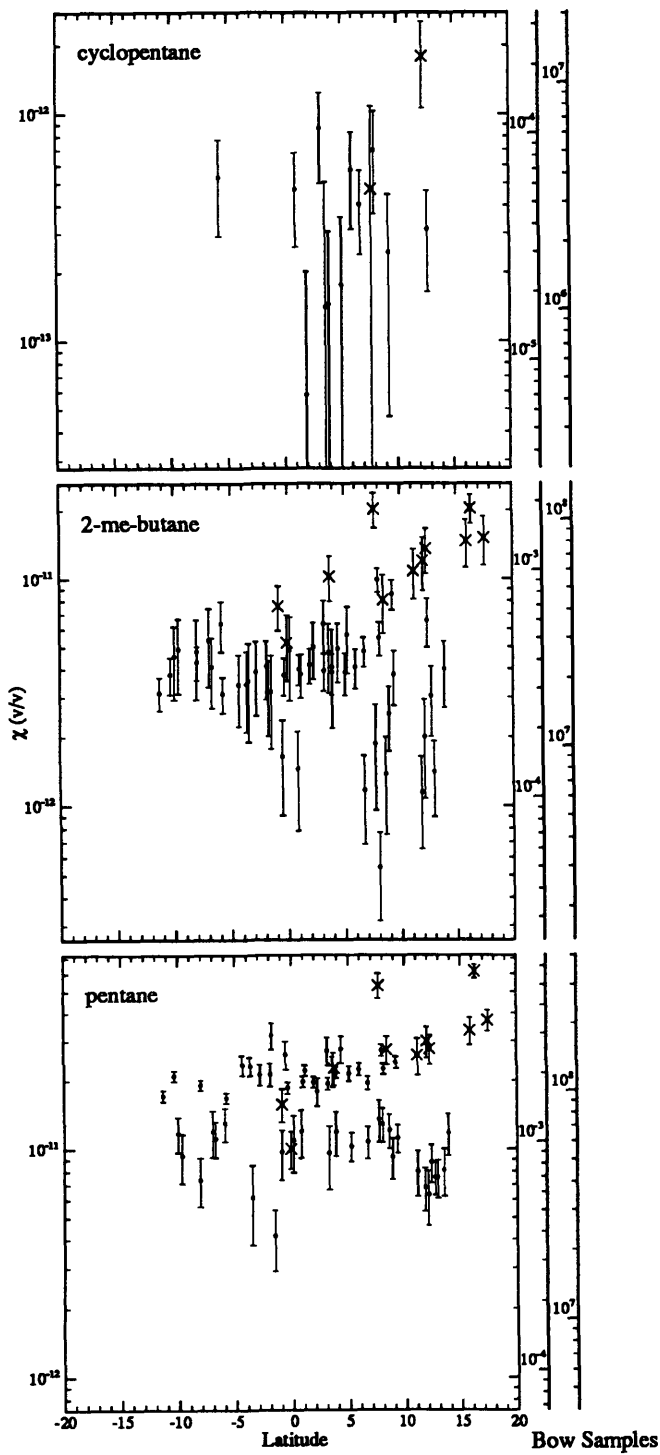
The early drop in the short lived compounds could be real or it could indicate a decaying line contamination problem; we consider contamination to be unlikely after the common minimum around JD 57. Several features in the data before JD 57 tend to support the

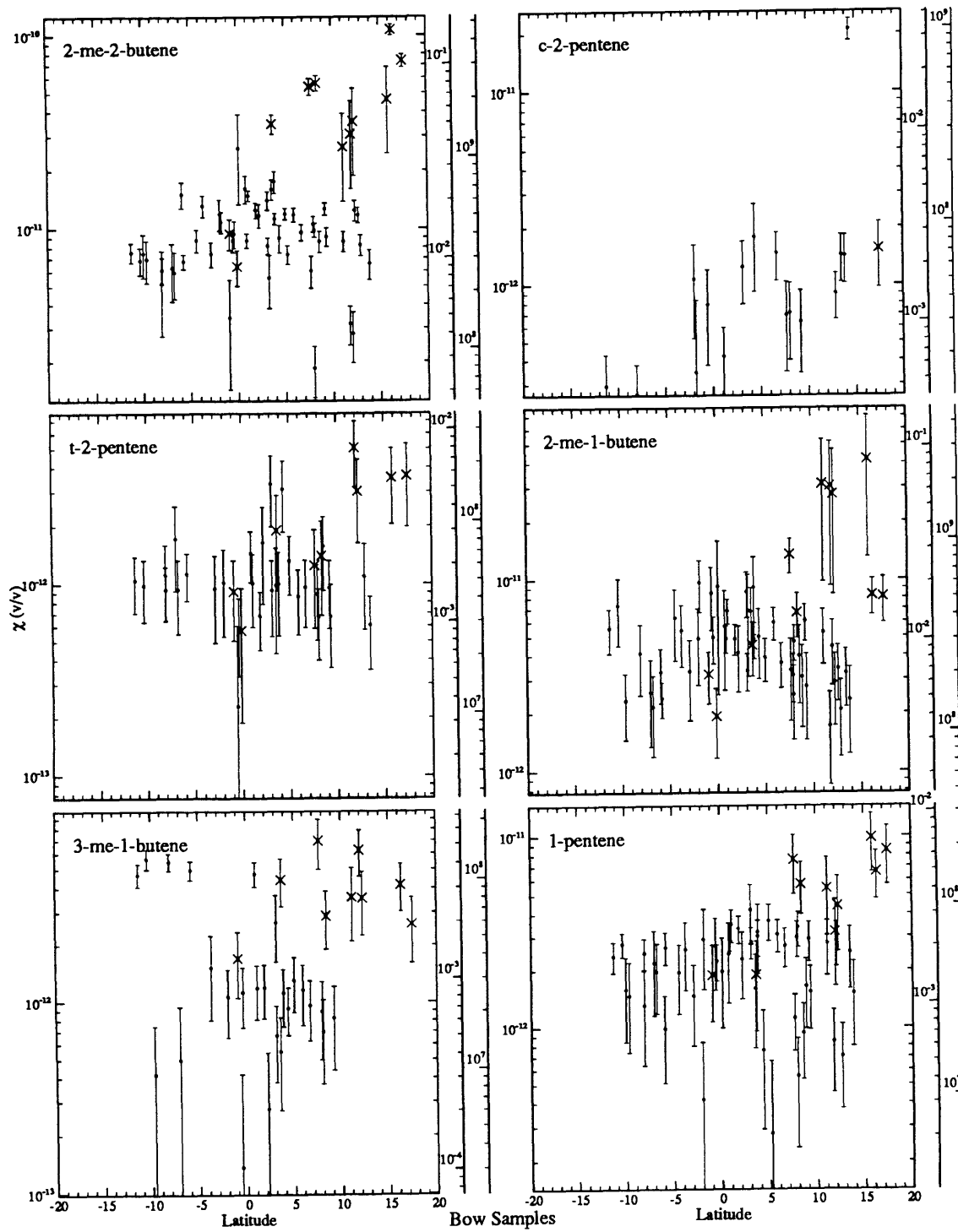
Figure 4.4.1

NMHC Mixing ratios in the marine boundary layer as a function of latitude. The primary axes are mixing ratios, with an absolute accuracy of $\pm 20\%$. The secondary axes are the OH removal frequency due to each NMHC, in sec^{-1} , with an absolute accuracy of $\sim \pm 30\%$. Finally, the tertiary axes are the NMHC column removal rates, in $\text{molec cm}^{-2} \text{ sec}$, with an accuracy of $\sim \pm 100\%$ (see text). Data collected before JD50, which is suspect, is indicated with a cross.









conclusion that it too is contamination free for most or all of the NMHCs shown. The first is the very presence of a common minimum; the diffusion constants of the NMHCs through FEP teflon, while unknown, are surely different. Assuming that permeation from the sample line would have been the source of any contamination, the cleansing time-scales for the various NMHCs should have scaled inversely with their diffusion constants. The second feature is the timing of the minimum at the turning point of our first leg; common degassing ending coincidentally at the southernmost point of our cruise seems a bit far-fetched. If the early data does represent conditions in the MBL, it could be a signature of a decaying continental influence. To check the sample line we conducted several tests. While our design precluded regularly running zero air down the length of the sample line, we were able to lash a zero air tank to the rail and test half of the line on one occasion. Two samples (shown as pentagons on Figure 4.3.1) were run, with mixed results. All compounds showed some response, and for no compound was the response lower than the minimum response observed on the cruise. For the alkanes the response was a factor of 2 - 5 less than the then current ambient levels, ethene and the butenes were a factor of two lower, while for propene and the pentenes zero air levels were similar to the ambient levels. Because the tests were run using a (borrowed) tank of zero air, the line was not flushed for more than 30 minutes before zero air sampling began; one explanation of the ensuing observations is thus that the sample line took over 30 minutes to equilibrate to changes in ambient concentrations. In the second test we slowed the bow line flow rate from 2.5 sl/min to 1 sl/min and watched for an increase in peak areas. These data points are indicated with a downward facing triangle in Figure 4.3.1. Almost all of the NMHCs showed a substantial increase, including those which passed the blank test. Unfortunately, a canister sample collected at the same time shows an almost identical mixing ratio for propane and increased levels for all NMHCs, suggesting that the observed increase may have been real, if unfortunately timed. After these two tests the bow flow was increased to in excess of 10 sl/min (the first high flow run is shown with an upward facing triangle in Figure 4.3.1). None of the NMHC data shows a sudden drop at this point, but rather a smooth continuation of the general decline from JD 45 to JD 53. Finally, we drew a sample from a different sample line, made of Dekabon, which was fixed to a 5 meter mast just aft of the bow. The line was flushed overnight before being analyzed. The results of that run are indicated with a square on Figure 4.3.1. For ethene, propene, 2-methyl-propane,

butane, and pentane, the mixing ratios were lower than others around them and similar to the lowest levels seen during the cruise. It must be noted that this line was not tested for NMHC destruction. In summary, the decline in observed mixing ratios for many of the NMHCs before JD 53 may have been real, or it may have been caused by an exponentially declining outgassing of the FEP sample line. The tests were inconclusive, yet on the whole favored inclusion of the data. Assuming that any contamination continued to decline exponentially, the data after JD 55 is very likely uncontaminated. Combined with the earlier demonstration that losses did not occur in the system, our upper limits on error bars are firm, while our lower ones are unquantifiably less firm. Conclusions will be drawn in this paper based on the data taken after JD 55. The earlier data is presented primarily because it may represent a continental influence, and we shall argue that the later data for the more reactive NMHCs cannot be so influenced.

It was also necessary to establish that the ship was not contaminating our air samples. This was accomplished in two ways: by occasionally sampling room air (these samples are indicated by an asterisk in Figure 4.3.1) and by drawing a sample from a shortened line extending off the port beam, just forward of the bridge and the forward laboratory and facing into a strong breeze (this run is indicated with a diamond in Figure 4.3.1). Both tests show a very consistent pattern of contamination, increasing in severity with carbon number and worse for alkanes than alkenes. The absence of elevated pentane levels in particular indicates that ship contamination was not a problem, especially for the lighter alkenes.

Our data agrees qualitatively with that reviewed by Singh and Zimmerman (1991), with discernible latitudinal gradients for ethane, ethyne, and propane (to which we add cyclopropane as a new result) and generally constant but scattered values for other NMHCs. For the former compounds, the agreement is also quantitatively good; we see roughly 1000 pptv ethane in the tropical northern hemisphere and as little as 300 pptv in the southern tropics. For propane our range is from 200 pptv to 20 pptv, falling within the distribution shown in Singh and Zimmerman (1991), while for ethyne we observe a range from roughly 100 pptv to 10 pptv, which is again consistent with previously reported ranges though on the low end of absolute values. While there are suggestions of a latitudinal gradient in the later ethyne data, overall there is only a hint of one in Figure 4.4.1. This may be an artifact of the partial co-elution with 2-methyl-propane for all but the last several data points. For

cyclopropane the gradient is smaller, with roughly 12 pptv in the northern tropics and 8 pptv in the southern tropics, amid considerable scatter. Note that the observed latitudinal gradients correlate very well with the lifetimes of these continentally influenced compounds; cyclopropane, with the longest lifetime (289 days) has the smallest gradient (a factor of 1.5 over the latitudinal range we covered), followed by ethane (86 days and a factor of 3), and finally propane and ethyne, which have similar short lifetimes (20 days) and equally large gradients (a factor of 10). Other compounds with (dominant) northern continental sources and shorter lifetimes would have even larger gradients. Butane may be an example of a compound with mixed sources; by the above argument it should have a substantial latitudinal gradient, but while it does show signs of one it is small (at most a factor of 1.5). There is not enough data to separate diurnal variations from the longer-scale variations, but data were collected at all times of day with no obvious signs of large diurnal variations, even for alkenes with lifetimes of well under 12 hours.

Published data on ethene and propene is very scattered among different investigators, with many individual data sets also showing a great deal of scatter. No consistent latitudinal gradients have been observed. Low ethene levels of 20 - 50 pptv are reported, mixed in with observations of hundreds of pptv to 1 ppbv. For propene, low values of a few tens of pptv are reported in data sets with values also frequently reaching 500 pptv. For total butenes, pentenes and hexenes, Bonsang and Lambert (1985) report mixing ratios with medians exceeding 150 pptv in the equatorial central Pacific, while Bonsang *et al.* (1988) observed these alkenes exceeding 1 ppbv in the western Indian Ocean. Tille and Bachman (1987) observed 25 - 200 pptv total butene and 5 - 10 pptv total pentene over the Atlantic. Recently, Koppmann *et al.* (1991) reported very low ethene south of 20 °N over the Atlantic, with mixing ratios ranging between 10 and 30 pptv. Propene data were not reported due to an interference problem with water. They also used an in-situ GC system. Our atmospheric ethene measurements fall at the low end of the previously reported range. They are consistently below 100 pptv, and generally cluster about 50 pptv. Excepting the first 4 days of the cruise, our propene measurements are also consistently low, with a median value near 30 pptv. Again excepting the first 4 days, the butenes measured were all very low. 1-butene was the most abundant at roughly 5 pptv, while trans-2-butene was close behind at 4 pptv and cis-2-butene was generally at 1 pptv. 2-methyl-2-butene appears to have been the most

Table 4.4.1 Concentrations of NMHCs dissolved in ocean water, in (10^9 molec/cc).

| Compound | C_P | | C_B | C_L |
|--------------|-----------|------------|-----------|----------|
| | 8°N - 3°S | 3°N - 30°S | | |
| ethane | 42 ± 31 | 7.8 ± 3.6 | 110 ± 100 | 5 |
| ethene | 99 ± 30 | 38 ± 8 | 380 ± 300 | 100 ± 50 |
| ethyne | 2.8 ± 0.6 | 2.5 ± 0.8 | | |
| propane | 12 ± 10 | 3.5 ± 1.1 | 62 ± 52 | 7.5 |
| propene | 47 ± 21 | 19 ± 5.4 | 180 ± 130 | 50 ± 30 |
| butane | 6.3 ± 5.0 | 1.7 ± 0.8 | 29 ± 25 | 2.5 |
| 2-me-propane | 1.7 ± 0.8 | 0.7 ± 0.5 | 18 ± 16 | 2.5 |
| Σ butene | 26 ± 9.6 | 10.8 ± 4.2 | 51 ± 41 | |
| pentane | | | 16 ± 16 | |
| 2-me-butane | | | 23 ± 41 | |
| Σ pentene | | | 44 ± 42 | |
| hexane | | | 36 ± 36 | |
| Σ hexene | | | 22 ± 23 | |

From (C_P) Plass *et al.* (1991), (C_B) Bonsang *et al.* (1988), and (C_L) Lamontagne *et al.* (1974).

common pentene, at 7 - 15 pptv, though its absolute calibration is uncertain. Of the other pentenes, only 1-pentene and 2-methyl-1-butene frequently exceeded 1 pptv, each averaging about 2 pptv. The 5 high determinations of 3-methyl-1-butene at the end of the cruise may be misidentification with a nearby coeluting compound after the chromatographic conditions were changed. Note that there is no consistent latitudinal gradient for any of the alkenes. There is certainly variability, and examination of Figure 4.3.1 reveals the common nature of that variability among the alkenes and pentane. One particularly obvious common event was the sudden jump in alkene (and pentane) mixing ratios around JD 59, a day of extensive convective activity during which we moved from a northern hemispheric air-mass (with low alkene mixing ratios) to a southern hemispheric one (with high alkene mixing ratios). Curiously, it was the alkanes which showed a sudden jump on another convectively active day around JD 66. The data for these short-lived NMHC is consistent with a spatially and temporally heterogeneous marine source.

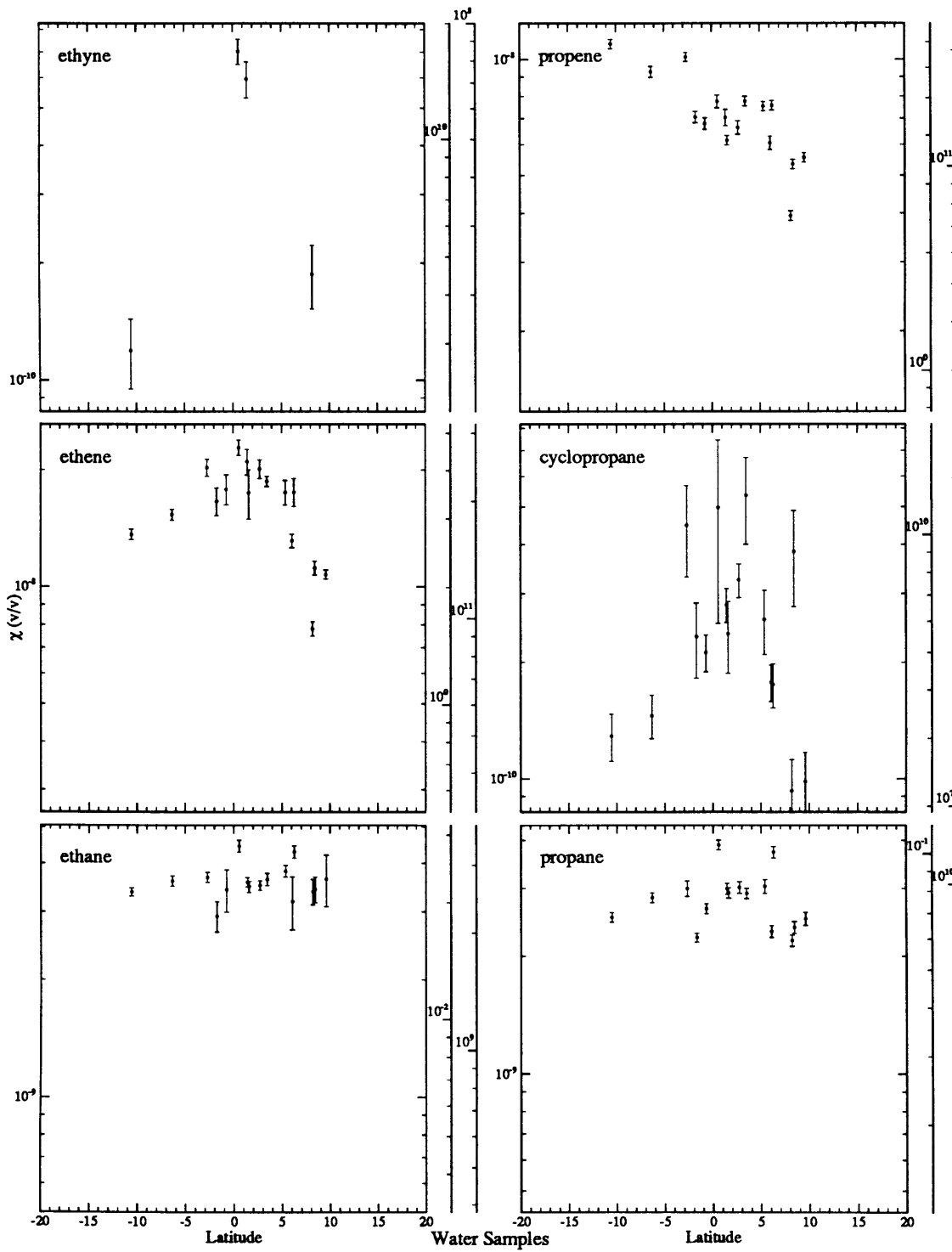
Our water measurements shown in Figure 4.3.2 are shown as a function of latitude in Figure 4.4.2. Most of the alkenes obey a common latitudinal pattern, with a minimum at 10°N (the northernmost extent of our track) and a maximum at 10°S (the southernmost point of the track), while the alkanes are relatively flat. Ethene and cyclopropane show signs of an

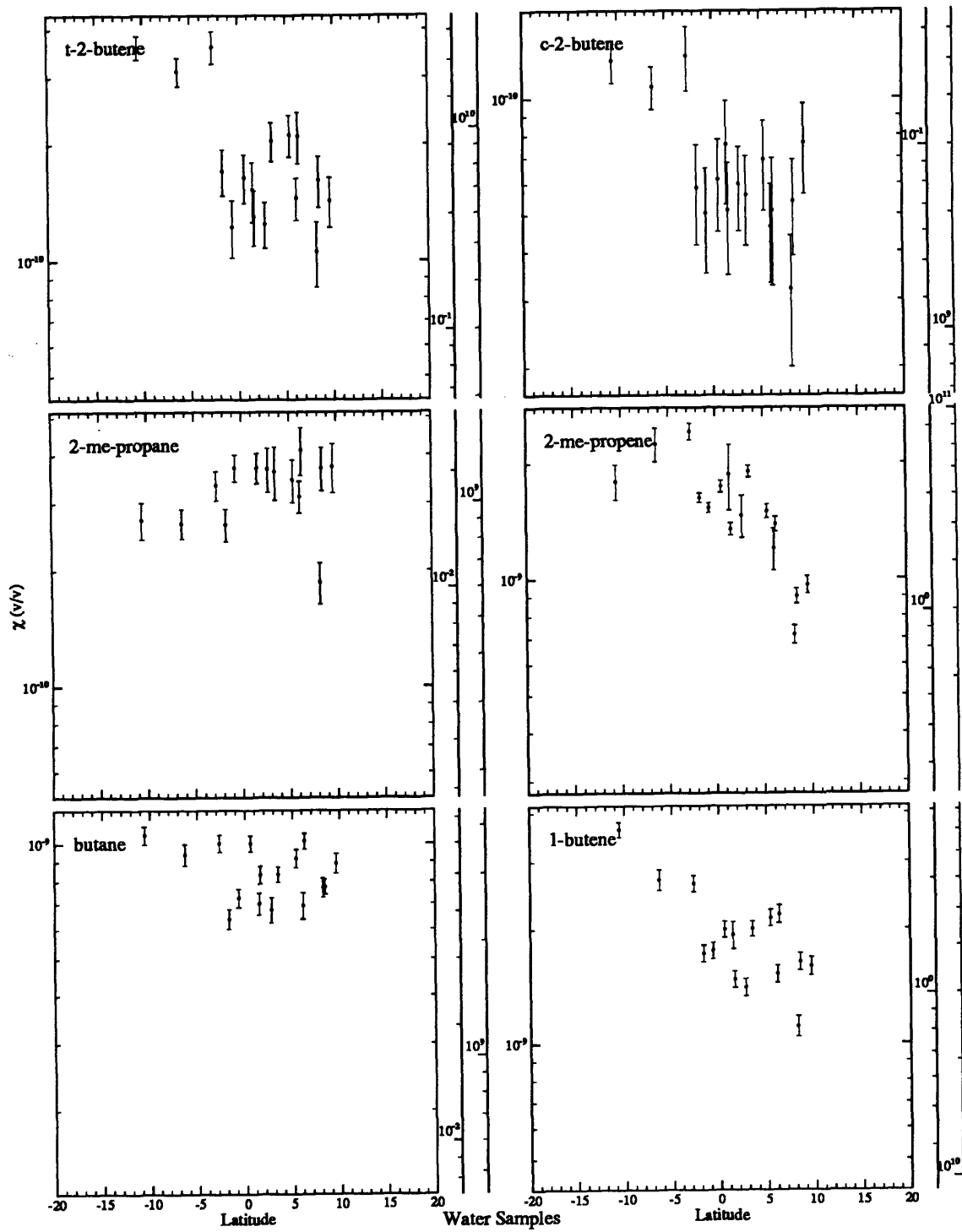
equatorial maximum. The 2-methyl-propene data are also shown; although we generally had contamination problems with this compound, the comparatively small sample size (100 cc), coupled with the very large 2-methyl-propene peak in the water samples, rendered these peaks far larger than the contamination peaks. We cannot discount the possibility that whatever was causing the contamination was most severe in the water samples, but note that the 2-methyl-propene shows a pattern almost identical to the other alkenes in sea water. If these data are real, 2-methyl-propene would be the most important butene, with a source strength roughly three times that of 1-butene. Our measurements are generally lower than those reported by other investigators, whose measurements are summarised in Table 4.4.1. A comparison with Plass *et al.* (1991) is particularly interesting. If we consider their data between 8°N and 30°S, which neglects their highest measurements for all compounds, our measurements fall short of theirs by roughly a factor of 3 for all compounds. For butane and 2-methyl-propane the discrepancy is roughly a factor of 4, while for ethene the distributions partially overlap, and for propene they differ by a factor of 2. Considering the different locations and the breadth of the individual distributions, this is good agreement. The common factors of 2 - 4 for the differences are also consistent with the general covariance of the NMHCs in water reported both by Bonsang *et al.* (1988) and Plass *et al.* (1991), although our water measurements are very much lower than those of Bonsang *et al.* (1988), by a factor closer to 30 than to 3.

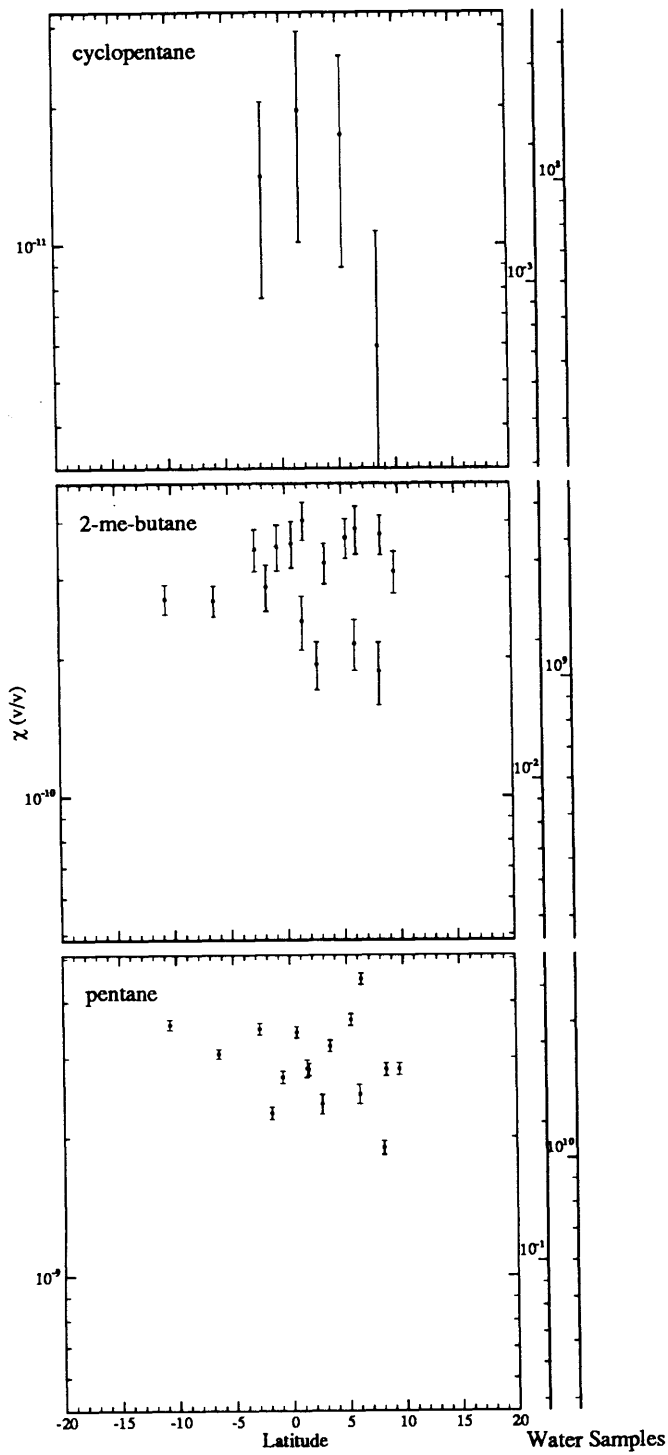
Provided that the NMHCs are generated in the ocean, emitted into the atmosphere, and locally removed principally through reaction with OH, the column destruction rate (the tertiary axis in Figure 4.3.1) and the oceanic emission rate (the tertiary axis in Figure 4.3.2) should be equal. This is discussed in Donahue and Prinn (1990) for previous NMHC measurements in terms of their photochemical model. While there is considerable uncertainty in calibrating the numbers on the two tertiary axes, the agreement of the atmospheric and oceanic rates is tenuous at best, with fluxes calculated from the water measurements lower than the atmospheric column removal rates by factors ranging from 3 for ethene to 200 for 2-methyl-2-butene. Note that we have assumed OH to be the sole atmospheric sink of the NMHCs in these calculations; inclusion of an ozone sink would aggravate the problem, especially for the 2-alkenes (see Table 4.1.1). Curiously, these factors are consistent with previous data (Donahue and Prinn (1990)), though both our atmospheric and oceanic measurements are in general lower than previous observations. There are five possible explanations for

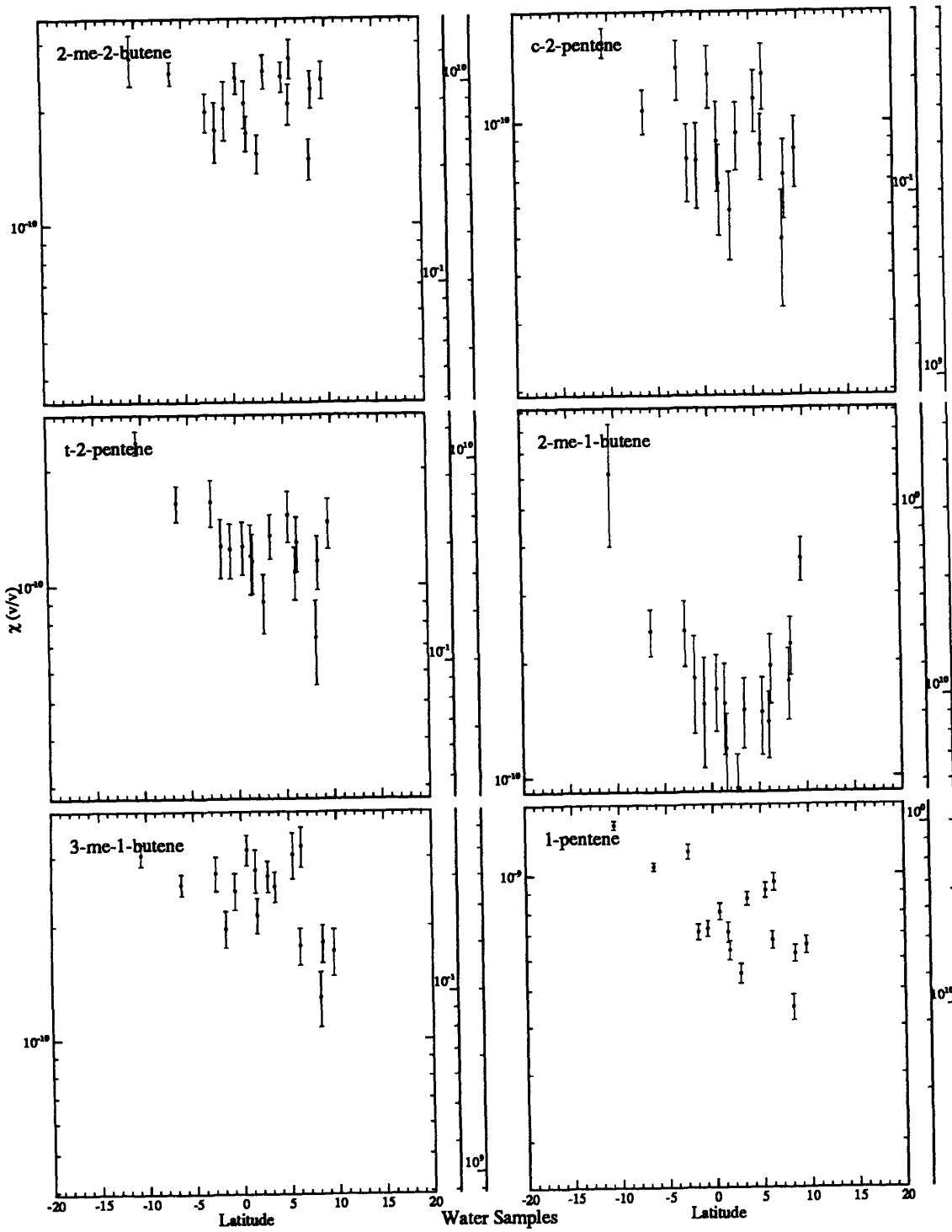
Figure 4.4.2

NMHC Mixing ratios for air in equilibrium with ocean water as a function of latitude. The primary axes are mixing ratios, with an absolute accuracy of $\pm 20\%$. The secondary axes are the NMHC concentrations in ocean water ($C_w = C_{eq}/H$) in molec cm^{-3} , with absolute accuracies of $\sim \pm 30 - 50\%$. Finally, the tertiary axes are the NMHC sea-air fluxes in molec $\text{cm}^{-2} \text{ sec}$, with an accuracy of $\sim \pm 100\%$ (see text).









the discrepancy represented by these large factors: the air measurements are falsely high, the water measurements are falsely low, sea-air NMHC fluxes are higher than the simple diffusive microlayer models (ie, Liss and Slater, 1974), the column removal rates are overestimated, or advection from continental or other remote sources makes up the difference. As already discussed, it is more likely that the air measurements are falsely high than low, but we have little evidence for a common, substantial contamination problem, especially very late in SAGA 3 when the air and water measurements overlap. With the equilibration system, undersaturation would be caused by outgassing before sea-water reached the equilibrator, leading to larger errors for less soluble compounds, which is what we found. The most obvious cause of failure in air-sea gas exchange models would be a microlayer source, which would flatten the microlayer gradient, driving more NMHCs into the atmosphere without greatly increasing the flux downward into the bulk mixed layer we were sampling. This is an intriguing possibility for the NMHCs, which could have as marine precursors hydrophobic surfactants confined to the surface layer. Factors making the estimated column removal rate falsely high would be overestimated scale heights or OH concentrations, The 500 m mixed layer has a mixing time scale of hours (Sarachick, 1985). We have assumed that the shorter lived NMHCs are confined to the mixed layer; given its mixing time, a substantially shorter scale height seems implausible. Likewise, 6×10^5 OH cm^{-3} could be high by a factor of two (Donahue and Prinn, 1990), but a greater factor is hard to justify. Furthermore, we have considered only OH initiated loss, neglecting ozone entirely and making it far more likely that we have underestimated than overestimated the column removal rates of most of the shorter lived alkenes. The last explanation (Singh and Zimmerman, 1991) suffers from at least three problems. The alkenes and heavier alkanes such as pentane do not display the characteristic latitudinal gradients of moderately short-lived compounds such as propane and radon which have continental sources contributing to their budgets in the remote marine atmosphere. As discussed above, compounds with lifetimes far shorter than propane and with primarily continental sources should display larger latitudinal gradients than propane, if their northern hemispheric continental sources are indeed stronger than their southern hemispheric sources. With the exception of the concentration drops during the early part of the cruise, which occurred on a southward leg and may well represent a continental influence, the alkenes (including ethene) as well as pentane do not display latitudinal variation but rather

a more complicated spatial variation not dependent on latitude. Also, if continental sources are important, the aforementioned factors should be largest for the longest lived alkenes. In fact the factors generally *increase* with *decreasing* compound lifetime, though far from monotonically. Back trajectories performed by Gary Herbert of NOAA (personal communication) indicate that for much of SAGA 3 the air being sampled was at least two weeks removed from continental influence. Neglecting mixing, even ethene concentrations would have been reduced to roughly 0.1 percent of their continental values, requiring a large-scale continental mixing ratio of 50 ppbv, which is more typical of a polluted urban setting (Singh and Zimmerman, 1991). Over two weeks 2-methyl-2-butene, with a lifetime of 0.25 days, would be depleted by a factor of 1.5×10^{-23} . Finally, our cruise track brought us to between 5°S and 10°S at 145°, 155°, and 165°W. Were there a continuous continental contribution to the NMHCs in the remote marine atmosphere, the air sampled at each of these southern points should have been roughly two days older than at the preceding point. For ethene, this would mean an expected e-fold decrease between each point. While there is a gradual decline in most alkene mixing ratios from day 60 on, even for ethene it is far too gentle. In summary, of the factors considered here for this problem, falsely low water measurements or incorrect air-sea gas exchange models are the most likely explanations.

It is of considerable interest to assess the role of the NMHCs in the remote marine OH budget. Here the alkenes are more important than the alkanes, of which only ethane and propane destroy OH more rapidly than $1 \times 10^{-3} \text{ sec}^{-1}$. The largest contributor appears to be propene, which removes OH at a rate of $(2 - 4) \times 10^{-2}$ per second, while ethene removes OH at roughly 1×10^{-2} per second. Both ethane and propane remove OH at rates between 1×10^{-2} and 1×10^{-3} removals per second depending on latitude. The heavier butenes may also contribute significantly, particularly 2-methyl-2-butene. The caveats made earlier about contamination force us to consider the OH removal rates for butenes and pentenes to be upper limits. With this consideration, the combined butenes may remove OH at rates of up to 2×10^{-2} per second, and the combined pentenes up to 3×10^{-2} per second. The total OH removal rate by NMHCs is roughly 0.1 per second, or 10 percent of the entire OH removal rate. This leaves the NMHCs as secondary but important players in the remote atmospheric OH budget, particularly considering the role played by their as yet unmeasured oxidation products, which could account for another 0.1 per second in the OH removal rate (Donahue

and Prinn, 1990).

As mentioned earlier, sample cylinders were filled on SAGA 3 by Anne Thompson and analyzed by Jim Greenberg (reported by Atlas *et al.*, 1990). Our measurements generally agree with Atlas *et al.* (1990) for alkanes, but again we observed much lower alkene levels. Bonsang *et al.* (1985) performed a hybrid measurement, taking flask samples but analyzing them aboard ship soon after sampling. They report some of the highest alkene observations. Singh and Zimmerman (1991) discuss this problem, indicating that light alkene concentrations in canisters have been observed to systematically increase with time, yet concluding that "It is likely that O₃ destroys alkenes during the cryogenic sampling process." We have demonstrated that, for our in-situ system, this is not the case. We therefore adopt the other conclusion, which is that alkenes are being generated in the canisters after sample collection. If this is true, the alkene production would have to be rapid in order to also explain the high observations of Bonsang and Lambert (1984), who analyzed canisters shortly after sampling.

4.5 Recommended Improvements

Several improvements should be made in this system:

1. The performance of the sample line is crucial. Our system could be improved in three ways: length, composition, and incorporation into the calibration. Our line was FEP teflon, some 50 meters long, and was not routinely included in either the calibrations or the blanks. On a ship, sample line length is not always under an investigator's control. A long line is not necessarily a problem but any loss or addition problems will scale with length. As bow sampling is essential, an in-situ instrument should therefore be located as close to the bow as possible unless a long sample line has been shown to be problem free (and is continuously tested during operation). The best solution would be to house the instrument in a small container which could be fixed forward of the bridge on a ship, if safety considerations allowed that. Teflon is non-reactive but permeable. We established the absence of loss in our line but not the absence of production. Production comes in three forms: permeation through the line, degassing of compounds impregnating the line, and true production in the line. All of these problems are reduced by short lines and high sample flow rates. Though hydrocarbon levels are vastly higher in air affected by the ship, they are not high enough to cause permeation

through the line to be a concern. Production in the line is certainly possible; if cannister sampling does suffer from rapid alkene production in the cannisters, one should also worry about rapid production in a sample line. Line degassing appears to be the most serious threat, however, particularly in the tropics. A line stored in an urban lab at 25°C will eventually reach equilibrium with that environment. When installed on a ship in the remote tropical atmosphere at 35°C, the line will degas. The only question is how much and for how long. Lines should therefore be thoroughly baked out immediately before shipment to the field and sealed in a hydrocarbon-free metal container. Our philosophy of treating standards exactly like samples applied on SAGA 3 to everything but the sampling line. Instead of being introduced at the bow, standards were introduced at the end of the sample line in the lab. This should be corrected in the future. If the instrument is far from the bow, sending the standard up a parallel line to the bow again means a long line and more chances for contamination or loss, but if a long line is acceptable for sampling, a factor of two is a healthy margin of error, and standards being sent to the bow will travel up the parallel line in a less rich gas mixture than samples heading to the instrument. An ideal configuration would consist of three lines, one running to the bow and two running from it, which would allow simultaneous sampling and either standard addition or calibration. Otherwise a rigorous cycle of samples, standards, zeros, and standard additions (and water samples) would allow only a sampling frequency of only a few per day.

2. The field instrument must be designed with tropical heat in mind. Aside from the concerns over the sample line, our actual instrument experienced some problems from the high temperatures. All of the surfaces outside of temperature controlled sections had been at 25°C for years before the system was placed aboard the Korolev. At 35°C in our inadequately air-conditioned lab, many surfaces degassed long-stored hydrocarbons (ethane and 2-methyl-propane in particular). Traps in gas lines should be avoided; we eventually found that ethane was degassing from one of the chemical traps in the carrier gas line, even though that trap had been conditioned before the cruise. The precision of all analyses improved markedly when the trap was removed, and because of this we were finally able to collect valid ethane data at the end of the cruise. The source of 2-methyl-propene contamination was never located. Zero air can only be obtained in

ship-board systems from a generator; too much is needed for blanking and calibration dilution for tanks to be practical. The zero air generator does involve large molecular sieve and activated charcoal traps and while we did not see severe problems from these, they were a source of concern. (The traps are followed in the generator by a methane reactor, but if large quantities of hydrocarbons were eluting from them the reactor may not have destroyed them all.) With the exception of any sample line problems, all of these degassing concerns could be met by an adequately air-conditioned laboratory; either integral to the ship or in the form of a container (the best option).

3. Water sampling must be explored more thoroughly and rigorously tested. Aboard the Korolev we took advantage of an available equilibration system. The system was, however, untested for the NMHCs. The system was a dynamic one, with a water flow rate of 20 liters per minute, and ocean water is an extremely rich collection of organisms and chemicals. The complexity of ocean water aside, either blanking or calibrating the system properly (by adding water with known NMHC levels, including zero) would be a formidable challenge. One possibility would be to put a high volume purge vessel ahead of the equilibrator. Also, the low solubility of hydrocarbons in water makes them poor candidates for equilibrator sampling. One problem is the slow response of the system; with a 20 liter per minute water flow rate and a 20 liter internal air volume, the equilibration time, expressed in minutes, will be equal to the Henry's law constant. For the NMHCs this is 5 - 50, meaning it will take 5 - 50 minutes for the equilibrator to respond to changes in water composition. Another problem is contamination; the high Henry's law constants mean that a relatively small air leak out of a water line would carry with it a substantial fraction of the highly supersaturated NMHC. Because the NMHC technique involves cryogenic sampling anyway, purge and trap water sampling is more suited to NMHC water analysis and should be used, in the very least to establish ground truth for the more convenient equilibrator samples.
4. The temperature program should be modified to allow sub-ambient initial temperatures. At 40 - 50 °C, ethane and ethene are not retained sufficiently on the PLOT column to erase any splitting caused by the cryofocussing. Their separation from each other and from an unknown compound between them is also only barely adequate. One extreme would be to bring or make liquid nitrogen and cool the GC oven enough to cryofocus on

the head of the column, rather than on a separate capillary loop; this would, however, eliminate the pre-column and its considerable benefits. Cryo-cooling of an oven also requires copious quantities of cryogen, rendering it impractical unless the cruise is short or an on-board cryogen source exists. Sufficient separation could be achieved by cooling the oven down to between 0 and 20°C, however, and this can be accomplished with a mechanical refrigeration system. Suitable prototype systems exist at NOAA/PMEL, operated by Tim Bates and Kim Kelley.

5. Methods for more rapidly collecting the necessarily large air samples (1 - 3 liters) should be explored. With a bare steel loop, we were limited to sample flows of 20 scc/m and barely trapped ethane and ethene. Any switch to a packed trap should be made, however, with the greatest caution after establishing with certainty that the traps do not clog with water, CO₂, or any other substance, and that 100 percent (neither more nor less) of all hydrocarbons can be desorbed from the loop. The cryofocussing reduces any requirement for instantaneous desorption, so in that regard packed traps are an option.
6. Sample drying and conditioning should be further explored. Our system consisted of a Nafion drier to remove most water, Ascarite (late in the cruise) to remove CO₂, and magnesium sulfate to further dry the sample and to remove any ozone which may have survived the first two traps. The Ascarite performed well, removing the CO₂ without affecting NMHCs (again demonstrated with standard additions). The Ascarite trap, borrowed from Jim Butler of GMCC, was well conditioned. Such conditioning may well be necessary. Likewise, Aquasorb (P₂O₅ impregnated vermiculite) is an unparalleled desiccant and completely destroys ozone. Well conditioned Aquasorb traps may be the best desiccant for marine air samples, provided that they do not destroy NMHCs.
7. Ship motion degrades FID performance. Because an FID combines a buoyant flame with charged collection plates, the FID baseline signal nicely records the orientation of the collector plates relative to the gravitational vector. This is a problem in two ways: the noise is increased, and the noise is far from white. Unfortunately, the resonant frequency of most ships is of order several seconds, which is similar to PLOT column peak widths; there is therefore no separation of scales between noise and signal frequencies, and thus no substantial reduction of noise from signal averaging. There are at least three potential solutions to this problem: the FID or the entire GC could be

gimballed, an accelerometer (perhaps an identical FID) could be used to correct for and subtract out the motion signal (Koppmann *et al.* (1991) use this approach), or the FID could be re-designed to reduce or eliminate the problem. At a minimum, the FID must have a cylindrical geometry (ours did); FID's with parallel plate collectors are rendered useless by even moderate seas (Kim Kelly, personal communication). A more radical re-design would be to eliminate buoyancy all together by confining the flame inside a relatively narrow tube. This is an intriguing possibility, as it would allow total control over the flame characteristics and could result in a more sensitive detector. Placing the instrument near the center of gravity of the ship will also reduce the problem, though this runs counter to the need for a short sample line.

8. The unknowns in our air analyses should be identified. If the instrument response for these compounds is similar to their nearest eluting NMHC neighbors, several of these unknowns have mixing ratios in the high tens of pptv. During SAGA 3, ethyne and cyclopropane were both unidentified; their identities were confirmed by later analysis of retention times. Two of the unknowns, the one eluting between ethane and ethene, and the one eluting in the large interval between butane and trans-2-pentene, appeared in lab tests in which ozone was being generated in zero air inside of a teflon tube before being mixed with an NMHC standard. Another peak, eluting slightly before cyclopentane, is in the position where we would expect to see 2-methyl-2-propane. The peaks eluting near the 2-butenes are also curiosities. The presence of cyclopropane suggests that the retention times of the other light cycloalkanes and cycloalkenes should be determined, although cyclopropane is quite long lived and appears to display the characteristics of a compound with a continental source.

4.6 Conclusions

We have obtained an interesting set of measurements that are relevant to NMHC concentrations, sources, and sinks over the equatorial Pacific, with measured NMHC mixing ratios which are generally low compared to other published observations. We were able to test both that the sampling line and the cryogenic trapping did not destroy NMHCs. The latter was tested routinely by adding a small flow of our standard into the sample flow from the bow in a standard addition. None of the NMHCs showed any signs of loss in these

tests. On one occasion the standard tank was lashed to the bow and the standard addition was performed over the entire length of the sampling line. Again, no losses were detected. Some doubt remains about possible sample line contamination early in the cruise, especially for propene and the pentenes. Our confidence that the atmospheric measurements are not too low is greater than our confidence that at least some of them are not too high.

We found the remote MBL to be an environment rich with unidentified compounds at the 10 pptv (hydrocarbon equivalent) level. Several of these compounds eluted very close to NMHCs we were measuring, and the temperature programmed GC technique inherently involved some variation in compound retention time. In most cases, we are confident that we have correctly identified the NMHC, using our integration software and the standard addition technique. We emphasize that for most of the hydrocarbons, the identification is unambiguous; both the retention times and peak shapes are consistent in standards, standard additions and samples. Late in the cruise we changed chromatographic conditions to improve separation, and achieved adequate separation for all compounds. Under the original conditions, coelution was a concern for ethene, propene, 2-methyl-propane and ethyne (with each other), trans-2-butene, and cis-2-butene. Using the later data, our integration software, and the standard additions performed while the earlier conditions applied, we have been able to unambiguously identify all of those compounds in the earlier data, excepting 2-methyl-propane and ethyne, where the picture is confused, and, when the peaks were very small, the 2-butenes. There being no indication of any negative interferences associated with these co-elutions, it is still possible to extract upper limits from the data, but positive detections are sometimes uncertain.

While the short lifetimes of the NMHCs preclude direct comparison of our data with any other data except that from simultaneously gathered samples, our atmospheric and oceanic measurements both fall at the lower limit of the broad range of currently published measurements. Revisiting the goals of the work, we have shown:

1. The in-situ GC/FID system works well. NMHCs are not lost during sample collection, and the ability to test in real time such problems as losses and contamination certainly render the method superior to flask sampling. Any problems we may have had with sample line contamination for some species can be eliminated through instrument redesign.

2. NMHCs play an important but secondary role in remote MBL chemistry, at least under the conditions encountered on SAGA 3.
3. The longer lived NMHCs, ethane, ethyne, propane, and cyclopropane, display strong latitudinal gradients, consistent with a northern hemispheric source. The shorter lived NMHCs display distributions consistent with a dispersed marine source, with at most occasional influences from continental advection.
4. We cannot confirm the conclusions of Koppman *et al.* (1991) that the NMHCs in the air and water are generally well balanced, concluding instead that, according to present understanding, marine sources are insufficient to maintain the levels seen in the atmosphere. However, the discrepancy is least severe for those compounds which Koppman *et al.* (1991) studied.

There is more to be gleaned from this data. The wealth of companion measurements in particular make the entire SAGA 3 data set, including these data, potentially lucrative for the examination of chemistry in the remote troposphere. For the atmospheric and oceanic NMHC measurements we need to determine whether one or the other is unreliable, or instead whether some revision of our concepts of air-sea gas exchange is required. Overall our NMHC measurements combined with earlier studies indicate that although the NMHCs are rare in the remote troposphere, they play an important secondary role in remote tropospheric chemistry and deserve continued attention.

Chapter 5 -- Conclusions

The concluding sentences of chapters 2 and 4 of this thesis stand in almost perfect disagreement. Is all hope lost? I would like to think that something has been gained, and that the questions raised in Chapter 2 (which is a largely unaltered version of a paper written in 1989) have been partially answered by the experimental work presented in Chapter 4. It should be noted that our observations fall within the ranges considered in Chapter 2; they fall very close to the lower limit, but they do in general lie above it. This applies to both the air and sea measurements, leading the curious consequence that we appear to have bolstered an apparent inconsistency in existing data. There are two possible explanations of this: either there are common systematic problems leading to either the consistent over-estimation of atmospheric NMHC mixing ratios or the consistent under-estimation of oceanic NMHC concentrations, or something is wrong with the air-sea gas exchange models we employ. Either possibility could be true, but the second one is sufficiently intriguing that it is well worth the necessary effort to either eliminate or confirm the first.

I hope there is an air of incompleteness about this as well, to be blunt. I have very much tried to let the data and the models tell me where to go, rather than blunder along with an *idée fixe* stuck in my mind like a seed between my teeth. I feel that they have led me along a path which should continue to be explored. I can describe some guideposts:

1. The remote, tropical, troposphere is not only a nice place to visit, it dominates global tropospheric chemistry as well.
2. There is a tremendous coupling of scales out there; compounds emitted from the ocean surface mix upward, continentally derived constituents are advected into the regions, and compounds from the stratosphere mix downward. All the while, diurnal cycling grinds on. Many of the most interesting compounds have chemical lifetimes which complicate attempts to separate these scales, being too short lived to ignore diurnal effects but too long lived to ignore either vertical mixing or horizontal advection.
3. We have passed the period of raw exploration, when more or less *ad hoc* attempts to measure compounds without careful planning and coordination with other measurements and models were useful as voyages of discovery. It is time to assess how combined measurements and models can be used to study these moderately short lived species to rigorously exclude hypotheses, rather than to simply indicate their plausibility. That is

not an easy problem, and it will require very active cooperation among meteorologists, chemical modelers, kineticists, and field experimentalists. Measurement programs need more design; necessary detection limits, key compounds, and rate constants, optimal spatial and temporal measurement resolution all need to be identified for a particular experiment, not by proclamation but by investigation.

I view this work as a very modest step along the path described. I was told in no uncertain terms by an early version of the model described in Chapter 2 that dimethyl sulfide could not be modeled without a better understanding of the nonmethane hydrocarbons, due to the coupling with OH, and I was told by a later version (the one in Chapter 2) that very low detection limits, substantially lower than reported for most systems, were necessary to understand the nonmethane hydrocarbons themselves. I hope I listened.

References

- Ackman, R.G., The Flame Ionization Detector: Further Comments on Molecular Breakdown and Fundamental Group Responses, *Journal of Gas Chromatography*, 6, 497 - 501, 1968.
- Aikin, A.C., F.R. Herman, E.J. Maier, and C.J. McQuillan, Atmospheric chemistry of ethane and ethylene, *Journ. Geophys. Res.*, 87, 3105 - 3118, 1982.
- Anastasi, C., I.W.M. Smith, D.A. Parkes, Flash photolysis study of the spectra of CH_3O_2 and $\text{C}(\text{CH}_3)\text{O}_2$ and the kinetics of their mutual reactions and with NO, *J. Chem. Soc., Faraday Trans. I*, 74, 1693 - 1701, 1978.
- Andreae, M.O., R.J. Ferek, F. Bermond, K.P. Byrd, R.T. Engstrom, S. Hardin, P.D. Houmère, F. LeMarrec, H. Raemndonck, and R.B. Chatfield, Dimethyl Sulfide in the marine atmosphere, *Journ. Geophys. Res.*, 90, 12,891 - 12,900, 1985.
- Atkinson, R., Kinetics and Mechanisms of the Gas-Phase Reactions of the Hydroxyl Radical with Organic Compounds, *J. Phys. Chem. Ref. Data* monograph 1, 268 pgs, 1989.
- Atkinson, R., A structure-activity relationship for the estimation of rate constants for the gas-phase reactions of OH radicals with organic compounds, *Int. J. Chem. Kin.*, 19, 799 - 828, 1987.
- Atkinson, R., and A.C. Lloyd, Evaluation of kinetic and mechanistic data for modeling of photochemical smog, *J. Phys. Chem. Ref. Data*, 13, 315 - 444, 1984.
- Atkinson, R., Kinetics and mechanisms of the gas-phase reactions of the hydroxyl radical with organic compounds under atmospheric conditions, *Chem. Rev.*, 85, 69 - 201, 1986.
- Atkinson, R., D.L. Baulch, R.A. Cox, R.F. Hampson, Jr., J.A. Kerr and J. Troe, Evaluated kinetic and photochemical data for atmospheric chemistry: supplement III, *J. Phys. Chem. Ref. Data*, 18, 881 - 917, 1989.
- Atkinson, R., and W.P.L. Carter, Kinetics and mechanisms of the gas-phase reactions of ozone with organic compounds under atmospheric conditions, *Chem. Rev.*, 83, 437 - 470, 1984.
- Atlas, E., W. Pollock, J. Greenberg, L. Heidt, and A. Thompson, Measurements of Organic Nitrates, NMHC, and Halocarbons During SAGA - III, *EOS*, 71, p1230, 1990.
- Barnes, I., K.H. Becker, P. Carlier, and G. Mouvier, FTIR study of the $\text{DMS}/\text{NO}_2/\text{I}_2/\text{N}_2$ photolysis system: the reaction of IO radicals with DMS, *Int. J. Chem. Kin.*, 19, 489 - 501, 1987.
- Bonsang, B., and G. Lambert, Nonmethane hydrocarbons in an oceanic atmosphere, *J. Atmos. Chem.*, 2, 257 - 271, 1985.
- Bonsang, B., M. Kanakidou, G. Lambert, and P. Monfray, The marine source of $\text{C}_2 - \text{C}_6$ aliphatic hydrocarbons, *J. Atmos. Chem.*, 6, 3 - 20, 1988.
- Butler, J.H., J.W. Elkins, and T.M. Thompson, Tropospheric and Dissolved N_2O of the West Pacific and East Indian Oceans During the El Nino Southern Oscillation Event of 1987, *Journ. Geophys. Res.*, 94, 14, 865 - 14, 877, 1989.
- Calvert, J.G., and S. Madronich, Theoretical study of the initial products of the atmospheric oxidation of hydrocarbons, *Journ. Geophys. Res.*, 92, 2211 - 2220, 1987.
- Carter, W.P.L., and R. Atkinson, Atmospheric chemistry of alkanes, *J. Atmos. Chem.*, 2, 377 - 405, 1985.
- Carroll, M. A., *An Experimental Study of the Fluxes of Reduced Sulfur Gases from a Salt Water Marsh*, MIT, Cambridge, 187 pp, 1983.
- Chandrasekhar, S., *Radiative Transfer*, (Dover, New York), 393 pgs, 1960.
- Chatfield, R.B., and P.J. Crutzen, Are there interactions of iodine and sulfur species in marine air photochemistry?, *Journ. Geophys. Res.*, in press, 1990.

- Cox, R.A., and G.S. Tyndall, Rate constants for the reactions of CH_3O_2 with HO_2 , NO , and NO_2 using Molecular Modulation Spectrometry, *J. Chem. Soc., Faraday Trans. II*, 76, 153 - 163, 1980.
- Crosley, D.R., and J.M. Hoell, *Future directions for H_xO_y detection*, NASA Conference publication 2448, 1986.
- Crutzen, P.J., The role of NO and NO_2 in the chemistry of the troposphere and stratosphere, *Ann. Rev. Earth Planet. Sci.*, 7, 443 - 472, 1979.
- Crutzen, P.J., *Tropospheric ozone: an overview*, in *Tropospheric Ozone*, D. Reidel, Boston, 1988. I.S.A. Isaksen (ed.),
- Dagaut, P., T.J. Wallington, and M.J. Kurylo, Flash photolysis kinetic absorption spectroscopy study of the gas-phase reactions $\text{HO}_2 + \text{C}_2\text{H}_5\text{O}_2$ over the temperature range 228 - 380 K, *J. Phys. Chem.*, 92, 3836-3839, 1988.
- Dagaut, P., T.J. Wallington, and M.J. Kurylo, Temperature dependence of the rate constant for the $\text{HO}_2 + \text{CH}_3\text{O}_2$ gas-phase reaction, *J. Phys. Chem.*, 92, 3833-3836, 1988.
- Dagaut, P., T.J. Wallington, R. Liu, and M.J. Kurylo, The gas phase reactions of hydroxyl radicals with a series of carboxylic acids over the temperature range 240 - 440 K, *Int. J. Chem. Kin.*, 20, 331 - 338, 1989.
- DeMore, W.B., M.J. Molina, S.P. Sander, D.M. Golden, R.F. Hampson, M.J. Kurylo, C.J. Howard, A.R. Ravishankara, *Chemical kinetics and photochemical data for use in stratospheric modeling*, JPL Publication 87-41, 1987.
- Donahue, N.M., and R.G. Prinn, Nonmethane Hydrocarbon Chemistry in the Remote Marine Boundary Layer, *Journ. Geophys. Res.*, 95, 18, 387 - 18, 411, 1990.
- Ehhalt, D.H., J. Rudolph, F. Meixner, and U. Schmidt., Measurements of selected C_2 - C_5 hydrocarbons in the background troposphere: vertical and latitudinal variations, *J. Atmos. Chem.*, 3, 29 - 52, 1985.
- Fishman, J., G.L. Gregory, G.W. Sachse, S.M. Beck, and G.F. Hill, Vertical profiles of ozone, carbon monoxide, and dew-point temperature obtained during GTE/CITE 1, October - November 1983. *Journ. Geophys. Res.*, 92, 2083 - 2094, 1987.
- Gammon, R.H., and K.C. Kelly, Reassessment of the flux of CO from the global ocean to the atmosphere, *EOS*, 69, 1072, 1988.
- Gelb, A. (ed.), *Applied Optimal Estimation*, (MIT Press, Cambridge, MA), 374 pgs, 1974.
- Greenberg, J.P., and P.R. Zimmerman, Nonmethane hydrocarbons in remote tropical, continental, and marine atmospheres, *Journ. Geophys. Res.*, 89, 4767 - 4778, 1984.
- Houghton, H.G., *Physical Meteorology*, (MIT Press, Cambridge, MA), 442 pgs, 1985.
- Jacob, D.J., Chemistry of OH in remote clouds and its role in the production of formic acid and peroxymonosulfate, *Journ. Geophys. Res.*, 91, 9807 - 9826, 1986.
- Jenkin, M.E., R.A. Cox, G.D. Hayman, and L.J. Whyte, Kinetic Study of the Reactions $\text{CH}_3\text{O}_2 + \text{CH}_3\text{O}_2$ and $\text{CH}_3\text{O}_2 + \text{HO}_2$ using Molecular Modulation Spectroscopy., *J. Chem. Soc., Faraday Trans. 2*, 84, 913 - 930, 1988.
- Johnson, J.E., R.H. Gammon, J. Larsen, T.S. Bates, S.J. Oltmans, and J.C. Farmer, Ozone in the marine boundary layer over the Pacific and Indian oceans: latitudinal gradients and diurnal cycles., *Journ. Geophys. Res.*, in press, 1990.
- Kasting, J., and H. Singh, Nonmethane hydrocarbons in the troposphere: impact on the odd hydrogen and odd nitrogen chemistry. *Journ. Geophys. Res.*, 91, 13239 - 13256, 1986.
- Koppmann, R., R. Bauer, F.R. Johnen, C. Plass, and J. Rudolph, The Distribution of Light Nonmethane Hydrocarbons over the mid-Atlantic: Results of the Polarstern cruise ANT VII/1, submitted to *J. Atmos. Chem.*, 1991.

- Kurylo, M.J., P. Dagaut, T.J. Wallington, D.M. Neuman, Kinetic measurements of the gas-phase HO₂ + CH₃O₂ cross-disproportionation reaction at 298 K, *Chem. Phys. Lett.*, 139, 513 - 518, 1987.
- Lamontagne, R.A., J.W. Swinnerton, and V.J. Linnebom, C₁ - C₄ hydrocarbons in the North and South Pacific, *Tellus*, 26, 71 - 77, 1974.
- Leone, J.A., and J.H. Seinfeld, Comparative analysis of chemical reactions mechanisms for photochemical smog, *Atmos. Env.*, 19, 437 - 464, 1985.
- Levy, H., Normal atmosphere: large radical and formaldehyde concentrations predicted, *Science*, 173, 141 - 143, 1971.
- Lightfoot, P.D., R. Lesclaux, and B. Veyret, Flash photolysis study of the CH₃O₂ + CH₃O₂ reaction: rate constants and branching ratios from 248 to 537 K, *J. Phys. Chem.*, 94, 700 - 707, 1990a.
- Lightfoot, P.D., B. Veyret, and R. Lesclaux, Flash photolysis study of the CH₃O₂ + HO₂ reaction between 248 and 537 K, *J. Phys. Chem.*, 94, 708 - 714, 1990b.
- Liss, P.S., and P.G. Slater, Flux of gases across the air-sea interface, *Nature*, 247, 181 - 184, 1974.
- Liu, S.C., M. McFarland, D. Kely, O. Zaririou, and B. Huebert, Tropospheric NO_x and O₃ budgets in the Equatorial Pacific, *Journ. Geophys. Res.*, 88, 1360 - 1368, 1983.
- Liu, S.C., S. McKean, and M. Trainer, Impacts of biogenic nonmethane hydrocarbons on the tropospheric chemistry, in *Our Changing Atmosphere*, Crutzen, P., K.C. Gerard, and R. Vander eds., 1989. Proc 28th Liege Int. Astrophys. Colloq., European Geophysical Union, Liege, Belgium, June 26-30, 1989.
- Logan, J.A., M.J. Prather, S.C. Wofsy, and M.B. McElroy, Tropospheric chemistry: a global perspective. *Journ. Geophys. Res.*, 86, 7210 - 7254, 1981.
- Mackay, D., and W.Y. Shiu, Critical Review of Henry's Law Constants for Chemicals of Environmental Interest, *J. Phys. Chem. Ref. Data*, 10, 1175 - 1199, 1981.
- Madronich, S., and J.G. Calvert, Alkyl and Acyl Peroxy radicals in the atmosphere: a study of the effect of their permutation reactions, *EOS*, 69, 1071, 1988.
- Madronich, S., and Jack G. Calvert, Permutation reactions of organic peroxy radicals in the troposphere, *Journ. Geophys. Res.*, 95, 5697 - 5716, 1990.
- McAdam, K., B. Veyret, and R. Lesclaux, UV absorption spectra of HO₂ and CH₃O₂ radicals and the kinetics of their mutual reactions at 298 K, *Chem. Phys. Lett.*, 133, 39 - 44, 1987.
- McAuliffe, C., Solubility in Water of Paraffin, Cycloparaffin, Olefin, Acetylene, Cycloolefin, and Aromatic Hydrocarbons, *J. Phys. Chem.*, 70, 1267 - 1275, 1966.
- Molina, M.J., and G. Arguello, Ultraviolet absorption spectrum of methylhydroperoxide vapor, *Geophys. Res. Lett.*, 6, 952 - 955, 1979.
- Moortgat, G., B. Veyret, and R. Lesclaux, Absorption spectrum and kinetics of reactions of the acetylperoxy radical, *J. Phys. Chem.*, 93, 2362 - 2368, 1989a.
- Moortgat, G., B. Veyret, and R. Lesclaux, Kinetics of the reaction of HO₂ with CH₃C(O)O₂ in the temperature range 253 - 368 K, *Chem. Phys. Lett.*, 160, 443 - 447, 1989 b.
- Niki, H., P.D. Maker, C.M. Savage, and L.P. Breitenbach, A fourier transform infrared study of the kinetics and mechanism for the reactions HO + CH₃OOH, *J. Phys. Chem.*, 87, 2190 - 219, 1983.
- Nutmagul, W., and D.R. Cronn, Determination of selected atmospheric aromatic hydrocarbons at remote continental and oceanic locations using photoionization/flame-ionization detection, *J. Atmos. Chem.*, 2, 415-433, 1985.
- Plass, C., R. Koppmann, and J. Rudolph, Light Hydrocarbons in the Surface Water of the Mid-Atlantic, submitted to *J. Atmos. Chem.*, 1991.

- Plum, C.N., E. Sanhueza, R. Atkinson, W.P. Carter, and J.N. Pitts, Jr., OH radical rate constants and photolysis rates of α -dicarbonyls, *Env. Sci. Tech.*, 17, 479 - 484, 1983.
- Piotrowicz, S.R., D.A. Boran, and C.K. Fischer, Ozone in the boundary layer of the equatorial Pacific Ocean, *Journ. Geophys. Res.*, 91, 13,113 - 13,119, 1986.
- Prinn, R. G., How have the atmospheric concentrations of the halocarbons changed? In, *The changing Atmosphere*, F.S. Rowland and I.S.A. Isaksen, eds., (John Wiley & Sons, New York) 33 - 48, 1988.
- Prinn, R.G., D. Cunnold, R. Rasmussen, P. Simmonds, F. Alyea, A. Crawford, P. Fraser, and R. Rosen, Atmospheric trends in methylchloroform and the global average for the hydroxyl radical, *Science*, 238, 945 - 950, 1987.
- Ridley, B.A., M.A. Carroll, and G.L. Gregory, Measurements of Nitric Oxide in the boundary layer and free troposphere over the Pacific Ocean, *Journ. Geophys. Res.*, 92, 2025 - 2047, 1987.
- Roether, W., Field measurements of gas exchange, in *Dynamic processes in the chemistry of the upper ocean*, Burton, J.D., P.G. Brewer, and R. Chesselet, eds., NATO Advanced Research Institute on Dynamic Processes in the Chemistry of the Upper Ocean, (1983: Jouy-en-Josas, France), Plenum Press, New York, 117 - 128, 1986.
- Rudolph, J., Two-dimensional distribution of light hydrocarbons: results from the STRATOZ III experiment, *Journ. Geophys. Res.*, 93, 8367 - 8377, 1988.
- Rudolph, J., and D.H. Ehhalt, Measurements of C₂ - C₅ hydrocarbons over the North Atlantic, *Journ. Geophys. Res.*, 86, 11,959 - 11,964, 1981.
- Sarachik, E. S., A Simple Theory of the Vertical Structure of the Tropical Atmosphere, *Pure and Applied Geophysics*, 123, 261 - 271, 1985.
- Schmidbauer, N., and M. Oehme, Analysis of Light Hydrocarbons (C₂ - C₆) at ppt Levels by High Resolution Gas Chromatography, *Journal of High Resolution Chromatography and Chromatography Communications*, 8, 404 - 406, 1985.
- Seiler, W., and J. Fishman, The distribution of carbon monoxide and ozone in the free troposphere, *Journ. Geophys. Res.*, 86, 7275-7256, 1981.
- Seiler, W., H. Giehl, E.G. Brunke, and E. A. Halliday, The seasonality of CO abundance in the southern hemisphere, *Tellus*, 36B, 219 - 231, 1984.
- Singh, H.B., and Zimmerman, P.B., Atmospheric Distributions and Sources of Nonmethane Hydrocarbons, submitted to *Adv. Env. Sci. Tech.*, 1991.
- Singh, H.B., and J.F. Kasting, Chlorine-hydrocarbon photochemistry in the marine troposphere and lower stratosphere, *J. Atmos. Chem.*, 7, 261 - 286, 1988.
- Singh, H.B., W. Viezee, and L.J. Salas, Measurements of selected C₂ - C₅ hydrocarbons in the troposphere, latitudinal, vertical, and temporal variations, *Journ. Geophys. Res.*, 93, 15,861 - 15,878, 1988.
- Singh, H.B., and L.J. Salas, Measurement of selected light hydrocarbons over the Pacific Ocean: latitudinal and seasonal variations, *Geophys. Res. Lett.*, 9, 842 - 845, 1982.
- Thompson A. M., and D. H. Lenschow, Mean profiles of trace reactive species in the unpolluted marine surface layer, *Journ. Geophys. Res.*, 89, 4788 - 4796, 1984.
- Thompson A., and R. Cicerone, Clouds and wet removal as causes of variability in the trace-gas composition of the marine atmosphere, *Journ. Geophys. Res.*, 87, 8811 - 8826, 1982.
- Tille, K.J.W., and K. Bachmann, Natural and anthropogenic hydrocarbons and halocarbons over the Atlantic Ocean: latitudinal distributions of mixing ratios and sources, pp 440 - 450 in *Physio-chemical behavior of atmospheric pollutants*, G. Angeletti and G. Restelli, eds, Proceedings of the Fourth European Symposium (23 - 25 Sept 1986: Stresa Italy), D. Reidel, Boston, 809 pgs., 1987.

U.S. Standard Atmosphere Supplements, (U.S. Government Printing Office, Washington, D.C.) 289 pgs, 1966.

Vaghjiani G.L., and A.R. Ravishankara, Kinetics and mechanism of OH reactions with CH₃OOH, *J. Phys. Chem.*, 93, 1948 - 1959, 1989b.

Vaghjiani G.L., and A.R. Ravishankara, Absorption cross sections of CH₃OOH, H₂O₂, and D₂O₂ vapors between 210 and 365 nm at 297 K, *Journ. Geophys. Res.*, 94, 3487 - 3492, 1989a.

Warneck, P., On the role of OH and HO₂ radicals in the troposphere, *Tellus*, 26, 39 - 46, 1974.

Wilhelm, E., R. Battino, and R.J. Wilcock, Low-Pressure Solubility of Gases in Liquid Water, *Chem. Rev.*, 77, 219 - 260, 1977.

World Meteorological Organization, *Atmospheric Ozone*, V1, (National Aeronautics and Space Administration, Washington, D.C.), 392 pgs, 1985.

Appendix 1

The complete reaction set used in Chapter 5, revised through May, 1990.

- *This file contains the reactions and rate expressions important to regulating atmospheric OH concentrations.
- *This set contains reactions up to C6
- *The rates here have been updated to include NASA 87 recommendations.
- *There are several symbols embedded in this file which must be changed before it can be used in a model. They are as follows:
- *1> "712" represents the activation energy boost from OOH in CH3OOH
- *2> "& " precedes the activation energy for any Atkinson estimated k with $E < -500$ Kelvin. These should generally be changed to 500K.
- *3> "3.2E-12" is the { RO2 } + HO2 reaction rate
- *4> Carboxylic acids from Dagaut et al (1988), all C4 and higher as i-butyric
- *5> Organic nitrates + OH are assumed to produce products like PAN, Atkinson ks

```
**      Reaction                      Rate
# define JNO2      J = crossec \ NO2.phd
# define JCH3OOH   J = crossec \ CH3OOH.phd
# define JCH3CHO_1 J = crossec \ CH3CHO_ 1.phd
# define JCH3CHO_2 J = crossec \ CH3CHO_ 2.phd
# define Jacetone  J = crossec \ acetone.phd
# define kROOHOOH  k = 5.9E-12
# define kRO2hh    k = 3.8E-13*exp(+580/T)*(1+3.2E-21*exp(+470/T)*(C[N2]+C[O2]))
# define kRO2hhH2O kd = 2.8E-18*kRO2hh
# define kRO2hm    k = 4.4E-13*exp(+780/T)
# define kRO2hp    k = 4.4E-13*exp(+780/T)
# define kRO2hs    k = 4.4E-13*exp(+780/T)
# define kRO2ht    k = 4.4E-13*exp(+780/T)
# define kRO2ho    k = 4.3E-13*exp(+1040/T)
# define kRO2mm    k = 8.8E-13
# define kRO2mp    k = 6.8E-13
# define kRO2ms    k = 1.1E-13
# define kRO2mt    k = 3.9E-14
# define kRO2mo    k = 1.4E-11
# define kRO2pp    k = 4.0E-13
# define kRO2ps    k = 6.3E-14
# define kRO2pt    k = 2.3E-14
# define kRO2po    k = 7.6E-12
# define kRO2ss    k = 1.6E-15
# define kRO2st    k = 5.8E-16
# define kRO2so    k = 1.2E-12
# define kRO2tt    k = 7.5E-17
# define kRO2to    k = 4.3E-13
# define kRO2oo    k = 3.3E-11
# define kRO2NOh   k = 3.7E-12*exp(+240/T)
# define kRO2NOm   k = 4.2E-12*exp(+180/T)
```

```

# define kRO2NOp  k = 4.2E-12*exp(+180/T)
# define kRO2NOs  k = 4.2E-12*exp(+180/T)
# define kRO2NOt  k = 4.2E-12*exp(+180/T)
# define kRO2NOo  k = 1.4E-11
# define kRO2NO2  k = 4.3E-12*exp(+180/T)
**      Reaction                      Rate
R1: N1   O3 -> O2 + O_ 1D; J = crosssec \ O3_ 1D.phd
R2: N1   O3 -> O2 + O_ 3P; J = crosssec \ O3_ 3P.phd
R3: C3   O_ 1D + N2 -> O_ 3P + N2; k = 1.8E-11*exp(+107/T)
R4: C3   O_ 1D + O2 -> O_ 3P + O2; k = 3.2E-11*exp(+67/T)
R5: C3   O_ 1D + H2O -> OH + OH; k = 2.2E-10
R6: C3   O_ 1D + H2O -> O_ 3P + H2O; k = 1.2E-11
R7: C3   O_ 1D + H2O -> H2 + O2; k = 2.3E-12
R8: C3   O_ 3P + O2 -> O3; L_ N2 = 5.7E-34*(T/300)^ (-2.8)
L_ O2 = 6.2E-34*(T/300)^ (-2.0)
ki = 2.8E-12
Fc = exp(-T/696)
R9: N7   HO2 + O3 -> OH + O2 + O2; k = 1.1E-14*exp(-500/T)
R10: N1  H2O2 -> OH + OH; J = crosssec \ H2O2_ OH.phd
R11: C3  HO2 + NO -> OH + NO2; kd = kRO2NOh
R12: C3  OH + H2O2 -> H2O + HO2; k = 2.9E-12*exp(-160/T)
R13: N7  OH + HO2 -> H2O + O2; k = 4.6E-11*exp(+230/T)
R14: C3  OH + O3 -> HO2 + O2; k = 1.9E-12*exp(-1000/T)
R15: H1  OH + CO -> CO2 + H; s1 = 1.47E-13*(1 + 0.59*(C[N2]+C[O2])/2.5E19)
R16: C3  OH + NO2 -> HONO2; L_ N2 = 2.6E-30*(T/300)^ (-2.9)
L_ O2 = 2.2E-30*(T/300)^ (-2.9)
ki = 5.2E-11
Fc = exp(-T/353)
R17: C3  HONO2 -> OH + NO2; J = crosssec \ HONO2.phd
R18: N7  OH + HONO2 -> H2O + NO3; s3 = 7.2E-15*exp(+785/T)
k2 = 4.1E-16*exp(+1440/T)
k3 = 1.9E-33*exp(+725/T)
R19: C3  OH + NO -> HONO; L_ N2 = 7.4E-31*(T/300)^ (-2.4)
L_ O2 = 7.4E-31*(T/300)^ (-2.4)
ki = 1.0E-11
Fc = exp(-T/1300)
R20: C3  HONO -> OH + NO; J = crosssec \ HONO.phd
R21: L1  OH + HONO -> H2O + NO2; k = 6.6E-12;
R22: N7  OH + H2 -> H2O + H; k = 5.5E-12*exp(-2000/T)
R23: N7  H + O2 -> HO2; L_ N2 = 5.7E-32*(T/300)^ (-1.6)
L_ O2 = 5.7E-32*(T/300)^ (-1.6)
ki = 7.5E-11
Fc = exp(-T/502)
R24: N7  HO2 + HO2 -> H2O2 + O2; kd = kRO2hh
R25: N7  HO2 + HO2 + H2O -> H2O2 + O2 + H2O; kd = kRO2hhH2O
R26: N7  HO2 + NO2 -> HO2NO2; L_ N2 = 1.8E-31*(T/300)^ (-3.2)

```

$L_{O2} = 1.8E-31*(T/300)^{-3.2}$
 $k_i = 4.7E-12*(T/300)^{-1.4}$
 $F_c = \exp(-T/517)$
R27: C3 HO2NO2 -> HO2 + NO2; $ko_{N2} = 5.0E-6*\exp(-10000/T)$
 $ko_{O2} = 3.6E-6*\exp(-10000/T)$
 $ji = 3.4E+14*\exp(-10420/T)$
 $F_c = \exp(-T/517)$
R28: C3 HO2NO2 -> HO2 + NO2; J = crosssec \ HO2NO2.phd
R29: C3 O3 + NO -> NO2 + O2; $k = 1.8E-12*\exp(-1370/T)$
R30: C3 O3 + NO2 -> O2 + NO3; $k = 1.2E-13*\exp(-2450/T)$
R31: N7 NO + NO3 -> NO2 + NO2; $k = 1.7E-11*\exp(+150/T)$
R32: N7 NO2 + NO3 -> N2O5; $L_{N2} = 2.2E-30*(T/300)^{-4.3}$
 $L_{O2} = 2.2E-30*(T/300)^{-4.3}$
 $k_i = 1.5E-12*(T/300)^{-0.5}$
 $F_c = \exp(-T/280)$
R33: C3 N2O5 -> NO2 + NO3; $ko_{N2} = 2.2E-3*(T/300)^{-4.4}*\exp(-11080/T)$
 $ko_{O2} = 2.2E-3*(T/300)^{-4.4}*\exp(-11080/T)$
 $ji = 9.7E+14*(T/300)^{+0.1}*\exp(-11080/T)$
 $F_c = \exp(-T/280)$
R34: C3 N2O5 -> NO2 + NO3; J = crosssec \ N2O5.phd
R35: C3 NO2 -> NO + O_ 3P; $kd = JNO2$
R36: C3 NO3 -> NO2 + O_ 3P; J = crosssec \ NO3_ O.phd
R37: C3 NO3 -> NO + O2; J = crosssec \ NO3_ O2.phd
***** Chlorine Chemistry *****
R38: N7 Cl + O3 -> ClO + O2; $k = 2.9E-11*\exp(-260/T)$
R39: N7 Cl + H2 -> HCl + H; $k = 3.7E-11*\exp(-2300/T)$
R40: N7 ClO + NO -> Cl + NO2; $k = 6.4E-12*\exp(290/T)$
R41: SK ClO + OH -> Cl + HO2; $k = 1E-11*\exp(120/T)$
R42: SK HCl -> H + Cl; $k = 8.11E-9$
R43: N7 ethane + Cl -> C2H5 + HCl; $k = 7.7E-11*\exp(-90/T)$
R44: A5 Cl + ethene -> HOC2H4; $k = 1.06E-10$
R45: SK CH3OOH + Cl -> CH3O2 + HCl; $k = 1.8E-11*\exp(-190/T)$
R46: SK C2H5OOH + Cl -> C2H5O2 + HCl; $k = 1.8E-11*\exp(-190/T)$
R47: SK CH3CHO + Cl -> CH3COO2 + HCl; $k = 1.1E-10$
R48: N7 HCl + OH -> Cl + H2O; $k = 2.6E-12*\exp(-350/T)$
R49: N7 Cl + methane -> HCl + CH3; $k = 1.1E-11*\exp(-1400/T)$
R50: SK ClONO2 -> Cl + NO2 + O_ 3P; $k = 4.79E-5$
R51: SK ClONO2 + OH -> Cl + HO2 + NO2; $k = 1.2E-12*\exp(-333/T)$
R52: N7 Cl + CH2O -> HCl + CHO; $k = 8.1E-11*\exp(-30/T)$
R53: N7 Cl + H2O2 -> HCl + HO2; $k = 1.1E-11*\exp(-980/T)$
R54: N7 Cl + HO2 -> ClO + OH; $k = 4.1E-11*\exp(-450/T)$
R55: N7 Cl + HO2 -> HCl + O2; $k = 1.8E-11*\exp(170/T)$
R56: N7 Cl + CH3OH -> CH2OH + HCl; $k = 5.7E-11$
R57: N7 Cl + NO3 -> ClO + NO2; $k = 5.2E-11$
R58: N7 ClO + O_ 3P -> Cl + O2; $k = 3E-11*\exp(70/T)$
R59: N7 ClO + NO -> NO2 + Cl; $k = 6.4E-12*\exp(290/T)$

R60: N7 $\text{ClO} + \text{NO}_2 \rightarrow \text{ClONO}_2$; $L_{\text{N}_2} = 1.8\text{E-}31 \cdot (\text{T}/300)^{\wedge} (-3.4)$
 $L_{\text{O}_2} = 1.8\text{E-}31 \cdot (\text{T}/300)^{\wedge} (-3.4)$
 $k_i = 1.5\text{E-}11$
 $F_c = 0.6$
R61: SK $\text{CH}_3\text{COCH}_3 + \text{Cl} \rightarrow \text{CH}_3\text{COCH}_2\text{O}_2$; $k = 9.0\text{E-}11$
R62: SK $\text{C}_2\text{H}_5\text{COO}_2\text{NO}_2 + \text{Cl} \rightarrow \text{CH}_3\text{CHO} + \text{CO}_2 + \text{NO}_2 + \text{HCl}$; $k = 9.1\text{E-}11 \cdot \exp(44/\text{T})$
R63: SK $\text{C}_3\text{H}_7\text{OOH} + \text{Cl} \rightarrow \text{C}_3\text{H}_7\text{O}_2 + \text{HCl}$; $k = 1.8\text{E-}11 \cdot \exp(-190/\text{T})$
R64: SK $\text{CH}_3\text{COCH}_2\text{OOH} + \text{Cl} \rightarrow \text{CH}_3\text{COCH}_2\text{O}_2 + \text{HCl}$; $k = 1.8\text{E-}11 \cdot \exp(-190/\text{T})$
R65: SK $\text{CH}_3\text{COCHO} + \text{Cl} \rightarrow \text{CH}_3\text{COO}_2 + \text{CO} + \text{HCl}$; $k = 1.8\text{E-}11 \cdot \exp(-190/\text{T})$
R66: SK $\text{C}_2\text{H}_5\text{CHO} + \text{Cl} \rightarrow \text{C}_2\text{H}_5\text{COO}_2 + \text{HCl}$; $k = 6.6\text{E-}11 \cdot \exp(250/\text{T})$
***** Methane *****
R67: C3 $\text{OH} + \text{methane} \rightarrow \text{CH}_3 + \text{H}_2\text{O}$; $k = 2.4\text{E-}12 \cdot \exp(-1710/\text{T})$
R68: N7 $\text{CH}_3 + \text{O}_2 \rightarrow \text{CH}_3\text{O}_2$; $L_{\text{N}_2} = 4.5\text{E-}31 \cdot (\text{T}/300)^{\wedge} (-2.0)$
 $L_{\text{O}_2} = 4.5\text{E-}31 \cdot (\text{T}/300)^{\wedge} (-2.0)$
 $k_i = 1.8\text{E-}12 \cdot (\text{T}/300)^{\wedge} (-2.0)$
 $F_c = \exp(-\text{T}/446)$
R69: K7 $\text{CH}_3\text{O}_2 + \text{HO}_2 \rightarrow \text{CH}_3\text{OOH} + \text{O}_2$; $k_d = 0.50 \cdot k_{\text{RO}_2\text{hm}}$
R70: 70 $\text{CH}_3\text{O}_2 + \text{HO}_2 \rightarrow \text{CH}_2\text{O} + \text{H}_2\text{O} + \text{O}_2$; $k_d = 0.50 \cdot k_{\text{RO}_2\text{hm}}$
R71: N7 $\text{CH}_3\text{O}_2 + \text{NO} \rightarrow \text{CH}_3\text{O} + \text{NO}_2$; $k_d = k_{\text{RO}_2\text{NOm}}$
R72: C3 $\text{CH}_3\text{O}_2 + \text{NO}_2 \rightarrow \text{CH}_3\text{O}_2\text{NO}_2$; $L_{\text{N}_2} = 2.3\text{E-}30 \cdot (\text{T}/300)^{\wedge} (-4.0)$
 $L_{\text{O}_2} = 2.3\text{E-}30 \cdot (\text{T}/300)^{\wedge} (-4.0)$
 $k_i = 8.0\text{E-}12$
 $F_c = \exp(-\text{T}/327)$
R73: ?? $\text{CH}_3\text{O}_2\text{NO}_2 \rightarrow \text{CH}_3\text{O}_2 + \text{NO}_2$; $k_{\text{a- N}_2} = 5.4\text{E-}2 \cdot \exp(-9600/\text{T})$
 $k_{\text{a- O}_2} = 5.4\text{E-}2 \cdot \exp(-9600/\text{T})$
 $j_i = 2.0\text{E+}17 \cdot \exp(-9600/\text{T})$
 $F_c = \exp(-\text{T}/327)$
R74: N7 $\text{CH}_3\text{O}_2 + \{ \text{CH}_3\text{O}_2 \} \rightarrow \text{CH}_3\text{O} + \{ \text{RO} \}$; $k_d = 0.25 \cdot k_{\text{RO}_2\text{mm}}$
R75: AA $\text{CH}_3\text{O}_2 + \{ \text{CH}_3\text{O}_2 \} \rightarrow \text{CH}_3\text{OH} + \{ \text{RO} \}$; $k_d = 0.38 \cdot k_{\text{RO}_2\text{mm}}$
R76: AA $\text{CH}_3\text{O}_2 + \{ \text{CH}_3\text{O}_2 \} \rightarrow \text{CH}_2\text{O} + \{ \text{ROH} \}$; $k_d = 0.38 \cdot k_{\text{RO}_2\text{mm}}$
R77: AA $\text{CH}_3\text{O}_2 + \{ \text{RCH}_2\text{O}_2 \} \rightarrow \text{CH}_3\text{O} + \{ \text{RO} \}$; $k_d = 0.40 \cdot k_{\text{RO}_2\text{mp}}$
R78: AA $\text{CH}_3\text{O}_2 + \{ \text{RCH}_2\text{O}_2 \} \rightarrow \text{CH}_3\text{OH} + \{ \text{RO} \}$; $k_d = 0.30 \cdot k_{\text{RO}_2\text{mp}}$
R79: AA $\text{CH}_3\text{O}_2 + \{ \text{RCH}_2\text{O}_2 \} \rightarrow \text{CH}_2\text{O} + \{ \text{ROH} \}$; $k_d = 0.30 \cdot k_{\text{RO}_2\text{mp}}$
R80: AA $\text{CH}_3\text{O}_2 + \{ \text{RCOO}_2 \} \rightarrow \text{CH}_3\text{O} + \{ \text{RO} \}$; $k_d = 0.50 \cdot k_{\text{RO}_2\text{mo}}$
R81: AA $\text{CH}_3\text{O}_2 + \{ \text{RCOO}_2 \} \rightarrow \text{CH}_2\text{O} + \{ \text{ROH} \}$; $k_d = 0.50 \cdot k_{\text{RO}_2\text{mo}}$
R82: A6 $\text{CH}_3\text{OH} + \text{OH} \rightarrow \text{CH}_3\text{O} + \text{H}_2\text{O}$; $k = 1.7\text{E-}12 \cdot \exp(-806/\text{T})$
R83: A6 $\text{CH}_3\text{OH} + \text{OH} \rightarrow \text{CH}_2\text{OH} + \text{H}_2\text{O}$; $k = 9.8\text{E-}12 \cdot \exp(-806/\text{T})$
R84: N7 $\text{CH}_2\text{OH} + \text{O}_2 \rightarrow \text{CH}_2\text{O} + \text{HO}_2$; $k = 9.6\text{E-}12$
R85: 72 $\text{CH}_3\text{OOH} + \text{OH} \rightarrow \text{CH}_3\text{O}_2 + \text{H}_2\text{O}$; $k_d = k_{\text{ROOH OH}}$
R86: 72 $\text{CH}_3\text{OOH} + \text{OH} \rightarrow \text{CH}_2\text{O} + \text{H}_2\text{O} + \text{OH}$; $k = 2.9\text{E-}12 \cdot \exp((-900+712)/\text{T})$
R87: C3 $\text{CH}_3\text{OOH} \rightarrow \text{CH}_3\text{O} + \text{OH}$; $k_d = J_{\text{CH}_3\text{OOH}}$
R88: N7 $\text{CH}_3\text{O} + \text{O}_2 \rightarrow \text{CH}_2\text{O} + \text{HO}_2$; $k = 1.9\text{E-}15 \cdot \exp(-900/\text{T})$
R89: C3 $\text{CH}_3\text{O} + \text{NO} \rightarrow \text{CH}_3\text{ONO}$; $k = 2\text{E-}11$
R90: ?? $\text{CH}_3\text{ONO} \rightarrow \text{CH}_3\text{O} + \text{NO}$; $k = 7.0\text{E+}16 \cdot \exp(-20500/\text{T})$
R91: C3 $\text{CH}_3\text{O} + \text{NO}_2 \rightarrow \text{CH}_3\text{ONO}_2$; $k = 1.2\text{E-}11$
R92: ?? $\text{CH}_3\text{ONO}_2 \rightarrow \text{CH}_3\text{O} + \text{NO}_2$; $k = 1.7\text{E+}17 \cdot \exp(-20125/\text{T})$

R93: N7 CH2O + OH -> CHO + H2O; k = 1.0E-11
R94: N1 CH2O -> CO + H2; J = crosssec \ CH2O_ H2.phd
R95: N1 CH2O -> CHO + H; J = crosssec \ CH2O_ H.phd
R96: N7 CHO + O2 -> CO + HO2; k = 3.5E-12*exp(+140/T)
***** DMS *****
R97: C4 DMS + OH -> CH3SCH2 + H2O; k = 9.6E-12*exp(-234/T)
R98: H6 DMS + OH -> CH3SOHCH3; k = 3.5E-12*exp(+353/T)
**a
R99: O2 CH3SCH2 + O2 -> CH3SCH2O2; k = 9.6E-12
R100: AA CH3SCH2O2 + HO2 -> CH3SCH2OOH + O2; k = 3.2E-12
R101: AA CH3SCH2O2 + NO -> CH3S + CH2O; kd = kRO2NOp
R102: AA CH3SCH2O2 + { CH3O2 } -> CH3S + CH2O + { RO } ; kd = 0.40*kRO2mp
R103: AA CH3SCH2O2 + { CH3O2 } -> CH3SCH2OH + { RO } ; kd = 0.30*kRO2mp
R104: AA CH3SCH2O2 + { CH3O2 } -> CH3SCHO + { ROH } ; kd = 0.30*kRO2mp
R105: AA CH3SCH2O2 + { RCH2O2 } -> CH3S + CH2O + { RO } ; kd = 0.6*kRO2pp
R106: AA CH3SCH2O2 + { RCH2O2 } -> CH3SCH2OH + { RO } ; kd = 0.2*kRO2pp
R107: AA CH3SCH2O2 + { RCH2O2 } -> CH3SCHO + { ROH } ; kd = 0.2*kRO2pp
R108: AA CH3SCH2O2 + { RCOO2 } -> CH3S + CH2O + { RO } ; kd = 0.80*kRO2po
R109: AA CH3SCH2O2 + { RCOO2 } -> CH3SCHO + { ROH } ; kd = 0.2*kRO2po
R110: ?N CH3SCH2OOH -> CH3S + CH2O + OH; kd = JCH3OOH
R111: ?N CH3SCH2OOH + OH -> CH3SCH2O2 + H2O; kd = kROOH OH
R112: ?N CH3SCH2OOH + OH -> CH3SCHO + H2O + OH; k = 2.9E-12*exp((-367+782)/T)
R113: ?N CH3SCH2OH + OH -> CH3SCH OH + H2O; k = 2.9E-12*exp((-367+435)/T)
R114: ?N CH3SCH OH + O2 -> CH3SCHO + HO2; k = 9.6E-12
R115: ?N CH3SCHO -> CH3S + CHO; kd = JCH3CHO_ 1
R116: ?N CH3SCHO + OH -> CH3S + CO + H2O; k = 1.3E-12*exp(+111+718)/T)
R117: ?N CH3S + O2 -> CH3 + SO2; k = 1E-17
**b
R118: H6 CH3SOHCH3 + O2 -> CH3SOCH3 + HO2; k = 5.53E-15*exp(+910/T)
R119: H6 CH3SOHCH3 -> DMS + OH; k = 1E16*exp(-6550/T)
R120: ?N CH3SOCH3 + OH -> CH3SOCH2 + H2O; k = 9.6E-12*exp(-234/T)
R121: ?N CH3SOCH3 + OH -> CH3SOOHCH3; k = 3.5E-12*exp(+353/T)
R122: ?N CH3SOOHCH3 + O2 -> CH3SO2CH3 + HO2; k = 9.7E-12
R123: ?N CH3SOCH2 + O2 -> CH3 + SO2 + CH2O; k = 1E-15
R124: ?N CH3SO2CH3 + OH -> CH3SO2CH2 + H2O; k = 9.6E-12*exp(-234/T)
R125: ?N CH3SO2CH2 + O2 -> CH3SO3 + CH2O; k = 1E-15
R126: ?N CH3SO3 + HO2 -> CH3SO2OH + O2; k = 3.2E-12
R127: C4 SO2 + OH -> HSO3; L N2 = 5.0E-31*(T/300)^(-3.3)
L N2 = 5.0E-31*(T/300)^(-3.3)
ki = 2E-12
Fc = exp(-T/380)
R128: C4 HSO3 + O2 -> SO3 + HO2; k = 4.0E-13
R129: Ta SO3 + H2O -> H2SO4; k = 9.1E-13
***** Ethane *****
R130: A6 ethane + OH -> C2H5 + H2O; k = 1.37E-17*T^(2)*exp(-444/T)
R131: C3 C2H5 + O2 -> C2H5O2; L N2 = 2E-28*(T/300)^(-3.8)

$$L_{O2} = 2E-28*(T/300)^{-3.8}$$

$$k_i = 5E-12$$

$$F_c = \exp(-T/840)$$

- R132: AL C2H5O2 + NO -> C2H5O + NO2; kd = kRO2NOp
R133: 73 C2H5O2 + HO2 -> C2H5OOH + O2; kd = 0.50*kRO2hp
R134: 73 C2H5O2 + HO2 -> CH3CHO + H2O + O2; kd = 0.34*kRO2hp
R135: 76 C2H5O2 + { CH3O2 } -> C2H5O + { RO }; kd = 0.40*kRO2mp
R136: AA C2H5O2 + { CH3O2 } -> C2H5OH + { RO }; kd = 0.30*kRO2mp
R137: AA C2H5O2 + { CH3O2 } -> CH3CHO + { ROH }; kd = 0.30*kRO2mp
R138: AA C2H5O2 + { RCH2O2 } -> C2H5O + { RO }; kd = 0.6*kRO2pp
R139: AA C2H5O2 + { RCH2O2 } -> C2H5OH + { RO }; kd = 0.2*kRO2pp
R140: AA C2H5O2 + { RCH2O2 } -> CH3CHO + { ROH }; kd = 0.2*kRO2pp
R141: AA C2H5O2 + { RCOO2 } -> C2H5O + { RO }; kd = 0.80*kRO2po
R142: AA C2H5O2 + { RCOO2 } -> CH3CHO + { RO }; kd = 0.2*kRO2po
R143: 74 C2H5OOH -> C2H5O + OH; kd = JCH3OOH
R144: 72 C2H5OOH + OH -> C2H5O2 + H2O; kd = kROOHOH
R145: 72 C2H5OOH + OH -> CH3CHO + H2O + OH; k = 2.9E-12*exp((-367+712)/T)
R146: 77 C2H5O + O2 -> CH3CHO + HO2; k = 3.9E-14*exp(-900/T)
R147: C3 CH3CHO -> methane + CO; kd = JCH3CHO_ 2
R148: C3 CH3CHO -> CH3 + CHO; kd = JCH3CHO_ 1
R149: C3 CH3CHO -> CH3CO + H; J = crossec \ CH3CHO_ 3.phd
R150: A6 CH3CHO + OH -> CH3CO + H2O; k = 6.9E-12*exp(260/T)
R151: 77 CH3CO + O2 -> CH3COO2; L N2 = 4.5E-31*(T/300)^{-2.0}

$$L_{O2} = 4.5E-31*(T/300)^{-2.0}$$

$$k_i = 1.8E-12*(T/300)^{-2.0}$$

$$F_c = \exp(-T/446)$$

- R152: 73 CH3COO2 + HO2 -> CH3COOOH + O2; kd = 0.670*kRO2ho
R153: 73 CH3COO2 + HO2 -> CH3COOH + O3; kd = 0.33*kRO2ho
R154: C3 CH3COO2 + NO -> CH3COO + NO2; kd = kRO2NOo
R155: C3 CH3COO2 + NO2 -> CH3COO2NO2; k = 6E-12
R156: 76 CH3COO2 + { CH3O2 } -> CH3COO + { RO }; kd = 0.50*kRO2mo
R157: AA CH3COO2 + { CH3O2 } -> CH3COOH + { RO }; kd = 0.50*kRO2mo
R158: AA CH3COO2 + { RCH2O2 } -> CH3COO + { RO }; kd = 0.80*kRO2po
R159: AA CH3COO2 + { RCH2O2 } -> CH3COOH + { RO }; kd = 0.2*kRO2po
R160: AA CH3COO2 + { RCOO2 } -> CH3COO + { RO }; kd = 1.00*kRO2oo
R161: 77 CH3COO -> CH3 + CO2; k = 1E+7
R162: C3 CH3COO2NO2 -> CH3COO2 + NO2; k = 1.12E+16*exp(-13330/T)
R163: C3 CH3COO2NO2 -> CH3COO2 + NO2; J = crossec \ PAN.phd
R164: KS CH3COO2NO2 + OH -> CH2O + CO2 + NO2 + H2O; k = 1.23E-12*exp(-651/T)
R165: 74 CH3COOOH -> CH3 + CO2 + OH; kd = JCH3OOH
R166: 72 CH3COOOH + OH -> CH3COO2 + H2O; kd = kROOHOH

***** Ethanol *****

- R167: A6 C2H5OH + OH -> CH3CHOH + H2O; k = 2.9E-12*exp(-84/T)
R168: A6 C2H5OH + OH -> HOC2H4 + H2O; k = 2.9E-12*exp(-430/T)
R169: 77 CH3CHOH + O2 -> CH3CHO + HO2; k = 9.6E-12

***** Ethene *****

R170: A6 ethene + OH -> HOC2H4; k = 2.15E-12*exp(+411/T)
R171: ?? HOC2H4 + O2 -> HOC2H4O2; k = 1E-12
R172: 75 HOC2H4O2 + NO -> HOC2H4O + NO2; kd = kRO2NOp
R173: 73 HOC2H4O2 + HO2 -> HOC2H4OOH + O2; kd = 0.50*kRO2hp
R174: 73 HOC2H4O2 + HO2 -> HOCH2CHO + H2O + O2; kd = 0.33*kRO2hp
R175: 76 HOC2H4O2 + { CH3O2 } -> HOC2H4O + { RO }; kd = 0.40*kRO2mp
R176: AA HOC2H4O2 + { CH3O2 } -> HOC2H4OH + { RO }; kd = 0.30*kRO2mp
R177: AA HOC2H4O2 + { CH3O2 } -> HOCH2CHO + { ROH }; kd = 0.30*kRO2mp
R178: AA HOC2H4O2 + { RCH2O2 } -> HOC2H4O + { RO }; kd = 0.6*kRO2pp
R179: AA HOC2H4O2 + { RCH2O2 } -> HOC2H4OH + { RO }; kd = 0.2*kRO2pp
R180: AA HOC2H4O2 + { RCH2O2 } -> HOCH2CHO + { ROH }; kd = 0.2*kRO2pp
R181: AA HOC2H4O2 + { RCOO2 } -> HOC2H4O + { RO }; kd = 0.80*kRO2po
R182: AA HOC2H4O2 + { RCOO2 } -> HOCH2CHO + { ROH }; kd = 0.2*kRO2po
R183: A6 HOC2H4OH + OH -> HOCH2CHOH + H2O; k = 7.7E-12
R184: A6 HOCH2CHOH + O2 -> HOCH2CHO + HO2; k = 9.6E-12
R185: 74 HOC2H4OOH -> HOC2H4O + OH; kd = JCH3OOH
R186: 72 HOC2H4OOH + OH -> HOC2H4O2 + H2O; kd = kROOHOH
R187: 72 HOC2H4OOH + OH -> HOCH2CHO + OH + H2O; k = 2.9E-12*exp((-291+712)/T)
R188: 72 HOC2H4OOH + OH -> HOCHCH2OOH + H2O; k = 2.9E-12*exp(+74/T)
R189: KS HOC2H4O -> CH2OH + CH2O; k = 1.4E+5
R190: CA HOC2H4O + O2 -> HOCH2CHO + HO2; k = 7.4E-15
R191: ?? HOCH2CHO -> CH3OH + CO; kd = JCH3CHO_ 2
R192: ?? HOCH2CHO -> CH2OH + CHO; kd = JCH3CHO_ 1
R193: A7 HOCH2CHO + OH -> HOCH2CO + H2O; k = 2.1E-11
R194: ?? HOCH2CO + O2 -> HOCH2COO2; k = 2E-12
R195: 73 HOCH2COO2 + HO2 -> HOCH2COOOH + O2; kd = 0.670*kRO2ho
R196: 73 HOCH2COO2 + HO2 -> HOCH2COOH + O3; kd = 0.33*kRO2ho
R197: N1 HOCH2CO + O2 -> HOCH2COO2; k = 2E-12
R198: KS HOCH2COO2 + NO2 -> HOCH2COO2NO2; k = 4.7E-12
R199: 75 HOCH2COO2 + NO -> HOCH2COO + NO2; kd = kRO2NOo
R200: 76 HOCH2COO2 + { CH3O2 } -> HOCH2COO + { RO }; kd = 0.50*kRO2mo
R201: AA HOCH2COO2 + { CH3O2 } -> HOCH2COOH + { ROH }; kd = 0.50*kRO2mo
R202: AA HOCH2COO2 + { RCH2O2 } -> HOCH2COO + { RO }; kd = 0.80*kRO2po
R203: AA HOCH2COO2 + { RCH2O2 } -> HOCH2COO + { ROH }; kd = 0.2*kRO2po
R204: AA HOCH2COO2 + { RCOO2 } -> HOCH2COO + { RO }; kd = 1.00*kRO2oo
R205: EA HOCH2COOH + OH -> CH2OH + CO2 + HO2; k = 1.3E-12*exp(-170/T)
R206: ?? HOCH2COO -> CH2OH + CO2; k = 1E+7
R207: ?? HOCH2COOOH -> CH2OH + CO2 + OH; kd = JCH3OOH
R208: 72 HOCH2COOOH + OH -> HOCH2COO2 + H2O; kd = kROOHOH
R209: 7A HOCH2COOOH + OH -> HOCHCOOOH + H2O; k = 2.9E-12
R210: 7N HOCHCOOOH + O2 -> CHO + CO2 + OH + HO2; k = 1.9E-15*exp(-900/T)
R211: KS HOCH2COO2NO2 -> HOCH2COO2 + NO2; k = 1.1E+16*exp(-13330/T)
R212: 75 HOCH2COO2NO2 + OH -> CH2O + CO2 + NO3 + H2O; k = 2.9E-12
R213: ?? HOCHCH2OOH + O2 -> OCHCH2OOH + HO2; k = 1E-12
R214: ?? OCHCH2OOH -> CHO + CH2O + OH; kd = JCH3CHO_ 1
R215: ?? OCHCH2OOH -> CHO + CH2O + OH; kd = JCH3OOH

R216: 72 OCHCH2OOH + OH -> OCHCH2O2 + H2O; kd = kROOHOH
R217: 72 OCHCH2OOH + OH -> OCHCHO + H2O + OH; k = 2.9E-12*exp((-449+712)/T)
R218: 72 OCHCH2OOH + OH -> OCCH2OOH + H2O; k = 1.3E-12*exp(+835/T)
R219: 73 OCHCH2O2 + HO2 -> OCHCH2OOH + O2; kd = 0.50*kRO2hp
R220: 73 OCHCH2O2 + HO2 -> OCHCHO + H2O + O2; kd = 0.33*kRO2hp
R221: 75 OCHCH2O2 + NO -> OCHCH2O + NO2; kd = kRO2NOp
R222: 76 OCHCH2O2 + { CH3O2 } -> OCHCH2O + { RO }; kd = 0.40*kRO2mp
R223: AA OCHCH2O2 + { CH3O2 } -> HOCH2CHO + { RO }; kd = 0.30*kRO2mp
R224: AA OCHCH2O2 + { CH3O2 } -> OCHCHO + { ROH }; kd = 0.30*kRO2mp
R225: AA OCHCH2O2 + { RCH2O2 } -> OCHCH2O + { RO }; kd = 0.6*kRO2pp
R226: AA OCHCH2O2 + { RCH2O2 } -> HOCH2CHO + { RO }; kd = 0.2*kRO2pp
R227: AA OCHCH2O2 + { RCH2O2 } -> OCHCHO + { ROH }; kd = 0.2*kRO2pp
R228: AA OCHCH2O2 + { RCOO2 } -> OCHCH2O + { RO }; kd = 0.80*kRO2po
R229: AA OCHCH2O2 + { RCOO2 } -> OCHCHO + { ROH }; kd = 0.2*kRO2po
R230: 77 OCHCH2O -> CHO + CH2O; k = 1E+7
R231: P3 OCHCHO -> CHO + CHO; kd = 8E-3*JNO2
R232: P3 OCHCHO + OH -> CO + CHO + H2O; k = 2.2E-12*exp(+500/T)
R233: 77 OCCH2OOH -> CO + CH2O + OH; k = 1E+5
** O3 **
R234: A84 ethene + O3 -> CH2OO + CH2O; k = 2.63E-14*exp(-2830/T)
R235: A84 CH2OO -> CH2O2; k = 4.0E+3
R236: A84 CH2OO -> CO + H2O; k = 4.2E+3
R237: A84 CH2OO -> CO2 + H2; k = 1.2E+3
R238: A84 CH2OO -> CHO2 + H; k = 6E+2
R239: N1 CHO2 + O2 -> CO2 + HO2; k = 2E-11
R240: A84 CH2O2 + H2O -> HCOOH; k = 1E-17
R241: D8 HCOOH + OH -> H2O + CO2 + H; k = 3.6E-13*exp(-77/T)
***** Propane *****
R242: CA propane + OH -> CH3CHCH3 + H2O; k = 4.99E-12*exp(-528/T)
R243: CA propane + OH -> C3H7 + H2O; k = 5.24E-12*exp(-823/T)
R244: 71 CH3CHCH3 + O2 -> CH3CHO2CH3; k = 2E-12
R245: 73 CH3CHO2CH3 + HO2 -> CH3CHOOHCH3 + O2; kd = 0.50*kRO2hs
R246: 73 CH3CHO2CH3 + HO2 -> CH3COCH3 + H2O + O2; kd = 0.16*kRO2hs
R247: 75 CH3CHO2CH3 + NO -> CH3CHOCH3 + NO2; kd = kRO2NOs
R248: 76 CH3CHO2CH3 + { CH3O2 } -> CH3CHOCH3 + { RO }; kd = 0.40*kRO2ms
R249: AA CH3CHO2CH3 + { CH3O2 } -> CH3CHOHCH3 + { RO }; kd = 0.30*kRO2ms
R250: AA CH3CHO2CH3 + { CH3O2 } -> CH3COCH3 + { ROH }; kd = 0.30*kRO2ms
R251: AA CH3CHO2CH3 + { RCH2O2 } -> CH3CHOCH3 + { RO }; kd = 0.6*kRO2ps
R252: AA CH3CHO2CH3 + { RCH2O2 } -> CH3CHOHCH3 + { RO }; kd = 0.2*kRO2ps
R253: AA CH3CHO2CH3 + { RCH2O2 } -> CH3COCH3 + { ROH }; kd = 0.2*kRO2ps
R254: AA CH3CHO2CH3 + { RCOO2 } -> CH3CHOCH3 + { RO }; kd = 0.80*kRO2so
R255: AA CH3CHO2CH3 + { RCOO2 } -> CH3COCH3 + { ROH }; kd = 0.2*kRO2so
R256: EA CH3CHOHCH3 + OH -> CH3COHCH3 + H2O; k = 1.3E-12*exp(+475/T)
R257: EA CH3COHCH3 + O2 -> CH3COCH3 + HO2; k = 9.6E-12
R258: 74 CH3CHOOHCH3 -> CH3CHOCH3 + OH; kd = JCH3OOH
R259: 72 CH3CHOOHCH3 + OH -> CH3CHO2CH3 + H2O; kd = kROOHOH

R260: 72 CH₃CHOHCH₃ + OH → CH₃COCH₃ + H₂O + OH; k = 1.3E-12*exp((+111 + 712)/T)
R261: CA CH₃CHOCH₃ + O₂ → CH₃COCH₃ + HO₂; k = 1.8E-14*exp(-196/T)
***** Acetone *****
R262: G4 CH₃COCH₃ → CH₃CO + CH₃; kd = Jacetone
R263: N1 CH₃COCH₃ + OH → CH₃COCH₂ + H₂O; k = 4.5E-12*exp(-886/T)
R264: N1 CH₃COCH₂ + O₂ → CH₃COCH₂O₂; k = 2E-12
R265: # 1 CH₃COCH₂O₂ + HO₂ → CH₃COCH₂OOH + O₂; kd = 0.50*kRO2hp
R266: # 1 CH₃COCH₂O₂ + HO₂ → CH₃COCHO + H₂O + O₂; kd = 0.33*kRO2hp
R267: N1 CH₃COCH₂O₂ + NO → CH₃COCH₂O + NO₂; kd = kRO2NOp
R268: 76 CH₃COCH₂O₂ + { CH₃O₂ } → CH₃COCH₂O + { RO } ; kd = 0.40*kRO2mp
R269: AA CH₃COCH₂O₂ + { CH₃O₂ } → CH₃COCH₂OH + { RO } ; kd = 0.30*kRO2mp
R270: AA CH₃COCH₂O₂ + { CH₃O₂ } → CH₃COCHO + { ROH } ; kd = 0.30*kRO2mp
R271: AA CH₃COCH₂O₂ + { RCH₂O₂ } → CH₃COCH₂O + { RO } ; kd = 0.6*kRO2pp
R272: AA CH₃COCH₂O₂ + { RCH₂O₂ } → CH₃COCH₂OH + { RO } ; kd = 0.2*kRO2pp
R273: AA CH₃COCH₂O₂ + { RCH₂O₂ } → CH₃COCHO + { ROH } ; kd = 0.2*kRO2pp
R274: AA CH₃COCH₂O₂ + { RCOO₂ } → CH₃COCH₂O + { RO } ; kd = 0.80*kRO2po
R275: AA CH₃COCH₂O₂ + { RCOO₂ } → CH₃COCHO + { ROH } ; kd = 0.2*kRO2po
R276: N1 CH₃COCH₂OOH → CH₃COCH₂O + OH; kd = JCH3OOH
R277: N1 CH₃COCH₂OOH → CH₃CO + CH₂O + OH; kd = Jacetone
R278: 72 CH₃COCH₂OOH + OH → CH₃COCH₂O₂ + H₂O; kd = kROOHOH
R279: 72 CH₃COCH₂OOH + OH → CH₃COCHO + H₂O + OH; k = 2.9E-12*exp((-449+712)/T)
R280: N1 CH₃COCH₂O + O₂ → CH₃COCHO + HO₂; k = 3.7E-14*exp(-484/T)
R281: N1 CH₃COCH₂O → CH₃CO + CH₂O; k = 1E+3
R282: N1 CH₃COCHO → CH₃CO + CHO; kd = 1.3E-2*JNO2
R283: N1 CH₃COCHO → CH₃ + CO + CHO; kd = 6.0E-3*JNO2
R284: P3 CH₃COCHO + OH → CH₃COCO + H₂O; k = 1.3E-12*exp(+770/T)
R285: N1 CH₃COCO → CH₃CO + CO; k = 1E+4
*
R286: N1 C₃H₇ + O₂ → C₃H₇O₂; k = 6E-12
R287: N1 C₃H₇O₂ + HO₂ → C₃H₇OOH + O₂; kd = 0.50*kRO2hp
R288: N1 C₃H₇O₂ + HO₂ → C₂H₅CHO + H₂O + O₂; kd = 0.33*kRO2hp
R289: N1 C₃H₇O₂ + NO → C₂H₅CH₂O + NO₂; kd = kRO2NOp
R290: 76 C₃H₇O₂ + { CH₃O₂ } → C₂H₅CH₂O + { RO } ; kd = 0.40*kRO2mp
R291: AA C₃H₇O₂ + { CH₃O₂ } → C₂H₅CH₂OH + { RO } ; kd = 0.30*kRO2mp
R292: AA C₃H₇O₂ + { CH₃O₂ } → C₂H₅CHO + { ROH } ; kd = 0.30*kRO2mp
R293: AA C₃H₇O₂ + { RCH₂O₂ } → C₂H₅CH₂O + { RO } ; kd = 0.6*kRO2pp
R294: AA C₃H₇O₂ + { RCH₂O₂ } → C₂H₅CH₂OH + { RO } ; kd = 0.2*kRO2pp
R295: AA C₃H₇O₂ + { RCH₂O₂ } → C₂H₅CHO + { ROH } ; kd = 0.2*kRO2pp
R296: AA C₃H₇O₂ + { RCOO₂ } → C₂H₅CH₂O + { RO } ; kd = 0.80*kRO2po
R297: AA C₃H₇O₂ + { RCOO₂ } → C₂H₅CHO + { ROH } ; kd = 0.2*kRO2po
R298: A6 C₂H₅CH₂OH + OH → C₂H₅CHOH + H₂O; k = 5E-12
R299: O2 C₂H₅CHOH + O₂ → C₂H₅CHO + HO₂; k = 9.6E-12
R300: N1 C₃H₇OOH → C₂H₅CH₂O; kd = JCH3OOH
R301: 72 C₃H₇OOH + OH → C₃H₇O₂ + H₂O; kd = kROOHOH
R302: 72 C₃H₇OOH + OH → C₂H₅CHO + H₂O + OH; k = 2.9E-12*exp((-291+712)/T)
R303: N1 C₂H₅CH₂O + O₂ → C₂H₅CHO + HO₂; k = 3.7E-14*exp(-484/T)

R304: N1 C2H5CH2O -> C2H5 + CH2O; k = 4.8E+3
R305: N1 C2H5CHO -> C2H5 + CHO; kd = 8.4E-4*JNO2
R306: N1 C2H5CHO -> C2H5CO + H; kd = 1.2E-5*JNO2
R307: N1 C2H5CHO + OH -> C2H5CO + H2O; k = 9.0E-12*exp(+250/T)
R308: N1 C2H5CO + O2 -> C2H5COO2; k = 2E-12
R309: N1 C2H5COO2 + NO -> C2H5COO + NO2; kd = kRO2NOo
R310: # 1 C2H5COO2 + HO2 -> C2H5COOOH + O2; kd = 0.670*kRO2ho
R311: # 1 C2H5COO2 + HO2 -> C2H5COOH + O3; kd = 0.33*kRO2ho
R312: 76 C2H5COO2 + { CH3O2 } -> C2H5COO + { RO }; kd = 0.50*kRO2mo
R313: AA C2H5COO2 + { CH3O2 } -> C2H5COOH + { RO }; kd = 0.50*kRO2mo
R314: AA C2H5COO2 + { RCH2O2 } -> C2H5COO + { RO }; kd = 0.80*kRO2po
R315: AA C2H5COO2 + { RCH2O2 } -> C2H5COOH + { RO }; kd = 0.2*kRO2po
R316: AA C2H5COO2 + { RCOO2 } -> C2H5COO + { RO }; kd = 1.00*kRO2oo
R317: D8 C2H5COOH + OH -> C2H5 + CO2 + H2O; k = 1.8E-12*exp(-120/T)
R318: 76 C2H5COO -> C2H5 + CO2; k = 1E+7
R319: N1 C2H5COO2 + NO2 -> C2H5COO2NO2; k = 4.7E-12
R320: N1 C2H5COOOH -> C2H5 + CO2 + OH; kd = JCH3OOH
R321: 72 C2H5COOOH + OH -> C2H5COO2 + H2O; kd = kROOHOH
R322: N1 C2H5COO2NO2 -> C2H5COO2 + NO2; k = 1.12E+16*exp(-13330/T)
R323: 75 C2H5COO2NO2 -> CH3CHO + CO2 + NO2 + H2O; k = 2.9E-12*exp(-367/T)

***** Propene *****

R324: A6 propene + O3 -> CH3CHOO + CH2O; k = 6.6E-15*exp(-2108/T)
R325: A6 propene + O3 -> CH3CHO + CH2OO; k = 6.6E-15*exp(-2108/T)
R326: N1 CH3CHOO -> CH3CHO2; k = 4.0E+3
R327: N1 CH3CHOO -> methane + CO2; k = 1.2E+3
R328: N1 CH3CHOO -> CH3 + CO2 + H; k = 2.4E+3
R329: N1 CH3CHOO -> CHO + CH3O; k = 5.0E+2
R330: N1 CH3CHOO -> CH3 + CO + OH; k = 1.9E+3
R331: N1 CH3CHO2 + H2O -> CH3COOH + H2O; k = 1E-17
R332: N1 CH3COOH + OH -> CH3 + CO2 + H2O; k = 1.3E-12*exp(-170/T)
R333: A6 propene + OH -> CH3CHCH2OH; k = 3.2E-12*exp(+504/T)
R334: A6 propene + OH -> CH3CHOHCH2; k = 1.65E-12*exp(+504/T)
R335: N1 CH3CHCH2OH + O2 -> CH3CHO2CH2OH; k = 2E-12
R336: # 1 CH3CHO2CH2OH + HO2 -> CH3CHOOHCH2OH + O2; kd = 0.50*kRO2hs
R337: # 1 CH3CHO2CH2OH + HO2 -> CH3COCH2OH + H2O + O2; kd = 0.16*kRO2hs
R338: N1 CH3CHO2CH2OH + NO -> CH3CHOCH2OH + NO2; kd = kRO2NOs
R339: 76 CH3CHO2CH2OH + { CH3O2 } -> CH3CHOCH2OH + { RO }; kd = 0.40*kRO2ms
R340: AA CH3CHO2CH2OH + { CH3O2 } -> CH3CHOHCH2OH + { RO }; kd = 0.30*kRO2ms
R341: AA CH3CHO2CH2OH + { CH3O2 } -> CH3COCH2OH + { ROH }; kd = 0.30*kRO2ms
R342: AA CH3CHO2CH2OH + { RCH2O2 } -> CH3CHOCH2OH + { RO }; kd = 0.6*kRO2ps
R343: AA CH3CHO2CH2OH + { RCH2O2 } -> CH3CHOHCH2OH + { RO }; kd = 0.2*kRO2ps
R344: AA CH3CHO2CH2OH + { RCH2O2 } -> CH3COCH2OH + { ROH }; kd = 0.2*kRO2ps
R345: AA CH3CHO2CH2OH + { RCOO2 } -> CH3CHOCH2OH + { RO }; kd = 0.80*kRO2so
R346: AA CH3CHO2CH2OH + { RCOO2 } -> CH3COCH2OH + { ROH }; kd = 0.80*kRO2so
R347: EA CH3CHOHCH2OH + OH -> CH3COHCH2OH + H2O; k = 1.3E-12*exp(+550/T)
R348: O2 CH3COHCH2OH + O2 -> CH3COCH2OH + HO2; k = 9.6E-12

R349: N1 CH3CHOOHCH2OH -> CH3CHOCH2OH + OH; kd = JCH3OOH
R350: 72 CH3CHOOHCH2OH + OH -> CH3CHO2CH2OH + H2O; kd = kROOHOH
R351: 72 CH3CHOOHCH2OH + OH -> CH3COCH2OH + H2O + OH; k = 1.3E-12*exp((+187+712)/T)
R352: 72 CH3CHOOHCH2OH + OH -> CH3CHOOHCHOH + H2O; k = 2.9E-12*exp(+74/T)
R353: N1 CH3CHOCH2OH -> CH3CHO + CH2OH; k = 1E+6
R354: N1 CH3COCH2OH -> CH3CO + CH2OH; kd = *Jacetone*
R355: N1 CH3COCH2OH -> CH3 + CO + CH2OH; kd = 0.5**Jacetone*
R356: 7A CH3COCH2OH + OH -> CH3COCHOH + H2O; k = 2.9E-12*exp(-84/T)
R357: N1 CH3COCHOH + O2 -> CH3COCHO + HO2; k = 9.6E-12
R358: N1 CH3CHOOHCHOH + O2 -> CH3CHOOHCHO + HO2; k = 9.6E-12
R359: N1 CH3CHOOHCHO -> CH3CHO + CHO + OH; kd = JCH3OOH
R360: N1 CH3CHOOHCHO -> CHO + CH3CHO + OH; kd = JCH3CHO_ 1
R361: 72 CH3CHOOHCHO + OH -> CH3CHO2CHO + H2O; kd = kROOHOH
R362: 72 CH3CHOOHCHO + OH -> CH3COCHO + H2O + OH; k = 1.3E-12*exp((+31+712)/T)
R363: 72 CH3CHOOHCHO + OH -> CH3CHO + CO + H2O + OH; k = 1.3E-12*exp(+500/T)
R364: N1 CH3CHO2CHO + HO2 -> CH3CHOOHCHO + O2; kd = 0.50*kRO2hs
R365: N1 CH3CHO2CHO + HO2 -> CH3COCHO + H2O + O2; kd = 0.16*kRO2hs
R366: N1 CH3CHO2CHO + NO -> CH3CHOCHO + NO2; kd = kRO2NOs
R367: 76 CH3CHO2CHO + { CH3O2 } -> CH3CHOCHO + { RO } ; kd = 0.40*kRO2ms
R368: AA CH3CHO2CHO + { CH3O2 } -> CH3CHOHCHO + { RO } ; kd = 0.30*kRO2ms
R369: AA CH3CHO2CHO + { CH3O2 } -> CH3COCHO + { ROH } ; kd = 0.30*kRO2ms
R370: AA CH3CHO2CHO + { RCH2O2 } -> CH3CHOCHO + { RO } ; kd = 0.6*kRO2ps
R371: AA CH3CHO2CHO + { RCH2O2 } -> CH3CHOHCHO + { RO } ; kd = 0.2*kRO2ps
R372: AA CH3CHO2CHO + { RCH2O2 } -> CH3COCHO + { ROH } ; kd = 0.2*kRO2ps
R373: AA CH3CHO2CHO + { RCOO2 } -> CH3CHOCHO + { RO } ; kd = 0.80*kRO2so
R374: AA CH3CHO2CHO + { RCOO2 } -> CH3COCHO + { ROH } ; kd = 0.2*kRO2so
R375: 76 CH3CHOCHO -> CH3CHO + CHO; k = 1E+7
*
R376: N1 CH3CHOHCH2 + O2 -> CH3CHOHCH2O2; k = 1E-10
R377: N1 CH3CHOHCH2O2 + HO2 -> CH3CHOHCH2OOH + O2; kd = 0.50*kRO2hp
R378: N1 CH3CHOHCH2O2 + HO2 -> CH3CHOHCHO + H2O + O2; kd = 0.33*kRO2hp
R379: N1 CH3CHOHCH2O2 + NO -> CH3CHOHCH2O + NO2; kd = kRO2NOp
R380: 76 CH3CHOHCH2O2 + { CH3O2 } -> CH3CHOHCH2O + { RO } ; kd = 0.40*kRO2mp
R381: AA CH3CHOHCH2O2 + { CH3O2 } -> CH3CHOHCH2OH + { RO } ; kd = 0.30*kRO2mp
R382: AA CH3CHOHCH2O2 + { CH3O2 } -> CH3CHOHCHO + { ROH } ; kd = 0.30*kRO2mp
R383: AA CH3CHOHCH2O2 + { RCH2O2 } -> CH3CHOHCH2O + { RO } ; kd = 0.6*kRO2pp
R384: AA CH3CHOHCH2O2 + { RCH2O2 } -> CH3CHOHCH2OH + { RO } ; kd = 0.2*kRO2pp
R385: AA CH3CHOHCH2O2 + { RCH2O2 } -> CH3CHOHCHO + { ROH } ; kd = 0.2*kRO2pp
R386: AA CH3CHOHCH2O2 + { RCOO2 } -> CH3CHOHCH2O + { RO } ; kd = 0.80*kRO2po
R387: AA CH3CHOHCH2O2 + { RCOO2 } -> CH3CHOHCHO + { ROH } ; kd = 0.2*kRO2po
R388: N1 CH3CHOHCH2OOH -> CH3CHOHCH2O + OH; kd = JCH3OOH
R389: 72 CH3CHOHCH2OOH + OH -> CH3CHOHCH2O2 + H2O; kd = kROOHOH
R390: 72 CH3CHOHCH2OOH + OH -> CH3CHOHCHO + H2O + OH; k = 2.9E-12*exp((-291+712)/T)
R391: 72 CH3CHOHCH2OOH + OH -> CH3COHCH2OOH + H2O; k = 1.3E-12*exp(+500/T)
R392: N1 CH3COHCH2OOH + O2 -> CH3COCH2OOH; k = 9.6E-12
R393: N1 CH3CHOHCH2O -> CH3CHOH + CH2O; k = 1E+6

R394: N1 CH3CHOHCHO -> C2H5OH + CO; kd = JCH3CHO_ 2
R395: N1 CH3CHOHCHO -> CH3CHOH + CHO; kd = JCH3CHO_ 1
R396: ?A CH3CHOHCHO + OH -> CH3CHOHCO + H2O; k = 1.3E-12*exp(+500/T)
R397: ?A CH3CHOHCHO + OH -> CH3COHCHO + H2O; k = 1.3E-12*exp(+394/T)
R398: N1 CH3COHCHO + O2 -> CH3COCHO + HO2; k = 9.6E-12
R399: N1 CH3CHOHCO + O2 -> CH3CHOHCOO2; k = 2E-12
R400: N1 CH3CHOHCO + O2 -> CH3CHO + CO + HO2; k = 1E-11
R401: N1 CH3CHOHCOO2 + NO -> CH3CHOHCOO + NO2; kd = kRO2NOo
R402: # 1 CH3CHOHCOO2 + HO2 -> CH3CHOHCOOOH + O2; kd = 0.670*kRO2ho
R403: # 1 CH3CHOHCOO2 + HO2 -> CH3CHOHCOOH + O3; kd = 0.33*kRO2ho
R404: N1 CH3CHOHCOO2 + NO2 -> CH3CHOHCOO2NO2; k = 4.7E-12
R405: ?6 CH3CHOHCOO2 + { CH3O2 } -> CH3CHOHCOO + { RO }; kd = 0.50*kRO2mo
R406: AA CH3CHOHCOO2 + { CH3O2 } -> CH3CHOHCOOH + { RO }; kd = 0.50*kRO2mo
R407: AA CH3CHOHCOO2 + { RCH2O2 } -> CH3CHOHCOO + { RO }; kd = 0.80*kRO2po
R408: AA CH3CHOHCOO2 + { RCH2O2 } -> CH3CHOHCOOH + { RO }; kd = 0.2*kRO2po
R409: AA CH3CHOHCOO2 + { RCOO2 } -> CH3CHOHCOO + { RO }; kd = 1.00*kRO2oo
R410: .D8 CH3CHOHCOOH + OH -> CH3CHOH + CO2 + H2O; k = 1.8E-12*exp(-120/T)
R411: ?6 CH3CHOHCOO -> CH3CHOH + CO2; k = 1E+7
R412: N1 CH3CHOHCOO2NO2 -> CH3CHOHCOO2 + NO2; k = 1.12E+16*exp(-13330/T)
R413: ?5 CH3CHOHCOO2NO2 + OH -> CH3CHO + CO2 + NO3 + H2O; k = 1.3E-12*exp(+475/T)
R414: N1 CH3CHOHCOOOH -> CH3CHOH + CO2 + OH; k = 1E+6

***** n-Butane *****

R415: N1 n- butane + OH -> C2H5CHCH3 + H2O; k = 1.49E-17*T²*exp(+196/T)
R416: N1 C2H5CHCH3 + O2 -> C2H5CHO2CH3; k = 1.8E-12
R417: N1 C2H5CHO2CH3 + HO2 -> C2H5CHOHCH3 + O2; kd = 0.50*kRO2hs
R418: N1 C2H5CHO2CH3 + HO2 -> C2H5COCH3 + H2O + O2; kd = 0.16*kRO2hs
R419: N1 C2H5CHO2CH3 + NO -> C2H5CHOCH3 + NO2; kd = kRO2NOs
R420: ?6 C2H5CHO2CH3 + { CH3O2 } -> C2H5CHOCH3 + { RO }; kd = 0.40*kRO2ms
R421: AA C2H5CHO2CH3 + { CH3O2 } -> C2H5CHOHCH3 + { RO }; kd = 0.30*kRO2ms
R422: AA C2H5CHO2CH3 + { CH3O2 } -> C2H5COCH3 + { ROH }; kd = 0.30*kRO2ms
R423: AA C2H5CHO2CH3 + { RCH2O2 } -> C2H5CHOCH3 + { RO }; kd = 0.6*kRO2ps
R424: AA C2H5CHO2CH3 + { RCH2O2 } -> C2H5CHOHCH3 + { RO }; kd = 0.2*kRO2ps
R425: AA C2H5CHO2CH3 + { RCH2O2 } -> C2H5COCH3 + { ROH }; kd = 0.2*kRO2ps
R426: AA C2H5CHO2CH3 + { RCOO2 } -> C2H5CHOCH3 + { RO }; kd = 0.80*kRO2so
R427: AA C2H5CHO2CH3 + { RCOO2 } -> C2H5COCH3 + { ROH }; kd = 0.2*kRO2so
R428: EA C2H5CHOHCH3 + OH -> C2H5COHCH3 + H2O; k = 1.3E-12*exp(+190/T)
R429: O2 C2H5COHCH3 + O2 -> C2H5COCH3 + HO2; k = 9.6E-12
R430: N1 C2H5CHOHCH3 -> C2H5CHOCH3 + OH; kd = JCH3OOH
R431: N1 C2H5CHOHCH3 + OH -> C2H5CHO2CH3 + H2O; kd = kROOHCH
R432: N1 C2H5CHOHCH3 + OH -> C2H5COCH3 + H2O + OH; k = 3.5E-11
R433: N1 C2H5CHOCH3 + O2 -> C2H5COCH3 + HO2; k = 1.8E-14*exp(-196/T)
R434: N1 C2H5CHOCH3 -> CH3CHO + C2H5; k = 4.8E+3

***** MEK *****

R435: N1 C2H5COCH3 -> CH3CO + C2H5; kd = 1.7E-3*JNO2
R436: N1 C2H5COCH3 + OH -> CH3CHCOCH3 + H2O; k = 5.5E-13
R437: N1 CH3CHCOCH3 + O2 -> CH3CHO2COCH3; k = 2E-12

R438: N1 CH3CHO2COCH3 + HO2 -> CH3CHOOHCOCH3 + O2; kd = 0.50*kRO2hs
R439: N1 CH3CHO2COCH3 + HO2 -> CH3COCOCH3 + O2; kd = 0.16*kRO2hs
R440: N1 CH3CHO2COCH3 + NO -> CH3CHOCOCH3 + NO2; kd = kRO2NOs
R441: 76 CH3CHO2COCH3 + { CH3O2 } -> CH3CHOCOCH3 + { RO }; kd = 0.40*kRO2ms
R442: AA CH3CHO2COCH3 + { CH3O2 } -> CH3CHOHCOCH3 + { RO }; kd = 0.30*kRO2ms
R443: AA CH3CHO2COCH3 + { CH3O2 } -> CH3COCOCH3 + { ROH }; kd = 0.30*kRO2ms
R444: AA CH3CHO2COCH3 + { RCH2O2 } -> CH3CHOCOCH3 + { RO }; kd = 0.6*kRO2ps
R445: AA CH3CHO2COCH3 + { RCH2O2 } -> CH3CHOHCOCH3 + { RO }; kd = 0.2*kRO2ps
R446: AA CH3CHO2COCH3 + { RCH2O2 } -> CH3COCOCH3 + { ROH }; kd = 0.2*kRO2ps
R447: AA CH3CHO2COCH3 + { RCOO2 } -> CH3CHOCOCH3 + { RO }; kd = 0.80*kRO2so
R448: AA CH3CHO2COCH3 + { RCOO2 } -> CH3COCOCH3 + { ROH }; kd = 0.2*kRO2so
R449: N1 CH3CHOOHCOCH3 -> CH3CHOCOCH3 + OH; kd = JCH3OOH
R450: N1 CH3CHOOHCOCH3 -> CH3CO + CH3CHO + OH; kd = 1.7E-3*JNO2
R451: N1 CH3CHOOHCOCH3 + OH -> CH3COCOCH3 + H2O + OH; k = 2.1E-11
R452: N1 CH3CHOOHCOCH3 + OH -> CH3CHO2COCH3 + H2O; kd = kROOHOH
R453: N1 CH3CHOCOCH3 -> CH3CHO + CH3CO; k = 7.8E+6
R454: N1 CH3COCOCH3 -> CH3CO + CH3CO; kd = 0.036*JNO2
***** ISO-BUTANE *****
R455: N1 i-butane + OH -> CH3CCH3CH3 + H2O; k = 1.89E-18*T^2*exp(+711/T)
R456: N1 i-butane + OH -> CH3CHCH3CH2 + H2O; k = 1.34E-17*T^2*exp(-227/T)
R457: N1 CH3CCH3CH3 + O2 -> CH3CO2CH3CH3; k = 2E-12
R458: N1 CH3CO2CH3CH3 + HO2 -> CH3COOHCH3CH3 + O2; kd = 0.50*kRO2ht
R459: N1 CH3CO2CH3CH3 + NO -> CH3COCH3CH3 + NO2; kd = kRO2NOt
R460: 76 CH3CO2CH3CH3 + { CH3O2 } -> CH3COCH3CH3 + { RO }; kd = 0.6*kRO2mt
R461: 76 CH3CO2CH3CH3 + { CH3O2 } -> CH3COHCH3CH3 + { RO }; kd = 0.40*kRO2mt
R462: N1 CH3COOHCH3CH3 -> CH3COCH3CH3 + OH; kd = JCH3OOH
R463: N1 CH3COOHCH3CH3 + OH -> CH3CO2CH3CH3 + H2O; kd = kROOHOH
R464: N1 CH3COCH3CH3 -> CH3COCH3 + CH3; k = 5.3E+2
*
R465: N1 CH3CHCH3CH2 + O2 -> CH3CHCH3CH2O2; k = 2E-12
R466: N1 CH3CHCH3CH2O2 + HO2 -> CH3CHCH3CH2OOH + O2; kd = 0.50*kRO2hp
R467: N1 CH3CHCH3CH2O2 + HO2 -> CH3CHCH3CHO + H2O + O2; kd = 0.33*kRO2hp
R468: N1 CH3CHCH3CH2O2 + NO -> CH3CHCH3CH2O + NO2; kd = kRO2NOp
R469: 76 CH3CHCH3CH2O2 + { CH3O2 } -> CH3CHCH3CH2O + { RO }; kd = 0.40*kRO2mp
R470: AA CH3CHCH3CH2O2 + { CH3O2 } -> CH3CHCH3CH2OH + { RO }; kd = 0.30*kRO2mp
R471: AA CH3CHCH3CH2O2 + { CH3O2 } -> CH3CHCH3CHO + { ROH }; kd = 0.30*kRO2mp
R472: AA CH3CHCH3CH2O2 + { RCH2O2 } -> CH3CHCH3CH2O + { RO }; kd = 0.6*kRO2pp
R473: AA CH3CHCH3CH2O2 + { RCH2O2 } -> CH3CHCH3CH2OH + { RO }; kd = 0.2*kRO2pp
R474: AA CH3CHCH3CH2O2 + { RCH2O2 } -> CH3CHCH3CHO + { ROH }; kd = 0.2*kRO2pp
R475: AA CH3CHCH3CH2O2 + { RCOO2 } -> CH3CHCH3CH2O + { RO }; kd = 0.80*kRO2po
R476: AA CH3CHCH3CH2O2 + { RCOO2 } -> CH3CHCH3CHO + { ROH }; kd = 0.2*kRO2po
R477: EA CH3CHCH3CH2OH + OH -> CH3CHCH3CHOH + H2O; k = 2.9E-12*exp(+73/T)
R478: O2 CH3CHCH3CHOH + O2 -> CH3CHCH3CHO + HO2; k = 9.6E-12
R479: N1 CH3CHCH3CH2OOH -> CH3CHCH3CH2O + OH; kd = JCH3OOH
R480: N1 CH3CHCH3CH2OOH + OH -> CH3CHCH3CH2O2 + H2O; kd = kROOHOH
R481: N1 CH3CHCH3CH2OOH + OH -> CH3CHCH3CHO + H2O + OH; k = 1.6E-11

R482: N1 CH3CHCH3CH2O + O2 -> CH3CHCH3CHO; k = 3.7E-14*exp(-484/T)
R483: N1 CH3CHCH3CHO -> CH3CHCH3 + CHO; kd = JCH3CHO_ 1
R484: N1 CH3CHCH3CHO + OH -> CH3CHCH3CO + H2O; k = 2.1E-11
R485: N1 CH3CHCH3CO + O2 -> CH3CHCH3COO2; k = 2E-12
R486: N1 CH3CHCH3COO2 + NO -> CH3CHCH3COO + NO2; kd = kRO2NOo
R487: N1 CH3CHCH3COO2 + HO2 -> CH3CHCH3COOOH + O2; kd = 0.670*kRO2ho
R488: N1 CH3CHCH3COO2 + HO2 -> CH3CHCH3COOH + O3; kd = 0.33*kRO2ho
R489: N1 CH3CHCH3COO2 + NO2 -> CH3CHCH3COO2NO2; k = 6E-12
R490: N1 CH3CHCH3COOOH -> CH3CHCH3COO + OH; kd = JCH3OOH
R491: N1 CH3CHCH3COOOH + OH -> CH3CHCH3COO2 + H2O; kd = kROOHOH
R492: N1 CH3CHCH3COO2NO2 -> CH3CHCH3COO2 + NO2; k = 1.12E+16*exp(-13330/T)
R493: 75 CH3CHCH3COO2NO2 + OH -> CH3COCH3 + CO2 + NO2 + H2O; k = 1.3E-12*exp(+111/T)
R494: 76 CH3CHCH3COO2 + { CH3O2 } -> CH3CHCH3COO + { RO } ; kd = 0.50*kRO2mo
R495: AA CH3CHCH3COO2 + { CH3O2 } -> CH3CHCH3COOH + { RO } ; kd = 0.50*kRO2mo
R496: AA CH3CHCH3COO2 + { RCH2O2 } -> CH3CHCH3COO + { RO } ; kd = 0.80*kRO2po
R497: AA CH3CHCH3COO2 + { RCH2O2 } -> CH3CHCH3COOH + { RO } ; kd = 0.2*kRO2po
R498: AA CH3CHCH3COO2 + { RCOO2 } -> CH3CHCH3COO + { RO } ; kd = 1.00*kRO2oo
R499: D8 CH3CHCH3COOH + OH -> CH3CHCH3 + CO2 + H2O; k = 2.6E-12*exp(-70/T)
R500: 76 CH3CHCH3COO -> CH3CHCH3 + CO2; k = 1E+7
***** 1-BUTENE *****
R501: N1 butene_ 1 + OH -> C2H5CHCH2OH; k = 4.38E-12*exp(+468/T)
R502: N1 butene_ 1 + OH -> C2H5CHOHCH2; k = 2.15E-12*exp(+468/T)
R503: N1 C2H5CHCH2OH + O2 -> C2H5CHO2CH2OH; k = 2E-12
R504: N1 C2H5CHO2CH2OH + HO2 -> C2H5CHOOHCH2OH + O2; kd = 0.50*kRO2hs
R505: N1 C2H5CHO2CH2OH + HO2 -> C2H5COCH2OH + H2O + O2; kd = 0.16*kRO2hs
R506: N1 C2H5CHO2CH2OH + NO -> C2H5CHOCH2OH + NO2; kd = kRO2NOs
R507: N1 C2H5CHO2CH2OH + { CH3O2 } -> C2H5CHOCH2OH + { RO } ; kd = 0.40*kRO2ms
R508: AA C2H5CHO2CH2OH + { CH3O2 } -> C2H5CHOHCH2OH + { RO } ; kd = 0.30*kRO2ms
R509: AA C2H5CHO2CH2OH + { CH3O2 } -> C2H5COCH2OH + { ROH } ; kd = 0.30*kRO2ms
R510: AA C2H5CHO2CH2OH + { RCH2O2 } -> C2H5CHOCH2OH + { RO } ; kd = 0.6*kRO2ps
R511: AA C2H5CHO2CH2OH + { RCH2O2 } -> C2H5CHOHCH2OH + { RO } ; kd = 0.2*kRO2ps
R512: AA C2H5CHO2CH2OH + { RCH2O2 } -> C2H5COCH2OH + { ROH } ; kd = 0.2*kRO2ps
R513: AA C2H5CHO2CH2OH + { RCOO2 } -> C2H5CHOCH2OH + { RO } ; kd = 0.80*kRO2so
R514: AA C2H5CHO2CH2OH + { RCOO2 } -> C2H5COCH2OH + { ROH } ; kd = 0.2*kRO2so
R515: N1 C2H5CHOOHCH2OH -> C2H5CHOCH2OH + OH; kd = JCH3OOH
R516: N1 C2H5CHOOHCH2OH + OH -> C2H5CHO2CH2OH + H2O; kd = kROOHOH
R517: N1 C2H5CHOOHCH2OH + OH -> C2H5COCH2OH + H2O + OH; k = 4.6E-11
R518: N1 C2H5CHOOHCH2OH + OH -> C2H5CHOOHCHOH + H2O; k = 3.7E-12
R519: N1 C2H5CHOCH2OH -> HOCH2CHO + C2H5; k = 1E+6
R520: N1 C2H5CHOOHCHOH + O2 -> C2H5CHOOHCHO + HO2; k = 9.6E-12
R521: N1 C2H5COCH2OH -> C2H5 + HOCH2CO; kd = 3.4E-3*JNO2
R522: N1 C2H5COCH2OH + OH -> C2H5COCHOH; k = 2.2E-12
R523: N1 C2H5COCHOH + O2 -> C2H5COCHO + HO2; k = 9.6E-12
R524: N1 C2H5COCHO -> C2H5CO + CHO; kd = 1.3E-2*JNO2
R525: N1 C2H5COCHO -> C2H5 + CO + CHO; kd = 6.0E-3*JNO2
R526: N1 C2H5COCHO + OH -> C2H5CO + CO + H2O; k = 1.4E-12

R527: N1 C2H5CHOHCHO -> C2H5CHO + CHO + OH; kd = JCH3OOH
R528: N1 C2H5CHOHCHO -> C2H5CHO + CHO + OH; kd = JCH3CHO_ 1
R529: N1 C2H5CHOHCHO + OH -> C2H5CHO2CHO + H2O; kd = kROOHCH
R530: N1 C2H5CHOHCHO + OH -> C2H5COCHO + H2O + OH; k = 2.6E-11
R531: N1 C2H5CHOHCHO + OH -> C2H5CHO + CO + H2O + OH; k = 7.8E-12
R532: N1 C2H5CHO2CHO + HO2 -> C2H5CHOHCHO + O2; kd = 0.50*kRO2hs
R533: N1 C2H5CHO2CHO + HO2 -> C2H5COCHO + H2O + O2; kd = 0.16*kRO2hs
R534: N1 C2H5CHO2CHO + NO -> C2H5CHOCHO + NO2; kd = kRO2NOs
R535: 76 C2H5CHO2CHO + { CH3O2 } -> C2H5CHOCHO + { RO }; kd = 0.40*kRO2ms
R536: AA C2H5CHO2CHO + { CH3O2 } -> C2H5CHOHCHO + { RO }; kd = 0.30*kRO2ms
R537: AA C2H5CHO2CHO + { CH3O2 } -> C2H5COCHO + { ROH }; kd = 0.30*kRO2ms
R538: AA C2H5CHO2CHO + { RCH2O2 } -> C2H5CHOCHO + { RO }; kd = 0.6*kRO2ps
R539: AA C2H5CHO2CHO + { RCH2O2 } -> C2H5CHOHCHO + { RO }; kd = 0.2*kRO2ps
R540: AA C2H5CHO2CHO + { RCH2O2 } -> C2H5COCHO + { ROH }; kd = 0.2*kRO2ps
R541: AA C2H5CHO2CHO + { RCOO2 } -> C2H5CHOCHO + { RO }; kd = 0.80*kRO2so
R542: AA C2H5CHO2CHO + { RCOO2 } -> C2H5COCHO + { ROH }; kd = 0.2*kRO2so
R543: 76 C2H5CHOCHO -> C2H5CHO + CHO; k = 1E+7

R544: N1 C2H5CHOHCH2 + O2 -> C2H5CHOHCH2O2; k = 1E-12
R545: N1 C2H5CHOHCH2O2 + HO2 -> C2H5CHOHCH2OOH + O2; kd = 0.50*kRO2hp
R546: N1 C2H5CHOHCH2O2 + HO2 -> C2H5CHOHCHO + H2O + O2; kd = 0.33*kRO2hp
R547: N1 C2H5CHOHCH2O2 + NO -> C2H5CHOHCH2O + NO2; kd = kRO2NOp
R548: 76 C2H5CHOHCH2O2 + { CH3O2 } -> C2H5CHOHCH2O + { RO }; kd = 0.40*kRO2mp
R549: AA C2H5CHOHCH2O2 + { CH3O2 } -> C2H5CHOHCH2OH + { RO }; kd = 0.30*kRO2mp
R550: AA C2H5CHOHCH2O2 + { CH3O2 } -> C2H5CHOHCHO + { ROH }; kd = 0.30*kRO2mp
R551: AA C2H5CHOHCH2O2 + { RCH2O2 } -> C2H5CHOHCH2O + { RO }; kd = 0.6*kRO2pp
R552: AA C2H5CHOHCH2O2 + { RCH2O2 } -> C2H5CHOHCH2OH + { RO }; kd = 0.2*kRO2pp
R553: AA C2H5CHOHCH2O2 + { RCH2O2 } -> C2H5CHOHCHO + { ROH }; kd = 0.2*kRO2pp
R554: AA C2H5CHOHCH2O2 + { RCOO2 } -> C2H5CHOHCH2O + { RO }; kd = 0.80*kRO2po
R555: AA C2H5CHOHCH2O2 + { RCOO2 } -> C2H5CHOHCHO + { ROH }; kd = 0.2*kRO2po
R556: EA C2H5CHOHCH2OH + OH -> C2H5COHCH2OH + H2O; k = 1.3E-12*exp(+625/T)
R557: O2 C2H5COHCH2OH + O2 -> C2H5COCH2OH + HO2; k = 9.6E-12
R558: N1 C2H5CHOHCH2OOH -> C2H5CHOHCH2O + OH; kd = JCH3OOH
R559: N1 C2H5CHOHCH2OOH + OH -> C2H5CHOHCH2O2 + H2O; kd = kROOHCH
R560: N1 C2H5CHOHCH2OOH + OH -> C2H5CHOHCHO + H2O + OH; k = 1.6E-11
R561: N1 C2H5CHOHCH2OOH + OH -> C2H5COHCH2OOH + H2O; k = 1.0E-11
R562: N1 C2H5CHOHCH2O -> C2H5CHOH + CH2O; k = 1.0E+4
R563: N1 C2H5CHOH + O2 -> C2H5CHO + HO2; k = 6.6E-12
R564: N1 C2H5CHOHCHO -> C2H5CHOH + CHO; kd = JCH3CHO_ 1
R565: N1 C2H5CHOHCHO + OH -> C2H5CHOHCO + H2O; k = 2.1E-11
R566: N1 C2H5CHOHCHO + OH -> C2H5COHCHO + H2O; k = 4.7E-12
R567: N1 C2H5COHCHO + O2 -> C2H5COCHO + HO2; k = 9.6E-12
R568: N1 C2H5CHOHCO + O2 -> C2H5CHOHCOO2; k = 2E-12
R569: N1 C2H5CHOHCO + O2 -> C2H5CHO + CO + HO2; k = 1E-11
R570: N1 C2H5CHOHCOO2 + NO -> C2H5CHOHCOO + NO2; kd = kRO2NOo
R571: N1 C2H5CHOHCOO2 + HO2 -> C2H5CHOHCOOOH + O2; kd = 0.670*kRO2ho

R572: N1 C2H5CHOHCOO2 + HO2 -> C2H5CHOHCOOH + O3; kd = 0.33*kRO2ho
R573: N1 C2H5CHOHCOO2 + NO2 -> C2H5CHOHCOO2NO2; kd = kRO2NO2
R574: 76 C2H5CHOHCOO2 + { CH3O2 } -> C2H5CHOHCOO + { RO } ; kd = 0.50*kRO2mo
R575: AA C2H5CHOHCOO2 + { CH3O2 } -> C2H5CHOHCOOH + { RO } ; kd = 0.50*kRO2mo
R576: AA C2H5CHOHCOO2 + { RCH2O2 } -> C2H5CHOHCOO + { RO } ; kd = 0.80*kRO2po
R577: AA C2H5CHOHCOO2 + { RCH2O2 } -> C2H5CHOHCOOH + { RO } ; kd = 0.2*kRO2po
R578: AA C2H5CHOHCOO2 + { RCOO2 } -> C2H5CHOHCOO + { RO } ; kd = 1.00*kRO2oo
R579: E6 C2H5CHOHCOOH + OH -> C2H5CHOH + CO2 + H2O; k = 2.6E-12*exp(-70/T)
R580: 76 C2H5CHOHCOO -> C2H5CHOH + CO2; k = 1E+7
R581: N1 C2H5CHOHCOOOH -> C2H5CHOH + CO2 + OH; kd = JCH3OOH
R582: N1 C2H5CHOHCOOOH + OH -> C2H5CHOHCOO2 + H2O; kd = kROOHOOH
R583: N1 C2H5CHOHCOOOH + OH -> C2H5COH + CO2 + OH + H2O; k = 6.1E-12
R584: N1 C2H5COH + O2 -> C2H5CO + HO2; k = 9.6E-12
R585: N1 C2H5CHOHCOO2NO2 -> C2H5CHOHCOO2 + NO2; k = 1.12E+16*exp(-13330/T)
R586: 75 C2H5CHOHCOO2NO2 + OH -> C2H5CHO + CO2 + NO3 + H2O; k = 1.3E-12*exp(+475/T)
R587: N1 C2H5COHCH2OOH + O2 -> C2H5COCH2OOH + HO2; kd = kROOHOOH
R588: N1 C2H5COCH2OOH -> C2H5CO + CH2O + OH; kd = JCH3OOH
R589: N1 C2H5COCH2OOH -> C2H5CO + CH2O + OH; kd = Jacetone
R590: N1 C2H5COCH2OOH + OH -> C2H5COCH2O2 + H2O; kd = kROOHOOH
R591: N1 C2H5COCH2OOH + OH -> C2H5COCHO + H2O + OH; k = 9.6E-12
R592: N1 C2H5COCH2O2 + HO2 -> C2H5COCH2OOH + O2; kd = 0.50*kRO2hp
R593: N1 C2H5COCH2O2 + HO2 -> C2H5COCHO + H2O + O2; kd = 0.33*kRO2hp
R594: N1 C2H5COCH2O2 + NO -> C2H5COCH2O + NO2; kd = kRO2NOp
R595: 76 C2H5COCH2O2 + { CH3O2 } -> C2H5COCH2O + { RO } ; kd = 0.40*kRO2mp
R596: AA C2H5COCH2O2 + { CH3O2 } -> C2H5COCH2OH + { RO } ; kd = 0.30*kRO2mp
R597: AA C2H5COCH2O2 + { CH3O2 } -> C2H5COCHO + { ROH } ; kd = 0.30*kRO2mp
R598: AA C2H5COCH2O2 + { RCH2O2 } -> C2H5COCH2O + { RO } ; kd = 0.6*kRO2pp
R599: AA C2H5COCH2O2 + { RCH2O2 } -> C2H5COCH2OH + { RO } ; kd = 0.2*kRO2pp
R600: AA C2H5COCH2O2 + { RCH2O2 } -> C2H5COCHO + { ROH } ; kd = 0.2*kRO2pp
R601: AA C2H5COCH2O2 + { RCOO2 } -> C2H5COCH2O + { RO } ; kd = 1.00*kRO2oo
R602: AA C2H5COCH2O2 + { RCOO2 } -> C2H5COCHO + { ROH } ; kd = 0.2*kRO2oo
R603: 76 C2H5COCH2O -> C2H5CO + CH2O; k = 1E+7
** O3 **
R604: N1 butene_ 1 + O3 -> C2H5CHOO + CH2O; k = 1.73E-15*exp(-1715/T)
R605: N1 butene_ 1 + O3 -> C2H5CHO + CH2OO; k = 1.73E-15*exp(-1715/T)
R606: N1 C2H5CHOO -> C2H5CHO2; k = 4.0E+3
R607: N1 C2H5CHOO -> ethane + CO2; k = 1.2E+3
R608: N1 C2H5CHOO -> C2H5 + CO2 + H; k = 2.4E+3
R609: N1 C2H5CHOO -> C2H5O + CHO; k = 3E+2
R610: N1 C2H5CHOO -> C2H5 + CO + OH; k = 2.1E+3
R611: N1 C2H5CHO2 + H2O -> C2H5COHO + H2O; k = 1E-17
R612: N1 C2H5COHO + OH -> C2H5 + CO2 + H2O; k = 1.8E-2*exp(-120/T)
***** ISO-BUTENE *****
R613: N1 i_ butene + OH -> CH3CCH3OHCH2; k = 3.14E-12*exp(+503/T)
R614: N1 i_ butene + OH -> HOCH2CCH3CH3; k = 6.37E-12*exp(+503/T)
R615: N1 CH3CCH3OHCH2 + O2 -> CH3CCH3OHCH2O2; k = 2E-12

R616: N1 CH₃CCH₃OHCH₂O₂ + HO₂ -> CH₃CCH₃OHCH₂OOH + O₂; kd = 0.50*kRO2hp
R617: N1 CH₃CCH₃OHCH₂O₂ + HO₂ -> CH₃CCH₃OHCHO + H₂O + O₂; kd = 0.33*kRO2hp
R618: N1 CH₃CCH₃OHCH₂O₂ + NO -> CH₃CCH₃OHCH₂O + NO₂; kd = kRO2NOp
R619: 76 CH₃CCH₃OHCH₂O₂ + { CH₃O₂ } -> CH₃CCH₃OHCH₂O + { RO } ; kd = 0.40*kRO2mp
R620: AA CH₃CCH₃OHCH₂O₂ + { CH₃O₂ } -> CH₃CCH₃OHCH₂OH + { RO } ; kd = 0.30*kRO2mp
R621: AA CH₃CCH₃OHCH₂O₂ + { CH₃O₂ } -> CH₃CCH₃OHCHO + { ROH } ; kd = 0.30*kRO2mp
R622: AA CH₃CCH₃OHCH₂O₂ + { RCH₂O₂ } -> CH₃CCH₃OHCH₂O + { RO } ; kd = 0.6*kRO2pp
R623: AA CH₃CCH₃OHCH₂O₂ + { RCH₂O₂ } -> CH₃CCH₃OHCH₂OH + { RO } ; kd = 0.2*kRO2pp
R624: AA CH₃CCH₃OHCH₂O₂ + { RCH₂O₂ } -> CH₃CCH₃OHCHO + { ROH } ; kd = 0.2*kRO2pp
R625: AA CH₃CCH₃OHCH₂O₂ + { RCOO₂ } -> CH₃CCH₃OHCH₂O + { RO } ; kd = 0.80*kRO2po
R626: AA CH₃CCH₃OHCH₂O₂ + { RCOO₂ } -> CH₃CCH₃OHCHO + { ROH } ; kd = 0.2*kRO2po
R627: EA CH₃CCH₃OHCH₂OH + OH -> CH₃CCH₃OHCHOH + H₂O; k = 2.9E-12*exp(+73/T)
R628: O2 CH₃CCH₃OHCHOH + O₂ -> CH₃CCH₃OHCHO + HO₂; k = 9.6E-12
R629: N1 CH₃CCH₃OHCH₂OOH -> CH₃CCH₃OHCH₂O + OH; kd = JCH3OOH
R630: N1 CH₃CCH₃OHCH₂OOH + OH -> CH₃CCH₃OHCH₂O₂ + H₂O; kd = kROOHOH
R631: N1 CH₃CCH₃OHCH₂OOH + OH -> CH₃CCH₃OHCHO + H₂O + OH; k = 1.62E-11
R632: N1 CH₃CCH₃OHCH₂O -> CH₃COHCH₃ + CHO; k = 1E+5
R633: N1 CH₃CCH₃OHCHO -> CH₃COHCH₃ + CHO; kd = JCH3CHO_ 1
R634: N1 CH₃CCH₃OHCHO + OH -> CH₃COHCH₃ + CO + H₂O; k = 2.1E-11
R635: N1 CH₃COHCH₃ + O₂ -> CH₃COCH₃ + HO₂; k = 9.6E-12
R636: N1 HOCH₂CCH₃CH₃ + O₂ -> HOCH₂CCH₃O₂CH₃; k = 2E-12
R637: N1 HOCH₂CCH₃O₂CH₃ + HO₂ -> HOCH₂CCH₃OOHCH₃ + O₂; kd = 0.50*kRO2ht
R638: N1 HOCH₂CCH₃O₂CH₃ + NO -> HOCH₂CCH₃OCH₃ + NO₂; kd = kRO2NOt
R639: 76 HOCH₂CCH₃O₂CH₃ + { CH₃O₂ } -> HOCH₂CCH₃OCH₃ + { RO } ; kd = 0.6*kRO2mt
R640: AA HOCH₂CCH₃O₂CH₃ + { CH₃O₂ } -> HOCH₂CCH₃OHCH₃ + { RO } ; kd = 0.40*kRO2mt
R641: N1 HOCH₂CCH₃OOHCH₃ -> HOCH₂CCH₃OCH₃ + OH; kd = JCH3OOH
R642: N1 HOCH₂CCH₃OOHCH₃ + OH -> HOCH₂CCH₃O₂CH₃ + H₂O; kd = kROOHOH
R643: N1 HOCH₂CCH₃OOHCH₃ + OH -> HOCH₂CCH₃OOHCH₃ + H₂O; k = 3.7E-12
R644: N1 HOCH₂CCH₃OCH₃ -> CH₃COCH₂OH + CH₃; k = 1E+4
R645: N1 HOCH₂CCH₃OOHCH₃ + O₂ -> CH₃CCH₃OOHCHO + HO₂; k = 9.6E-12
R646: N1 CH₃CCH₃OOHCHO -> CH₃COCH₃ + OH + CHO; kd = JCH3OOH
R647: N1 CH₃CCH₃OOHCHO -> CH₃COCH₃ + OH + CHO; kd = 1.7E-3*JNO2
R648: N1 CH₃CCH₃OOHCHO + OH -> CH₃CCH₃O₂CHO + H₂O; kd = kROOHOH
R649: N1 CH₃CCH₃OOHCHO + OH -> CH₃COCH₃ + OH + CO + H₂O; k = 2.1E-12
R650: N1 CH₃CCH₃O₂CHO + HO₂ -> CH₃CCH₃OOHCHO + O₂; kd = 0.50*kRO2ht
R651: N1 CH₃CCH₃O₂CHO + NO -> CH₃CCH₃OCHO + NO₂; kd = kRO2NOt
R652: 76 CH₃CCH₃O₂CHO + { CH₃O₂ } -> CH₃CCH₃OCHO + { RO } ; kd = 0.6*kRO2mt
R653: AA CH₃CCH₃O₂CHO + { CH₃O₂ } -> CH₃CCH₃OHCHO + { RO } ; kd = 0.40*kRO2mt
R654: 76 CH₃CCH₃OCHO -> CH₃COCH₃ + CHO; k = 1E+7
**** O3 ****
R655: N1 iL butene + O₃ -> CH₃CCH₃OO + CH₂O; k = 1.8E-15*exp(-1695/T)
R656: N1 iL butene + O₃ -> CH₃COCH₃ + CH₂OO; k = 1.8E-15*exp(-1695/T)
R657: N1 CH₃CCH₃OO -> CH₃CCH₃O₂; k = 4.0E+3
R658: N1 CH₃CCH₃OO -> CH₃CO + CH₃O; k = 1.5E+3
R659: N1 CH₃CCH₃OO -> CH₃ + CH₃ + CO₂; k = 2.5E+3
R660: N1 CH₃CCH₃OO -> CH₃O + CH₃ + CO; k = 2.0E+3

R661: N1 CH₃CCH₃O₂ + NO → CH₃COCH₃ + NO₂; kd = kRO₂NO_t
R662: ?6 CH₃CCH₃O₂ + { CH₃O₂ } → CH₃COCH₃ + { RO } ; kd = 0.6*kRO₂mt
R663: AA CH₃CCH₃O₂ + { CH₃O₂ } → CH₃COHCH₃ + { RO } ; kd = 0.6*kRO₂mt
***** TRANS-2 BUTENE *****
R664: N1 butene_ 2 + O₃ → CH₃CHOO + CH₃CHO; k = 9.08E-15*exp(-1138/T)
R665: N1 butene_ 2 + OH → CH₃CHOHCHCH₃; k = 1.01E-11*exp(+549/T)
R666: N1 CH₃CHOHCHCH₃ + O₂ → CH₃CHOHCHO₂CH₃; k = 2E-12
R667: N1 CH₃CHOHCHO₂CH₃ + HO₂ → CH₃CHOHCHOOHCH₃ + O₂; kd = 0.50*kRO₂hs
R668: N1 CH₃CHOHCHO₂CH₃ + HO₂ → CH₃CHOHCOCH₃ + H₂O + O₂; kd = 0.16*kRO₂hs
R669: N1 CH₃CHOHCHO₂CH₃ + NO → CH₃CHOHCHOCH₃ + NO₂; kd = kRO₂NO_s
R670: ?6 CH₃CHOHCHO₂CH₃ + { CH₃O₂ } → CH₃CHOHCHOCH₃ + { RO } ; kd = 0.40*kRO₂ms
R671: AA CH₃CHOHCHO₂CH₃ + { CH₃O₂ } → CH₃CHOHCHOHCH₃ + { RO } ; kd = 0.30*kRO₂ms
R672: AA CH₃CHOHCHO₂CH₃ + { CH₃O₂ } → CH₃CHOHCOCH₃ + { ROH } ; kd = 0.30*kRO₂ms
R673: AA CH₃CHOHCHO₂CH₃ + { RCH₂O₂ } → CH₃CHOHCHOCH₃ + { RO } ; kd = 0.6*kRO₂ps
R674: AA CH₃CHOHCHO₂CH₃ + { RCH₂O₂ } → CH₃CHOHCHOHCH₃ + { RO } ; kd = 0.2*kRO₂ps
R675: AA CH₃CHOHCHO₂CH₃ + { RCH₂O₂ } → CH₃CHOHCOCH₃ + { ROH } ; kd = 0.2*kRO₂ps
R676: AA CH₃CHOHCHO₂CH₃ + { RCOO₂ } → CH₃CHOHCHOCH₃ + { RO } ; kd = 0.80*kRO₂so
R677: AA CH₃CHOHCHO₂CH₃ + { RCOO₂ } → CH₃CHOHCOCH₃ + { ROH } ; kd = 0.2*kRO₂so
R678: EA CH₃CHOHCHOHCH₃ + OH → CH₃COHCHOHCH₃ + H₂O; k = 2.6E-12*exp(+475/T)
R679: O₂ CH₃COHCHOHCH₃ + O₂ → CH₃COCHOHCH₃ + HO₂; k = 9.6E-12
R680: N1 CH₃CHOHCHOOHCH₃ → CH₃CHOHCHOCH₃ + OH; kd = JCH₃OOH
R681: N1 CH₃CHOHCHOOHCH₃ + OH → CH₃CHOHCHO₂CH₃ + H₂O; kd = kROOHOH
R682: N1 CH₃CHOHCHOOHCH₃ + OH → CH₃CHOHCOCH₃ + H₂O + OH; k = 3.5E-11
R683: N1 CH₃CHOHCHOOHCH₃ + OH → CH₃COHCHOOHCH₃; k = 8.0E-12
R684: N1 CH₃CHOHCHOCH₃ → CH₃CHOH + CH₃CHO; k = 1E+6
R685: N1 CH₃CHOHCOCH₃ → CH₃CHOH + CH₃CO; kd = JCH₃CHO_ 1
R686: N1 CH₃CHOHCOCH₃ + OH → CH₃COHCOCH₃ + H₂O; k = 4.7E-12
R687: N1 CH₃COHCOCH₃ + O₂ → CH₃COCOCH₃ + HO₂; k = 9.6E-12
R688: N1 CH₃COHCHOOHCH₃ + O₂ → CH₃COCHOOHCH₃ + HO₂; k = 9.6E-12
R689: N1 CH₃COCHOOHCH₃ → CH₃COCHOCH₃ + OH; kd = JCH₃OOH
R690: N1 CH₃COCHOOHCH₃ → CH₃CO + CH₃CHO + OH; kd = 1.7E-3*JNO₂
R691: N1 CH₃COCHOOHCH₃ + OH → CH₃COCOCH₃ + H₂O + OH; k = 2.1E-11
R692: N1 CH₃COCHOOHCH₃ + OH → CH₃COCHO₂CH₃ + H₂O; kd = kROOHOH
R693: N1 CH₃COCHO₂CH₃ + HO₂ → CH₃COCHOOHCH₃ + O₂; kd = 0.50*kRO₂hs
R694: N1 CH₃COCHO₂CH₃ + HO₂ → CH₃COCOCH₃ + H₂O + O₂; kd = 0.16*kRO₂hs
R695: N1 CH₃COCHO₂CH₃ + NO → CH₃COCHOCH₃ + NO₂; kd = kRO₂NO_s
R696: N1 CH₃COCHO₂CH₃ + { CH₃O₂ } → CH₃COCHOCH₃ + { RO } ; kd = 0.40*kRO₂ms
R697: AA CH₃COCHO₂CH₃ + { CH₃O₂ } → CH₃COCHOHCH₃ + { RO } ; kd = 0.30*kRO₂ms
R698: AA CH₃COCHO₂CH₃ + { CH₃O₂ } → CH₃COCOCH₃ + { ROH } ; kd = 0.30*kRO₂ms
R699: AA CH₃COCHO₂CH₃ + { RCH₂O₂ } → CH₃COCHOCH₃ + { RO } ; kd = 0.6*kRO₂ps
R700: AA CH₃COCHO₂CH₃ + { RCH₂O₂ } → CH₃COCHOHCH₃ + { RO } ; kd = 0.2*kRO₂ps
R701: AA CH₃COCHO₂CH₃ + { RCH₂O₂ } → CH₃COCOCH₃ + { ROH } ; kd = 0.2*kRO₂ps
R702: AA CH₃COCHO₂CH₃ + { RCOO₂ } → CH₃COCHOCH₃ + { RO } ; kd = 0.80*kRO₂so
R703: AA CH₃COCHO₂CH₃ + { RCOO₂ } → CH₃COCOCH₃ + { ROH } ; kd = 0.2*kRO₂so
R704: EA CH₃COCHOHCH₃ + OH → CH₃COCOHCH₃ + H₂O; k = 1.3E-12*exp(+475/T)
R705: O₂ CH₃COCOHCH₃ + O₂ → CH₃COCOCH₃ + HO₂; k = 9.6E-12

R706: N1 CH3COCHOCH3 -> CH3CHO + CH3CO; k = 1E+6
 ***** 2-Pentene *****
 R707: A6 pentene_2 + O3 -> CH3CHOO + C2H5CHO; k = 1.0E-16
 R708: A6 pentene_2 + O3 -> CH3CHO + C2H5CHOO; k = 1.0E-16
 R709: A6 pentene_2 + OH -> CH3CHOHCHC2H5; k = 5.5E-11
 R710: N1 CH3CHOHCHC2H5 + O2 -> CH3CHOHCHO2C2H5; k = 2.0E-12
 R711: N1 CH3CHOHCHO2C2H5 + HO2 -> CH3CHOHCHOOHC2H + O2; kd = 0.50*kRO2hs
 R712: N1 CH3CHOHCHO2C2H5 + HO2 -> CH3CHOHCOC2H5 + O2; kd = 0.16*kRO2hs
 R713: N1 CH3CHOHCHO2C2H5 + NO -> CH3CHOHCHOC2H5 + NO2; kd = kRO2NOs
 R714: N1 CH3CHOHCHO2C2H5 + { CH3O2 } -> CH3CHOHCHOC2H5 + { RO }; kd = 0.40*kRO2ms
 R715: AA CH3CHOHCHO2C2H5 + { CH3O2 } -> CH3CHOHCHOHC2H5 + { RO }; kd = 0.30*kRO2ms
 R716: AA CH3CHOHCHO2C2H5 + { CH3O2 } -> CH3CHOHCOC2H5 + { ROH }; kd = 0.30*kRO2ms
 R717: AA CH3CHOHCHO2C2H5 + { RCH2O2 } -> CH3CHOHCHOC2H5 + { RO }; kd = 0.6*kRO2ps
 R718: AA CH3CHOHCHO2C2H5 + { RCH2O2 } -> CH3CHOHCHOHC2H5 + { RO }; kd = 0.2*kRO2ps
 R719: AA CH3CHOHCHO2C2H5 + { RCH2O2 } -> CH3CHOHCOC2H5 + { ROH }; kd = 0.2*kRO2ps
 R720: AA CH3CHOHCHO2C2H5 + { RCOO2 } -> CH3CHOHCHOC2H5 + { RO }; kd = 0.80*kRO2so
 R721: AA CH3CHOHCHO2C2H5 + { RCOO2 } -> CH3CHOHCOC2H5 + { ROH }; kd = 0.2*kRO2so
 R722: EA CH3CHOHCHOHC2H5 + OH -> CH3COHCHOHC2H5 + H2O; k = 2.6E-12*exp(+475/T)
 R723: O2 CH3COHCHOHC2H5 + O2 -> CH3CHOHCOC2H5 + HO2; k = 9.6E-12
 R724: N1 CH3CHOHCHOHC2H5 -> CH3CHOHCHOC2H5 + OH; kd = JCH3OOH
 R725: N1 CH3CHOHCHOHC2H5 + OH -> CH3CHOHCHO2C2H5 + H2O; kd = kROOHOH
 R726: N1 CH3CHOHCHOHC2H5 + OH -> CH3CHOHCOC2H5 + H2O + OH; k = 4.6E-11
 R727: N1 CH3CHOHCHOC2H5 -> CH3CHOH + C2H5CHO; k = 1.0E+06
 R728: N1 CH3CHOHCOC2H5 -> CH3CHOH + C2H5CO; kd = JCH3CHO_1
 R729: N1 CH3CHOHCOC2H5 + OH -> CH3COHCOC2H5 + H2O; k = 4.7E-12
 R730: N1 CH3COHCOC2H5 + O2 -> CH3COCOC2H5 + HO2; k = 1.0E-11
 R731: N1 CH3COCOC2H5 -> CH3CO + C2H5CO; kd = 3.6E-02*JNO2
 ***** 2-Hexene *****
 R732: A6 hexene_2 + O3 -> CH3CHOO + C3H7CHO; k = 1.0E-16
 R733: A6 hexene_2 + O3 -> CH3CHO + C3H7CHOO; k = 1.0E-16
 R734: A6 hexene_2 + OH -> CH3CHOHCHC3H7; k = 6.4E-11
 R735: N1 CH3CHOHCHC3H7 + O2 -> CH3CHOHCHO2C3H7; k = 2.0E-12
 R736: N1 CH3CHOHCHO2C3H7 + HO2 -> CH3CHOHCHOOHC3H + O2; kd = 0.50*kRO2hs
 R737: N1 CH3CHOHCHO2C3H7 + HO2 -> CH3CHOHCOC3H7 + H2O + O2; kd = 0.16*kRO2hs
 R738: N1 CH3CHOHCHO2C3H7 + NO -> CH3CHOHCHOC3H7 + NO2; kd = kRO2NOs
 R739: N1 CH3CHOHCHO2C3H7 + { CH3O2 } -> CH3CHOHCHOC3H7 + { RO }; kd = 0.40*kRO2ms
 R740: AA CH3CHOHCHO2C3H7 + { CH3O2 } -> CH3CHOHCHOHC3H7 + { RO }; kd = 0.30*kRO2ms
 R741: AA CH3CHOHCHO2C3H7 + { CH3O2 } -> CH3CHOHCOC3H7 + { ROH }; kd = 0.30*kRO2ms
 R742: AA CH3CHOHCHO2C3H7 + { RCH2O2 } -> CH3CHOHCHOC3H7 + { RO }; kd = 0.6*kRO2ps
 R743: AA CH3CHOHCHO2C3H7 + { RCH2O2 } -> CH3CHOHCHOHC3H7 + { RO }; kd = 0.2*kRO2ps
 R744: AA CH3CHOHCHO2C3H7 + { RCH2O2 } -> CH3CHOHCOC3H7 + { ROH }; kd = 0.2*kRO2ps
 R745: AA CH3CHOHCHO2C3H7 + { RCOO2 } -> CH3CHOHCHOC3H7 + { RO }; kd = 0.80*kRO2so
 R746: AA CH3CHOHCHO2C3H7 + { RCOO2 } -> CH3CHOHCOC3H7 + { ROH }; kd = 0.2*kRO2so
 R747: EA CH3CHOHCHOHC3H7 + OH -> CH3CHOHCHOHC3H7 + H2O; k = 2.6E-12*exp(+475/T)
 R748: O2 CH3CHOHCHOHC3H7 + O2 -> CH3CHOHCOC3H7 + HO2; k = 9.6E-12
 R749: N1 CH3CHOHCHOHC3H7 -> CH3CHOHCHOC3H7 + OH; kd = JCH3OOH

R750: N1 CH3CHOHCHOOHC3H + OH -> CH3CHOHCHO2C3H7 + H2O; kd = kROOHOH
R751: N1 CH3CHOHCHOOHC3H + OH -> CH3CHOHCOC3H7 + H2O + OH; k = 4.6E-11
R752: N1 CH3CHOHCHOC3H7 -> CH3CHOH + C3H7CHO; k = 1.0E+06
R753: N1 CH3CHOHCOC3H7 -> CH3CHOH + C3H7CO; kd = JCH3CHO_ 1
R754: N1 CH3CHOHCOC3H7 + OH -> CH3COHCOC3H7 + H2O; k = 6.1E-12
R755: N1 CH3COHCOC3H7 + O2 -> CH3COCOC3H7 + HO2; k = 1.0E-11
R756: N1 CH3COCOC3H7 -> CH3CO + C3H7CO; kd = 3.6E-02*JNO2
R757: N1 C3H7CHOO -> C3H7CHO2; k = 4.0E+3
R758: N1 C3H7CHOO -> propane + CO2; k = 1.2E+3
R759: N1 C3H7CHOO -> C3H7 + CO2 + H; k = 2.4E+3
R760: N1 C3H7CHOO -> C2H5CH2O + CHO; k = 3E+2
R761: N1 C3H7CHOO -> C3H7 + CO + OH; k = 2.1E+3
R762: N1 C3H7CHO2 + H2O -> C3H7COHO + H2O; k = 1E-17
R763: N1 C3H7COHO + OH -> C3H7 + CO2 + H2O; k = 1.8E-2*exp(-120/T)
***** (Some choice butene selections: Butanal) ***
R764: N1 C3H7CHO -> C3H7 + CHO; kd = 8.4E-4*JNO2
R765: N1 C3H7CHO + OH -> C3H7CO + H2O; k = 9.0E-12*exp(+250/T)
R766: N1 C3H7CO + O2 -> C3H7COO2; k = 2E-12
R767: N1 C3H7COO2 + NO -> C3H7COO + NO2; kd = kRO2NOo
R768: N1 C3H7COO2 + HO2 -> C3H7COOOH + O2; kd = 0.670*kRO2ho
R769: N1 C3H7COO2 + HO2 -> C3H7COOH + O3; kd = 0.33*kRO2ho
R770: N1 C3H7COO2 + NO2 -> C3H7COO2NO2; kd = kRO2NO2
R771: 76 C3H7COO2 + { CH3O2 } -> C3H7COO + { RO } ; kd = 0.50*kRO2mo
R772: AA C3H7COO2 + { CH3O2 } -> C3H7COOH + { RO } ; kd = 0.50*kRO2mo
R773: AA C3H7COO2 + { RCH2O2 } -> C3H7COO + { RO } ; kd = 0.80*kRO2po
R774: AA C3H7COO2 + { RCH2O2 } -> C3H7COOH + { RO } ; kd = 0.2*kRO2po
R775: AA C3H7COO2 + { RCOO2 } -> C3H7COO + { RO } ; kd = 1.00*kRO2oo
R776: D8 C3H7COOH + OH -> C3H7 + CO2 + OH; k = 2.6E-12*exp(-70/T)
R777: 76 C3H7COO -> C3H7 + CO2; k = 1E+7
R778: N1 C3H7COOOH -> C3H7 + CO2 + OH; kd = JCH3OOH
R779: N1 C3H7COOOH + OH -> C3H7COO2 + H2O; kd = kROOHOH
R780: N1 C3H7COO2NO2 -> C3H7COO2 + NO2; k = 1.12E+16*exp(-13330/T)
R781: 75 C3H7COO2NO2 + OH -> C2H5CHO + CO2 + NO2 + H2O; k = 2.9E-12*exp(-367/T)
R782: 00 { R2CHO2 } + { R3CO2 } -> { ROOH } + { RO2NO2 } ; k = 1
R783: 00 { OROH } -> { RONO2 } ; k = 1

***** End of Reaction list *****

*Nix[O2]

*Nix[H2O]

*Nix[CO2]

*Families

{ CH3O2 } = { CH3O2 }

{ RO } = { CH2O,CH3CHO,HOCH2CHO,OCHCH2OOH,OCHCHO,CH3COCH3,CH3COCH2OOH,CH3COCHO,
C2H5CHO,CH3COCH2OH,CH3CHOHCHO,CH3CHOHCHO,C2H5COCH3,CH3CHOHCOCH3,
CH3CHOHCOCH3,CH3COCOCH3,CH3CHCH3CHO,C2H5COCH2OH,C2H5CHOHCHO,C2H5COCHO,
C2H5CHOHCHO,C2H5COCH2OOH,CH3CCH3OHCHO,CH3CCH3OOHCHO,CH3COCHOHCH3,
CH3COCHOHCH3,CH3CHOHCOC2H5,CH3COCOC2H5,CH3CHOHCOC3H7,CH3COCOC3H7 }

$\{ ROH \} = \{ CH_3OH, C_2H_5OH, HOC_2H_4OOH, HOCH_2CHO, HOCH_2COOOH, HOC_2H_4OH, CH_3CHOHCH_3, CH_3COCH_2OH, C_2H_5CH_2OH, CH_3CHOHCH_2OH, CH_3CHOHCHO, CH_3CHOHCH_2OOH, C_2H_5CHOHCH_3, CH_3CHOHCOCH_3, CH_3CHCH_3CH_2OH, C_2H_5CHOHCH_2OH, C_2H_5CHOHCH_2OH, C_2H_5COCH_2OH, C_2H_5CHOHCHO, C_2H_5CHOHCH_2OOH, C_2H_5CHOHCOOOH, CH_3CCH_3OHCH_2OOH, CH_3CCH_3OHCH_2OH, CH_3CCH_3OHCHO, HOCH_2CCH_3OOHCH_3, CH_3CHOHCHOHCH_3, CH_3CHOHCHOHCH_3, CH_3COCHOHCH_3, CH_3CHOHCHOHCH_2H, CH_3CHOHCHOHCH_2H_5, CH_3CHOHCOCH_2H_5, CH_3CHOHCHOHCH_3H, CH_3CHOHCHOHCH_3H_7, CH_3CHOHCOCH_3H_7, CH_3COHCH_3CH_3, HOCH_2CCH_3OHCH_3 \}$

$\{ RCH_2O_2 \} = \{ C_2H_5O_2, HOC_2H_4O_2, OCHCH_2O_2, CH_3COCH_2O_2, C_3H_7O_2, CH_3CHOHCH_2O_2, C_2H_5COCH_2O_2, CH_3CHCH_3CH_2O_2, C_2H_5CHOHCH_2O_2, CH_3CCH_3OHCH_2O_2, CH_3SCH_2O_2 \}$

$\{ RCOO_2 \} = \{ CH_3COO_2, HOCH_2COO_2, C_2H_5COO_2, CH_3CHOHCOO_2, CH_3CHCH_3COO_2, C_3H_7COO_2, C_2H_5CHOHCOO_2 \}$

$\{ R_2CHO_2 \} = \{ CH_3CHO_2CH_3, CH_3CHO_2CH_2OH, CH_3CHO_2CHO, CH_3CHO_2COCH_3, C_2H_5CHO_2CH_3, C_2H_5CHO_2CH_2OH, C_2H_5CHO_2CHO, CH_3CHOHCHO_2CH_3, CH_3COCHO_2CH_3, CH_3CHOHCHO_2C_2H_5, CH_3CHOHCHO_2C_3H_7 \}$

$\{ R_3CO_2 \} = \{ CH_3CO_2CH_3CH_3, HOCH_2CCH_3O_2CH_3, CH_3CCH_3O_2CHO \}$

$\{ ROOH \} = \{ CH_3OOH, C_2H_5OOH, CH_3COOOH, HOC_2H_4OOH, HOCH_2COOOH, OCHCH_2OOH, C_3H_7OOH, CH_3COCH_2OOH, CH_3CHOHCH_3, C_2H_5COOOH, CH_3CHOHCH_2OH, CH_3CHOHCHO, CH_3CHOHCH_2OOH, C_2H_5CHOHCH_3, CH_3CHOHCOCH_3, CH_3COOHCH_3CH_3, CH_3CHCH_3CH_2OOH, CH_3CHCH_3COOOH, C_2H_5CHOHCH_2OH, C_2H_5CHOHCHO, C_2H_5CHOHCH_2OOH, C_2H_5CHOHCOOOH, C_2H_5COCH_2OOH, CH_3CCH_3OHCH_2OOH, HOCH_2CCH_3OOHCH_3, CH_3CCH_3OOHCHO, CH_3CHOHCHOHCH_3, CH_3COCHOHCH_3, CH_3CHOHCHOHCH_2H, CH_3CHOHCHOHCH_3H, C_3H_7COOOH \}$

$\{ RO_2NO_2 \} = \{ CH_3COO_2NO_2, HOCH_2COO_2NO_2, C_2H_5COO_2NO_2, CH_3CHOHCOO_2NO_2, CH_3CHCH_3COO_2NO_2, C_2H_5CHOHCOO_2NO_2, C_3H_7COO_2NO_2 \}$

$\{ OROH \} = \{ HCOOH, CH_3COOH, HOCH_2COOH, C_2H_5COOH, CH_3CHOHCOOH, CH_3CHCH_3COOH, C_2H_5CHOHCOOH, C_3H_7COOH \}$

$\{ O_x \} = \{ O_3, O_-, 3P, O_-, 1D \}$

$\{ HO_y \} = \{ OH, H, HO_2, 2 \cdot H_2O_2 \}$

$\{ NO_y \} = \{ NO, NO_2, NO_3, 2 \cdot N_2O_5, HONO, CH_3O_2NO_2, CH_3COO_2NO_2, HOCH_2COO_2NO_2, HO_2NO_2, ClONO_2, C_2H_5COO_2NO_2, CH_3CHOHCOO_2NO_2, C_3H_7COO_2NO_2, C_2H_5CHOHCOO_2NO_2, CH_3CHCH_3COO_2NO_2 \}$

$\{ NO_z \} = \{ \{ NO_y \}, HONO_2 \}$

Appendix 2

Marine air samples from SAGA 3.

NMHC Data for SAGA3 bow samples.

Note that dChi does not include the absolute accuracy of the standards, which is 20%.

Data before JD50 may have had line contamination.

ethane

| JD | lat | lon | Chi | dChi |
|--------|--------|---------|-----------|-----------|
| 70.323 | -11.29 | -166.71 | 3.153e-10 | 6.089e-12 |
| 69.854 | -10.35 | -165.48 | 3.556e-10 | 5.907e-12 |
| 69.323 | -8.03 | -165.07 | 4.555e-10 | 7.576e-12 |
| 68.844 | -5.78 | -165.00 | 4.446e-10 | 8.415e-12 |
| 67.312 | 0.95 | -165.00 | 7.247e-10 | 1.153e-11 |
| 67.115 | 1.88 | -165.00 | 8.065e-10 | 4.474e-11 |
| 66.844 | 3.15 | -165.00 | 8.488e-10 | 7.099e-11 |
| 66.083 | 6.68 | -165.00 | 7.885e-10 | 4.142e-11 |
| 65.812 | 7.93 | -165.00 | 1.067e-09 | 4.602e-11 |
| 65.125 | 9.20 | -164.48 | 1.246e-09 | 6.979e-11 |
| 64.833 | 8.05 | -163.72 | 9.230e-10 | 4.327e-11 |
| 64.302 | 5.92 | -162.33 | 7.930e-10 | 4.415e-11 |
| 64.083 | 5.01 | -161.76 | 9.128e-10 | 5.011e-11 |
| 63.802 | 3.87 | -161.04 | 9.216e-10 | 5.245e-11 |
| 63.125 | 1.12 | -159.15 | 8.854e-10 | 4.852e-11 |
| 62.792 | -0.39 | -158.22 | 8.477e-10 | 3.745e-11 |
| 62.417 | -1.93 | -157.13 | 8.028e-10 | 2.924e-11 |
| 62.208 | -2.86 | -156.54 | 7.953e-10 | 2.785e-11 |
| 62.021 | -3.69 | -155.96 | 8.179e-10 | 3.386e-11 |
| 61.854 | -4.37 | -155.50 | 7.902e-10 | 2.595e-11 |

ethene

| JD | lat | lon | Chi | dChi |
|--------|--------|---------|-----------|-----------|
| 70.323 | -11.29 | -166.71 | 4.175e-11 | 2.166e-12 |
| 69.854 | -10.35 | -165.48 | 4.678e-11 | 2.287e-12 |
| 69.323 | -8.03 | -165.07 | 4.048e-11 | 5.259e-12 |
| 68.844 | -5.78 | -165.00 | 3.941e-11 | 2.213e-12 |
| 67.312 | 0.95 | -165.00 | 4.654e-11 | 1.971e-12 |
| 67.115 | 1.88 | -165.00 | 5.641e-11 | 2.027e-12 |
| 66.844 | 3.15 | -165.00 | 4.835e-11 | 1.952e-12 |
| 66.083 | 6.68 | -165.00 | 5.245e-11 | 2.693e-12 |
| 65.812 | 7.93 | -165.00 | 5.291e-11 | 2.788e-12 |
| 65.125 | 9.20 | -164.48 | 5.669e-11 | 2.257e-12 |
| 64.833 | 8.05 | -163.72 | 5.570e-11 | 2.484e-12 |
| 64.302 | 5.92 | -162.33 | 5.758e-11 | 2.895e-12 |
| 64.083 | 5.01 | -161.76 | 6.206e-11 | 1.861e-12 |
| 63.802 | 3.87 | -161.04 | 5.936e-11 | 2.541e-12 |
| 63.125 | 1.12 | -159.15 | 6.581e-11 | 1.857e-12 |
| 62.792 | -0.39 | -158.22 | 5.544e-11 | 2.692e-12 |
| 62.417 | -1.93 | -157.13 | 4.943e-11 | 4.124e-12 |
| 62.208 | -2.86 | -156.54 | 5.772e-11 | 4.343e-12 |
| 62.021 | -3.69 | -155.96 | 7.134e-11 | 5.022e-12 |
| 61.854 | -4.37 | -155.50 | 6.248e-11 | 4.477e-12 |
| 61.062 | -1.78 | -154.99 | 7.011e-11 | 7.551e-12 |
| 60.802 | -0.53 | -155.00 | 8.305e-11 | 4.591e-12 |
| 60.208 | 2.22 | -154.98 | 6.864e-11 | 4.017e-12 |

| | | | | |
|--------|--------|---------|-----------|-----------|
| 60.052 | 3.13 | -154.97 | 7.986e-11 | 1.006e-11 |
| 59.927 | 3.57 | -155.02 | 9.673e-11 | 5.472e-12 |
| 59.792 | 4.37 | -155.00 | 8.794e-11 | 4.850e-12 |
| 59.240 | 6.68 | -155.00 | 1.842e-11 | 1.934e-12 |
| 58.948 | 7.99 | -155.00 | 2.549e-11 | 2.687e-12 |
| 58.792 | 8.88 | -154.98 | 4.770e-11 | 5.892e-12 |
| 58.312 | 11.12 | -155.01 | 4.310e-11 | 3.360e-12 |
| 58.177 | 11.77 | -154.99 | 5.015e-11 | 3.748e-12 |
| 58.052 | 12.32 | -154.98 | 5.526e-11 | 5.578e-12 |
| 57.917 | 12.90 | -154.98 | 4.416e-11 | 2.700e-12 |
| 57.792 | 13.47 | -154.99 | 2.834e-11 | 4.288e-12 |
| 57.312 | 14.43 | -154.79 | 0.000e+00 | 1.245e-13 |
| 57.188 | 13.85 | -154.56 | 5.268e-11 | 4.649e-12 |
| 56.938 | 12.66 | -154.11 | 4.373e-11 | 5.875e-12 |
| 56.812 | 12.07 | -153.88 | 5.358e-11 | 3.347e-12 |
| 56.208 | 9.33 | -152.69 | 6.544e-11 | 3.812e-12 |
| 56.042 | 8.59 | -152.36 | 6.806e-11 | 3.533e-12 |
| 55.833 | 7.69 | -151.96 | 6.500e-11 | 4.670e-12 |
| 55.292 | 5.22 | -151.11 | 4.934e-11 | 3.098e-12 |
| 54.927 | 3.87 | -150.62 | 5.985e-11 | 7.389e-12 |
| 54.792 | 3.26 | -150.40 | 4.427e-11 | 7.591e-12 |
| 54.281 | 0.82 | -149.42 | 4.370e-11 | 6.507e-12 |
| 54.135 | 0.13 | -149.21 | 1.066e-10 | 1.589e-11 |
| 53.917 | -0.92 | -148.84 | 3.477e-11 | 5.877e-12 |
| 53.792 | -1.52 | -148.68 | 3.147e-11 | 4.191e-12 |
| 53.333 | -3.51 | -147.79 | 3.012e-11 | 5.047e-12 |
| 52.365 | -8.05 | -145.86 | 4.848e-11 | 7.498e-12 |
| 51.958 | -10.00 | -145.03 | 4.274e-11 | 2.853e-12 |
| 51.802 | -9.64 | -145.07 | 4.179e-11 | 3.796e-12 |
| 51.229 | -6.97 | -144.99 | 3.995e-11 | 3.772e-12 |
| 51.167 | -6.73 | -145.02 | 4.418e-11 | 4.184e-12 |
| 50.927 | -5.89 | -145.00 | 5.446e-11 | 3.750e-12 |
| 49.917 | -0.88 | -144.95 | 5.771e-11 | 4.981e-12 |
| 49.781 | -0.10 | -144.97 | 0.000e+00 | 0.000e+00 |
| 48.865 | 3.69 | -145.05 | 9.620e-11 | 5.648e-12 |
| 47.917 | 7.67 | -144.03 | 1.388e-10 | 9.537e-12 |
| 47.792 | 8.40 | -144.05 | 1.035e-10 | 7.869e-12 |
| 47.042 | 11.14 | -145.66 | 1.247e-10 | 5.503e-12 |
| 46.875 | 11.97 | -146.22 | 1.162e-10 | 1.310e-11 |
| 46.802 | 12.24 | -146.40 | 9.963e-11 | 8.517e-12 |
| 45.896 | 15.86 | -148.71 | 1.125e-10 | 9.104e-12 |
| 45.708 | 16.30 | -149.31 | 7.970e-11 | 8.749e-12 |
| 45.271 | 17.45 | -151.09 | 9.237e-11 | 8.101e-12 |
| ethyne | | | | |
| JD | lat | lon | Chi | dChi |
| 70.323 | -11.29 | -166.71 | 1.057e-11 | 1.297e-12 |
| 69.854 | -10.35 | -165.48 | 1.073e-11 | 1.273e-12 |
| 69.323 | -8.03 | -165.07 | 1.712e-11 | 1.892e-12 |
| 68.844 | -5.78 | -165.00 | 1.257e-11 | 1.299e-12 |
| 67.312 | 0.95 | -165.00 | 4.193e-11 | 3.005e-12 |
| 67.115 | 1.88 | -165.00 | 0.000e+00 | 2.350e-13 |
| 66.844 | 3.15 | -165.00 | 5.673e-11 | 1.932e-12 |
| 66.083 | 6.68 | -165.00 | 1.894e-15 | 2.492e-13 |
| 65.812 | 7.93 | -165.00 | 1.365e-10 | 4.133e-12 |
| 65.125 | 9.20 | -164.48 | 4.356e-14 | 3.235e-13 |

| | | | | |
|--------|--------|---------|-----------|-----------|
| 64.833 | 8.05 | -163.72 | 1.204e-10 | 3.501e-12 |
| 64.302 | 5.92 | -162.33 | 6.061e-14 | 2.987e-13 |
| 64.083 | 5.01 | -161.76 | 1.648e-13 | 2.953e-13 |
| 63.802 | 3.87 | -161.04 | 6.391e-11 | 2.171e-12 |
| 63.125 | 1.12 | -159.15 | 5.152e-13 | 2.617e-13 |
| 62.792 | -0.39 | -158.22 | 6.273e-11 | 2.320e-12 |
| 62.417 | -1.93 | -157.13 | 2.614e-13 | 6.313e-13 |
| 62.208 | -2.86 | -156.54 | 9.091e-14 | 6.313e-13 |
| 62.021 | -3.69 | -155.96 | 1.989e-13 | 7.267e-13 |
| 61.854 | -4.37 | -155.50 | 6.201e-11 | 4.187e-12 |
| 61.062 | -1.78 | -154.99 | 2.347e-12 | 1.113e-12 |
| 60.802 | -0.53 | -155.00 | 2.613e-11 | 2.826e-12 |
| 60.208 | 2.22 | -154.98 | 1.023e-12 | 5.517e-13 |
| 60.052 | 3.13 | -154.97 | 0.000e+00 | 5.835e-13 |
| 59.927 | 3.57 | -155.02 | 0.000e+00 | 5.835e-13 |
| 59.792 | 4.37 | -155.00 | 2.848e-11 | 3.280e-12 |
| 59.240 | 6.68 | -155.00 | 3.869e-11 | 2.711e-12 |
| 58.948 | 7.99 | -155.00 | 9.489e-13 | 4.318e-13 |
| 58.792 | 8.88 | -154.98 | 5.918e-11 | 3.137e-12 |
| 58.312 | 11.12 | -155.01 | 2.131e-12 | 9.182e-13 |
| 58.177 | 11.77 | -154.99 | 8.920e-13 | 3.932e-13 |
| 58.052 | 12.32 | -154.98 | 0.000e+00 | 4.563e-13 |
| 57.917 | 12.90 | -154.98 | 3.125e-12 | 1.135e-12 |
| 57.792 | 13.47 | -154.99 | 5.840e-11 | 5.534e-12 |
| 57.312 | 14.43 | -154.79 | 2.455e-12 | 1.164e-12 |
| 57.188 | 13.85 | -154.56 | 4.375e-13 | 6.256e-13 |
| 56.938 | 12.66 | -154.11 | 2.415e-12 | 1.047e-12 |
| 56.812 | 12.07 | -153.88 | 3.681e-11 | 3.909e-12 |
| 56.208 | 9.33 | -152.69 | 1.165e-12 | 5.295e-13 |
| 56.042 | 8.59 | -152.36 | 6.534e-13 | 5.142e-13 |
| 55.833 | 7.69 | -151.96 | 2.750e-12 | 1.310e-12 |
| 55.292 | 5.22 | -151.11 | 9.977e-12 | 2.451e-12 |
| 54.927 | 3.87 | -150.62 | 0.000e+00 | 7.318e-13 |
| 54.792 | 3.26 | -150.40 | 1.116e-11 | 4.071e-12 |
| 54.281 | 0.82 | -149.42 | 3.063e-12 | 1.432e-12 |
| 54.135 | 0.13 | -149.21 | 1.648e-13 | 8.273e-13 |
| 53.917 | -0.92 | -148.84 | 5.682e-15 | 7.955e-13 |
| 53.792 | -1.52 | -148.68 | 5.682e-15 | 8.324e-13 |
| 53.333 | -3.51 | -147.79 | 5.682e-15 | 1.283e-12 |
| 52.365 | -8.05 | -145.86 | 9.091e-14 | 7.580e-13 |
| 51.958 | -10.00 | -145.03 | 3.085e-12 | 1.528e-12 |
| 51.802 | -9.64 | -145.07 | 1.282e-11 | 3.304e-12 |
| 51.229 | -6.97 | -144.99 | 4.865e-12 | 2.156e-12 |
| 51.167 | -6.73 | -145.02 | 3.920e-13 | 6.949e-13 |
| 50.927 | -5.89 | -145.00 | 0.000e+00 | 6.790e-13 |
| 49.917 | -0.88 | -144.95 | 6.534e-13 | 5.835e-13 |
| 49.781 | -0.10 | -144.97 | 2.865e-11 | 3.201e-12 |
| 48.865 | 3.69 | -145.05 | 0.000e+00 | 7.477e-13 |
| 47.917 | 7.67 | -144.03 | 2.159e-12 | 1.023e-12 |
| 47.792 | 8.40 | -144.05 | 0.000e+00 | 8.006e-13 |
| 47.042 | 11.14 | -145.66 | 9.722e-12 | 3.014e-12 |
| 46.875 | 11.97 | -146.22 | 0.000e+00 | 1.023e-12 |
| 46.802 | 12.24 | -146.40 | 1.070e-11 | 3.706e-12 |
| 45.896 | 15.86 | -148.71 | 3.145e-10 | 1.599e-11 |
| 45.708 | 16.30 | -149.31 | 4.746e-11 | 4.791e-12 |

| | | | | |
|---------|--------|---------|-----------|-----------|
| 45.271 | 17.45 | -151.09 | 6.057e-11 | 5.120e-12 |
| propane | | | | |
| JD | lat | lon | Chi | dChi |
| 70.323 | -11.29 | -166.71 | 2.470e-11 | 1.578e-12 |
| 69.854 | -10.35 | -165.48 | 2.854e-11 | 1.958e-12 |
| 69.323 | -8.03 | -165.07 | 3.131e-11 | 1.776e-12 |
| 68.844 | -5.78 | -165.00 | 2.923e-11 | 1.828e-12 |
| 67.312 | 0.95 | -165.00 | 5.740e-11 | 2.432e-12 |
| 67.115 | 1.88 | -165.00 | 5.946e-11 | 2.261e-12 |
| 66.844 | 3.15 | -165.00 | 6.979e-11 | 2.840e-12 |
| 66.083 | 6.68 | -165.00 | 6.084e-11 | 2.231e-12 |
| 65.812 | 7.93 | -165.00 | 1.423e-10 | 4.210e-12 |
| 65.125 | 9.20 | -164.48 | 1.984e-10 | 4.381e-12 |
| 64.833 | 8.05 | -163.72 | 1.150e-10 | 8.340e-12 |
| 64.302 | 5.92 | -162.33 | 6.031e-11 | 2.188e-12 |
| 64.083 | 5.01 | -161.76 | 7.744e-11 | 2.732e-12 |
| 63.802 | 3.87 | -161.04 | 7.609e-11 | 2.517e-12 |
| 63.125 | 1.12 | -159.15 | 7.560e-11 | 2.216e-12 |
| 62.792 | -0.39 | -158.22 | 6.858e-11 | 1.949e-12 |
| 62.417 | -1.93 | -157.13 | 6.151e-11 | 4.024e-12 |
| 62.208 | -2.86 | -156.54 | 6.209e-11 | 3.003e-12 |
| 62.021 | -3.69 | -155.96 | 6.201e-11 | 3.792e-12 |
| 61.854 | -4.37 | -155.50 | 6.455e-11 | 3.981e-12 |
| 61.062 | -1.78 | -154.99 | 6.392e-11 | 4.353e-12 |
| 60.802 | -0.53 | -155.00 | 6.483e-11 | 8.649e-12 |
| 60.208 | 2.22 | -154.98 | 4.570e-11 | 6.311e-12 |
| 60.052 | 3.13 | -154.97 | 6.625e-11 | 8.878e-12 |
| 59.927 | 3.57 | -155.02 | 5.459e-11 | 5.716e-12 |
| 59.792 | 4.37 | -155.00 | 6.476e-11 | 6.875e-12 |
| 59.240 | 6.68 | -155.00 | 6.119e-11 | 9.258e-12 |
| 58.948 | 7.99 | -155.00 | 6.404e-11 | 7.090e-12 |
| 58.792 | 8.88 | -154.98 | 7.967e-11 | 8.036e-12 |
| 58.312 | 11.12 | -155.01 | 8.944e-11 | 9.632e-12 |
| 58.177 | 11.77 | -154.99 | 7.493e-11 | 8.535e-12 |
| 58.052 | 12.32 | -154.98 | 9.982e-11 | 1.076e-11 |
| 57.917 | 12.90 | -154.98 | 7.138e-11 | 8.541e-12 |
| 57.792 | 13.47 | -154.99 | 7.643e-11 | 6.440e-12 |
| 57.312 | 14.43 | -154.79 | 1.809e-11 | 3.552e-12 |
| 57.188 | 13.85 | -154.56 | 1.011e-10 | 7.691e-12 |
| 56.938 | 12.66 | -154.11 | 7.363e-11 | 3.224e-12 |
| 56.812 | 12.07 | -153.88 | 2.393e-11 | 2.603e-12 |
| 56.208 | 9.33 | -152.69 | 7.020e-11 | 4.593e-12 |
| 56.042 | 8.59 | -152.36 | 7.872e-11 | 4.565e-12 |
| 55.833 | 7.69 | -151.96 | 7.864e-11 | 9.588e-12 |
| 55.292 | 5.22 | -151.11 | 5.500e-11 | 5.863e-12 |
| 54.927 | 3.87 | -150.62 | 7.251e-11 | 8.381e-12 |
| 54.792 | 3.26 | -150.40 | 5.097e-11 | 7.435e-12 |
| 54.281 | 0.82 | -149.42 | 4.438e-11 | 4.778e-12 |
| 54.135 | 0.13 | -149.21 | 5.716e-11 | 7.724e-12 |
| 53.917 | -0.92 | -148.84 | 2.953e-11 | 4.536e-12 |
| 53.792 | -1.52 | -148.68 | 3.352e-11 | 3.840e-12 |
| 53.333 | -3.51 | -147.79 | 1.591e-11 | 4.230e-12 |
| 52.365 | -8.05 | -145.86 | 1.532e-11 | 2.448e-12 |
| 51.958 | -10.00 | -145.03 | 1.942e-11 | 2.914e-12 |
| 51.802 | -9.64 | -145.07 | 2.305e-11 | 3.531e-12 |

| | | | | |
|--------|-------|---------|-----------|-----------|
| 51.229 | -6.97 | -144.99 | 3.109e-11 | 3.393e-12 |
| 51.167 | -6.73 | -145.02 | 2.815e-11 | 3.415e-12 |
| 50.927 | -5.89 | -145.00 | 3.174e-11 | 5.046e-12 |
| 49.917 | -0.88 | -144.95 | 5.066e-11 | 7.215e-12 |
| 49.781 | -0.10 | -144.97 | 4.260e-11 | 5.851e-12 |
| 48.865 | 3.69 | -145.05 | 9.480e-11 | 1.394e-11 |
| 47.917 | 7.67 | -144.03 | 1.304e-10 | 1.648e-11 |
| 47.792 | 8.40 | -144.05 | 1.476e-10 | 1.925e-11 |
| 47.042 | 11.14 | -145.66 | 1.584e-10 | 1.650e-11 |
| 46.875 | 11.97 | -146.22 | 1.420e-10 | 1.515e-11 |
| 46.802 | 12.24 | -146.40 | 1.201e-10 | 1.311e-11 |
| 45.896 | 15.86 | -148.71 | 3.768e-10 | 4.093e-11 |
| 45.708 | 16.30 | -149.31 | 4.548e-10 | 2.369e-11 |
| 45.271 | 17.45 | -151.09 | 3.819e-10 | 1.810e-11 |

cyclopropane

| JD | lat | lon | Chi | dChi |
|--------|--------|---------|-----------|-----------|
| 70.323 | -11.29 | -166.71 | 7.613e-12 | 1.034e-12 |
| 69.854 | -10.35 | -165.48 | 9.289e-12 | 1.259e-12 |
| 69.323 | -8.03 | -165.07 | 8.218e-12 | 9.851e-13 |
| 68.844 | -5.78 | -165.00 | 7.974e-12 | 9.093e-13 |
| 67.312 | 0.95 | -165.00 | 9.988e-12 | 8.869e-13 |
| 67.115 | 1.88 | -165.00 | 1.112e-11 | 9.577e-13 |
| 66.844 | 3.15 | -165.00 | 1.478e-11 | 1.455e-12 |
| 66.083 | 6.68 | -165.00 | 1.273e-11 | 1.858e-12 |
| 65.812 | 7.93 | -165.00 | 1.313e-11 | 1.507e-12 |
| 65.125 | 9.20 | -164.48 | 1.269e-11 | 1.241e-12 |
| 64.833 | 8.05 | -163.72 | 1.114e-11 | 9.758e-13 |
| 64.302 | 5.92 | -162.33 | 1.264e-11 | 1.544e-12 |
| 64.083 | 5.01 | -161.76 | 1.190e-11 | 1.374e-12 |
| 63.802 | 3.87 | -161.04 | 1.325e-11 | 1.573e-12 |
| 63.125 | 1.12 | -159.15 | 1.200e-11 | 1.233e-12 |
| 62.792 | -0.39 | -158.22 | 1.061e-11 | 1.027e-12 |
| 62.417 | -1.93 | -157.13 | 1.005e-11 | 1.572e-12 |
| 62.208 | -2.86 | -156.54 | 1.029e-11 | 1.685e-12 |
| 62.021 | -3.69 | -155.96 | 1.133e-11 | 2.070e-12 |
| 61.854 | -4.37 | -155.50 | 9.971e-12 | 1.619e-12 |
| 61.062 | -1.78 | -154.99 | 2.121e-11 | 4.724e-12 |
| 60.802 | -0.53 | -155.00 | 1.195e-11 | 1.932e-12 |
| 60.208 | 2.22 | -154.98 | 8.975e-12 | 1.321e-12 |
| 60.052 | 3.13 | -154.97 | 1.154e-11 | 1.801e-12 |
| 59.927 | 3.57 | -155.02 | 1.106e-11 | 1.839e-12 |
| 59.792 | 4.37 | -155.00 | 9.285e-12 | 1.509e-12 |
| 59.240 | 6.68 | -155.00 | 1.480e-11 | 2.109e-12 |
| 58.948 | 7.99 | -155.00 | 8.219e-12 | 1.276e-12 |
| 58.792 | 8.88 | -154.98 | 9.183e-12 | 1.182e-12 |
| 58.312 | 11.12 | -155.01 | 1.139e-11 | 1.813e-12 |
| 58.177 | 11.77 | -154.99 | 1.087e-11 | 1.809e-12 |
| 58.052 | 12.32 | -154.98 | 4.886e-12 | 1.172e-12 |
| 57.917 | 12.90 | -154.98 | 2.655e-13 | 3.689e-13 |
| 57.792 | 13.47 | -154.99 | 1.473e-11 | 2.544e-12 |
| 57.312 | 14.43 | -154.79 | 9.314e-13 | 4.739e-13 |
| 57.188 | 13.85 | -154.56 | 2.208e-11 | 3.408e-12 |
| 56.938 | 12.66 | -154.11 | 1.617e-11 | 2.692e-12 |
| 56.812 | 12.07 | -153.88 | 1.140e-12 | 5.707e-13 |
| 56.208 | 9.33 | -152.69 | 1.228e-11 | 1.706e-12 |

| | | | | |
|--------|--------|---------|-----------|-----------|
| 56.042 | 8.59 | -152.36 | 1.470e-11 | 3.191e-12 |
| 55.833 | 7.69 | -151.96 | 1.878e-11 | 2.491e-12 |
| 55.292 | 5.22 | -151.11 | 1.773e-11 | 3.782e-12 |
| 54.927 | 3.87 | -150.62 | 8.317e-12 | 1.948e-12 |
| 54.792 | 3.26 | -150.40 | 9.028e-13 | 8.288e-13 |
| 54.281 | 0.82 | -149.42 | 1.056e-11 | 2.060e-12 |
| 54.135 | 0.13 | -149.21 | 6.842e-12 | 2.039e-12 |
| 53.917 | -0.92 | -148.84 | 3.121e-12 | 1.207e-12 |
| 53.792 | -1.52 | -148.68 | 3.574e-12 | 1.264e-12 |
| 53.333 | -3.51 | -147.79 | 8.170e-15 | 1.102e-12 |
| 52.365 | -8.05 | -145.86 | 5.249e-12 | 1.725e-12 |
| 51.958 | -10.00 | -145.03 | 8.378e-12 | 2.702e-12 |
| 51.802 | -9.64 | -145.07 | 3.609e-11 | 1.103e-11 |
| 51.229 | -6.97 | -144.99 | 7.879e-12 | 2.005e-12 |
| 51.167 | -6.73 | -145.02 | 1.278e-11 | 3.293e-12 |
| 50.927 | -5.89 | -145.00 | 2.010e-11 | 2.849e-12 |
| 49.917 | -0.88 | -144.95 | 2.032e-11 | 5.161e-12 |
| 49.781 | -0.10 | -144.97 | 1.065e-11 | 1.971e-12 |
| 48.865 | 3.69 | -145.05 | 3.440e-11 | 2.964e-12 |
| 47.917 | 7.67 | -144.03 | 1.268e-11 | 2.815e-12 |
| 47.792 | 8.40 | -144.05 | 2.022e-12 | 1.076e-12 |
| 47.042 | 11.14 | -145.66 | 9.003e-12 | 2.549e-12 |
| 46.875 | 11.97 | -146.22 | 1.032e-11 | 2.527e-12 |
| 46.802 | 12.24 | -146.40 | 9.849e-12 | 2.664e-12 |
| 45.896 | 15.86 | -148.71 | 1.846e-12 | 9.804e-13 |
| 45.708 | 16.30 | -149.31 | 1.007e-11 | 2.001e-12 |
| 45.271 | 17.45 | -151.09 | 1.940e-11 | 3.155e-12 |

propene

| JD | lat | lon | Chi | dChi |
|--------|--------|---------|-----------|-----------|
| 70.323 | -11.29 | -166.71 | 2.445e-11 | 1.562e-12 |
| 69.854 | -10.35 | -165.48 | 3.058e-11 | 1.640e-12 |
| 69.323 | -8.03 | -165.07 | 2.469e-11 | 1.741e-12 |
| 68.844 | -5.78 | -165.00 | 2.171e-11 | 1.478e-12 |
| 67.312 | 0.95 | -165.00 | 2.518e-11 | 1.517e-12 |
| 67.115 | 1.88 | -165.00 | 4.138e-11 | 2.088e-12 |
| 66.844 | 3.15 | -165.00 | 2.561e-11 | 1.220e-12 |
| 66.083 | 6.68 | -165.00 | 2.324e-11 | 1.285e-12 |
| 65.812 | 7.93 | -165.00 | 3.065e-11 | 1.456e-12 |
| 65.125 | 9.20 | -164.48 | 4.141e-11 | 1.679e-12 |
| 64.833 | 8.05 | -163.72 | 3.456e-11 | 1.517e-12 |
| 64.302 | 5.92 | -162.33 | 3.150e-11 | 1.364e-12 |
| 64.083 | 5.01 | -161.76 | 4.192e-11 | 1.510e-12 |
| 63.802 | 3.87 | -161.04 | 3.234e-11 | 1.243e-12 |
| 63.125 | 1.12 | -159.15 | 4.799e-11 | 1.580e-12 |
| 62.792 | -0.39 | -158.22 | 3.176e-11 | 1.322e-12 |
| 62.417 | -1.93 | -157.13 | 3.208e-11 | 2.366e-12 |
| 62.208 | -2.86 | -156.54 | 4.342e-11 | 2.507e-12 |
| 62.021 | -3.69 | -155.96 | 5.926e-11 | 3.528e-12 |
| 61.854 | -4.37 | -155.50 | 4.811e-11 | 2.596e-12 |
| 61.062 | -1.78 | -154.99 | 7.492e-11 | 1.111e-11 |
| 60.802 | -0.53 | -155.00 | 4.313e-11 | 8.601e-12 |
| 60.208 | 2.22 | -154.98 | 3.423e-11 | 7.019e-12 |
| 60.052 | 3.13 | -154.97 | 7.039e-11 | 1.364e-11 |
| 59.927 | 3.57 | -155.02 | 3.478e-11 | 6.636e-12 |
| 59.792 | 4.37 | -155.00 | 4.818e-11 | 9.231e-12 |

| | | | | |
|--------|--------|---------|-----------|-----------|
| 59.240 | 6.68 | -155.00 | 1.147e-11 | 2.840e-12 |
| 58.948 | 7.99 | -155.00 | 1.878e-11 | 3.832e-12 |
| 58.792 | 8.88 | -154.98 | 1.528e-11 | 2.943e-12 |
| 58.312 | 11.12 | -155.01 | 3.330e-11 | 6.050e-12 |
| 58.177 | 11.77 | -154.99 | 3.350e-11 | 5.753e-12 |
| 58.052 | 12.32 | -154.98 | 5.858e-11 | 1.038e-11 |
| 57.917 | 12.90 | -154.98 | 4.171e-11 | 8.430e-12 |
| 57.792 | 13.47 | -154.99 | 1.619e-11 | 3.490e-12 |
| 57.312 | 14.43 | -154.79 | 2.374e-12 | 1.082e-12 |
| 57.188 | 13.85 | -154.56 | 3.321e-11 | 3.943e-12 |
| 56.938 | 12.66 | -154.11 | 5.026e-11 | 3.356e-12 |
| 56.812 | 12.07 | -153.88 | 3.366e-11 | 5.750e-12 |
| 56.208 | 9.33 | -152.69 | 3.939e-11 | 4.740e-12 |
| 56.042 | 8.59 | -152.36 | 5.365e-11 | 6.303e-12 |
| 55.833 | 7.69 | -151.96 | 3.392e-11 | 5.221e-12 |
| 55.292 | 5.22 | -151.11 | 4.124e-11 | 5.813e-12 |
| 54.927 | 3.87 | -150.62 | 8.007e-11 | 5.388e-12 |
| 54.792 | 3.26 | -150.40 | 5.009e-11 | 8.298e-12 |
| 54.281 | 0.82 | -149.42 | 4.140e-11 | 4.332e-12 |
| 54.135 | 0.13 | -149.21 | 6.194e-11 | 1.248e-11 |
| 53.917 | -0.92 | -148.84 | 4.591e-11 | 9.620e-12 |
| 53.792 | -1.52 | -148.68 | 2.181e-11 | 2.232e-12 |
| 53.333 | -3.51 | -147.79 | 2.168e-11 | 4.334e-12 |
| 52.365 | -8.05 | -145.86 | 2.807e-11 | 3.383e-12 |
| 51.958 | -10.00 | -145.03 | 5.715e-11 | 3.539e-12 |
| 51.802 | -9.64 | -145.07 | 2.322e-11 | 2.531e-12 |
| 51.229 | -6.97 | -144.99 | 4.135e-11 | 3.164e-12 |
| 51.167 | -6.73 | -145.02 | 5.325e-11 | 4.634e-12 |
| 50.927 | -5.89 | -145.00 | 6.837e-11 | 1.041e-11 |
| 49.917 | -0.88 | -144.95 | 6.608e-11 | 9.939e-12 |
| 49.781 | -0.10 | -144.97 | 4.322e-11 | 6.752e-12 |
| 48.865 | 3.69 | -145.05 | 1.164e-10 | 1.817e-11 |
| 47.917 | 7.67 | -144.03 | 2.724e-10 | 4.027e-11 |
| 47.792 | 8.40 | -144.05 | 1.754e-10 | 2.623e-11 |
| 47.042 | 11.14 | -145.66 | 3.000e-10 | 4.549e-11 |
| 46.875 | 11.97 | -146.22 | 2.236e-10 | 3.425e-11 |
| 46.802 | 12.24 | -146.40 | 1.578e-10 | 2.435e-11 |
| 45.896 | 15.86 | -148.71 | 2.853e-10 | 4.617e-11 |
| 45.708 | 16.30 | -149.31 | 7.866e-11 | 5.533e-12 |
| 45.271 | 17.45 | -151.09 | 5.635e-11 | 5.964e-12 |

butane

| JD | lat | lon | Chi | dChi |
|--------|--------|---------|-----------|-----------|
| 70.323 | -11.29 | -166.71 | 6.985e-12 | 9.009e-13 |
| 69.854 | -10.35 | -165.48 | 6.806e-12 | 8.327e-13 |
| 69.323 | -8.03 | -165.07 | 7.489e-12 | 1.052e-12 |
| 68.844 | -5.78 | -165.00 | 6.591e-12 | 8.228e-13 |
| 67.312 | 0.95 | -165.00 | 9.587e-12 | 1.052e-12 |
| 67.115 | 1.88 | -165.00 | 7.279e-12 | 7.470e-13 |
| 66.844 | 3.15 | -165.00 | 7.259e-12 | 7.049e-13 |
| 66.083 | 6.68 | -165.00 | 9.908e-12 | 1.126e-12 |
| 65.812 | 7.93 | -165.00 | 2.712e-11 | 1.468e-12 |
| 65.125 | 9.20 | -164.48 | 3.297e-11 | 1.657e-12 |
| 64.833 | 8.05 | -163.72 | 1.915e-11 | 1.265e-12 |
| 64.302 | 5.92 | -162.33 | 7.401e-12 | 7.597e-13 |
| 64.083 | 5.01 | -161.76 | 9.112e-12 | 1.170e-12 |

| | | | | |
|------------------|--------|---------|-----------|-----------|
| 63.802 | 3.87 | -161.04 | 8.285e-12 | 7.854e-13 |
| 63.125 | 1.12 | -159.15 | 8.324e-12 | 8.848e-13 |
| 62.792 | -0.39 | -158.22 | 8.506e-12 | 7.498e-13 |
| 62.417 | -1.93 | -157.13 | 9.018e-12 | 1.538e-12 |
| 62.208 | -2.86 | -156.54 | 9.074e-12 | 1.448e-12 |
| 62.021 | -3.69 | -155.96 | 1.032e-11 | 1.760e-12 |
| 61.854 | -4.37 | -155.50 | 1.032e-11 | 1.705e-12 |
| 61.062 | -1.78 | -154.99 | 1.087e-11 | 2.247e-12 |
| 60.802 | -0.53 | -155.00 | 1.313e-11 | 2.697e-12 |
| 60.208 | 2.22 | -154.98 | 1.021e-11 | 2.072e-12 |
| 60.052 | 3.13 | -154.97 | 1.349e-11 | 2.486e-12 |
| 59.927 | 3.57 | -155.02 | 1.451e-11 | 2.945e-12 |
| 59.792 | 4.37 | -155.00 | 1.496e-11 | 2.599e-12 |
| 59.240 | 6.68 | -155.00 | 1.079e-11 | 2.072e-12 |
| 58.948 | 7.99 | -155.00 | 9.823e-12 | 1.929e-12 |
| 58.792 | 8.88 | -154.98 | 9.580e-12 | 1.774e-12 |
| 58.312 | 11.12 | -155.01 | 9.566e-12 | 1.928e-12 |
| 58.177 | 11.77 | -154.99 | 8.478e-12 | 1.871e-12 |
| 58.052 | 12.32 | -154.98 | 1.281e-11 | 2.506e-12 |
| 57.917 | 12.90 | -154.98 | 1.787e-12 | 6.337e-13 |
| 57.792 | 13.47 | -154.99 | 1.036e-11 | 1.868e-12 |
| 57.312 | 14.43 | -154.79 | 0.000e+00 | 4.098e-13 |
| 57.188 | 13.85 | -154.56 | 9.733e-12 | 2.315e-12 |
| 56.938 | 12.66 | -154.11 | 1.214e-11 | 1.759e-12 |
| 56.812 | 12.07 | -153.88 | 3.502e-12 | 1.153e-12 |
| 56.208 | 9.33 | -152.69 | 1.249e-11 | 1.611e-12 |
| 56.042 | 8.59 | -152.36 | 9.261e-12 | 1.618e-12 |
| 55.833 | 7.69 | -151.96 | 7.100e-12 | 2.134e-12 |
| 55.292 | 5.22 | -151.11 | 6.543e-12 | 1.710e-12 |
| 54.927 | 3.87 | -150.62 | 1.017e-11 | 2.660e-12 |
| 54.792 | 3.26 | -150.40 | 6.495e-12 | 2.712e-12 |
| 54.281 | 0.82 | -149.42 | 7.428e-12 | 2.307e-12 |
| 54.135 | 0.13 | -149.21 | 1.047e-11 | 2.760e-12 |
| 53.917 | -0.92 | -148.84 | 5.258e-12 | 1.811e-12 |
| 53.792 | -1.52 | -148.68 | 6.108e-12 | 1.838e-12 |
| 53.333 | -3.51 | -147.79 | 3.476e-12 | 1.504e-12 |
| 52.365 | -8.05 | -145.86 | 6.528e-12 | 1.899e-12 |
| 51.958 | -10.00 | -145.03 | 6.802e-12 | 1.890e-12 |
| 51.802 | -9.64 | -145.07 | 1.414e-12 | 6.846e-13 |
| 51.229 | -6.97 | -144.99 | 7.267e-12 | 1.909e-12 |
| 51.167 | -6.73 | -145.02 | 7.690e-12 | 1.903e-12 |
| 50.927 | -5.89 | -145.00 | 8.215e-12 | 1.663e-12 |
| 49.917 | -0.88 | -144.95 | 8.392e-12 | 1.545e-12 |
| 49.781 | -0.10 | -144.97 | 4.889e-12 | 1.326e-12 |
| 48.865 | 3.69 | -145.05 | 1.079e-11 | 2.859e-12 |
| 47.917 | 7.67 | -144.03 | 2.433e-11 | 3.465e-12 |
| 47.792 | 8.40 | -144.05 | 1.476e-11 | 2.923e-12 |
| 47.042 | 11.14 | -145.66 | 1.761e-11 | 3.175e-12 |
| 46.875 | 11.97 | -146.22 | 1.856e-11 | 3.442e-12 |
| 46.802 | 12.24 | -146.40 | 1.664e-11 | 3.515e-12 |
| 45.896 | 15.86 | -148.71 | 4.814e-11 | 6.447e-12 |
| 45.708 | 16.30 | -149.31 | 6.653e-11 | 6.541e-12 |
| 45.271 | 17.45 | -151.09 | 3.467e-15 | 7.340e-13 |
| 2-methyl-propane | | | | |
| JD | lat | lon | Chi | dChi |

| | | | | |
|--------|--------|---------|-----------|-----------|
| 70.323 | -11.29 | -166.71 | 1.726e-11 | 1.634e-12 |
| 69.854 | -10.35 | -165.48 | 1.765e-11 | 1.404e-12 |
| 69.323 | -8.03 | -165.07 | 1.502e-11 | 1.326e-12 |
| 68.844 | -5.78 | -165.00 | 1.374e-11 | 1.125e-12 |
| 67.312 | 0.95 | -165.00 | 1.630e-11 | 1.451e-12 |
| 67.115 | 1.88 | -165.00 | 4.353e-11 | 3.018e-12 |
| 66.844 | 3.15 | -165.00 | 1.389e-11 | 9.224e-13 |
| 66.083 | 6.68 | -165.00 | 4.471e-11 | 2.339e-12 |
| 65.812 | 7.93 | -165.00 | 1.473e-11 | 1.113e-12 |
| 65.125 | 9.20 | -164.48 | 1.188e-10 | 4.032e-12 |
| 64.833 | 8.05 | -163.72 | 0.000e+00 | 0.000e+00 |
| 64.302 | 5.92 | -162.33 | 4.287e-11 | 1.922e-12 |
| 64.083 | 5.01 | -161.76 | 4.954e-11 | 2.369e-12 |
| 63.802 | 3.87 | -161.04 | 9.629e-12 | 8.566e-13 |
| 63.125 | 1.12 | -159.15 | 4.714e-11 | 1.744e-12 |
| 62.792 | -0.39 | -158.22 | 3.168e-12 | 5.444e-13 |
| 62.417 | -1.93 | -157.13 | 3.515e-11 | 3.669e-12 |
| 62.208 | -2.86 | -156.54 | 3.733e-11 | 2.659e-12 |
| 62.021 | -3.69 | -155.96 | 2.515e-11 | 2.858e-12 |
| 61.854 | -4.37 | -155.50 | 2.066e-12 | 9.004e-13 |
| 61.062 | -1.78 | -154.99 | 4.214e-11 | 3.873e-12 |
| 60.802 | -0.53 | -155.00 | 2.082e-11 | 1.690e-12 |
| 60.208 | 2.22 | -154.98 | 3.418e-11 | 3.123e-12 |
| 60.052 | 3.13 | -154.97 | 2.843e-11 | 2.155e-12 |
| 59.927 | 3.57 | -155.02 | 3.233e-11 | 2.942e-12 |
| 59.792 | 4.37 | -155.00 | 2.385e-11 | 2.195e-12 |
| 59.240 | 6.68 | -155.00 | 2.170e-11 | 2.088e-12 |
| 58.948 | 7.99 | -155.00 | 3.800e-11 | 1.998e-12 |
| 58.792 | 8.88 | -154.98 | 2.170e-11 | 1.936e-12 |
| 58.312 | 11.12 | -155.01 | 5.056e-11 | 2.184e-12 |
| 58.177 | 11.77 | -154.99 | 4.798e-11 | 2.325e-12 |
| 58.052 | 12.32 | -154.98 | 5.443e-11 | 2.958e-12 |
| 57.917 | 12.90 | -154.98 | 4.917e-11 | 3.035e-12 |
| 57.792 | 13.47 | -154.99 | 2.101e-11 | 2.288e-12 |
| 57.312 | 14.43 | -154.79 | 0.000e+00 | 3.361e-13 |
| 57.188 | 13.85 | -154.56 | 1.588e-11 | 1.924e-12 |
| 56.938 | 12.66 | -154.11 | 4.851e-11 | 2.377e-12 |
| 56.812 | 12.07 | -153.88 | 2.992e-11 | 4.617e-12 |
| 56.208 | 9.33 | -152.69 | 5.049e-11 | 2.925e-12 |
| 56.042 | 8.59 | -152.36 | 4.965e-11 | 3.679e-12 |
| 55.833 | 7.69 | -151.96 | 3.500e-11 | 4.073e-12 |
| 55.292 | 5.22 | -151.11 | 4.046e-11 | 3.451e-12 |
| 54.927 | 3.87 | -150.62 | 3.900e-11 | 4.913e-12 |
| 54.792 | 3.26 | -150.40 | 1.780e-11 | 3.646e-12 |
| 54.281 | 0.82 | -149.42 | 2.074e-11 | 2.174e-12 |
| 54.135 | 0.13 | -149.21 | 3.537e-11 | 3.612e-12 |
| 53.917 | -0.92 | -148.84 | 1.487e-11 | 2.035e-12 |
| 53.792 | -1.52 | -148.68 | 2.234e-11 | 3.275e-12 |
| 53.333 | -3.51 | -147.79 | 1.415e-11 | 4.947e-12 |
| 52.365 | -8.05 | -145.86 | 2.344e-11 | 2.862e-12 |
| 51.958 | -10.00 | -145.03 | 2.541e-11 | 2.699e-12 |
| 51.802 | -9.64 | -145.07 | 1.526e-11 | 1.822e-12 |
| 51.229 | -6.97 | -144.99 | 3.231e-11 | 3.870e-12 |
| 51.167 | -6.73 | -145.02 | 3.374e-11 | 3.164e-12 |
| 50.927 | -5.89 | -145.00 | 3.636e-11 | 3.538e-12 |

| | | | | |
|--------|-------|---------|-----------|-----------|
| 49.917 | -0.88 | -144.95 | 2.824e-11 | 2.564e-12 |
| 49.781 | -0.10 | -144.97 | 2.321e-11 | 2.716e-12 |
| 48.865 | 3.69 | -145.05 | 8.634e-11 | 7.087e-12 |
| 47.917 | 7.67 | -144.03 | 7.750e-11 | 6.164e-12 |
| 47.792 | 8.40 | -144.05 | 1.115e-10 | 8.142e-12 |
| 47.042 | 11.14 | -145.66 | 1.254e-10 | 7.221e-12 |
| 46.875 | 11.97 | -146.22 | 6.540e-11 | 4.555e-12 |
| 46.802 | 12.24 | -146.40 | 5.797e-11 | 4.246e-12 |
| 45.896 | 15.86 | -148.71 | 8.453e-13 | 6.939e-13 |
| 45.708 | 16.30 | -149.31 | 0.000e+00 | 4.364e-13 |
| 45.271 | 17.45 | -151.09 | 1.422e-10 | 9.406e-12 |

trans-2-butene

| JD | lat | lon | Chi | dChi |
|--------|--------|---------|-----------|-----------|
| 70.323 | -11.29 | -166.71 | 3.190e-12 | 4.991e-13 |
| 69.854 | -10.35 | -165.48 | 4.976e-12 | 8.203e-13 |
| 69.323 | -8.03 | -165.07 | 4.182e-12 | 6.523e-13 |
| 68.844 | -5.78 | -165.00 | 4.213e-12 | 7.426e-13 |
| 67.312 | 0.95 | -165.00 | 3.777e-12 | 6.127e-13 |
| 67.115 | 1.88 | -165.00 | 3.488e-12 | 5.353e-13 |
| 66.844 | 3.15 | -165.00 | 3.281e-12 | 5.002e-13 |
| 66.083 | 6.68 | -165.00 | 2.557e-12 | 5.161e-13 |
| 65.812 | 7.93 | -165.00 | 4.303e-12 | 7.994e-13 |
| 65.125 | 9.20 | -164.48 | 3.341e-12 | 6.543e-13 |
| 64.833 | 8.05 | -163.72 | 5.049e-12 | 8.586e-13 |
| 64.302 | 5.92 | -162.33 | 4.449e-12 | 7.010e-13 |
| 64.083 | 5.01 | -161.76 | 5.061e-12 | 7.691e-13 |
| 63.802 | 3.87 | -161.04 | 3.084e-12 | 5.847e-13 |
| 63.125 | 1.12 | -159.15 | 4.174e-12 | 6.962e-13 |
| 62.792 | -0.39 | -158.22 | 4.084e-12 | 6.485e-13 |
| 62.417 | -1.93 | -157.13 | 2.247e-12 | 9.016e-13 |
| 62.208 | -2.86 | -156.54 | 1.747e-12 | 8.130e-13 |
| 62.021 | -3.69 | -155.96 | 0.000e+00 | 4.430e-13 |
| 61.854 | -4.37 | -155.50 | 4.112e-12 | 1.475e-12 |
| 61.062 | -1.78 | -154.99 | 4.356e-12 | 1.626e-12 |
| 60.802 | -0.53 | -155.00 | 3.153e-12 | 1.239e-12 |
| 60.208 | 2.22 | -154.98 | 1.905e-12 | 9.655e-13 |
| 60.052 | 3.13 | -154.97 | 4.996e-12 | 1.706e-12 |
| 59.927 | 3.57 | -155.02 | 5.493e-12 | 1.789e-12 |
| 59.792 | 4.37 | -155.00 | 6.257e-12 | 1.732e-12 |
| 59.240 | 6.68 | -155.00 | 3.142e-12 | 1.011e-12 |
| 58.948 | 7.99 | -155.00 | 0.000e+00 | 3.402e-13 |
| 58.792 | 8.88 | -154.98 | 1.503e-12 | 7.254e-13 |
| 58.312 | 11.12 | -155.01 | 1.968e-13 | 3.704e-13 |
| 58.177 | 11.77 | -154.99 | 0.000e+00 | 3.339e-13 |
| 58.052 | 12.32 | -154.98 | 2.140e-12 | 8.928e-13 |
| 57.917 | 12.90 | -154.98 | 1.718e-13 | 3.661e-13 |
| 57.792 | 13.47 | -154.99 | 1.879e-12 | 7.992e-13 |
| 57.312 | 14.43 | -154.79 | 1.767e-12 | 8.489e-13 |
| 57.188 | 13.85 | -154.56 | 3.203e-12 | 1.165e-12 |
| 56.938 | 12.66 | -154.11 | 9.951e-13 | 4.922e-13 |
| 56.812 | 12.07 | -153.88 | 0.000e+00 | 5.505e-13 |
| 56.208 | 9.33 | -152.69 | 3.706e-12 | 1.021e-12 |
| 56.042 | 8.59 | -152.36 | 1.580e-12 | 7.057e-13 |
| 55.833 | 7.69 | -151.96 | 3.465e-12 | 1.621e-12 |
| 55.292 | 5.22 | -151.11 | 4.040e-12 | 1.217e-12 |

| | | | | |
|--------|--------|---------|-----------|-----------|
| 54.927 | 3.87 | -150.62 | 3.277e-12 | 1.578e-12 |
| 54.792 | 3.26 | -150.40 | 1.751e-12 | 8.859e-13 |
| 54.281 | 0.82 | -149.42 | 1.841e-13 | 6.073e-13 |
| 54.135 | 0.13 | -149.21 | 2.701e-12 | 1.353e-12 |
| 53.917 | -0.92 | -148.84 | 3.068e-12 | 1.531e-12 |
| 53.792 | -1.52 | -148.68 | 2.577e-12 | 1.089e-12 |
| 53.333 | -3.51 | -147.79 | 9.024e-13 | 9.507e-13 |
| 52.365 | -8.05 | -145.86 | 4.332e-12 | 1.494e-12 |
| 51.958 | -10.00 | -145.03 | 3.338e-12 | 1.344e-12 |
| 51.802 | -9.64 | -145.07 | 3.722e-12 | 1.616e-12 |
| 51.229 | -6.97 | -144.99 | 7.177e-12 | 2.266e-12 |
| 51.167 | -6.73 | -145.02 | 4.306e-12 | 1.395e-12 |
| 50.927 | -5.89 | -145.00 | 8.066e-12 | 2.063e-12 |
| 49.917 | -0.88 | -144.95 | 0.000e+00 | 4.131e-13 |
| 49.781 | -0.10 | -144.97 | 4.512e-12 | 1.433e-12 |
| 48.865 | 3.69 | -145.05 | 8.626e-12 | 2.206e-12 |
| 47.917 | 7.67 | -144.03 | 1.292e-11 | 3.298e-12 |
| 47.792 | 8.40 | -144.05 | 7.622e-12 | 2.160e-12 |
| 47.042 | 11.14 | -145.66 | 1.465e-11 | 2.871e-12 |
| 46.875 | 11.97 | -146.22 | 1.450e-11 | 3.166e-12 |
| 46.802 | 12.24 | -146.40 | 1.066e-11 | 3.107e-12 |
| 45.896 | 15.86 | -148.71 | 0.000e+00 | 9.466e-13 |
| 45.708 | 16.30 | -149.31 | 4.486e-12 | 1.915e-12 |
| 45.271 | 17.45 | -151.09 | 2.439e-12 | 1.249e-12 |

1-butene

| JD | lat | lon | Chi | dChi |
|--------|--------|---------|-----------|-----------|
| 70.323 | -11.29 | -166.71 | 4.660e-12 | 6.621e-13 |
| 69.854 | -10.35 | -165.48 | 5.885e-12 | 9.137e-13 |
| 69.323 | -8.03 | -165.07 | 4.955e-12 | 7.468e-13 |
| 68.844 | -5.78 | -165.00 | 4.340e-12 | 6.840e-13 |
| 67.312 | 0.95 | -165.00 | 4.808e-12 | 8.153e-13 |
| 67.115 | 1.88 | -165.00 | 5.309e-12 | 9.216e-13 |
| 66.844 | 3.15 | -165.00 | 4.346e-12 | 6.670e-13 |
| 66.083 | 6.68 | -165.00 | 3.430e-12 | 6.171e-13 |
| 65.812 | 7.93 | -165.00 | 6.514e-12 | 1.080e-12 |
| 65.125 | 9.20 | -164.48 | 4.587e-12 | 8.680e-13 |
| 64.833 | 8.05 | -163.72 | 6.353e-12 | 1.138e-12 |
| 64.302 | 5.92 | -162.33 | 5.849e-12 | 8.895e-13 |
| 64.083 | 5.01 | -161.76 | 5.186e-12 | 8.451e-13 |
| 63.802 | 3.87 | -161.04 | 4.913e-12 | 8.865e-13 |
| 63.125 | 1.12 | -159.15 | 5.526e-12 | 9.048e-13 |
| 62.792 | -0.39 | -158.22 | 4.438e-12 | 6.514e-13 |
| 62.417 | -1.93 | -157.13 | 2.128e-12 | 7.860e-13 |
| 62.208 | -2.86 | -156.54 | 4.910e-12 | 1.269e-12 |
| 62.021 | -3.69 | -155.96 | 6.470e-12 | 1.619e-12 |
| 61.854 | -4.37 | -155.50 | 4.598e-12 | 1.300e-12 |
| 61.062 | -1.78 | -154.99 | 6.713e-12 | 2.072e-12 |
| 60.802 | -0.53 | -155.00 | 5.208e-12 | 1.592e-12 |
| 60.208 | 2.22 | -154.98 | 3.456e-12 | 1.274e-12 |
| 60.052 | 3.13 | -154.97 | 5.112e-12 | 1.644e-12 |
| 59.927 | 3.57 | -155.02 | 5.341e-12 | 1.523e-12 |
| 59.792 | 4.37 | -155.00 | 6.206e-12 | 1.580e-12 |
| 59.240 | 6.68 | -155.00 | 0.000e+00 | 2.947e-13 |
| 58.948 | 7.99 | -155.00 | 2.514e-12 | 8.498e-13 |
| 58.792 | 8.88 | -154.98 | 1.570e-12 | 6.387e-13 |

| | | | | |
|--------------|--------|---------|-----------|-----------|
| 58.312 | 11.12 | -155.01 | 2.044e-12 | 8.342e-13 |
| 58.177 | 11.77 | -154.99 | 2.597e-12 | 8.069e-13 |
| 58.052 | 12.32 | -154.98 | 1.051e-12 | 5.396e-13 |
| 57.917 | 12.90 | -154.98 | 1.536e-12 | 6.366e-13 |
| 57.792 | 13.47 | -154.99 | 1.040e-12 | 4.814e-13 |
| 57.312 | 14.43 | -154.79 | 0.000e+00 | 3.936e-13 |
| 57.188 | 13.85 | -154.56 | 3.372e-12 | 1.316e-12 |
| 56.938 | 12.66 | -154.11 | 4.906e-12 | 9.154e-13 |
| 56.812 | 12.07 | -153.88 | 3.573e-12 | 1.237e-12 |
| 56.208 | 9.33 | -152.69 | 5.779e-12 | 1.217e-12 |
| 56.042 | 8.59 | -152.36 | 3.897e-12 | 1.063e-12 |
| 55.833 | 7.69 | -151.96 | 2.660e-12 | 1.147e-12 |
| 55.292 | 5.22 | -151.11 | 2.592e-12 | 1.018e-12 |
| 54.927 | 3.87 | -150.62 | 4.973e-12 | 1.602e-12 |
| 54.792 | 3.26 | -150.40 | 3.629e-15 | 7.356e-13 |
| 54.281 | 0.82 | -149.42 | 1.967e-12 | 9.355e-13 |
| 54.135 | 0.13 | -149.21 | 3.900e-12 | 1.655e-12 |
| 53.917 | -0.92 | -148.84 | 3.179e-12 | 1.180e-12 |
| 53.792 | -1.52 | -148.68 | 3.030e-15 | 5.299e-13 |
| 53.333 | -3.51 | -147.79 | 3.030e-15 | 8.169e-13 |
| 52.365 | -8.05 | -145.86 | 4.224e-12 | 1.292e-12 |
| 51.958 | -10.00 | -145.03 | 2.780e-12 | 1.038e-12 |
| 51.802 | -9.64 | -145.07 | 3.036e-12 | 1.035e-12 |
| 51.229 | -6.97 | -144.99 | 5.609e-12 | 1.793e-12 |
| 51.167 | -6.73 | -145.02 | 7.518e-13 | 4.246e-13 |
| 50.927 | -5.89 | -145.00 | 7.043e-12 | 1.734e-12 |
| 49.917 | -0.88 | -144.95 | 0.000e+00 | 3.478e-13 |
| 49.781 | -0.10 | -144.97 | 2.101e-12 | 8.660e-13 |
| 48.865 | 3.69 | -145.05 | 1.008e-11 | 2.181e-12 |
| 47.917 | 7.67 | -144.03 | 1.576e-11 | 3.349e-12 |
| 47.792 | 8.40 | -144.05 | 1.236e-11 | 2.731e-12 |
| 47.042 | 11.14 | -145.66 | 1.674e-11 | 2.871e-12 |
| 46.875 | 11.97 | -146.22 | 1.321e-11 | 2.791e-12 |
| 46.802 | 12.24 | -146.40 | 1.492e-11 | 3.077e-12 |
| 45.896 | 15.86 | -148.71 | 1.489e-11 | 3.336e-12 |
| 45.708 | 16.30 | -149.31 | 1.473e-11 | 3.015e-12 |
| 45.271 | 17.45 | -151.09 | 0.000e+00 | 7.268e-13 |
| cis-2-butene | | | | |
| JD | lat | lon | Chi | dChi |
| 70.323 | -11.29 | -166.71 | 7.768e-13 | 3.283e-13 |
| 69.854 | -10.35 | -165.48 | 1.213e-12 | 4.023e-13 |
| 69.323 | -8.03 | -165.07 | 9.769e-13 | 3.439e-13 |
| 68.844 | -5.78 | -165.00 | 5.308e-13 | 2.365e-13 |
| 67.312 | 0.95 | -165.00 | 1.013e-12 | 2.899e-13 |
| 67.115 | 1.88 | -165.00 | 1.096e-12 | 3.831e-13 |
| 66.844 | 3.15 | -165.00 | 5.901e-13 | 2.937e-13 |
| 66.083 | 6.68 | -165.00 | 1.463e-12 | 5.528e-13 |
| 65.812 | 7.93 | -165.00 | 1.373e-12 | 4.635e-13 |
| 65.125 | 9.20 | -164.48 | 1.637e-12 | 6.783e-13 |
| 64.833 | 8.05 | -163.72 | 1.411e-12 | 5.315e-13 |
| 64.302 | 5.92 | -162.33 | 1.074e-12 | 4.244e-13 |
| 64.083 | 5.01 | -161.76 | 1.134e-12 | 4.657e-13 |
| 63.802 | 3.87 | -161.04 | 1.059e-12 | 3.929e-13 |
| 63.125 | 1.12 | -159.15 | 8.487e-13 | 3.714e-13 |
| 62.792 | -0.39 | -158.22 | 6.173e-13 | 2.752e-13 |

| | | | | |
|---------|--------|---------|-----------|-----------|
| 62.417 | -1.93 | -157.13 | 4.519e-13 | 3.999e-13 |
| 62.208 | -2.86 | -156.54 | 1.187e-12 | 5.866e-13 |
| 62.021 | -3.69 | -155.96 | 1.325e-12 | 6.756e-13 |
| 61.854 | -4.37 | -155.50 | 8.601e-13 | 4.383e-13 |
| 61.062 | -1.78 | -154.99 | 1.330e-12 | 6.711e-13 |
| 60.802 | -0.53 | -155.00 | 1.170e-12 | 5.931e-13 |
| 60.208 | 2.22 | -154.98 | 0.000e+00 | 3.806e-13 |
| 60.052 | 3.13 | -154.97 | 1.196e-12 | 6.031e-13 |
| 59.927 | 3.57 | -155.02 | 1.668e-12 | 7.057e-13 |
| 59.792 | 4.37 | -155.00 | 8.950e-13 | 5.202e-13 |
| 59.240 | 6.68 | -155.00 | 1.294e-13 | 3.299e-13 |
| 58.948 | 7.99 | -155.00 | 1.146e-13 | 3.299e-13 |
| 58.792 | 8.88 | -154.98 | 3.701e-13 | 3.440e-13 |
| 58.312 | 11.12 | -155.01 | 2.895e-13 | 3.483e-13 |
| 58.177 | 11.77 | -154.99 | 0.000e+00 | 3.141e-13 |
| 58.052 | 12.32 | -154.98 | 0.000e+00 | 3.650e-13 |
| 57.917 | 12.90 | -154.98 | 7.329e-15 | 3.441e-13 |
| 57.792 | 13.47 | -154.99 | 4.060e-13 | 4.580e-13 |
| 57.312 | 14.43 | -154.79 | 3.593e-15 | 4.330e-13 |
| 57.188 | 13.85 | -154.56 | 2.533e-12 | 1.107e-12 |
| 56.938 | 12.66 | -154.11 | 3.614e-15 | 3.477e-13 |
| 56.812 | 12.07 | -153.88 | 0.000e+00 | 5.148e-13 |
| 56.208 | 9.33 | -152.69 | 1.423e-12 | 7.124e-13 |
| 56.042 | 8.59 | -152.36 | 1.575e-12 | 7.377e-13 |
| 55.833 | 7.69 | -151.96 | 3.295e-13 | 6.793e-13 |
| 55.292 | 5.22 | -151.11 | 3.173e-13 | 4.864e-13 |
| 54.927 | 3.87 | -150.62 | 6.256e-12 | 2.615e-12 |
| 54.792 | 3.26 | -150.40 | 2.676e-12 | 1.315e-12 |
| 54.281 | 0.82 | -149.42 | 4.025e-12 | 1.554e-12 |
| 54.135 | 0.13 | -149.21 | 9.512e-13 | 6.596e-13 |
| 53.917 | -0.92 | -148.84 | 2.456e-12 | 1.216e-12 |
| 53.792 | -1.52 | -148.68 | 2.055e-12 | 1.048e-12 |
| 53.333 | -3.51 | -147.79 | 3.147e-15 | 8.824e-13 |
| 52.365 | -8.05 | -145.86 | 1.249e-12 | 5.274e-13 |
| 51.958 | -10.00 | -145.03 | 1.881e-12 | 9.311e-13 |
| 51.802 | -9.64 | -145.07 | 2.127e-13 | 4.685e-13 |
| 51.229 | -6.97 | -144.99 | 4.530e-13 | 6.292e-13 |
| 51.167 | -6.73 | -145.02 | 1.707e-12 | 8.234e-13 |
| 50.927 | -5.89 | -145.00 | 2.920e-12 | 1.261e-12 |
| 49.917 | -0.88 | -144.95 | 1.333e-12 | 6.502e-13 |
| 49.781 | -0.10 | -144.97 | 1.978e-12 | 9.251e-13 |
| 48.865 | 3.69 | -145.05 | 5.072e-12 | 1.684e-12 |
| 47.917 | 7.67 | -144.03 | 5.091e-12 | 1.910e-12 |
| 47.792 | 8.40 | -144.05 | 0.000e+00 | 5.527e-13 |
| 47.042 | 11.14 | -145.66 | 7.103e-12 | 2.443e-12 |
| 46.875 | 11.97 | -146.22 | 7.802e-12 | 2.502e-12 |
| 46.802 | 12.24 | -146.40 | 4.889e-12 | 2.116e-12 |
| 45.896 | 15.86 | -148.71 | 1.102e-11 | 3.141e-12 |
| 45.708 | 16.30 | -149.31 | 1.200e-12 | 5.390e-13 |
| 45.271 | 17.45 | -151.09 | 7.631e-13 | 7.579e-13 |
| pentane | | | | |
| JD | lat | lon | Chi | dChi |
| 70.323 | -11.29 | -166.71 | 1.714e-11 | 9.775e-13 |
| 69.854 | -10.35 | -165.48 | 2.102e-11 | 1.203e-12 |
| 69.323 | -8.03 | -165.07 | 1.910e-11 | 1.039e-12 |

| | | | | |
|--------|--------|---------|-----------|-----------|
| 68.844 | -5.78 | -165.00 | 1.675e-11 | 8.486e-13 |
| 67.312 | 0.95 | -165.00 | 1.971e-11 | 1.128e-12 |
| 67.115 | 1.88 | -165.00 | 1.958e-11 | 1.130e-12 |
| 66.844 | 3.15 | -165.00 | 1.931e-11 | 1.216e-12 |
| 66.083 | 6.68 | -165.00 | 1.947e-11 | 1.350e-12 |
| 65.812 | 7.93 | -165.00 | 2.728e-11 | 1.597e-12 |
| 65.125 | 9.20 | -164.48 | 2.410e-11 | 1.448e-12 |
| 64.833 | 8.05 | -163.72 | 2.252e-11 | 1.253e-12 |
| 64.302 | 5.92 | -162.33 | 2.238e-11 | 1.471e-12 |
| 64.083 | 5.01 | -161.76 | 2.143e-11 | 1.643e-12 |
| 63.802 | 3.87 | -161.04 | 2.170e-11 | 1.261e-12 |
| 63.125 | 1.12 | -159.15 | 2.209e-11 | 1.230e-12 |
| 62.792 | -0.39 | -158.22 | 1.853e-11 | 1.089e-12 |
| 62.417 | -1.93 | -157.13 | 2.134e-11 | 2.571e-12 |
| 62.208 | -2.86 | -156.54 | 2.126e-11 | 2.295e-12 |
| 62.021 | -3.69 | -155.96 | 2.316e-11 | 2.198e-12 |
| 61.854 | -4.37 | -155.50 | 2.351e-11 | 2.398e-12 |
| 61.062 | -1.78 | -154.99 | 3.176e-11 | 4.278e-12 |
| 60.802 | -0.53 | -155.00 | 2.607e-11 | 3.698e-12 |
| 60.208 | 2.22 | -154.98 | 1.786e-11 | 2.546e-12 |
| 60.052 | 3.13 | -154.97 | 2.711e-11 | 3.850e-12 |
| 59.927 | 3.57 | -155.02 | 2.205e-11 | 3.414e-12 |
| 59.792 | 4.37 | -155.00 | 2.759e-11 | 3.785e-12 |
| 59.240 | 6.68 | -155.00 | 1.075e-11 | 1.702e-12 |
| 58.948 | 7.99 | -155.00 | 1.285e-11 | 2.161e-12 |
| 58.792 | 8.88 | -154.98 | 9.241e-12 | 1.858e-12 |
| 58.312 | 11.12 | -155.01 | 7.974e-12 | 1.785e-12 |
| 58.177 | 11.77 | -154.99 | 6.782e-12 | 1.472e-12 |
| 58.052 | 12.32 | -154.98 | 8.761e-12 | 1.660e-12 |
| 57.917 | 12.90 | -154.98 | 7.505e-12 | 1.428e-12 |
| 57.792 | 13.47 | -154.99 | 8.104e-12 | 1.903e-12 |
| 57.312 | 14.43 | -154.79 | 0.000e+00 | 4.385e-13 |
| 57.188 | 13.85 | -154.56 | 1.177e-11 | 2.429e-12 |
| 56.938 | 12.66 | -154.11 | 7.522e-12 | 1.247e-12 |
| 56.812 | 12.07 | -153.88 | 6.306e-12 | 1.715e-12 |
| 56.208 | 9.33 | -152.69 | 1.116e-11 | 1.557e-12 |
| 56.042 | 8.59 | -152.36 | 1.207e-11 | 2.016e-12 |
| 55.833 | 7.69 | -151.96 | 1.348e-11 | 2.796e-12 |
| 55.292 | 5.22 | -151.11 | 1.026e-11 | 1.465e-12 |
| 54.927 | 3.87 | -150.62 | 1.189e-11 | 2.607e-12 |
| 54.792 | 3.26 | -150.40 | 9.590e-12 | 2.952e-12 |
| 54.281 | 0.82 | -149.42 | 1.193e-11 | 2.804e-12 |
| 54.135 | 0.13 | -149.21 | 1.091e-11 | 3.014e-12 |
| 53.917 | -0.92 | -148.84 | 9.696e-12 | 2.352e-12 |
| 53.792 | -1.52 | -148.68 | 4.148e-12 | 1.243e-12 |
| 53.333 | -3.51 | -147.79 | 6.136e-12 | 2.359e-12 |
| 52.365 | -8.05 | -145.86 | 7.366e-12 | 1.774e-12 |
| 51.958 | -10.00 | -145.03 | 1.171e-11 | 2.017e-12 |
| 51.802 | -9.64 | -145.07 | 9.370e-12 | 2.261e-12 |
| 51.229 | -6.97 | -144.99 | 1.195e-11 | 2.720e-12 |
| 51.167 | -6.73 | -145.02 | 1.114e-11 | 1.962e-12 |
| 50.927 | -5.89 | -145.00 | 1.295e-11 | 2.156e-12 |
| 49.917 | -0.88 | -144.95 | 1.566e-11 | 2.621e-12 |
| 49.781 | -0.10 | -144.97 | 1.003e-11 | 1.849e-12 |
| 48.865 | 3.69 | -145.05 | 2.270e-11 | 3.761e-12 |

| | | | | |
|--------|-------|---------|-----------|-----------|
| 47.917 | 7.67 | -144.03 | 5.323e-11 | 6.672e-12 |
| 47.792 | 8.40 | -144.05 | 2.748e-11 | 3.952e-12 |
| 47.042 | 11.14 | -145.66 | 2.589e-11 | 4.837e-12 |
| 46.875 | 11.97 | -146.22 | 2.986e-11 | 4.711e-12 |
| 46.802 | 12.24 | -146.40 | 2.767e-11 | 4.150e-12 |
| 45.896 | 15.86 | -148.71 | 3.338e-11 | 4.601e-12 |
| 45.708 | 16.30 | -149.31 | 6.136e-11 | 4.139e-12 |
| 45.271 | 17.45 | -151.09 | 3.714e-11 | 4.003e-12 |

2-methyl-butane

| JD | lat | lon | Chi | dChi |
|--------|--------|---------|-----------|-----------|
| 70.323 | -11.29 | -166.71 | 3.133e-12 | 5.180e-13 |
| 69.854 | -10.35 | -165.48 | 3.774e-12 | 6.951e-13 |
| 69.323 | -8.03 | -165.07 | 4.282e-12 | 7.169e-13 |
| 68.844 | -5.78 | -165.00 | 3.107e-12 | 5.589e-13 |
| 67.312 | 0.95 | -165.00 | 3.984e-12 | 6.104e-13 |
| 67.115 | 1.88 | -165.00 | 4.158e-12 | 7.290e-13 |
| 66.844 | 3.15 | -165.00 | 3.911e-12 | 7.203e-13 |
| 66.083 | 6.68 | -165.00 | 4.758e-12 | 7.068e-13 |
| 65.812 | 7.93 | -165.00 | 9.891e-12 | 1.194e-12 |
| 65.125 | 9.20 | -164.48 | 8.548e-12 | 1.296e-12 |
| 64.833 | 8.05 | -163.72 | 5.470e-12 | 9.363e-13 |
| 64.302 | 5.92 | -162.33 | 4.048e-12 | 8.040e-13 |
| 64.083 | 5.01 | -161.76 | 3.854e-12 | 8.152e-13 |
| 63.802 | 3.87 | -161.04 | 3.843e-12 | 7.830e-13 |
| 63.125 | 1.12 | -159.15 | 3.777e-12 | 8.198e-13 |
| 62.792 | -0.39 | -158.22 | 3.741e-12 | 6.994e-13 |
| 62.417 | -1.93 | -157.13 | 4.108e-12 | 1.185e-12 |
| 62.208 | -2.86 | -156.54 | 3.867e-12 | 1.393e-12 |
| 62.021 | -3.69 | -155.96 | 3.422e-12 | 1.327e-12 |
| 61.854 | -4.37 | -155.50 | 3.406e-12 | 1.183e-12 |
| 61.062 | -1.78 | -154.99 | 3.165e-12 | 1.148e-12 |
| 60.802 | -0.53 | -155.00 | 1.635e-12 | 7.279e-13 |
| 60.208 | 2.22 | -154.98 | 4.991e-12 | 1.407e-12 |
| 60.052 | 3.13 | -154.97 | 6.323e-12 | 1.655e-12 |
| 59.927 | 3.57 | -155.02 | 4.708e-12 | 1.580e-12 |
| 59.792 | 4.37 | -155.00 | 4.899e-12 | 1.429e-12 |
| 59.240 | 6.68 | -155.00 | 1.164e-12 | 4.823e-13 |
| 58.948 | 7.99 | -155.00 | 5.416e-13 | 2.274e-13 |
| 58.792 | 8.88 | -154.98 | 2.530e-12 | 8.028e-13 |
| 58.312 | 11.12 | -155.01 | 0.000e+00 | 3.546e-13 |
| 58.177 | 11.77 | -154.99 | 1.141e-12 | 4.888e-13 |
| 58.052 | 12.32 | -154.98 | 6.542e-12 | 1.586e-12 |
| 57.917 | 12.90 | -154.98 | 1.401e-12 | 5.058e-13 |
| 57.792 | 13.47 | -154.99 | 0.000e+00 | 4.862e-13 |
| 57.312 | 14.43 | -154.79 | 0.000e+00 | 4.598e-13 |
| 57.188 | 13.85 | -154.56 | 3.988e-12 | 1.298e-12 |
| 56.938 | 12.66 | -154.11 | 3.038e-12 | 1.041e-12 |
| 56.812 | 12.07 | -153.88 | 1.995e-12 | 9.222e-13 |
| 56.208 | 9.33 | -152.69 | 3.765e-12 | 1.016e-12 |
| 56.042 | 8.59 | -152.36 | 1.372e-12 | 6.205e-13 |
| 55.833 | 7.69 | -151.96 | 1.862e-12 | 9.061e-13 |
| 55.292 | 5.22 | -151.11 | 5.642e-12 | 1.848e-12 |
| 54.927 | 3.87 | -150.62 | 4.060e-12 | 1.882e-12 |
| 54.792 | 3.26 | -150.40 | 0.000e+00 | 7.971e-13 |
| 54.281 | 0.82 | -149.42 | 1.443e-12 | 6.642e-13 |

| | | | | |
|--------|--------|---------|-----------|-----------|
| 54.135 | 0.13 | -149.21 | 4.832e-12 | 1.942e-12 |
| 53.917 | -0.92 | -148.84 | 0.000e+00 | 6.690e-13 |
| 53.792 | -1.52 | -148.68 | 3.162e-12 | 1.398e-12 |
| 53.333 | -3.51 | -147.79 | 3.524e-12 | 1.635e-12 |
| 52.365 | -8.05 | -145.86 | 4.758e-12 | 1.842e-12 |
| 51.958 | -10.00 | -145.03 | 4.535e-12 | 1.616e-12 |
| 51.802 | -9.64 | -145.07 | 4.888e-12 | 1.775e-12 |
| 51.229 | -6.97 | -144.99 | 5.364e-12 | 2.033e-12 |
| 51.167 | -6.73 | -145.02 | 4.078e-12 | 1.388e-12 |
| 50.927 | -5.89 | -145.00 | 6.338e-12 | 1.604e-12 |
| 49.917 | -0.88 | -144.95 | 7.558e-12 | 1.684e-12 |
| 49.781 | -0.10 | -144.97 | 5.208e-12 | 1.684e-12 |
| 48.865 | 3.69 | -145.05 | 1.022e-11 | 2.306e-12 |
| 47.917 | 7.67 | -144.03 | 2.014e-11 | 3.464e-12 |
| 47.792 | 8.40 | -144.05 | 8.044e-12 | 2.343e-12 |
| 47.042 | 11.14 | -145.66 | 1.078e-11 | 2.706e-12 |
| 46.875 | 11.97 | -146.22 | 1.198e-11 | 3.167e-12 |
| 46.802 | 12.24 | -146.40 | 1.355e-11 | 3.034e-12 |
| 45.896 | 15.86 | -148.71 | 1.463e-11 | 3.444e-12 |
| 45.708 | 16.30 | -149.31 | 2.031e-11 | 2.911e-12 |
| 45.271 | 17.45 | -151.09 | 1.511e-11 | 3.652e-12 |

cyclopentane

| JD | lat | lon | Chi | dChi |
|--------|--------|---------|-----------|-----------|
| 70.323 | -11.29 | -166.71 | 0.000e+00 | 1.196e-13 |
| 69.854 | -10.35 | -165.48 | 0.000e+00 | 1.233e-13 |
| 69.323 | -8.03 | -165.07 | 0.000e+00 | 1.173e-13 |
| 68.844 | -5.78 | -165.00 | 5.307e-13 | 2.398e-13 |
| 67.312 | 0.95 | -165.00 | 4.684e-13 | 2.085e-13 |
| 67.115 | 1.88 | -165.00 | 5.776e-14 | 1.442e-13 |
| 66.844 | 3.15 | -165.00 | 7.784e-16 | 1.290e-13 |
| 66.083 | 6.68 | -165.00 | 4.032e-13 | 1.634e-13 |
| 65.812 | 7.93 | -165.00 | 6.951e-13 | 3.306e-13 |
| 65.125 | 9.20 | -164.48 | 2.463e-13 | 1.999e-13 |
| 64.833 | 8.05 | -163.72 | 1.163e-14 | 1.838e-13 |
| 64.302 | 5.92 | -162.33 | 5.700e-13 | 2.587e-13 |
| 64.083 | 5.01 | -161.76 | 1.760e-13 | 1.774e-13 |
| 63.802 | 3.87 | -161.04 | 1.451e-13 | 1.599e-13 |
| 63.125 | 1.12 | -159.15 | 0.000e+00 | 1.599e-13 |
| 62.792 | -0.39 | -158.22 | 2.263e-14 | 1.450e-13 |
| 62.417 | -1.93 | -157.13 | 0.000e+00 | 3.952e-13 |
| 62.208 | -2.86 | -156.54 | 0.000e+00 | 4.036e-13 |
| 62.021 | -3.69 | -155.96 | 0.000e+00 | 4.645e-13 |
| 61.854 | -4.37 | -155.50 | 0.000e+00 | 4.137e-13 |
| 61.062 | -1.78 | -154.99 | 0.000e+00 | 4.520e-13 |
| 60.802 | -0.53 | -155.00 | 0.000e+00 | 3.620e-13 |
| 60.208 | 2.22 | -154.98 | 0.000e+00 | 3.486e-13 |
| 60.052 | 3.13 | -154.97 | 8.666e-13 | 3.695e-13 |
| 59.927 | 3.57 | -155.02 | 1.405e-13 | 3.651e-13 |
| 59.792 | 4.37 | -155.00 | 0.000e+00 | 3.782e-13 |
| 59.240 | 6.68 | -155.00 | 0.000e+00 | 2.699e-13 |
| 58.948 | 7.99 | -155.00 | 0.000e+00 | 2.699e-13 |
| 58.792 | 8.88 | -154.98 | 0.000e+00 | 2.867e-13 |
| 58.312 | 11.12 | -155.01 | 0.000e+00 | 2.901e-13 |
| 58.177 | 11.77 | -154.99 | 0.000e+00 | 2.618e-13 |
| 58.052 | 12.32 | -154.98 | 0.000e+00 | 3.043e-13 |

| | | | | |
|--------|--------|---------|-----------|-----------|
| 57.917 | 12.90 | -154.98 | 0.000e+00 | 2.867e-13 |
| 57.792 | 13.47 | -154.99 | 0.000e+00 | 3.836e-13 |
| 57.312 | 14.43 | -154.79 | 0.000e+00 | 3.626e-13 |
| 57.188 | 13.85 | -154.56 | 0.000e+00 | 4.079e-13 |
| 56.938 | 12.66 | -154.11 | 3.130e-13 | 1.490e-13 |
| 56.812 | 12.07 | -153.88 | 0.000e+00 | 4.357e-13 |
| 56.208 | 9.33 | -152.69 | 0.000e+00 | 2.976e-13 |
| 56.042 | 8.59 | -152.36 | 0.000e+00 | 3.436e-13 |
| 55.833 | 7.69 | -151.96 | 0.000e+00 | 5.225e-13 |
| 55.292 | 5.22 | -151.11 | 0.000e+00 | 3.738e-13 |
| 54.927 | 3.87 | -150.62 | 0.000e+00 | 4.937e-13 |
| 54.792 | 3.26 | -150.40 | 0.000e+00 | 6.526e-13 |
| 54.281 | 0.82 | -149.42 | 0.000e+00 | 4.590e-13 |
| 54.135 | 0.13 | -149.21 | 0.000e+00 | 5.645e-13 |
| 53.917 | -0.92 | -148.84 | 0.000e+00 | 5.428e-13 |
| 53.792 | -1.52 | -148.68 | 0.000e+00 | 5.192e-13 |
| 53.333 | -3.51 | -147.79 | 0.000e+00 | 8.003e-13 |
| 52.365 | -8.05 | -145.86 | 0.000e+00 | 4.730e-13 |
| 51.958 | -10.00 | -145.03 | 0.000e+00 | 5.239e-13 |
| 51.802 | -9.64 | -145.07 | 0.000e+00 | 4.211e-13 |
| 51.229 | -6.97 | -144.99 | 0.000e+00 | 5.654e-13 |
| 51.167 | -6.73 | -145.02 | 0.000e+00 | 4.086e-13 |
| 50.927 | -5.89 | -145.00 | 0.000e+00 | 4.021e-13 |
| 49.917 | -0.88 | -144.95 | 0.000e+00 | 3.454e-13 |
| 49.781 | -0.10 | -144.97 | 0.000e+00 | 3.517e-13 |
| 48.865 | 3.69 | -145.05 | 0.000e+00 | 4.429e-13 |
| 47.917 | 7.67 | -144.03 | 4.711e-13 | 6.062e-13 |
| 47.792 | 8.40 | -144.05 | 0.000e+00 | 4.741e-13 |
| 47.042 | 11.14 | -145.66 | 0.000e+00 | 6.729e-13 |
| 46.875 | 11.97 | -146.22 | 0.000e+00 | 6.660e-13 |
| 46.802 | 12.24 | -146.40 | 1.791e-12 | 7.350e-13 |
| 45.896 | 15.86 | -148.71 | 0.000e+00 | 7.385e-13 |
| 45.708 | 16.30 | -149.31 | 0.000e+00 | 4.330e-13 |
| 45.271 | 17.45 | -151.09 | 0.000e+00 | 6.170e-13 |

3-methyl-1-butene

| JD | lat | lon | Chi | dChi |
|--------|--------|---------|-----------|-----------|
| 70.323 | -11.29 | -166.71 | 4.690e-12 | 6.263e-13 |
| 69.854 | -10.35 | -165.48 | 5.653e-12 | 6.539e-13 |
| 69.323 | -8.03 | -165.07 | 5.454e-12 | 5.471e-13 |
| 68.844 | -5.78 | -165.00 | 4.965e-12 | 5.419e-13 |
| 67.312 | 0.95 | -165.00 | 4.737e-12 | 6.811e-13 |
| 67.115 | 1.88 | -165.00 | 1.197e-12 | 3.783e-13 |
| 66.844 | 3.15 | -165.00 | 6.663e-13 | 2.874e-13 |
| 66.083 | 6.68 | -165.00 | 9.577e-13 | 3.355e-13 |
| 65.812 | 7.93 | -165.00 | 8.911e-13 | 3.924e-13 |
| 65.125 | 9.20 | -164.48 | 8.250e-13 | 3.862e-13 |
| 64.833 | 8.05 | -163.72 | 6.986e-13 | 3.278e-13 |
| 64.302 | 5.92 | -162.33 | 1.162e-12 | 4.097e-13 |
| 64.083 | 5.01 | -161.76 | 1.304e-12 | 4.224e-13 |
| 63.802 | 3.87 | -161.04 | 1.116e-12 | 3.756e-13 |
| 63.125 | 1.12 | -159.15 | 1.186e-12 | 3.758e-13 |
| 62.792 | -0.39 | -158.22 | 1.126e-12 | 3.913e-13 |
| 62.417 | -1.93 | -157.13 | 1.072e-12 | 4.193e-13 |
| 62.208 | -2.86 | -156.54 | 0.000e+00 | 3.052e-13 |
| 62.021 | -3.69 | -155.96 | 1.523e-12 | 7.198e-13 |

| | | | | |
|-----------------|--------|---------|-----------|-----------|
| 61.854 | -4.37 | -155.50 | 0.000e+00 | 3.129e-13 |
| 61.062 | -1.78 | -154.99 | 0.000e+00 | 3.459e-13 |
| 60.802 | -0.53 | -155.00 | 1.370e-13 | 2.794e-13 |
| 60.208 | 2.22 | -154.98 | 2.740e-13 | 2.690e-13 |
| 60.052 | 3.13 | -154.97 | 2.654e-12 | 1.020e-12 |
| 59.927 | 3.57 | -155.02 | 5.490e-13 | 2.796e-13 |
| 59.792 | 4.37 | -155.00 | 9.264e-13 | 2.606e-13 |
| 59.240 | 6.68 | -155.00 | 0.000e+00 | 2.167e-13 |
| 58.948 | 7.99 | -155.00 | 0.000e+00 | 2.167e-13 |
| 58.792 | 8.88 | -154.98 | 0.000e+00 | 2.229e-13 |
| 58.312 | 11.12 | -155.01 | 0.000e+00 | 2.258e-13 |
| 58.177 | 11.77 | -154.99 | 0.000e+00 | 2.038e-13 |
| 58.052 | 12.32 | -154.98 | 0.000e+00 | 2.369e-13 |
| 57.917 | 12.90 | -154.98 | 0.000e+00 | 2.229e-13 |
| 57.792 | 13.47 | -154.99 | 0.000e+00 | 3.029e-13 |
| 57.312 | 14.43 | -154.79 | 0.000e+00 | 2.863e-13 |
| 57.188 | 13.85 | -154.56 | 0.000e+00 | 3.283e-13 |
| 56.938 | 12.66 | -154.11 | 2.610e-15 | 2.310e-13 |
| 56.812 | 12.07 | -153.88 | 0.000e+00 | 3.471e-13 |
| 56.208 | 9.33 | -152.69 | 0.000e+00 | 2.370e-13 |
| 56.042 | 8.59 | -152.36 | 0.000e+00 | 2.738e-13 |
| 55.833 | 7.69 | -151.96 | 0.000e+00 | 4.417e-13 |
| 55.292 | 5.22 | -151.11 | 0.000e+00 | 3.160e-13 |
| 54.927 | 3.87 | -150.62 | 0.000e+00 | 4.184e-13 |
| 54.792 | 3.26 | -150.40 | 0.000e+00 | 5.067e-13 |
| 54.281 | 0.82 | -149.42 | 0.000e+00 | 3.562e-13 |
| 54.135 | 0.13 | -149.21 | 0.000e+00 | 4.393e-13 |
| 53.917 | -0.92 | -148.84 | 0.000e+00 | 4.223e-13 |
| 53.792 | -1.52 | -148.68 | 0.000e+00 | 4.116e-13 |
| 53.333 | -3.51 | -147.79 | 0.000e+00 | 6.344e-13 |
| 52.365 | -8.05 | -145.86 | 0.000e+00 | 3.747e-13 |
| 51.958 | -10.00 | -145.03 | 0.000e+00 | 4.124e-13 |
| 51.802 | -9.64 | -145.07 | 4.168e-13 | 3.314e-13 |
| 51.229 | -6.97 | -144.99 | 4.980e-13 | 4.451e-13 |
| 51.167 | -6.73 | -145.02 | 6.217e-14 | 3.215e-13 |
| 50.927 | -5.89 | -145.00 | 0.000e+00 | 3.233e-13 |
| 49.917 | -0.88 | -144.95 | 1.702e-12 | 6.482e-13 |
| 49.781 | -0.10 | -144.97 | 2.370e-15 | 2.830e-13 |
| 48.865 | 3.69 | -145.05 | 4.420e-12 | 1.215e-12 |
| 47.917 | 7.67 | -144.03 | 6.982e-12 | 2.002e-12 |
| 47.792 | 8.40 | -144.05 | 2.884e-12 | 9.815e-13 |
| 47.042 | 11.14 | -145.66 | 3.588e-12 | 1.498e-12 |
| 46.875 | 11.97 | -146.22 | 6.246e-12 | 1.662e-12 |
| 46.802 | 12.24 | -146.40 | 3.550e-12 | 1.303e-12 |
| 45.896 | 15.86 | -148.71 | 0.000e+00 | 5.683e-13 |
| 45.708 | 16.30 | -149.31 | 4.163e-12 | 1.141e-12 |
| 45.271 | 17.45 | -151.09 | 2.601e-12 | 9.867e-13 |
| trans-2-pentene | | | | |
| JD | lat | lon | Chi | dChi |
| 70.323 | -11.29 | -166.71 | 1.046e-12 | 3.415e-13 |
| 69.854 | -10.35 | -165.48 | 9.829e-13 | 3.511e-13 |
| 69.323 | -8.03 | -165.07 | 9.354e-13 | 2.901e-13 |
| 68.844 | -5.78 | -165.00 | 1.134e-12 | 3.157e-13 |
| 67.312 | 0.95 | -165.00 | 1.448e-12 | 4.287e-13 |
| 67.115 | 1.88 | -165.00 | 6.795e-13 | 2.283e-13 |

| | | | | |
|--------|--------|---------|-----------|-----------|
| 66.844 | 3.15 | -165.00 | 9.275e-13 | 3.968e-13 |
| 66.083 | 6.68 | -165.00 | 9.603e-13 | 3.707e-13 |
| 65.812 | 7.93 | -165.00 | 8.847e-13 | 3.787e-13 |
| 65.125 | 9.20 | -164.48 | 9.542e-13 | 3.712e-13 |
| 64.833 | 8.05 | -163.72 | 6.697e-13 | 2.711e-13 |
| 64.302 | 5.92 | -162.33 | 8.642e-13 | 3.218e-13 |
| 64.083 | 5.01 | -161.76 | 1.325e-12 | 4.495e-13 |
| 63.802 | 3.87 | -161.04 | 1.002e-12 | 4.673e-13 |
| 63.125 | 1.12 | -159.15 | 1.011e-12 | 4.173e-13 |
| 62.792 | -0.39 | -158.22 | 5.844e-13 | 2.553e-13 |
| 62.417 | -1.93 | -157.13 | 1.022e-12 | 4.915e-13 |
| 62.208 | -2.86 | -156.54 | 9.495e-13 | 4.570e-13 |
| 62.021 | -3.69 | -155.96 | 0.000e+00 | 3.959e-13 |
| 61.854 | -4.37 | -155.50 | 2.834e-15 | 3.526e-13 |
| 61.062 | -1.78 | -154.99 | 3.349e-15 | 4.507e-13 |
| 60.802 | -0.53 | -155.00 | 2.291e-13 | 3.732e-13 |
| 60.208 | 2.22 | -154.98 | 1.651e-12 | 8.639e-13 |
| 60.052 | 3.13 | -154.97 | 3.295e-12 | 1.307e-12 |
| 59.927 | 3.57 | -155.02 | 9.862e-13 | 5.530e-13 |
| 59.792 | 4.37 | -155.00 | 3.100e-12 | 1.233e-12 |
| 59.240 | 6.68 | -155.00 | 3.298e-15 | 2.955e-13 |
| 58.948 | 7.99 | -155.00 | 0.000e+00 | 2.955e-13 |
| 58.792 | 8.88 | -154.98 | 3.291e-15 | 3.100e-13 |
| 58.312 | 11.12 | -155.01 | 0.000e+00 | 3.139e-13 |
| 58.177 | 11.77 | -154.99 | 0.000e+00 | 2.833e-13 |
| 58.052 | 12.32 | -154.98 | 0.000e+00 | 3.291e-13 |
| 57.917 | 12.90 | -154.98 | 1.096e-12 | 5.218e-13 |
| 57.792 | 13.47 | -154.99 | 6.072e-13 | 2.511e-13 |
| 57.312 | 14.43 | -154.79 | 0.000e+00 | 3.602e-13 |
| 57.188 | 13.85 | -154.56 | 0.000e+00 | 4.566e-13 |
| 56.938 | 12.66 | -154.11 | 0.000e+00 | 3.209e-13 |
| 56.812 | 12.07 | -153.88 | 3.157e-15 | 4.517e-13 |
| 56.208 | 9.33 | -152.69 | 6.787e-13 | 3.133e-13 |
| 56.042 | 8.59 | -152.36 | 1.578e-12 | 6.540e-13 |
| 55.833 | 7.69 | -151.96 | 0.000e+00 | 5.079e-13 |
| 55.292 | 5.22 | -151.11 | 0.000e+00 | 3.632e-13 |
| 54.927 | 3.87 | -150.62 | 0.000e+00 | 4.752e-13 |
| 54.792 | 3.26 | -150.40 | 0.000e+00 | 6.907e-13 |
| 54.281 | 0.82 | -149.42 | 0.000e+00 | 4.858e-13 |
| 54.135 | 0.13 | -149.21 | 3.350e-15 | 6.080e-13 |
| 53.917 | -0.92 | -148.84 | 3.350e-15 | 5.845e-13 |
| 53.792 | -1.52 | -148.68 | 0.000e+00 | 4.965e-13 |
| 53.333 | -3.51 | -147.79 | 2.719e-15 | 7.654e-13 |
| 52.365 | -8.05 | -145.86 | 1.118e-12 | 4.797e-13 |
| 51.958 | -10.00 | -145.03 | 5.156e-15 | 5.038e-13 |
| 51.802 | -9.64 | -145.07 | 0.000e+00 | 4.048e-13 |
| 51.229 | -6.97 | -144.99 | 1.727e-12 | 8.079e-13 |
| 51.167 | -6.73 | -145.02 | 9.411e-13 | 3.941e-13 |
| 50.927 | -5.89 | -145.00 | 2.846e-15 | 4.238e-13 |
| 49.917 | -0.88 | -144.95 | 9.137e-13 | 4.102e-13 |
| 49.781 | -0.10 | -144.97 | 5.693e-13 | 3.807e-13 |
| 48.865 | 3.69 | -145.05 | 1.901e-12 | 9.818e-13 |
| 47.917 | 7.67 | -144.03 | 1.250e-12 | 6.663e-13 |
| 47.792 | 8.40 | -144.05 | 1.403e-12 | 7.197e-13 |
| 47.042 | 11.14 | -145.66 | 0.000e+00 | 6.776e-13 |

| | | | | |
|--------|-------|---------|-----------|-----------|
| 46.875 | 11.97 | -146.22 | 5.064e-12 | 1.899e-12 |
| 46.802 | 12.24 | -146.40 | 3.020e-12 | 1.385e-12 |
| 45.896 | 15.86 | -148.71 | 3.537e-12 | 1.493e-12 |
| 45.708 | 16.30 | -149.31 | 0.000e+00 | 5.234e-13 |
| 45.271 | 17.45 | -151.09 | 3.642e-12 | 1.658e-12 |

2-methyl-2-butene

| JD | lat | lon | Chi | dChi |
|--------|--------|---------|-----------|-----------|
| 70.323 | -11.29 | -166.71 | 7.539e-12 | 8.699e-13 |
| 69.854 | -10.35 | -165.48 | 6.846e-12 | 1.095e-12 |
| 69.323 | -8.03 | -165.07 | 6.095e-12 | 9.584e-13 |
| 68.844 | -5.78 | -165.00 | 6.777e-12 | 5.894e-13 |
| 67.312 | 0.95 | -165.00 | 8.700e-12 | 7.527e-13 |
| 67.115 | 1.88 | -165.00 | 1.249e-11 | 1.126e-12 |
| 66.844 | 3.15 | -165.00 | 8.143e-12 | 8.047e-13 |
| 66.083 | 6.68 | -165.00 | 9.565e-12 | 9.344e-13 |
| 65.812 | 7.93 | -165.00 | 1.057e-11 | 9.706e-13 |
| 65.125 | 9.20 | -164.48 | 1.267e-11 | 9.133e-13 |
| 64.833 | 8.05 | -163.72 | 9.837e-12 | 8.150e-13 |
| 64.302 | 5.92 | -162.33 | 1.184e-11 | 9.776e-13 |
| 64.083 | 5.01 | -161.76 | 1.195e-11 | 7.928e-13 |
| 63.802 | 3.87 | -161.04 | 1.128e-11 | 7.573e-13 |
| 63.125 | 1.12 | -159.15 | 1.483e-11 | 9.194e-13 |
| 62.792 | -0.39 | -158.22 | 9.406e-12 | 1.482e-12 |
| 62.417 | -1.93 | -157.13 | 1.197e-11 | 2.195e-12 |
| 62.208 | -2.86 | -156.54 | 7.418e-12 | 1.099e-12 |
| 62.021 | -3.69 | -155.96 | 1.315e-11 | 1.674e-12 |
| 61.854 | -4.37 | -155.50 | 8.722e-12 | 1.151e-12 |
| 61.062 | -1.78 | -154.99 | 1.088e-11 | 1.353e-12 |
| 60.802 | -0.53 | -155.00 | 8.679e-12 | 1.157e-12 |
| 60.208 | 2.22 | -154.98 | 1.176e-11 | 1.631e-12 |
| 60.052 | 3.13 | -154.97 | 1.400e-11 | 1.538e-12 |
| 59.927 | 3.57 | -155.02 | 1.599e-11 | 1.903e-12 |
| 59.792 | 4.37 | -155.00 | 8.956e-12 | 1.467e-12 |
| 59.240 | 6.68 | -155.00 | 0.000e+00 | 1.886e-13 |
| 58.948 | 7.99 | -155.00 | 1.853e-12 | 5.537e-13 |
| 58.792 | 8.88 | -154.98 | 8.779e-13 | 3.312e-13 |
| 58.312 | 11.12 | -155.01 | 8.584e-12 | 1.043e-12 |
| 58.177 | 11.77 | -154.99 | 3.179e-12 | 7.335e-13 |
| 58.052 | 12.32 | -154.98 | 1.242e-11 | 1.518e-12 |
| 57.917 | 12.90 | -154.98 | 8.231e-12 | 1.001e-12 |
| 57.792 | 13.47 | -154.99 | 1.001e-12 | 3.843e-13 |
| 57.312 | 14.43 | -154.79 | 0.000e+00 | 2.465e-13 |
| 57.188 | 13.85 | -154.56 | 6.578e-12 | 1.175e-12 |
| 56.938 | 12.66 | -154.11 | 1.179e-11 | 1.086e-12 |
| 56.812 | 12.07 | -153.88 | 2.815e-12 | 8.463e-13 |
| 56.208 | 9.33 | -152.69 | 9.093e-12 | 1.013e-12 |
| 56.042 | 8.59 | -152.36 | 8.604e-12 | 1.098e-12 |
| 55.833 | 7.69 | -151.96 | 6.035e-12 | 1.155e-12 |
| 55.292 | 5.22 | -151.11 | 7.367e-12 | 8.162e-13 |
| 54.927 | 3.87 | -150.62 | 1.756e-11 | 2.293e-12 |
| 54.792 | 3.26 | -150.40 | 5.543e-12 | 1.713e-12 |
| 54.281 | 0.82 | -149.42 | 1.617e-11 | 2.651e-12 |
| 54.135 | 0.13 | -149.21 | 2.613e-11 | 1.276e-11 |
| 53.917 | -0.92 | -148.84 | 3.417e-12 | 1.984e-12 |
| 53.792 | -1.52 | -148.68 | 0.000e+00 | 6.649e-13 |

| | | | | |
|--------|--------|---------|-----------|-----------|
| 53.333 | -3.51 | -147.79 | 0.000e+00 | 1.025e-12 |
| 52.365 | -8.05 | -145.86 | 5.191e-12 | 2.457e-12 |
| 51.958 | -10.00 | -145.03 | 7.446e-12 | 1.897e-12 |
| 51.802 | -9.64 | -145.07 | 6.949e-12 | 1.729e-12 |
| 51.229 | -6.97 | -144.99 | 6.265e-12 | 2.095e-12 |
| 51.167 | -6.73 | -145.02 | 5.930e-12 | 1.622e-12 |
| 50.927 | -5.89 | -145.00 | 1.508e-11 | 2.324e-12 |
| 49.917 | -0.88 | -144.95 | 9.436e-12 | 1.721e-12 |
| 49.781 | -0.10 | -144.97 | 6.361e-12 | 1.346e-12 |
| 48.865 | 3.69 | -145.05 | 3.482e-11 | 3.939e-12 |
| 47.917 | 7.67 | -144.03 | 5.402e-11 | 5.337e-12 |
| 47.792 | 8.40 | -144.05 | 5.640e-11 | 5.209e-12 |
| 47.042 | 11.14 | -145.66 | 2.646e-11 | 1.267e-11 |
| 46.875 | 11.97 | -146.22 | 3.081e-11 | 1.479e-11 |
| 46.802 | 12.24 | -146.40 | 3.582e-11 | 1.699e-11 |
| 45.896 | 15.86 | -148.71 | 4.639e-11 | 2.190e-11 |
| 45.708 | 16.30 | -149.31 | 1.071e-10 | 6.851e-12 |
| 45.271 | 17.45 | -151.09 | 7.363e-11 | 5.724e-12 |

1-pentene

| JD | lat | lon | Chi | dChi |
|--------|--------|---------|-----------|-----------|
| 70.323 | -11.29 | -166.71 | 2.371e-12 | 4.349e-13 |
| 69.854 | -10.35 | -165.48 | 2.750e-12 | 3.954e-13 |
| 69.323 | -8.03 | -165.07 | 2.466e-12 | 4.563e-13 |
| 68.844 | -5.78 | -165.00 | 2.644e-12 | 5.087e-13 |
| 67.312 | 0.95 | -165.00 | 3.027e-12 | 5.212e-13 |
| 67.115 | 1.88 | -165.00 | 3.317e-12 | 5.709e-13 |
| 66.844 | 3.15 | -165.00 | 2.802e-12 | 5.259e-13 |
| 66.083 | 6.68 | -165.00 | 2.682e-12 | 6.257e-13 |
| 65.812 | 7.93 | -165.00 | 2.971e-12 | 6.333e-13 |
| 65.125 | 9.20 | -164.48 | 2.908e-12 | 6.953e-13 |
| 64.833 | 8.05 | -163.72 | 3.363e-12 | 7.121e-13 |
| 64.302 | 5.92 | -162.33 | 3.086e-12 | 6.031e-13 |
| 64.083 | 5.01 | -161.76 | 3.646e-12 | 7.991e-13 |
| 63.802 | 3.87 | -161.04 | 3.006e-12 | 6.547e-13 |
| 63.125 | 1.12 | -159.15 | 3.492e-12 | 7.042e-13 |
| 62.792 | -0.39 | -158.22 | 2.231e-12 | 4.858e-13 |
| 62.417 | -1.93 | -157.13 | 4.180e-13 | 4.189e-13 |
| 62.208 | -2.86 | -156.54 | 1.466e-12 | 6.670e-13 |
| 62.021 | -3.69 | -155.96 | 2.574e-12 | 1.008e-12 |
| 61.854 | -4.37 | -155.50 | 1.946e-12 | 7.701e-13 |
| 61.062 | -1.78 | -154.99 | 2.905e-12 | 1.321e-12 |
| 60.802 | -0.53 | -155.00 | 2.663e-12 | 1.097e-12 |
| 60.208 | 2.22 | -154.98 | 2.288e-12 | 8.818e-13 |
| 60.052 | 3.13 | -154.97 | 4.175e-12 | 1.451e-12 |
| 59.927 | 3.57 | -155.02 | 1.596e-12 | 8.214e-13 |
| 59.792 | 4.37 | -155.00 | 7.574e-13 | 4.661e-13 |
| 59.240 | 6.68 | -155.00 | 0.000e+00 | 3.148e-13 |
| 58.948 | 7.99 | -155.00 | 5.540e-13 | 3.200e-13 |
| 58.792 | 8.88 | -154.98 | 1.641e-12 | 6.558e-13 |
| 58.312 | 11.12 | -155.01 | 2.768e-12 | 8.929e-13 |
| 58.177 | 11.77 | -154.99 | 8.454e-13 | 3.900e-13 |
| 58.052 | 12.32 | -154.98 | 0.000e+00 | 3.478e-13 |
| 57.917 | 12.90 | -154.98 | 3.097e-15 | 3.276e-13 |
| 57.792 | 13.47 | -154.99 | 2.496e-12 | 8.975e-13 |
| 57.312 | 14.43 | -154.79 | 0.000e+00 | 3.852e-13 |

| | | | | |
|--------|--------|---------|-----------|-----------|
| 57.188 | 13.85 | -154.56 | 1.515e-12 | 7.163e-13 |
| 56.938 | 12.66 | -154.11 | 7.084e-13 | 3.347e-13 |
| 56.812 | 12.07 | -153.88 | 2.843e-12 | 7.463e-13 |
| 56.208 | 9.33 | -152.69 | 1.536e-12 | 5.607e-13 |
| 56.042 | 8.59 | -152.36 | 9.329e-13 | 3.981e-13 |
| 55.833 | 7.69 | -151.96 | 1.115e-12 | 3.652e-13 |
| 55.292 | 5.22 | -151.11 | 2.772e-13 | 3.886e-13 |
| 54.927 | 3.87 | -150.62 | 3.166e-12 | 1.264e-12 |
| 54.792 | 3.26 | -150.40 | 2.957e-15 | 7.029e-13 |
| 54.281 | 0.82 | -149.42 | 2.440e-12 | 1.105e-12 |
| 54.135 | 0.13 | -149.21 | 1.969e-12 | 9.771e-13 |
| 53.917 | -0.92 | -148.84 | 0.000e+00 | 6.162e-13 |
| 53.792 | -1.52 | -148.68 | 0.000e+00 | 5.594e-13 |
| 53.333 | -3.51 | -147.79 | 0.000e+00 | 8.621e-13 |
| 52.365 | -8.05 | -145.86 | 1.306e-12 | 6.754e-13 |
| 51.958 | -10.00 | -145.03 | 1.586e-12 | 7.460e-13 |
| 51.802 | -9.64 | -145.07 | 1.470e-12 | 7.281e-13 |
| 51.229 | -6.97 | -144.99 | 2.188e-12 | 1.035e-12 |
| 51.167 | -6.73 | -145.02 | 1.972e-12 | 7.909e-13 |
| 50.927 | -5.89 | -145.00 | 9.863e-13 | 4.769e-13 |
| 49.917 | -0.88 | -144.95 | 1.890e-12 | 8.189e-13 |
| 49.781 | -0.10 | -144.97 | 0.000e+00 | 6.692e-13 |
| 48.865 | 3.69 | -145.05 | 1.890e-12 | 9.383e-13 |
| 47.917 | 7.67 | -144.03 | 7.563e-12 | 2.538e-12 |
| 47.792 | 8.40 | -144.05 | 5.681e-12 | 1.692e-12 |
| 47.042 | 11.14 | -145.66 | 5.404e-12 | 2.356e-12 |
| 46.875 | 11.97 | -146.22 | 3.189e-12 | 1.538e-12 |
| 46.802 | 12.24 | -146.40 | 4.388e-12 | 1.868e-12 |
| 45.896 | 15.86 | -148.71 | 9.809e-12 | 3.213e-12 |
| 45.708 | 16.30 | -149.31 | 6.599e-12 | 1.816e-12 |
| 45.271 | 17.45 | -151.09 | 8.483e-12 | 2.806e-12 |

2-methyl-1-butene

| JD | lat | lon | Chi | dChi |
|--------|--------|---------|-----------|-----------|
| 70.323 | -11.29 | -166.71 | 5.540e-12 | 1.451e-12 |
| 69.854 | -10.35 | -165.48 | 7.314e-12 | 2.805e-12 |
| 69.323 | -8.03 | -165.07 | 4.118e-12 | 1.644e-12 |
| 68.844 | -5.78 | -165.00 | 2.397e-12 | 5.023e-13 |
| 67.312 | 0.95 | -165.00 | 4.898e-12 | 7.955e-13 |
| 67.115 | 1.88 | -165.00 | 4.880e-12 | 8.792e-13 |
| 66.844 | 3.15 | -165.00 | 3.328e-12 | 7.355e-13 |
| 66.083 | 6.68 | -165.00 | 3.655e-12 | 9.537e-13 |
| 65.812 | 7.93 | -165.00 | 3.151e-12 | 8.950e-13 |
| 65.125 | 9.20 | -164.48 | 6.058e-12 | 1.311e-12 |
| 64.833 | 8.05 | -163.72 | 4.706e-12 | 9.885e-13 |
| 64.302 | 5.92 | -162.33 | 5.920e-12 | 1.143e-12 |
| 64.083 | 5.01 | -161.76 | 3.888e-12 | 9.807e-13 |
| 63.802 | 3.87 | -161.04 | 4.848e-12 | 1.034e-12 |
| 63.125 | 1.12 | -159.15 | 6.833e-12 | 1.030e-12 |
| 62.792 | -0.39 | -158.22 | 4.967e-12 | 1.361e-12 |
| 62.417 | -1.93 | -157.13 | 4.910e-12 | 2.105e-12 |
| 62.208 | -2.86 | -156.54 | 3.311e-12 | 1.487e-12 |
| 62.021 | -3.69 | -155.96 | 5.394e-12 | 1.911e-12 |
| 61.854 | -4.37 | -155.50 | 6.285e-12 | 2.544e-12 |
| 61.062 | -1.78 | -154.99 | 9.667e-12 | 2.962e-12 |
| 60.802 | -0.53 | -155.00 | 8.468e-12 | 3.081e-12 |

| | | | | |
|---------------|--------|---------|-----------|-----------|
| 60.208 | 2.22 | -154.98 | 4.131e-12 | 1.552e-12 |
| 60.052 | 3.13 | -154.97 | 8.579e-12 | 2.321e-12 |
| 59.927 | 3.57 | -155.02 | 6.765e-12 | 2.245e-12 |
| 59.792 | 4.37 | -155.00 | 5.002e-12 | 1.990e-12 |
| 59.240 | 6.68 | -155.00 | 0.000e+00 | 5.350e-13 |
| 58.948 | 7.99 | -155.00 | 2.486e-12 | 1.041e-12 |
| 58.792 | 8.88 | -154.98 | 3.091e-12 | 1.415e-12 |
| 58.312 | 11.12 | -155.01 | 5.253e-12 | 1.668e-12 |
| 58.177 | 11.77 | -154.99 | 1.707e-12 | 8.588e-13 |
| 58.052 | 12.32 | -154.98 | 2.899e-12 | 1.182e-12 |
| 57.917 | 12.90 | -154.98 | 2.086e-12 | 8.969e-13 |
| 57.792 | 13.47 | -154.99 | 3.242e-12 | 1.085e-12 |
| 57.312 | 14.43 | -154.79 | 0.000e+00 | 6.599e-13 |
| 57.188 | 13.85 | -154.56 | 2.355e-12 | 1.126e-12 |
| 56.938 | 12.66 | -154.11 | 3.416e-12 | 1.111e-12 |
| 56.812 | 12.07 | -153.88 | 4.433e-12 | 1.639e-12 |
| 56.208 | 9.33 | -152.69 | 2.762e-12 | 1.314e-12 |
| 56.042 | 8.59 | -152.36 | 3.965e-12 | 1.735e-12 |
| 55.833 | 7.69 | -151.96 | 3.339e-12 | 1.533e-12 |
| 55.292 | 5.22 | -151.11 | 0.000e+00 | 1.126e-12 |
| 54.927 | 3.87 | -150.62 | 9.076e-12 | 3.971e-12 |
| 54.792 | 3.26 | -150.40 | 6.851e-12 | 3.750e-12 |
| 54.281 | 0.82 | -149.42 | 5.670e-12 | 3.033e-12 |
| 54.135 | 0.13 | -149.21 | 9.190e-12 | 6.693e-12 |
| 53.917 | -0.92 | -148.84 | 5.559e-15 | 1.147e-12 |
| 53.792 | -1.52 | -148.68 | 2.585e-15 | 5.583e-13 |
| 53.333 | -3.51 | -147.79 | 0.000e+00 | 8.604e-13 |
| 52.365 | -8.05 | -145.86 | 5.169e-15 | 5.084e-13 |
| 51.958 | -10.00 | -145.03 | 5.192e-15 | 5.999e-13 |
| 51.802 | -9.64 | -145.07 | 2.331e-12 | 8.827e-13 |
| 51.229 | -6.97 | -144.99 | 2.570e-12 | 1.233e-12 |
| 51.167 | -6.73 | -145.02 | 2.165e-12 | 9.776e-13 |
| 50.927 | -5.89 | -145.00 | 3.288e-12 | 1.035e-12 |
| 49.917 | -0.88 | -144.95 | 3.197e-12 | 9.608e-13 |
| 49.781 | -0.10 | -144.97 | 1.927e-12 | 7.610e-13 |
| 48.865 | 3.69 | -145.05 | 4.513e-12 | 1.404e-12 |
| 47.917 | 7.67 | -144.03 | 1.350e-11 | 2.782e-12 |
| 47.792 | 8.40 | -144.05 | 6.678e-12 | 1.754e-12 |
| 47.042 | 11.14 | -145.66 | 3.128e-11 | 2.156e-11 |
| 46.875 | 11.97 | -146.22 | 3.048e-11 | 2.121e-11 |
| 46.802 | 12.24 | -146.40 | 2.766e-11 | 1.931e-11 |
| 45.896 | 15.86 | -148.71 | 4.176e-11 | 2.867e-11 |
| 45.708 | 16.30 | -149.31 | 8.272e-12 | 1.779e-12 |
| 45.271 | 17.45 | -151.09 | 8.118e-12 | 2.204e-12 |
| cis-2-pentene | | | | |
| JD | lat | lon | Chi | dChi |
| 70.323 | -11.29 | -166.71 | 2.947e-13 | 1.312e-13 |
| 69.854 | -10.35 | -165.48 | 1.925e-13 | 1.193e-13 |
| 69.323 | -8.03 | -165.07 | 2.661e-13 | 1.135e-13 |
| 68.844 | -5.78 | -165.00 | 0.000e+00 | 1.151e-13 |
| 67.312 | 0.95 | -165.00 | 2.176e-13 | 1.138e-13 |
| 67.115 | 1.88 | -165.00 | 2.426e-13 | 1.501e-13 |
| 66.844 | 3.15 | -165.00 | 2.346e-14 | 1.275e-13 |
| 66.083 | 6.68 | -165.00 | 2.021e-13 | 1.485e-13 |
| 65.812 | 7.93 | -165.00 | 7.606e-14 | 1.917e-13 |

| | | | | |
|--------|--------|---------|-----------|-----------|
| 65.125 | 9.20 | -164.48 | 6.381e-13 | 2.944e-13 |
| 64.833 | 8.05 | -163.72 | 7.100e-13 | 3.088e-13 |
| 64.302 | 5.92 | -162.33 | 1.707e-13 | 1.904e-13 |
| 64.083 | 5.01 | -161.76 | 0.000e+00 | 1.881e-13 |
| 63.802 | 3.87 | -161.04 | 0.000e+00 | 1.676e-13 |
| 63.125 | 1.12 | -159.15 | 4.200e-13 | 1.768e-13 |
| 62.792 | -0.39 | -158.22 | 0.000e+00 | 1.480e-13 |
| 62.417 | -1.93 | -157.13 | 1.076e-12 | 5.537e-13 |
| 62.208 | -2.86 | -156.54 | 5.012e-14 | 4.095e-13 |
| 62.021 | -3.69 | -155.96 | 3.538e-14 | 4.717e-13 |
| 61.854 | -4.37 | -155.50 | 2.093e-13 | 4.198e-13 |
| 61.062 | -1.78 | -154.99 | 3.466e-13 | 4.861e-13 |
| 60.802 | -0.53 | -155.00 | 7.868e-13 | 4.108e-13 |
| 60.208 | 2.22 | -154.98 | 0.000e+00 | 3.915e-13 |
| 60.052 | 3.13 | -154.97 | 1.242e-12 | 4.486e-13 |
| 59.927 | 3.57 | -155.02 | 0.000e+00 | 3.913e-13 |
| 59.792 | 4.37 | -155.00 | 1.777e-12 | 8.577e-13 |
| 59.240 | 6.68 | -155.00 | 1.469e-12 | 4.122e-13 |
| 58.948 | 7.99 | -155.00 | 0.000e+00 | 2.856e-13 |
| 58.792 | 8.88 | -154.98 | 0.000e+00 | 2.952e-13 |
| 58.312 | 11.12 | -155.01 | 0.000e+00 | 2.988e-13 |
| 58.177 | 11.77 | -154.99 | 0.000e+00 | 2.698e-13 |
| 58.052 | 12.32 | -154.98 | 9.582e-14 | 3.135e-13 |
| 57.917 | 12.90 | -154.98 | 9.013e-13 | 2.449e-13 |
| 57.792 | 13.47 | -154.99 | 1.433e-12 | 3.995e-13 |
| 57.312 | 14.43 | -154.79 | 2.113e-11 | 2.773e-12 |
| 57.188 | 13.85 | -154.56 | 1.421e-12 | 4.009e-13 |
| 56.938 | 12.66 | -154.11 | 0.000e+00 | 3.041e-13 |
| 56.812 | 12.07 | -153.88 | 0.000e+00 | 4.428e-13 |
| 56.208 | 9.33 | -152.69 | 0.000e+00 | 3.026e-13 |
| 56.042 | 8.59 | -152.36 | 2.958e-15 | 3.493e-13 |
| 55.833 | 7.69 | -151.96 | 6.911e-13 | 3.429e-13 |
| 55.292 | 5.22 | -151.11 | 0.000e+00 | 3.957e-13 |
| 54.927 | 3.87 | -150.62 | 0.000e+00 | 5.145e-13 |
| 54.792 | 3.26 | -150.40 | 0.000e+00 | 6.269e-13 |
| 54.281 | 0.82 | -149.42 | 0.000e+00 | 4.407e-13 |
| 54.135 | 0.13 | -149.21 | 2.933e-15 | 5.570e-13 |
| 53.917 | -0.92 | -148.84 | 5.280e-14 | 5.356e-13 |
| 53.792 | -1.52 | -148.68 | 0.000e+00 | 5.523e-13 |
| 53.333 | -3.51 | -147.79 | 5.780e-15 | 8.514e-13 |
| 52.365 | -8.05 | -145.86 | 0.000e+00 | 5.031e-13 |
| 51.958 | -10.00 | -145.03 | 0.000e+00 | 5.654e-13 |
| 51.802 | -9.64 | -145.07 | 0.000e+00 | 4.542e-13 |
| 51.229 | -6.97 | -144.99 | 0.000e+00 | 6.100e-13 |
| 51.167 | -6.73 | -145.02 | 0.000e+00 | 4.410e-13 |
| 50.927 | -5.89 | -145.00 | 2.796e-15 | 4.356e-13 |
| 49.917 | -0.88 | -144.95 | 0.000e+00 | 3.744e-13 |
| 49.781 | -0.10 | -144.97 | 0.000e+00 | 3.811e-13 |
| 48.865 | 3.69 | -145.05 | 2.796e-15 | 4.798e-13 |
| 47.917 | 7.67 | -144.03 | 7.270e-14 | 6.568e-13 |
| 47.792 | 8.40 | -144.05 | 0.000e+00 | 5.139e-13 |
| 47.042 | 11.14 | -145.66 | 1.184e-13 | 6.693e-13 |
| 46.875 | 11.97 | -146.22 | 2.819e-15 | 6.622e-13 |
| 46.802 | 12.24 | -146.40 | 8.457e-15 | 7.276e-13 |
| 45.896 | 15.86 | -148.71 | 5.638e-15 | 7.343e-13 |

| | | | | |
|--------|-------|---------|-----------|-----------|
| 45.708 | 16.30 | -149.31 | 0.000e+00 | 4.979e-13 |
| 45.271 | 17.45 | -151.09 | 1.546e-12 | 5.790e-13 |

Appendix 3

Equilibrator samples from SAGA 3.

NMHC data for SAGA 3 Equilibrator Samples
 Data must be converted to concentration and divided by the appropriate Henry's law constant to determine the water concentrations. Henry's law constants are listed after each compound name. A good average dry air density for SAGA 3 is 2.36(19) molec/cc. Uncertainties do not include absolute calibration uncertainties (20%).

ethane 20.4

| JD | lat | lon | Chi | dChi |
|--------|--------|---------|-----------|-----------|
| 69.944 | -10.56 | -165.76 | 3.375e-09 | 8.534e-11 |
| 68.944 | -6.34 | -164.99 | 3.603e-09 | 1.146e-10 |
| 67.181 | 1.44 | -165.00 | 3.578e-09 | 9.887e-11 |
| 66.917 | 2.73 | -165.00 | 3.510e-09 | 9.553e-11 |
| 66.181 | 6.07 | -165.00 | 3.191e-09 | 5.010e-10 |
| 65.705 | 8.20 | -165.00 | 3.382e-09 | 2.528e-10 |
| 65.205 | 9.60 | -164.74 | 3.647e-09 | 5.518e-10 |
| 64.938 | 8.44 | -163.98 | 3.430e-09 | 2.660e-10 |
| 64.385 | 6.27 | -162.59 | 4.287e-09 | 1.595e-10 |
| 64.167 | 5.37 | -161.97 | 3.822e-09 | 1.330e-10 |
| 63.705 | 3.48 | -160.78 | 3.638e-09 | 1.355e-10 |
| 63.250 | 1.60 | -159.43 | 3.482e-09 | 1.135e-10 |
| 63.021 | 0.58 | -158.83 | 4.433e-09 | 1.575e-10 |
| 62.708 | -0.72 | -157.99 | 3.423e-09 | 4.292e-10 |
| 62.479 | -1.70 | -157.28 | 2.920e-09 | 2.638e-10 |
| 62.250 | -2.70 | -156.65 | 3.682e-09 | 1.127e-10 |

ethene 8.8

| JD | lat | lon | Chi | dChi |
|--------|--------|---------|-----------|-----------|
| 69.944 | -10.56 | -165.76 | 1.360e-08 | 4.224e-10 |
| 68.944 | -6.34 | -164.99 | 1.530e-08 | 4.910e-10 |
| 67.181 | 1.44 | -165.00 | 2.099e-08 | 1.593e-09 |
| 66.917 | 2.73 | -165.00 | 2.011e-08 | 1.116e-09 |
| 66.181 | 6.07 | -165.00 | 1.310e-08 | 5.206e-10 |
| 65.705 | 8.20 | -165.00 | 7.815e-09 | 3.262e-10 |
| 65.205 | 9.60 | -164.74 | 1.074e-08 | 2.908e-10 |
| 64.938 | 8.44 | -163.98 | 1.116e-08 | 4.480e-10 |
| 64.385 | 6.27 | -162.59 | 1.751e-08 | 1.454e-09 |
| 64.167 | 5.37 | -161.97 | 1.748e-08 | 1.281e-09 |
| 63.705 | 3.48 | -160.78 | 1.868e-08 | 5.699e-10 |
| 63.250 | 1.60 | -159.43 | 1.745e-08 | 2.543e-09 |
| 63.021 | 0.58 | -158.83 | 2.282e-08 | 1.049e-09 |
| 62.708 | -0.72 | -157.99 | 1.781e-08 | 1.595e-09 |
| 62.479 | -1.70 | -157.28 | 1.656e-08 | 1.382e-09 |
| 62.250 | -2.70 | -156.65 | 2.027e-08 | 1.031e-09 |

ethyne 0.98

| JD | lat | lon | Chi | dChi |
|--------|--------|---------|-----------|-----------|
| 69.944 | -10.56 | -165.76 | 1.194e-10 | 2.452e-11 |
| 68.944 | -6.34 | -164.99 | 4.250e-11 | 1.217e-11 |
| 67.181 | 1.44 | -165.00 | 5.949e-10 | 6.417e-11 |

| | | | | |
|--------|-------|---------|-----------|-----------|
| 66.917 | 2.73 | -165.00 | 7.784e-12 | 6.847e-12 |
| 66.181 | 6.07 | -165.00 | 0.000e+00 | 6.682e-12 |
| 65.705 | 8.20 | -165.00 | 1.873e-10 | 3.472e-11 |
| 65.205 | 9.60 | -164.74 | 0.000e+00 | 8.858e-12 |
| 64.938 | 8.44 | -163.98 | 0.000e+00 | 7.847e-12 |
| 64.385 | 6.27 | -162.59 | 0.000e+00 | 1.066e-11 |
| 64.167 | 5.37 | -161.97 | 0.000e+00 | 8.699e-12 |
| 63.705 | 3.48 | -160.78 | 5.341e-12 | 7.324e-12 |
| 63.250 | 1.60 | -159.43 | 5.682e-14 | 8.699e-12 |
| 63.021 | 0.58 | -158.83 | 7.015e-10 | 5.344e-11 |
| 62.708 | -0.72 | -157.99 | 0.000e+00 | 8.006e-12 |
| 62.479 | -1.70 | -157.28 | 3.807e-12 | 7.636e-12 |
| 62.250 | -2.70 | -156.65 | 2.256e-11 | 1.034e-11 |

propane 28.9

| JD | lat | lon | Chi | dChi |
|--------|--------|---------|-----------|-----------|
| 69.944 | -10.56 | -165.76 | 2.525e-09 | 7.265e-11 |
| 68.944 | -6.34 | -164.99 | 2.842e-09 | 8.305e-11 |
| 67.181 | 1.44 | -165.00 | 2.994e-09 | 1.004e-10 |
| 66.917 | 2.73 | -165.00 | 3.018e-09 | 1.060e-10 |
| 66.181 | 6.07 | -165.00 | 2.319e-09 | 8.316e-11 |
| 65.705 | 8.20 | -165.00 | 2.198e-09 | 7.559e-11 |
| 65.205 | 9.60 | -164.74 | 2.504e-09 | 9.811e-11 |
| 64.938 | 8.44 | -163.98 | 2.377e-09 | 8.379e-11 |
| 64.385 | 6.27 | -162.59 | 3.726e-09 | 1.289e-10 |
| 64.167 | 5.37 | -161.97 | 3.039e-09 | 1.216e-10 |
| 63.705 | 3.48 | -160.78 | 2.913e-09 | 8.920e-11 |
| 63.250 | 1.60 | -159.43 | 2.922e-09 | 8.790e-11 |
| 63.021 | 0.58 | -158.83 | 3.886e-09 | 1.124e-10 |
| 62.708 | -0.72 | -157.99 | 2.660e-09 | 7.640e-11 |
| 62.479 | -1.70 | -157.28 | 2.237e-09 | 5.945e-11 |
| 62.250 | -2.70 | -156.65 | 2.999e-09 | 1.385e-10 |

cyclopropane 1?

| JD | lat | lon | Chi | dChi |
|--------|--------|---------|-----------|-----------|
| 69.944 | -10.56 | -165.76 | 1.289e-10 | 1.812e-11 |
| 68.944 | -6.34 | -164.99 | 1.455e-10 | 1.853e-11 |
| 67.181 | 1.44 | -165.00 | 2.804e-10 | 2.765e-11 |
| 66.917 | 2.73 | -165.00 | 3.243e-10 | 3.188e-11 |
| 66.181 | 6.07 | -165.00 | 1.774e-10 | 1.927e-11 |
| 65.705 | 8.20 | -165.00 | 9.293e-11 | 1.896e-11 |
| 65.205 | 9.60 | -164.74 | 9.824e-11 | 1.853e-11 |
| 64.938 | 8.44 | -163.98 | 3.833e-10 | 1.058e-10 |
| 64.385 | 6.27 | -162.59 | 1.752e-10 | 2.289e-11 |
| 64.167 | 5.37 | -161.97 | 2.573e-10 | 4.788e-11 |
| 63.705 | 3.48 | -160.78 | 5.356e-10 | 1.357e-10 |
| 63.250 | 1.60 | -159.43 | 2.368e-10 | 4.944e-11 |
| 63.021 | 0.58 | -158.83 | 4.980e-10 | 2.465e-10 |
| 62.708 | -0.72 | -157.99 | 2.118e-10 | 2.298e-11 |
| 62.479 | -1.70 | -157.28 | 2.328e-10 | 5.082e-11 |
| 62.250 | -2.70 | -156.65 | 4.487e-10 | 1.185e-10 |

propene 8.6

| JD | lat | lon | Chi | dChi |
|--------|--------|---------|-----------|-----------|
| 69.944 | -10.56 | -165.76 | 1.096e-08 | 3.062e-10 |

| | | | | |
|--------|-------|---------|-----------|-----------|
| 68.944 | -6.34 | -164.99 | 9.267e-09 | 3.004e-10 |
| 67.181 | 1.44 | -165.00 | 7.047e-09 | 3.368e-10 |
| 66.917 | 2.73 | -165.00 | 6.637e-09 | 2.630e-10 |
| 66.181 | 6.07 | -165.00 | 6.053e-09 | 2.405e-10 |
| 65.705 | 8.20 | -165.00 | 3.937e-09 | 1.143e-10 |
| 65.205 | 9.60 | -164.74 | 5.554e-09 | 1.540e-10 |
| 64.938 | 8.44 | -163.98 | 5.342e-09 | 1.491e-10 |
| 64.385 | 6.27 | -162.59 | 7.576e-09 | 2.141e-10 |
| 64.167 | 5.37 | -161.97 | 7.533e-09 | 2.150e-10 |
| 63.705 | 3.48 | -160.78 | 7.766e-09 | 2.238e-10 |
| 63.250 | 1.60 | -159.43 | 6.146e-09 | 1.703e-10 |
| 63.021 | 0.58 | -158.83 | 7.756e-09 | 3.001e-10 |
| 62.708 | -0.72 | -157.99 | 6.796e-09 | 2.302e-10 |
| 62.479 | -1.70 | -157.28 | 7.061e-09 | 2.340e-10 |
| 62.250 | -2.70 | -156.65 | 1.013e-08 | 2.717e-10 |

butane 38.7

| JD | lat | lon | Chi | dChi |
|--------|--------|---------|-----------|-----------|
| 69.944 | -10.56 | -165.76 | 1.054e-09 | 5.560e-11 |
| 68.944 | -6.34 | -164.99 | 9.396e-10 | 5.902e-11 |
| 67.181 | 1.44 | -165.00 | 7.008e-10 | 4.561e-11 |
| 66.917 | 2.73 | -165.00 | 6.759e-10 | 4.927e-11 |
| 66.181 | 6.07 | -165.00 | 6.934e-10 | 5.392e-11 |
| 65.705 | 8.20 | -165.00 | 7.716e-10 | 4.427e-11 |
| 65.205 | 9.60 | -164.74 | 8.924e-10 | 5.111e-11 |
| 64.938 | 8.44 | -163.98 | 7.764e-10 | 3.464e-11 |
| 64.385 | 6.27 | -162.59 | 1.017e-09 | 4.726e-11 |
| 64.167 | 5.37 | -161.97 | 9.179e-10 | 4.917e-11 |
| 63.705 | 3.48 | -160.78 | 8.346e-10 | 3.844e-11 |
| 63.250 | 1.60 | -159.43 | 8.333e-10 | 4.375e-11 |
| 63.021 | 0.58 | -158.83 | 1.003e-09 | 4.655e-11 |
| 62.708 | -0.72 | -157.99 | 7.252e-10 | 4.008e-11 |
| 62.479 | -1.70 | -157.28 | 6.398e-10 | 3.836e-11 |
| 62.250 | -2.70 | -156.65 | 1.004e-09 | 5.084e-11 |

2-methyl-propane 48.4

| JD | lat | lon | Chi | dChi |
|--------|--------|---------|-----------|-----------|
| 69.944 | -10.56 | -165.76 | 2.714e-10 | 2.955e-11 |
| 68.944 | -6.34 | -164.99 | 2.656e-10 | 2.344e-11 |
| 67.181 | 1.44 | -165.00 | 0.000e+00 | 6.085e-12 |
| 66.917 | 2.73 | -165.00 | 3.683e-10 | 4.772e-11 |
| 66.181 | 6.07 | -165.00 | 3.119e-10 | 2.954e-11 |
| 65.705 | 8.20 | -165.00 | 1.867e-10 | 2.283e-11 |
| 65.205 | 9.60 | -164.74 | 3.736e-10 | 5.403e-11 |
| 64.938 | 8.44 | -163.98 | 3.703e-10 | 4.738e-11 |
| 64.385 | 6.27 | -162.59 | 4.119e-10 | 5.806e-11 |
| 64.167 | 5.37 | -161.97 | 3.449e-10 | 4.386e-11 |
| 63.705 | 3.48 | -160.78 | 3.622e-10 | 5.670e-11 |
| 63.250 | 1.60 | -159.43 | 3.705e-10 | 3.337e-11 |
| 63.021 | 0.58 | -158.83 | 1.173e-11 | 5.148e-12 |
| 62.708 | -0.72 | -157.99 | 3.708e-10 | 2.971e-11 |
| 62.479 | -1.70 | -157.28 | 2.639e-10 | 2.525e-11 |
| 62.250 | -2.70 | -156.65 | 3.341e-10 | 2.918e-11 |

trans-2-butene 7.8

| JD | lat | lon | Chi | dChi |
|--------|--------|---------|-----------|-----------|
| 69.944 | -10.56 | -165.76 | 3.592e-10 | 2.540e-11 |
| 68.944 | -6.34 | -164.99 | 3.106e-10 | 2.642e-11 |
| 67.181 | 1.44 | -165.00 | 1.528e-10 | 2.673e-11 |
| 66.917 | 2.73 | -165.00 | 1.249e-10 | 1.688e-11 |
| 66.181 | 6.07 | -165.00 | 1.455e-10 | 1.798e-11 |
| 65.705 | 8.20 | -165.00 | 1.059e-10 | 2.043e-11 |
| 65.205 | 9.60 | -164.74 | 1.433e-10 | 2.094e-11 |
| 64.938 | 8.44 | -163.98 | 1.619e-10 | 2.432e-11 |
| 64.385 | 6.27 | -162.59 | 2.102e-10 | 3.216e-11 |
| 64.167 | 5.37 | -161.97 | 2.121e-10 | 2.651e-11 |
| 63.705 | 3.48 | -160.78 | 2.045e-10 | 2.370e-11 |
| 63.250 | 1.60 | -159.43 | 1.305e-10 | 2.114e-11 |
| 63.021 | 0.58 | -158.83 | 1.647e-10 | 2.356e-11 |
| 62.708 | -0.72 | -157.99 | 1.228e-10 | 2.072e-11 |
| 62.479 | -1.70 | -157.28 | 1.708e-10 | 2.335e-11 |
| 62.250 | -2.70 | -156.65 | 3.603e-10 | 3.529e-11 |

1-butene 10.3

| JD | lat | lon | Chi | dChi |
|--------|--------|---------|-----------|-----------|
| 69.944 | -10.56 | -165.76 | 3.629e-09 | 1.625e-10 |
| 68.944 | -6.34 | -164.99 | 2.694e-09 | 1.645e-10 |
| 67.181 | 1.44 | -165.00 | 1.930e-09 | 1.583e-10 |
| 66.917 | 2.73 | -165.00 | 1.404e-09 | 7.401e-11 |
| 66.181 | 6.07 | -165.00 | 1.520e-09 | 7.837e-11 |
| 65.705 | 8.20 | -165.00 | 1.108e-09 | 6.793e-11 |
| 65.205 | 9.60 | -164.74 | 1.594e-09 | 8.671e-11 |
| 64.938 | 8.44 | -163.98 | 1.636e-09 | 8.506e-11 |
| 64.385 | 6.27 | -162.59 | 2.193e-09 | 1.180e-10 |
| 64.167 | 5.37 | -161.97 | 2.145e-09 | 1.076e-10 |
| 63.705 | 3.48 | -160.78 | 2.003e-09 | 9.408e-11 |
| 63.250 | 1.60 | -159.43 | 1.473e-09 | 7.422e-11 |
| 63.021 | 0.58 | -158.83 | 1.998e-09 | 9.889e-11 |
| 62.708 | -0.72 | -157.99 | 1.755e-09 | 8.707e-11 |
| 62.479 | -1.70 | -157.28 | 1.726e-09 | 8.617e-11 |
| 62.250 | -2.70 | -156.65 | 2.634e-09 | 1.241e-10 |

2-methyl-propene 48.4

| JD | lat | lon | Chi | dChi |
|--------|--------|---------|-----------|-----------|
| 69.944 | -10.56 | -165.76 | 1.796e-09 | 1.881e-10 |
| 68.944 | -6.34 | -164.99 | 2.245e-09 | 2.232e-10 |
| 67.181 | 1.44 | -165.00 | 1.872e-09 | 3.628e-10 |
| 66.917 | 2.73 | -165.00 | 1.465e-09 | 1.842e-10 |
| 66.181 | 6.07 | -165.00 | 1.201e-09 | 1.510e-10 |
| 65.705 | 8.20 | -165.00 | 7.156e-10 | 3.972e-11 |
| 65.205 | 9.60 | -164.74 | 9.643e-10 | 4.994e-11 |
| 64.938 | 8.44 | -163.98 | 9.015e-10 | 4.044e-11 |
| 64.385 | 6.27 | -162.59 | 1.389e-09 | 6.140e-11 |
| 64.167 | 5.37 | -161.97 | 1.500e-09 | 6.266e-11 |
| 63.705 | 3.48 | -160.78 | 1.904e-09 | 6.701e-11 |
| 63.250 | 1.60 | -159.43 | 1.349e-09 | 5.000e-11 |
| 63.021 | 0.58 | -158.83 | 1.743e-09 | 6.239e-11 |
| 62.708 | -0.72 | -157.99 | 1.533e-09 | 4.516e-11 |
| 62.479 | -1.70 | -157.28 | 1.629e-09 | 4.661e-11 |
| 62.250 | -2.70 | -156.65 | 2.417e-09 | 1.191e-10 |

cis-2-butene 5.8

| JD | lat | lon | Chi | dChi |
|--------|--------|---------|-----------|-----------|
| 69.944 | -10.56 | -165.76 | 1.257e-10 | 1.597e-11 |
| 68.944 | -6.34 | -164.99 | 1.072e-10 | 1.366e-11 |
| 67.181 | 1.44 | -165.00 | 7.588e-11 | 2.270e-11 |
| 66.917 | 2.73 | -165.00 | 6.002e-11 | 1.477e-11 |
| 66.181 | 6.07 | -165.00 | 4.648e-11 | 1.337e-11 |
| 65.705 | 8.20 | -165.00 | 3.202e-11 | 1.199e-11 |
| 65.205 | 9.60 | -164.74 | 7.655e-11 | 2.016e-11 |
| 64.938 | 8.44 | -163.98 | 5.404e-11 | 1.500e-11 |
| 64.385 | 6.27 | -162.59 | 5.121e-11 | 1.854e-11 |
| 64.167 | 5.37 | -161.97 | 6.916e-11 | 1.804e-11 |
| 63.705 | 3.48 | -160.78 | 5.609e-11 | 1.458e-11 |
| 63.250 | 1.60 | -159.43 | 5.139e-11 | 1.654e-11 |
| 63.021 | 0.58 | -158.83 | 6.164e-11 | 1.652e-11 |
| 62.708 | -0.72 | -157.99 | 5.046e-11 | 1.530e-11 |
| 62.479 | -1.70 | -157.28 | 5.871e-11 | 1.703e-11 |
| 62.250 | -2.70 | -156.65 | 1.292e-10 | 2.475e-11 |

pentane 50.4

| JD | lat | lon | Chi | dChi |
|--------|--------|---------|-----------|-----------|
| 69.944 | -10.56 | -165.76 | 3.557e-09 | 9.125e-11 |
| 68.944 | -6.34 | -164.99 | 3.066e-09 | 7.714e-11 |
| 67.181 | 1.44 | -165.00 | 2.847e-09 | 1.239e-10 |
| 66.917 | 2.73 | -165.00 | 2.373e-09 | 1.170e-10 |
| 66.181 | 6.07 | -165.00 | 2.497e-09 | 1.245e-10 |
| 65.705 | 8.20 | -165.00 | 1.898e-09 | 6.678e-11 |
| 65.205 | 9.60 | -164.74 | 2.838e-09 | 8.402e-11 |
| 64.938 | 8.44 | -163.98 | 2.832e-09 | 9.187e-11 |
| 64.385 | 6.27 | -162.59 | 4.497e-09 | 1.331e-10 |
| 64.167 | 5.37 | -161.97 | 3.648e-09 | 1.075e-10 |
| 63.705 | 3.48 | -160.78 | 3.191e-09 | 9.250e-11 |
| 63.250 | 1.60 | -159.43 | 2.837e-09 | 8.818e-11 |
| 63.021 | 0.58 | -158.83 | 3.422e-09 | 9.896e-11 |
| 62.708 | -0.72 | -157.99 | 2.724e-09 | 8.608e-11 |
| 62.479 | -1.70 | -157.28 | 2.268e-09 | 7.027e-11 |
| 62.250 | -2.70 | -156.65 | 3.478e-09 | 1.034e-10 |

2-methyl-butane 48.4

| JD | lat | lon | Chi | dChi |
|--------|--------|---------|-----------|-----------|
| 69.944 | -10.56 | -165.76 | 2.709e-10 | 2.053e-11 |
| 68.944 | -6.34 | -164.99 | 2.682e-10 | 2.108e-11 |
| 67.181 | 1.44 | -165.00 | 2.416e-10 | 3.300e-11 |
| 66.917 | 2.73 | -165.00 | 1.937e-10 | 2.335e-11 |
| 66.181 | 6.07 | -165.00 | 2.154e-10 | 2.777e-11 |
| 65.705 | 8.20 | -165.00 | 1.871e-10 | 2.923e-11 |
| 65.205 | 9.60 | -164.74 | 3.110e-10 | 3.283e-11 |
| 64.938 | 8.44 | -163.98 | 3.749e-10 | 3.760e-11 |
| 64.385 | 6.27 | -162.59 | 3.859e-10 | 4.663e-11 |
| 64.167 | 5.37 | -161.97 | 3.686e-10 | 3.647e-11 |
| 63.705 | 3.48 | -160.78 | 3.246e-10 | 3.303e-11 |
| 63.250 | 1.60 | -159.43 | 4.027e-10 | 3.865e-11 |
| 63.021 | 0.58 | -158.83 | 3.582e-10 | 4.166e-11 |
| 62.708 | -0.72 | -157.99 | 3.526e-10 | 4.066e-11 |
| 62.479 | -1.70 | -157.28 | 2.878e-10 | 3.377e-11 |

62.250 -2.70 -156.65 3.475e-10 3.657e-11

cyclopentane 7.5

| JD | lat | lon | Chi | dChi |
|--------|--------|---------|-----------|-----------|
| 69.944 | -10.56 | -165.76 | 2.895e-12 | 2.975e-12 |
| 68.944 | -6.34 | -164.99 | 0.000e+00 | 2.639e-12 |
| 67.181 | 1.44 | -165.00 | 0.000e+00 | 6.795e-12 |
| 66.917 | 2.73 | -165.00 | 0.000e+00 | 4.127e-12 |
| 66.181 | 6.07 | -165.00 | 0.000e+00 | 4.031e-12 |
| 65.705 | 8.20 | -165.00 | 0.000e+00 | 5.600e-12 |
| 65.205 | 9.60 | -164.74 | 3.085e-12 | 5.470e-12 |
| 64.938 | 8.44 | -163.98 | 5.956e-12 | 4.720e-12 |
| 64.385 | 6.27 | -162.59 | 0.000e+00 | 6.405e-12 |
| 64.167 | 5.37 | -161.97 | 1.738e-11 | 8.475e-12 |
| 63.705 | 3.48 | -160.78 | 0.000e+00 | 4.472e-12 |
| 63.250 | 1.60 | -159.43 | 1.969e-11 | 9.573e-12 |
| 63.021 | 0.58 | -158.83 | 0.000e+00 | 5.283e-12 |
| 62.708 | -0.72 | -157.99 | 0.000e+00 | 5.014e-12 |
| 62.479 | -1.70 | -157.28 | 1.406e-11 | 6.459e-12 |
| 62.250 | -2.70 | -156.65 | 0.000e+00 | 5.561e-12 |

3-methyl-1-butene 22.1

| JD | lat | lon | Chi | dChi |
|--------|--------|---------|-----------|-----------|
| 69.944 | -10.56 | -165.76 | 3.043e-10 | 1.955e-11 |
| 68.944 | -6.34 | -164.99 | 2.554e-10 | 1.612e-11 |
| 67.181 | 1.44 | -165.00 | 2.777e-10 | 3.507e-11 |
| 66.917 | 2.73 | -165.00 | 2.683e-10 | 2.484e-11 |
| 66.181 | 6.07 | -165.00 | 1.764e-10 | 1.969e-11 |
| 65.705 | 8.20 | -165.00 | 1.291e-10 | 2.141e-11 |
| 65.205 | 9.60 | -164.74 | 1.709e-10 | 2.407e-11 |
| 64.938 | 8.44 | -163.98 | 1.800e-10 | 2.078e-11 |
| 64.385 | 6.27 | -162.59 | 3.200e-10 | 3.775e-11 |
| 64.167 | 5.37 | -161.97 | 3.051e-10 | 4.142e-11 |
| 63.705 | 3.48 | -160.78 | 2.520e-10 | 2.281e-11 |
| 63.250 | 1.60 | -159.43 | 2.124e-10 | 2.207e-11 |
| 63.021 | 0.58 | -158.83 | 3.141e-10 | 2.833e-11 |
| 62.708 | -0.72 | -157.99 | 2.458e-10 | 2.665e-11 |
| 62.479 | -1.70 | -157.28 | 1.964e-10 | 2.160e-11 |
| 62.250 | -2.70 | -156.65 | 2.730e-10 | 2.749e-11 |

trans-2-pentene 10

| JD | lat | lon | Chi | dChi |
|--------|--------|---------|-----------|-----------|
| 69.944 | -10.56 | -165.76 | 2.363e-10 | 1.701e-11 |
| 68.944 | -6.34 | -164.99 | 1.640e-10 | 1.764e-11 |
| 67.181 | 1.44 | -165.00 | 1.190e-10 | 2.440e-11 |
| 66.917 | 2.73 | -165.00 | 9.091e-11 | 1.588e-11 |
| 66.181 | 6.07 | -165.00 | 1.083e-10 | 1.676e-11 |
| 65.705 | 8.20 | -165.00 | 7.334e-11 | 1.795e-11 |
| 65.205 | 9.60 | -164.74 | 1.455e-10 | 2.163e-11 |
| 64.938 | 8.44 | -163.98 | 1.155e-10 | 1.819e-11 |
| 64.385 | 6.27 | -162.59 | 1.290e-10 | 2.078e-11 |
| 64.167 | 5.37 | -161.97 | 1.519e-10 | 2.298e-11 |
| 63.705 | 3.48 | -160.78 | 1.343e-10 | 1.753e-11 |
| 63.250 | 1.60 | -159.43 | 1.153e-10 | 2.019e-11 |
| 63.021 | 0.58 | -158.83 | 1.262e-10 | 1.955e-11 |

| | | | | |
|--------|-------|---------|-----------|-----------|
| 62.708 | -0.72 | -157.99 | 1.241e-10 | 2.000e-11 |
| 62.479 | -1.70 | -157.28 | 1.266e-10 | 2.206e-11 |
| 62.250 | -2.70 | -156.65 | 1.646e-10 | 2.286e-11 |

2-methyl-2-butene 6.3

| JD | lat | lon | Chi | dChi |
|--------|--------|---------|-----------|-----------|
| 69.944 | -10.56 | -165.76 | 2.735e-10 | 4.172e-11 |
| 68.944 | -6.34 | -164.99 | 2.504e-10 | 1.755e-11 |
| 67.181 | 1.44 | -165.00 | 2.086e-10 | 2.955e-11 |
| 66.917 | 2.73 | -165.00 | 1.540e-10 | 1.808e-11 |
| 66.181 | 6.07 | -165.00 | 2.078e-10 | 2.541e-11 |
| 65.705 | 8.20 | -165.00 | 1.488e-10 | 1.854e-11 |
| 65.205 | 9.60 | -164.74 | 2.400e-10 | 2.663e-11 |
| 64.938 | 8.44 | -163.98 | 2.268e-10 | 2.505e-11 |
| 64.385 | 6.27 | -162.59 | 2.730e-10 | 3.229e-11 |
| 64.167 | 5.37 | -161.97 | 2.447e-10 | 2.192e-11 |
| 63.705 | 3.48 | -160.78 | 2.526e-10 | 2.590e-11 |
| 63.250 | 1.60 | -159.43 | 1.741e-10 | 1.824e-11 |
| 63.021 | 0.58 | -158.83 | 2.432e-10 | 2.253e-11 |
| 62.708 | -0.72 | -157.99 | 2.020e-10 | 3.568e-11 |
| 62.479 | -1.70 | -157.28 | 1.778e-10 | 3.203e-11 |
| 62.250 | -2.70 | -156.65 | 1.981e-10 | 2.281e-11 |

1-pentene 16.3

| JD | lat | lon | Chi | dChi |
|--------|--------|---------|-----------|-----------|
| 69.944 | -10.56 | -165.76 | 1.343e-09 | 3.391e-11 |
| 68.944 | -6.34 | -164.99 | 1.050e-09 | 2.512e-11 |
| 67.181 | 1.44 | -165.00 | 7.052e-10 | 4.427e-11 |
| 66.917 | 2.73 | -165.00 | 5.506e-10 | 3.263e-11 |
| 66.181 | 6.07 | -165.00 | 6.717e-10 | 3.495e-11 |
| 65.705 | 8.20 | -165.00 | 4.479e-10 | 3.497e-11 |
| 65.205 | 9.60 | -164.74 | 6.516e-10 | 3.357e-11 |
| 64.938 | 8.44 | -163.98 | 6.197e-10 | 3.188e-11 |
| 64.385 | 6.27 | -162.59 | 9.541e-10 | 4.893e-11 |
| 64.167 | 5.37 | -161.97 | 9.103e-10 | 4.025e-11 |
| 63.705 | 3.48 | -160.78 | 8.661e-10 | 3.534e-11 |
| 63.250 | 1.60 | -159.43 | 6.319e-10 | 3.683e-11 |
| 63.021 | 0.58 | -158.83 | 8.021e-10 | 4.013e-11 |
| 62.708 | -0.72 | -157.99 | 7.220e-10 | 3.420e-11 |
| 62.479 | -1.70 | -157.28 | 7.093e-10 | 3.349e-11 |
| 62.250 | -2.70 | -156.65 | 1.146e-09 | 5.085e-11 |

2-methyl-1-butene 22.1

| JD | lat | lon | Chi | dChi |
|--------|--------|---------|-----------|-----------|
| 69.944 | -10.56 | -165.76 | 6.148e-10 | 2.170e-10 |
| 68.944 | -6.34 | -164.99 | 2.402e-10 | 3.316e-11 |
| 67.181 | 1.44 | -165.00 | 1.558e-10 | 4.168e-11 |
| 66.917 | 2.73 | -165.00 | 9.352e-11 | 2.085e-11 |
| 66.181 | 6.07 | -165.00 | 1.392e-10 | 2.763e-11 |
| 65.705 | 8.20 | -165.00 | 1.783e-10 | 3.775e-11 |
| 65.205 | 9.60 | -164.74 | 3.688e-10 | 4.770e-11 |
| 64.938 | 8.44 | -163.98 | 2.218e-10 | 3.768e-11 |
| 64.385 | 6.27 | -162.59 | 1.951e-10 | 3.970e-11 |
| 64.167 | 5.37 | -161.97 | 1.480e-10 | 3.403e-11 |
| 63.705 | 3.48 | -160.78 | 1.498e-10 | 3.107e-11 |

| | | | | |
|--------|-------|---------|-----------|-----------|
| 63.250 | 1.60 | -159.43 | 1.187e-10 | 2.763e-11 |
| 63.021 | 0.58 | -158.83 | 1.702e-10 | 3.832e-11 |
| 62.708 | -0.72 | -157.99 | 1.553e-10 | 4.968e-11 |
| 62.479 | -1.70 | -157.28 | 1.823e-10 | 5.182e-11 |
| 62.250 | -2.70 | -156.65 | 2.412e-10 | 4.620e-11 |

cis-2-pentene 9.2

| JD | lat | lon | Chi | dChi |
|--------|--------|---------|-----------|-----------|
| 69.944 | -10.56 | -165.76 | 1.619e-10 | 1.450e-11 |
| 68.944 | -6.34 | -164.99 | 1.072e-10 | 1.430e-11 |
| 67.181 | 1.44 | -165.00 | 8.888e-11 | 2.357e-11 |
| 66.917 | 2.73 | -165.00 | 5.846e-11 | 1.509e-11 |
| 66.181 | 6.07 | -165.00 | 8.691e-11 | 1.731e-11 |
| 65.705 | 8.20 | -165.00 | 4.925e-11 | 1.647e-11 |
| 65.205 | 9.60 | -164.74 | 8.459e-11 | 1.797e-11 |
| 64.938 | 8.44 | -163.98 | 7.235e-11 | 1.696e-11 |
| 64.385 | 6.27 | -162.59 | 1.331e-10 | 2.599e-11 |
| 64.167 | 5.37 | -161.97 | 1.147e-10 | 2.114e-11 |
| 63.705 | 3.48 | -160.78 | 9.317e-11 | 1.892e-11 |
| 63.250 | 1.60 | -159.43 | 6.852e-11 | 1.829e-11 |
| 63.021 | 0.58 | -158.83 | 1.330e-10 | 2.471e-11 |
| 62.708 | -0.72 | -157.99 | 7.912e-11 | 2.004e-11 |
| 62.479 | -1.70 | -157.28 | 8.010e-11 | 1.859e-11 |
| 62.250 | -2.70 | -156.65 | 1.384e-10 | 2.463e-11 |

Appendix 4

CURRICULUM VITA

April 1991

NEIL McPHERSON DONAHUE

Personal:

Born: 8 May 1963 in Pittsburgh, Pennsylvania
Social Security No. 181-42-3079

Education:

| | |
|---|------|
| Brown University, Providence, Rhode Island; A.B. in Physics | 1985 |
| Massachusetts Institute of Technology; Ph.D. in Meteorology | 1991 |

Professional Positions:

| | |
|---|---------|
| NCAR Summer Intern, Atmospheric Chemistry and Aeronomy Division | 1984 |
| NASA Graduate Student Researcher | 1985-88 |
| Research Assistant, MIT | 1988-91 |
| Post-doctoral Associate, Harvard University | 1991- |

Research Experience:

Worked with Dr. Brian Ridley during Summer 1984 to develop a chromatographic instrument to measure peroxyacetyl nitrate (PAN) in the remote atmosphere.

Research during 1987-88 with Dr. James Anderson of Harvard University using discharge flow techniques and computer models to study the hydroxyl radical - dimethyl sulfide reaction.

Thesis research with Dr. Ronald Prinn: Developed a detailed chemical model of the remote marine boundary layer, focusing on sources of uncertainty in determinations of the hydroxyl radical. Found non-methane hydrocarbon observations to be the largest source of uncertainty in OH predictions. Developed a chromatographic system to measure C₂ - C₅ hydrocarbons at part-per-trillion mixing ratios. Participated in SAGA3 Soviet and American Gases and Aerosols Expedition in February and March, 1990, measuring nonmethane hydrocarbons at the pptv level.

Honors:

| | |
|--|------|
| State of Michigan Legislative Merit Award | 1981 |
| A.B. Brown University, Magna Cum Laude | 1985 |
| Center for Meteorology and Physical Oceanography Charney Award | 1985 |

Research Interests:

Global Tropospheric Chemistry, focusing on Marine Boundary Layer chemistry. Development of instrumentation suitable for use in remote field studies. Detailed chemical modeling of varied tropospheric chemical environments geared toward identifying key sources of uncertainty and optimal measurement protocols to constrain local fast-photochemistry. Development of accurate standards for compounds of interest. Measuring reaction rate coefficients at temperatures and pressures pertinent to a wide range of tropospheric conditions using absolute techniques. Using absolute kinetic techniques to probe reaction potential surfaces over a wide range of conditions, looking in particular for weakly bound intermediate species.

1. PUBLICATIONS

(* = sole or principal author)

- 1985: Relationship between Peroxyacetyl Nitrate (PAN) and Nitrogen Oxides in the Clean Troposphere, *Nature*, **318**, 347-349 (with H.L. Singh, B. Ridley, J. Shetter, F. Fehsenfeld, D. Fahey, D. Parish, E. Williams, S. Liu, G. Hebler, and P. Murphy).
- 1990: *Non-Methane Hydrocarbon Chemistry in the Remote Marine Boundary Layer. *Journ. Geophys. Res.*, **95**, 18,387 - 18,411, (with R. Prinn).
- 1991: *Nonmethane Hydrocarbon Chemistry in the Remote Marine Atmosphere. *MIT Doctoral Thesis*.
- 1991: *Nonmethane Hydrocarbon Measurements in and over the Remote Pacific during the SAGA III Cruise. *Manuscript in preparation*, (with A. Thompson, J. Greenberg, and R. Prinn)

THE END